

UNIVERSITÉ DU QUÉBEC À CHICOUTIMI

MÉMOIRE PRÉSENTÉ À L'UNIVERSITÉ DU QUÉBEC À CHICOUTIMI COMME
EXIGENCE PARTIELLE DE LA MAÎTRISE EN SCIENCES DE LA TERRE

PAR

CARLOS MARIO MUNOZ TABORDA

DISTRIBUTION OF PLATINUM-GROUP ELEMENTS IN THE EBAY CLAIM,
CENTRAL PART OF THE BELL RIVER COMPLEX, MATAGAMI, QUEBEC

OCTOBER 2010

ABSTRACT

The Bell River Complex (BRC) is a mafic layered complex located 30 kilometers southeast of Matagami in northern Abitibi. The complex is divided into three parts: The East, the Central and the West. The Central part of the intrusion contains the Platinum Group Elements (PGE) occurrences Bwest, Dotcom and Ebay.

This project is focused on the Ebay claim (property of *Hinterland Metals Inc.*) which is centered on the Elizabeth Bay and Opaoca River. The BRC around Ebay consists of layers of leucocratic and melanocratic metagabbros that are folded with an orientation that is predominantly E-W and dipping south 70-80 degrees. The leucocratic layers consist of a sequence of meta-leucogabbro-norites, meta-leucogabbros, meta-leucotroctolites and meta-anorthosites. The melanocratic layers consist of a sequence of meta-melanogabbros, meta-olivine-gabbro-norites, meta-gabbro-norites and meta-pyroxenites. The layered mafic complex is crosscut by sills, dykes and quartz veins associated with the Opaoca and Olga granitic plutons.

The BRC is visibly and polymetamorphosed with regional metamorphism reaching greenschist to amphibolite facies (Goutier, 2005) and contact

metamorphism at albite-epidote hornfels facies and in few places to hornblende hornfels facies.

A series of boreholes made by *Hinterland* were used to reconstruct the BRC stratigraphic sequence in the area of Ebay. A total of 65 samples were taken from 28 boreholes at Ebay for detailed analyses of petrology and geochemistry.

The analyses show that there is a concentration of PGE values that can reach 1-2 g/tonne Pt+Pd, with Pt/Pd ~ 1. Many of these high values are found at the top of a melanocratic layer and therefore the presence of a reef is proposed. Disseminated sulphides are present, however the PGE are not associated with them. The PGE are present as PGM mainly bismuth-tellurides and arsenides of Pt and Pd.

It is suggested that in the magmatic chamber a sulphide liquid collected Ni, Cu and PGE. Then gravity settling gathered together all of the sulphide droplets in a layer. Some time later during metamorphism S and Cu were mobilized, but left the PGE as PGM phases.

RÉSUMÉ

Le Complexe de la Rivière Bell (CRB) est un complexe mafique stratifié situé dans la sous-province de l'Abitibi à 30 km au Sud-Est de Matagami. Le complexe est divisé en trois parties, Est, Centrale et Ouest. La partie Centrale de l'intrusion est celle contenant les occurrences des EGP Bwest, Dotcom et Ebay.

Ce projet s'effectue dans la propriété minière Ebay (propriété de *Hinterland Metals Inc.*) laquelle est située près la baie Elizabeth et de la Rivière Opaoca. Le CRB à Ebay est composé d'une séquence interstratifiée de lits leucocratiques et mélanocratiques foliée avec une orientation prédominante E-O et inclinés vers le sud à 70-80 degrés. Les lits leucocratiques se composent d'une séquence de meta-leucogabbros, de meta-leucogabbronorites, de meta-leucotroctolites et de meta-anorthosites. Les lits mélanocratiques sont constitués d'une séquence de meta-mélanogabbros, de meta-olivine-gabbronorites, de meta-gabbronorites et de meta-pyroxenites. Le complexe mafique stratifié est traversé par des reefs, dykes et veines de quartz associés avec les plutons d'Opaoca et du lac Olga.

Le CRB est visiblement altéré et polymétamorphisé par le métamorphisme régional qui a atteint les faciès schiste vert à amphibolites (Goutier, 2005) et par le métamorphisme de contact qui a atteint les faciès albite-epidote à cornéenne et de hornblende à cornéenne localement.

Une série de forages effectués par *Hinterland* a été utilisée pour reconstruire la séquence stratigraphique de CRB à Ebay. Un total de 65 échantillons ont été

collectés à partir de 28 forages pour les analyses plus détaillées de pétrologie et géochimie.

Les analyses montrent qu'il y a une concentration d'EGP qui peut atteindre 1-2 g/ton Pt+Pd, avec Pt/Pd ~ 1. Plusieurs de ces échantillons sont situés dans le toit d'un des lits mélanocratiques, et par conséquent la présence d'un *reef* y est proposé.

Des sulfures disséminés sont présents, mais les EGP ne sont pas associés avec eux. Les EGP sont présents comme minéraux du groupe du platine (MGP), principalement bismuth-tellurides et arséniures de Pt et Pd.

Il est suggéré que dans la chambre magmatique un liquide sulfuré a collecté le Ni, le Cu et les EGP. Après, la décantation par gravité a déposé toutes les gouttelettes de sulfures dans un lit. Quelques temps après, pendant le métamorphisme agit, le soufre et le cuivre ont été mobilisés en laissant les EGP comme des MGP.

ACKNOWLEDGEMENTS

I would like to thank Sarah Jane Barnes who brought me this valious opportunity; she gave me the chance to came to Canada and let me became a better person. I really admire her. Words cannot express my gratitude.

I would like to thank Hinterland metals and Mark Fekete (President and CEO) whom kindly support economically many things of the project, the field trip, sampling and some analyses.

I would like to thank Natural Sciences and Engineering Research Council of Canada (NSERC) and the Canada Research Chair in Magmatic Metallogeny for the founding.

I would like to acknowledge the debt I owe to Edward Sawyer, Philippe Pagé and Sarah Dare, Sarah was very helpful with comments, suggestions and English things like gramma and spelling, I have learnt much from her.

The colleagues at REDIST-UQAC whom I consider my friends, Carlos, Steph, Samuel and Dominique, I owe them many of the knowledge I have got of the French language. They helped with comments, suggestions and everything else related to oral presentations and texts. Also thanks to Lionnel, Levin, Daphne, Lucas, Clifford, Laetitia, Matthias and Jérôme, merci beaucoup each.

My no-REDIST friends who I had not mention before, they motivated me to stand winter, some of them are Luis, Karla, Memo, Jacobo, Audrey, Juanito, Anita, Juan Cynthia and Jeannette, muchas gracias.

Sandra, she gave me a new smile and has contributed with her love, support and affection.

My family, they have built the person I have become, they always know how to overcome from the difficulties. Without them this could not be possible.

A mi papá, mamá y hermanos, muchas gracias por toda la ayuda que me han brindado, por aguantarme y por darme la posibilidad de estudiar, el esfuerzo de esta maestria también es de ustedes. Los llevo en el corazón a cualquier lugar y en todo momento.

CONTENTS

ABSTRACT	II
RÉSUMÉ	IV
AKNOWLEDGEMENTS	VI
LIST OF FIGURES	XI
LIST OF TABLES	XIV
LIST OF APPENDICES	XV
CHAPTER 1	1
INTRODUCTION	1
1.1. Objectives of the Study	1
1.2. Classification of Platinum-Group Element Resources	3
1.3 Layered Intrusion Hosted Platinum-Group Deposits	5
CHAPTER 2	11
GEOLOGY	11
2.1 Previous Work	11
2.2 Stratigraphic profiles	17
2.1.1. North-South profile	21
2.1.2. East-West profile	24

2.1.3. Generalized stratigraphic column	27
CHAPTER 3	32
PETROLOGY	32
3.1. Silicate assemblage	34
3.1.1. Metagabbros	34
3.1.2. Felsic rock	44
3.2. Sulphide assemblage.....	47
3.3. Platinum Group Minerals (PGM)	50
CHAPTER 4	54
GEOCHEMISTRY	54
4.1. Analytical Methods.....	54
4.1.1 Whole Rock Major and Trace Element Methods.....	54
4.1.2 Whole Rock Nickel, Copper, Sulphur and PGE-Au Analyses.....	54
4.2 Major elements	55
4.2.1. CIPW Norm and Rock Classification	61
4.3. Trace elements	65
4.4. Sulphur, Ni-Cu & PGE-Au geochemistry	69
4.4.1. Relationships among the PGE.....	75

CHAPTER 5	84
DISCUSSION	84
5.1. Magmatic events in the Bell River Complex	84
5.1.1 The sulphides	88
5.2. PGE behaviour and implications for exploration	89
5.3. PGE layer location	100
5.4. Formation processes of the Ebay's PGE reef	103
5.5. Comparison to other PGE deposits	110
CHAPTER 6	117
CONCLUSIONS	117
BIBLIOGRAPHY	121

LIST OF FIGURES

Figure 1.1 Generalized geological map of the Bell River Complex and its contacts..	2
Figure 2.1 Location of the Bell River Complex within the sub-province of Abitibi, Canada.	15
Figure 2.2 Aeromagnetic survey of the Bell River Complex.....	16
Figure 2.3 a) centimetric dyke crosscutting the gneiss; b) veins crosscutting the sequence of gneiss	18
Figure 2.4 Above: Granite dyke intruding the sequence of leucogabbros, Below: Contact between the leuco- and melanogabbros.....	19
Figure 2.5 Location of the Stratigraphic profiles in the area.....	20
Figure 2.6 Stratigraphic profile N-S	23
Figure 2.7 Stratigraphic profile E-W.....	25
Figure 2.8 Generalized stratigraphic column	28
Figure 3.1 Location of the samples.....	33
Figure 3.2 Meta-gabbroic samples.	39
Figure 3.3 calcite vein and quartz veins cross-cutting the rocks	40
Figure 3.4 type 3 rocks	43
Figure 3.5 Felsic rock ML-52	46
Figure 3.6 Sulphide assemblages.	49

Figure 3.7 PGM pictures.....	51
Figure 4.1 Major elements plotted on Harker diagrams	59
Figure 4.2 diagram of alkali vs. silica and AFM of Irvine and Baragar (1971).....	60
Figure 4.3 a) plagioclase, pyroxene and olivine diagram of Streckeisen (1979) and QAP diagram of Streckeisen (1976)	63
Figure 4. 4 MgO vs. Al ₂ O ₃ and SiO ₂ vs. Al ₂ O ₃	64
Figure 4.5 Multi-element spider diagrams for Ebay samples, normalized to the primitive mantle (Sun and McDonough, 1989) after CIPW.....	67
Figure 4.6 Sm vs. La diagram.....	68
Figure 4.7 Variation of S and PGE with depth	72
Figure 4.8 MgO vs. Ni diagram.....	73
Figure 4.9 Diagram of sulphur vs. Cu	74
Figure 4.10 Sulphur vs. Pt and Pd.....	77
Figure 4.11 Pd vs PGE and Pd vs. Bi and Sb (main constituents of PGM)	78
Figure 4.12 Ni-PGE-Cu normalized to primitive mantle	80
Figure 4.13 Cu/Ir vs. Ni/Pd and Ni/Cu vs. Pd/Ir.....	81
Figure 5.1 Al ₂ O ₃ vs. FeO _T diagram	86
Figure 5.2 multi-element plots showing the patterns for the olivine gabbros and the pyroxene rich rocks.	87
Figure 5.3 Pt vs. Pd for the Ebay samples, compared to Bushveld's Merensky and Stillwater.....	93
Figure 5.4 Variation of S, Cu/(Cu+Ni) and PGE at depth.....	94

Figure 5.5 Cu/Ir vs. Ni/Pd and Ni/Cu vs. Pd/Ir.....	97
Figure 5.6 Pd vs. Cu/Pd for BRC and other different layered complexes.....	99
Figure 5.7 The proposed location of the reef	102
Figure 5.8 Ni-PGE-Au-Cu Spidergrams normalized to primitive mantle	105
Figure 5.9 Diagram that represents the processes in the BRC at the Ebay zone and the PGM concentration.....	109
Figure 5.10 PGE Ni, Au and Cu Spidergrams after Cu/Pd ratios.	111
Figure 5.11 Mg number $[Mg\# = Mg/(Mg+Fe_T)]$ for different PGE deposits	114
Figure 5.12 Comparison of the Mg# between BRC in a generalized stratigraphic column and the interval Critical-Main Zones of Bushveld.....	115

LIST OF TABLES

Table 1.1 Classification of PGE Resources in Mafic and Ultramafic Rocks	4
Table 1.2 Classification of PGE deposits in layered intrusions	10
Table 2.1 Sample location	29
Table 3.1 Characterization of grains of Platinum-Group Minerals detected with the Scanning Electron Microscope	52
Table 3.2 Statistical Results of PGM grains	53
Table 4.1 S, Ni, Cu, Au and PGE values	71
Table 5.1 Characteristics of the different PGE deposits of the world	116

LIST OF APPENDICES

APPENDIX 1 Major elements by XRF, Untreated.....	130
APPENDIX 2 Major elements after treatment.....	132
APPENDIX 3 REE analyses by ICP-MS (in ppm).....	134
APPENDIX 4 Ni, Cu analyses by atomic absorption spectrometry	142
APPENDIX 5 Whole rock sulphur by infrared light absorption	144
APPENDIX 6 Whole rock PGE analyses by ICP-MS.....	146
APPENDIX 7 Profile reconstructions from the borehole stratigraphic columns ...	154
APPENDIX 8 Thin section descriptions	155
APPENDIX 9 CIPW norm classification.....	160
APPENDIX 10 SEM sessions, pictures and histograms	162
APPENDIX 11 Proposed sampling	186

CHAPTER 1

INTRODUCTION

1.1. Objectives of the Study

A number of reports have suggested that the Bell River and Lac Dore intrusions of the north-western region of Abitibi in Quebec (Fig. 1.1) are layered intrusions similar to the Bushveld Complex (Allard, 1970, Maier et al., 1996). This prompted an initial sampling of both bodies for platinum-group elements (PGE) as part of a *Géologie Québec* survey of the Abitibi for PGE resources (Barnes et al., 1993). The samples were very poor in PGE and the Cu/Pd ratios were greater than mantle values suggesting that there could be a PGE enrichment in the rocks stratigraphically lower than those sampled (Barnes et al., 1993, Maier et al., 1996). *Géologie Québec* sampled the Bell River intrusion more intensively (Goutier, 2005) and reported a number of PGE occurrences in the eastern portion (Figure 1.1). Hinterland Metals have been conducting an exploration program in the area since 2000 and have found more PGE occurrences. Many of these are close to the Lac Olga granite pluton in the Elizabeth Bay and Opaoca River. This thesis will examine one of the PGE occurrences, Ebay, with the aim of characterizing and classifying the deposit and investigating whether the intrusion of the granite pluton played a role in forming the PGE occurrence.

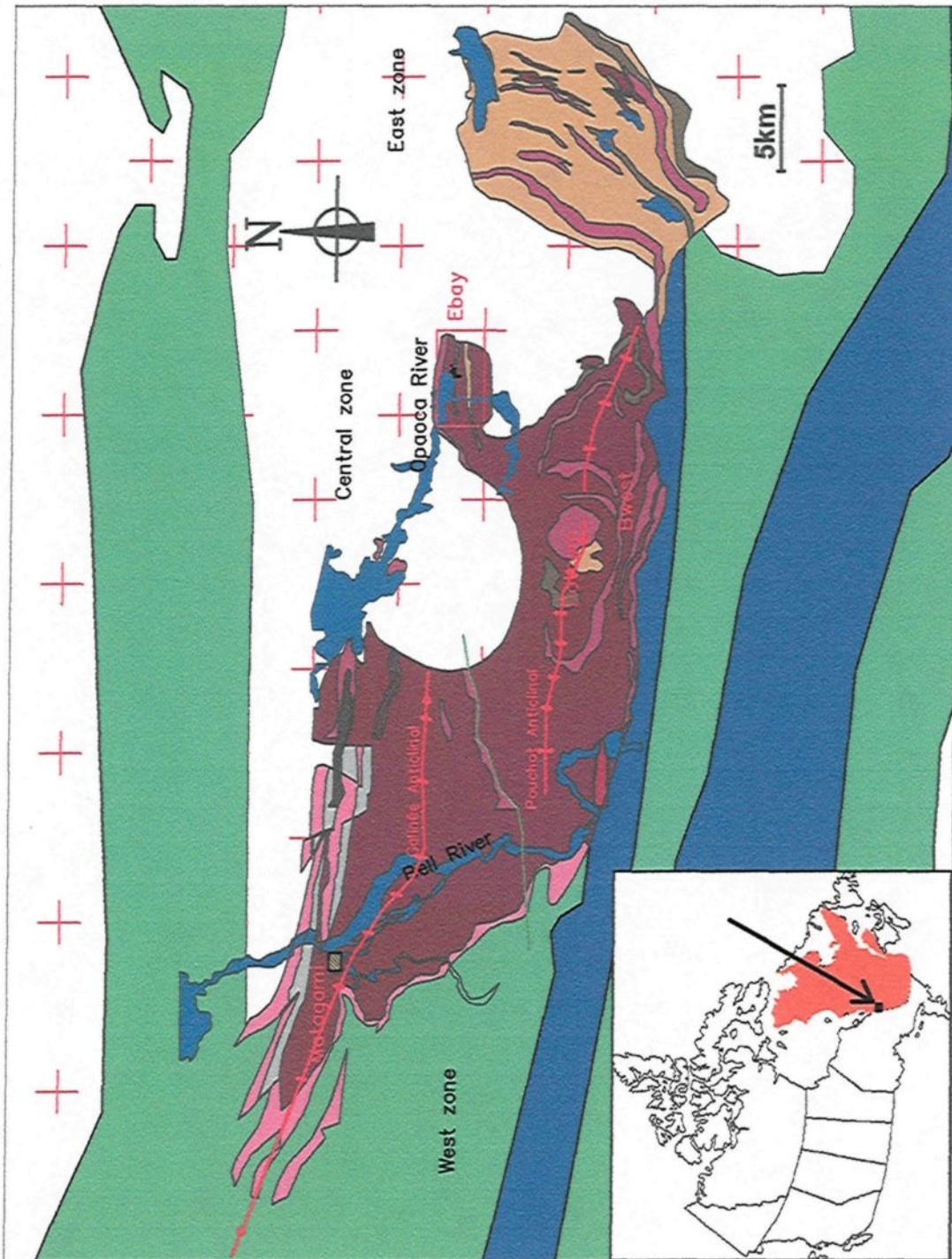


Figure 1.1 Generalized geological map of the Bell River Complex and its contacts. Modified after Piche et al., 1990; Barnes et al., 1993 and Goutier, 2005.

1.2. Classification of Platinum-Group Element Resources

The platinum-group elements (PGE) resources of the world have different characteristics in terms of geological setting, form, host rock and the minerals that host the PGE (e.g. Naldrett, 2004; Maier, 2005; Green and Peck 2005). Most are found within mafic and ultramafic intrusions. These have been classified into sulphide rich deposits, which produce mainly Ni and Cu with PGE as by-products (e.g. the Creighton deposit of Sudbury, Farrow and Lightfoot, 2002), and PGE-dominated deposits which are exploited for the PGE (e.g. the Merensky reef of the Bushveld). The PGE-dominated deposits may be further divided based on the nature of the intrusion (Table 1) into layered intrusions, concentrically zoned intrusions and ophiolites. Most of the ore deposits (i.e. those that are mined) occur within layered intrusions. An exception to this is the Roby Zone of the Lac des Iles Complex, which occurs in a concentrically zoned intrusion (Lavigne and Michaud, 2001).

Table 1.1 Classification of PGE Resources in Mafic and Ultramafic Rocks

1. Ni-Cu sulphide deposits > 5 % sulphides, PGE produced as a by-product
(e.g. deposits of Noril'sk and Sudbury)
2. PGE-dominated deposits < 5 % sulphides, PGE principle product
 - 2.1 Layered Intrusion Hosted (e.g. Bushveld, Stillwater, Great Dyke)
 - 2.1.1 Contact (e.g. Platreef, Bushveld)
 - 2.1.2 Lower Third Stratiform (reef)
 - 2.1.2.1 Chromite-bearing (e.g. UG-2, Bushveld)
 - 2.1.2.2 Sulphide-bearing (e.g. JM, Stillwater)
 - 2.1.3 Upper Third
 - 2.1.3.1. Magnetite layers (e.g. Rio Jacare)
 - 2.1.3.2. Cryptic (e.g. Platinova, Skaergaard)
 - 2.1.4 Discordant
 - 2.1.4.1 Fe-rich dunite pipes (e.g. Driekop pipe, Bushveld)
 - 2.1.4.2 Fe-oxide lenses/pipe (e.g. OUI Duluth)
3. Concentrically Zoned Complexes
 - 3.1 Magmatic Breccia (e.g. Roby Zone Lac des Iles)
 - 3.2 Chromitite lenses (e.g. Alaskan type complexes)
4. Ophiolites
 - 4.1 Podiform chromites (e.g. Leka, Norway)
 - 4.2 Stratiform chromites (e.g. Thetford, Quebec)

1.3 Layered Intrusion Hosted Platinum-Group Deposits

The Bell River Complex (BRC) is clearly a layered intrusion (Goutier, 2005) and thus a more detailed description of the types of PGE deposits found in layered intrusions will be outlined (Table 1.2). We will then try to characterize the BRC in terms of these properties.

PGE deposits in layered intrusions may be divided on the basis of their form and position within the intrusion into contact, stratiform and discordant deposits. The contact deposits occur at the margins of a layered intrusion in a wide zone (100-200m). The only mined example is the Platreef of the Bushveld. The Platreef is a broad heterogeneous zone of up to 200 m of pyroxenite to norite containing large xenoliths of dolomite, serpentinites and calcsilicates (Cawthorn *et al.*, 1985, Maier *et al.*, 2008). The rocks contain 1-10 % disseminated sulphides. The sulphide assemblage is igneous: pentlandite, pyrrhotite and chalcopyrite. The PGE are hosted in solid solution in the sulphides and as PGM associated with sulphides (Holwell and McDonald, 2007).

Within the intrusions, stratiform layers enriched in Pt and Pd occur. They are referred to as reefs. They may be subdivided based on their position in the intrusion into those occurring in the lower third and those occurring in the upper third. All of the reefs that are mined occur in the lower third. The reefs in the lower third of the intrusions may be divided into those which are rich in chromite and those which contain disseminated sulphide.

Most of the mined reefs (e.g. Merensky Reef, Bushveld, Main Sulphide Reef Great Dyke, JM reef Stillwater) are stratiform with disseminated sulphides and occur in the lower third of the intrusions. There are also a number of important occurrences in this category: The AP reef of the Penikat intrusion and the Ferguson reef of the Munni Munni intrusion. The common features of these reefs are that they are narrow (1-3 m). The host rock type is generally a pyroxenite or gabbro-norite. The sulphides present represent an igneous assemblage of pyrrhotite, pentlandite and chalcopyrite. The PGE are mainly found in a solid solution within the sulphides or as platinum-group minerals associated with the sulphides (Barnes and Maier, 2002b; Godel et al. 2007; Godel and Barnes, 2008; Barnes et al., 2008; Oberthür, 2002, Zientek et al., 2002; Hoatson and Keays, 1989).

The overall model for the formation of both the contact and sulphide-bearing stratiform reefs is that a mafic magma became saturated in a sulphide liquid. The sulphide liquid collected the platinum-group elements and the sulphide liquid in turn was collected either at the margins of the intrusion or into the layers that now form the stratiform reefs (Naldrett 2004).

The chromite-bearing reefs occur in the lower-most part of the intrusions. The only mined example is the UG2-reef of the Bushveld Complex. Other examples of this type of enrichment exist such as the Dream reef of the Great Dyke, the A-chromitite of the Stillwater, and the SJ reef of the Penikat intrusion. These aforementioned examples however are not continuous or rich enough to be mined.

They are between 1 and 3 metres thick and are comprised of a number of layers of chromite with the intervening layers consisting of pyroxenites. In most cases there is very little sulphide present (<1 %) and it consists mainly of chalcopyrite with minor pentlandite. The PGE are hosted by PGM, which are associated with the sulphides in the rocks where sulphides are present. The origin of the chromite-bearing reefs is more difficult to explain than the sulphide bearing reefs. The extremely low sulphide content and lack of correlation between PGE and S suggest that a simple model with collection of PGE by a sulphide liquid will not suffice to explain the PGE enrichment. Two models are generally proposed; a) PGE crystallized directly from the silicate magma (Tredoux et al 1995) and b) sulphides were originally present along with the PGE, but S has been remobilized (Barnes, 2002b).

The upper portions of many layered intrusions are magnetite-bearing and consist of gabbro-norites or diorites and leucogabbro-norites. In some cases they consist of cyclic units of magnetite layers; gabbro-norite and leucogabbro-norite are also present. Enrichment of PGE has been reported from this setting for a number of intrusions. In some cases the enrichment is found in the magnetite layers (e.g. Rio Jacare, Brazil, Sa et al. 2005; Birch Lake, Duluth, Ripley et al. 2008). In some cases both the magnetite-rich rocks and the surrounding rocks are enriched in PGE (e.g. Platinova reef Skaergaard, Nielsen and Brooks, 1995; Sonju Lake, Duluth, Nabil, 2003; Rincon del Tigre, Bolivia, Prendergast, 2000; Stella intrusion South Africa, Maier et al., 2003). In these cases the enriched zones can span from

20 m up to a width of 200 m. Both the sulphide and magnetite content of the rocks can be very low and the zone is extremely difficult to identify in the field. In most cases some sulphides are present, but the assemblage is not igneous. Minerals however, such as chalcopyrite, pyrite, bornite and chalcocite, have been reported. The PGE are present as PGM. The PGM are found in association with both silicates and oxides. Correlations between PGE content and S content of the rocks are poor. It is impossible to propose a model of collection of PGE by a sulphide liquid considering that magnetite-rich stratiform reefs and the sulphide assemblage itself does not support it. It is generally suggested that the PGE were initially collected by a sulphide liquid and that the rocks contained disseminated sulphides. Late magmatic fluids or metamorphic fluids however dissolved the sulphides and removed much of the S (Andersen et al., 1998, Sa et al., 2005, Maier, 2005).

Discordant lenses or pipes enriched in PGE have been found in a number of intrusions (Bushveld, Duluth and Rio Jacare). The Bushveld pipes were mined. The mineralized rocks consisted of Fe-rich dunites and wherlites pipes approximately 10-30 meters in diameter (Scoon and Mitchell, 2004) surrounded by unmineralized Mg-dunite pipes up to 100 meters in diameter. The sulphide contents of the rocks were very low and the main PGM reported were FePt alloy and PtAs₂. The origin of both the pipes and the PGE deposits within them is poorly understood (Scoon and Mitchell, 2004).

The pipes in Duluth and Rio Jacare consist largely of Fe-oxides with minor sulphides. The Rio Jacare body was metamorphized and the PGE are found as

PGM in association with the magnetite (Sa et al., 2005). In Duluth an igneous assemblage of sulphides, pyrrhotite, pentlandite and chalcopyrite are present and PGE correlate with S suggesting a sulphide control of the elements (Nabil, 2003). In both cases the pipes could have been formed from overlying magnetite rich layers which were gravitationally unstable and collapsed into the partially consolidated underlying cumulates during seismic activity and/or when a new magma was emplaced.

Table 1.2 Classification of PGE deposits in layered intrusions

Position	Form	Classification	Example	Intrusion	Host rocks	Associated Sulphides	Oxide	Refs
Margins	Wide zone 200m, Heterogeneous	Contact	Platreef	Bushveld	Pyroxenite, norite	Pn, Ccp, Po	Mgt, Ilm	1,2
Lower 1/3	Narrow layer 1-2 m, chromite layer	Stratiform, Chromite	UG-2 reef	Bushveld	Chromitite, pyroxenite	Ccp, py, Pn	Chr	3,4
	Narrow layer 1-2 m, disseminated sulphides	Stratiform Sulphide	Merensky Reef	Bushveld	Melanorite, Chromitite	Pn, Ccp, Po	Chr	5,6
	Narrow layer 1-2 m, disseminated sulphides	Stratiform Sulphide	Main Sulphide zone	Great Dyke	Pyroxenite, Gabbronorite	Pn, Ccp, Po	Chr	7,8,9
	Narrow layer 1-2 m, disseminated sulphides	Stratiform Sulphide	JM reef	Stillwater	Troctolite, Gabbronorite	Pn, Ccp, Po	Chr	10,11
Upper 1/3	Narrow layer 1-2 m, magnetite layer	Stratiform, Fe-oxide		Rio Jacare	Magnetitite, metagabbro	Pn	Mgt	12
	Wide Zone (20-100m)	Stratiform Cryptic	Platinova reef	Skaergaard	Leucogabbronorite	Bn, Dg, Ccp	Mgt	13,14
Discordant	Pipe Dunite	Discordant	Driekop	Bushveld	Fe-rich dunite	None	Mgt	15
	Pipe/lense Magnetite	Discordant	OUI	Duluth	Magnetitite	Po, Pn, Ccp	Mgt, Ilm	16

1) Maier et al. (2008)

2) Holwell and McDonald (2007)

3) McLaren and De Villiers (1982)

4) Maier and Barnes (2008)

5) Prichard et al. (2004)

6) Vermaak and Hendriks (1976)

7) Prendergast (1990)

8) Barnes et al. (2008)

9) Oberthur (2002)

10) Zientek et al. (2002)

11) Godel and Barnes (2008)

12) Sa et al. (2005)

13) Nielsen and Brooks (1995)

14) Andersen et al. (1998)

15) Scoon and Mitchell (2004)

16) Nabil (2003)

CHAPTER 2

GEOLOGY

2.1 Previous Work

The Bell River Complex (BRC) is located close to the town of Matagami on the northern edge of the Abitibi sub-province, 782 kilometres northwest of Montreal (Figure 1.1).

This region is composed of volcanic, sedimentary and plutonic rocks following a series of antiforms and synclinals oriented E-W (Card and Ciesielski, 1986). The age of the synvolcanic plutons and volcanic rocks ranges from 2790 Ma to 2690 Ma (Goutier and Melançon, 2007). Turbidite bodies were deposited between 2690 Ma and 2682 Ma, and form long bands W-E between the volcanic rocks (Ayer et al., 2002 and Davis, 2002). The last volcanic -sedimentary event (2687-2673 Ma; Ayer et al., 2002 and Davis, 2002) is represented by polygenic conglomerates and alkaline volcanic rocks deposited in a continental setting (Goutier and Melançon, 2007).

The BRC (2724.6 ± 2.5 Ma U-Pb on zircons, Mortensen 1993) intruded the volcanic rocks of Watson Lake and the Wabasse Group and is interpreted to be a feeder chamber to the Wabasse basalts (Maier et al., 1996). The basalts themselves are tholeiitic with flat REE patterns (Maier et al., 1996) and were interpreted as island arc tholeiites. The BRC is clearly cut by subsequent tonalitic

and dioritic intrusions, such as the Opaoca tonalite and Olga pluton (2693 ± 2 Ma U-Pb on zircons, Mortensen, 1993; in Goutier, 2005).

The BRC is a stratified complex (20 Km x 65 Km) and was first recognized by Bancroft in 1912. The Bell River body was described as a complex by Freeman in 1939, who made a comparison with the Stillwater Complex (Montana, U.S.A.). Both Maier et al. (1996) and Goutier (2005) make comparisons with the Bushveld Complex (South Africa). Magmatic structures can be observed in the outcrop, however the primary minerals were now replaced by amphibole, serpentine, talc, chlorite and quartz. The complex was metamorphized to greenschist facies in the west and amphibolite facies in the east (Goutier, 2005). All rocks were completely metamorphized and should contain the prefix meta in front of their igneous name. In the interest of readability however, the prefix will not added to the rock names and should be inferred. The BRC consists of meta- pyroxenites, gabbronorite, anorthosites, granophyres, magnetitite layers and dunite (Goutier, 2005).

The complex is folded with the anticlines Galinée and Puchot being recognized. The axes of the anticlines have a WNW-ESE orientation and plunge to the east Goutier (2005) (Figure 1.1). Goutier (2005) divided the BRC into three parts: Western, Central and Eastern Zones (Figures 1.1 and 1.2). He interprets the Western Zone to be the youngest, the Central Zone to be oldest and the Eastern Zone to be of intermediate age. The Western Zone had previously been divided into the Granophyre Zone at the margins, underlain by the Layered Zone, which consists of numerous layers of magnetite-bearing gabbros and anorthosites; the

Main Zone consists of magnetite-bearing gabbro-norites (Goutier, 2005; Maier et al 1996). The magnetite-bearing units are clearly visible on the aeromagnetic map. Based on the whole rock geochemistry and the presence of magnetite Maier et al. (1996) equated this portion of the intrusion with the Upper Zone of the Bushveld. The Eastern Zone consists of leucogabbros and anorthosites. The Central Zone consists mainly of leucocratic to melanocratic gabbro-norites with minor pyroxenites (Goutier, 2005). Many of the units are magnetite-bearing as can be seen on the aeromagnetic map (Figure 2.2).

The current study is centered on the Ebay claim (Elizabeth Bay), 30 kilometres southeast of Matagami town, the northeastern border of the central part of BRC to the east of Opaoca River and Elizabeth Bay (Figure 2.3). The rocks in the area consist of leucocratic to melanocratic gabbro-norite layers, crosscut by granitic sills, dykes, and quartz veins (figures 2.3 and 2.4). According to the aeromagnetic map, the rocks at Ebay do not appear to be magnetite-bearing.

The leucocratic layers consist of a sequence of leucogabbros, anorthosites and a minor proportion of foliated granites. These leucocratic rocks are hard to differentiate in a hand specimen. The rocks are coarse-grained, and are composed of amphibole, plagioclase and minor biotite and quartz. Phaneritic relict texture has been preserved from igneous protoliths, which in some outcrops is gneissic or migmatitic (Figures 2.3 and 2.4).

The melanocratic layers consist of a sequence of dark green meta-melanogabbros to fine-medium grained meta-pyroxenites containing minor relicts of amphibole and plagioclase (Figure 2.4).

The layers are folded into an orientation predominantly E-W and dipping south 70-80 degrees.

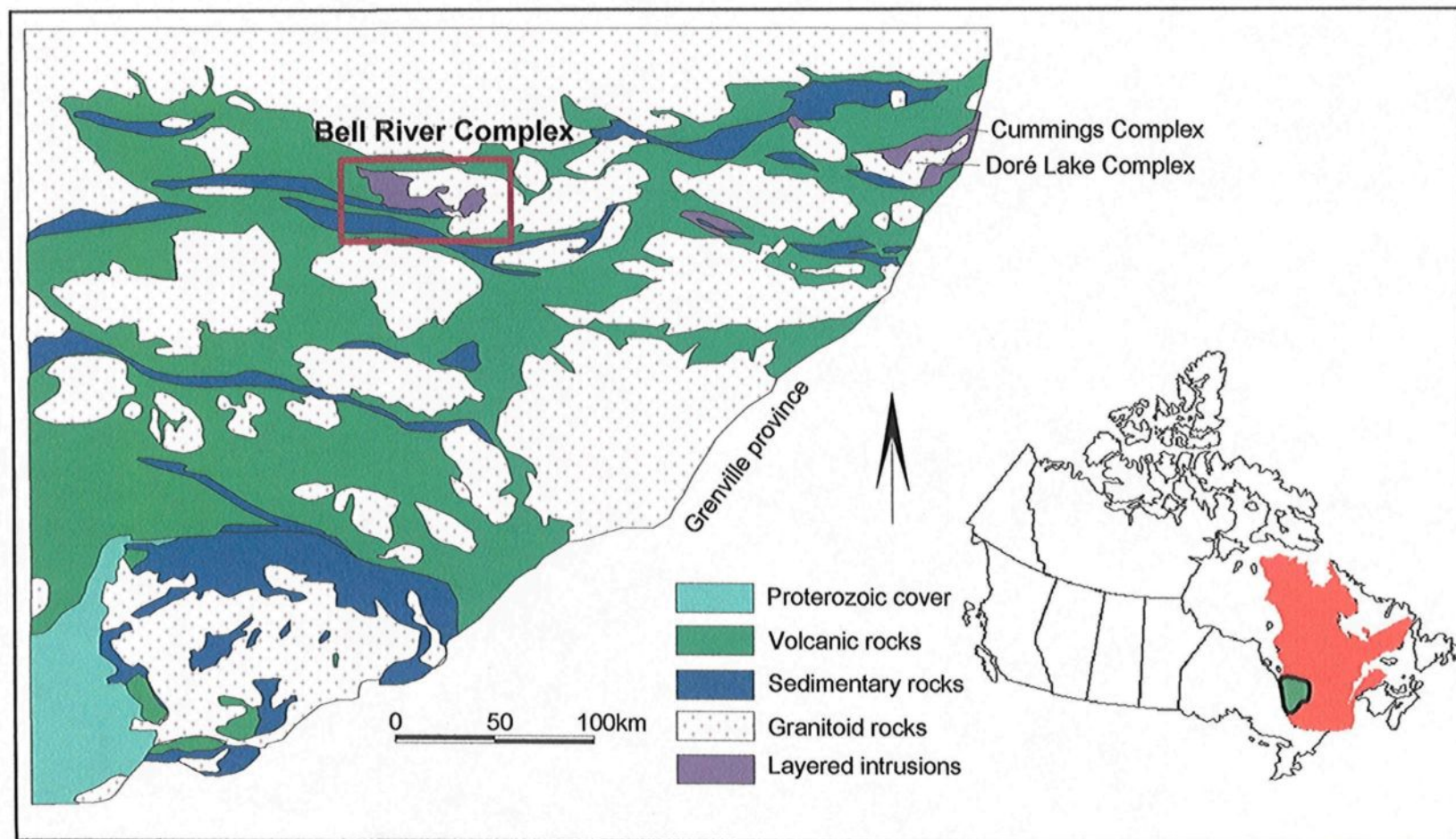


Figure 2.1 Location of the Bell River Complex within the sub-province of Abitibi, Canada (Modified from MERQ-OGS, 1983).

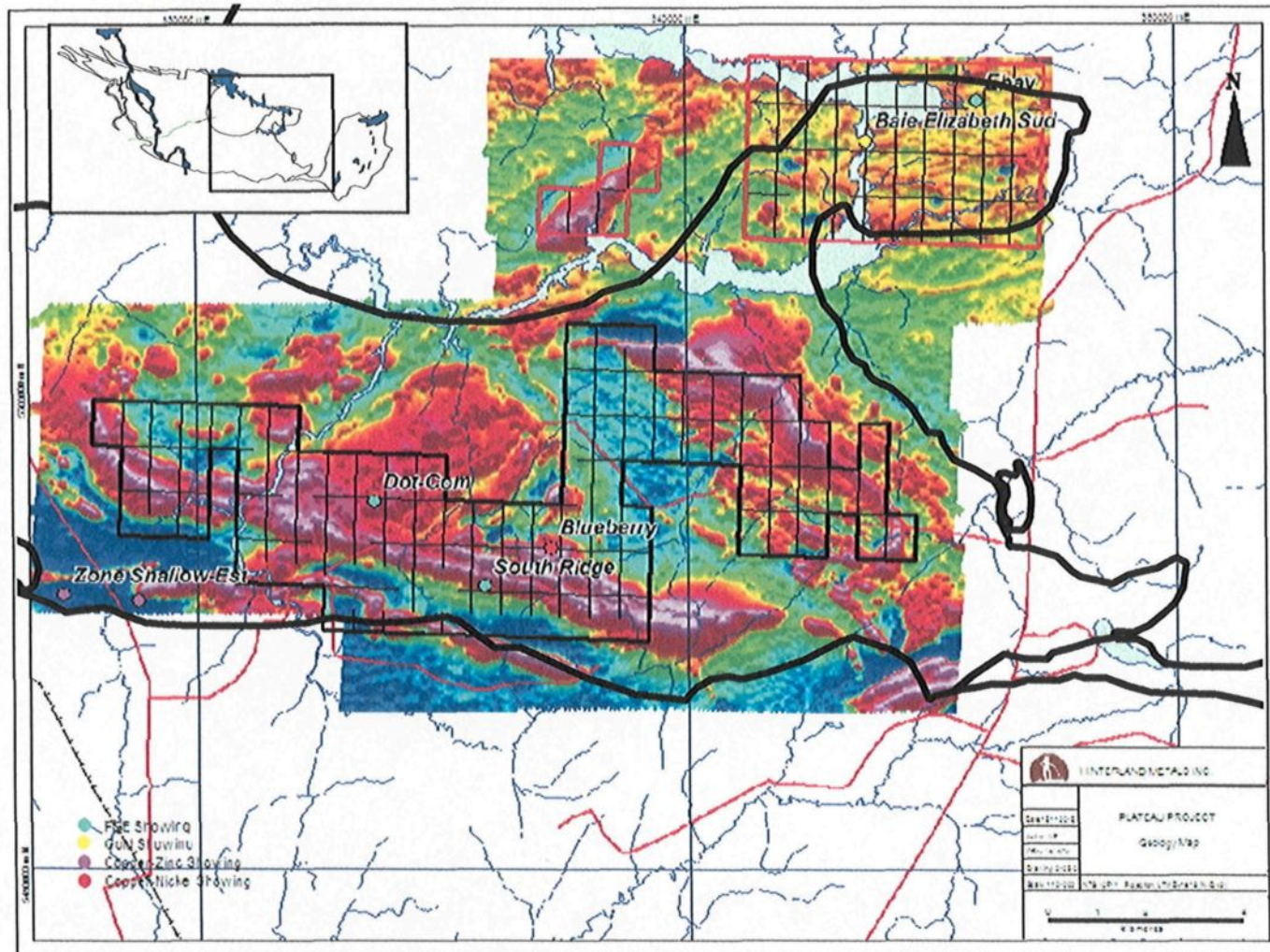


Figure 2.2 Aeromagnetic survey of the Bell River Complex, the black line denotes the BRC border (RGB chart from SIGÉOM after Hinterland)

2.2 Stratigraphic profiles

Two stratigraphic profiles were reconstructed from hand specimen descriptions done by *Hinterland Metals* between 2006 and 2008 (Figure 2.5). The boreholes were distributed along two traverses aligned approximately E-W and N-S plunging 50-53 degrees north (except the drill hole EB07-14 plunging south, see Appendix 7 for descriptions). The area that has been drilled is 2.4km² (1715 m x 1402 m) and is covered by 35 holes from 120 to 195 meters deep (Figure 2.5).

From these surveys, the stratigraphic columns were reconstructed and placed at their respective coordinates and elevations in order to reconstruct the layers at depth (Figures 2.6 and 2.7).

The correlation was made from Hinterland's hand specimen descriptions, and we incorporated the samples we collected. The lithological layering occurs on a fine scale (<1m) thus the division of the units into melagabbronitic and leucogabbronitic is based on the dominant rock type in each layer.



Figure 2.3 a) centimetric dyke crosscutting the gneiss; b) veins crosscutting the sequence of gneiss, defined in this work as leucogabbros protoliths, note the interlayering of leucocratic and melanocratic mineral beds and some movement along the sides of the veins.

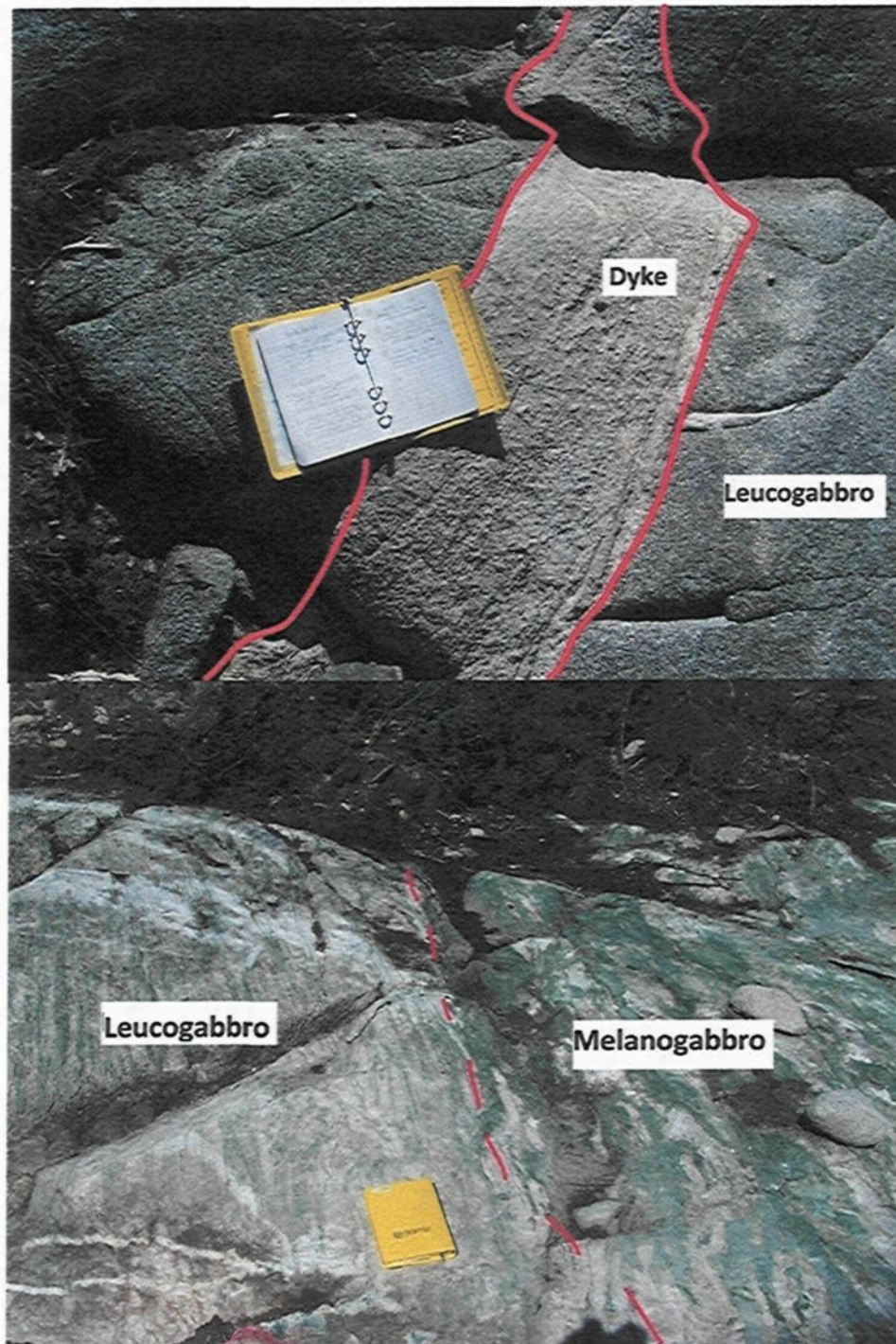
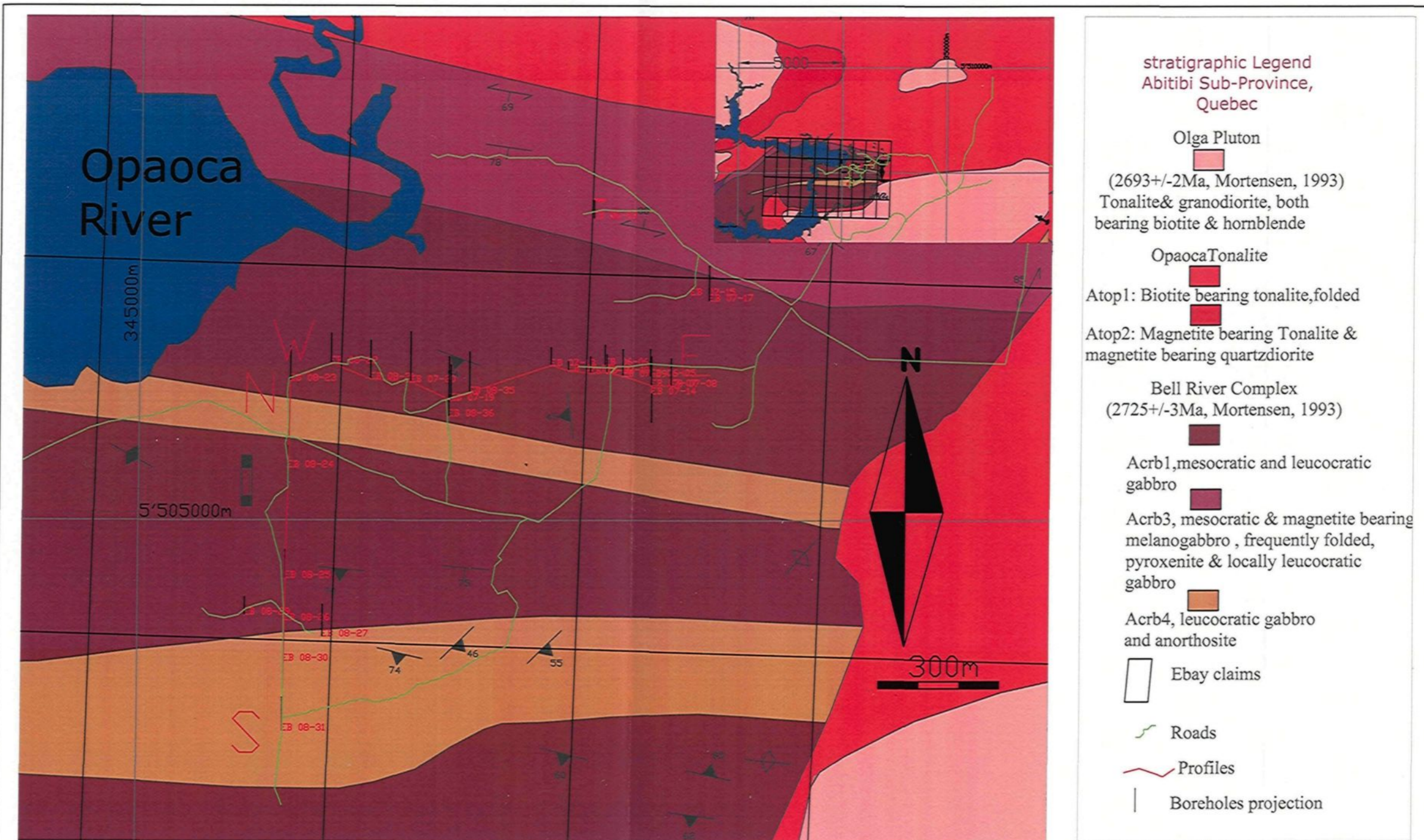


Figure 2.4 Above: Granite dyke intruding the sequence of leucogabbros, this one is relatively fresh and not foliated. Below: Contact between the leuco- and melanogabbros.




 UNIVERSITÉ DU QUÉBEC À CHICOUTIMI	UNIVERSITÉ DU QUÉBEC À CHICOUTIMI	HINTERLANDS METALS	Modified after Goutier et Melancon, 2007	Figure 2.5: position of the geological profiles N-S and W-E; geological map from the 32F11-200-0202 Rivière Opaoca	<h1>2.5</h1>
	DEPARTAMENT DU SCIENCES DE LA TERRE	DISTRIBUTION OF PLATINUM GROUP ELEMENTS IN THE HINTERLAND'S EBAY CLAIM, CENTRAL PART OF THE BELL RIVER COMPLEX, MATAGAMI, QUEBEC	DATE: JULY 2010		

Figure 2.5 Location of the Stratigraphic profiles in the area

2.1.1. North-South profile

On the N-S profile (Figures 2.5 and 2.6), the layers dip predominantly to the south with an open synform in the center of the section and some pinch and swell of the layers. Eight layers were defined from south to north and from the top to bottom. The sequence can be described as follows:

The top of the sequence, the southernmost layer (1) (Figure 2.6), corresponds to the map unit Acrb4 from Goutier (2005) and this layer is a leucogabbro. It is a grey-green gabbro, medium to coarse grained equigranular, and massive overall. It contains minor disseminated pyrite. The granitic dykes that intrude this leucogabbro are light grey/pink, coarse to very coarse grained with a pegmatitic texture; muscovite and minor disseminated sulphides are visible locally.

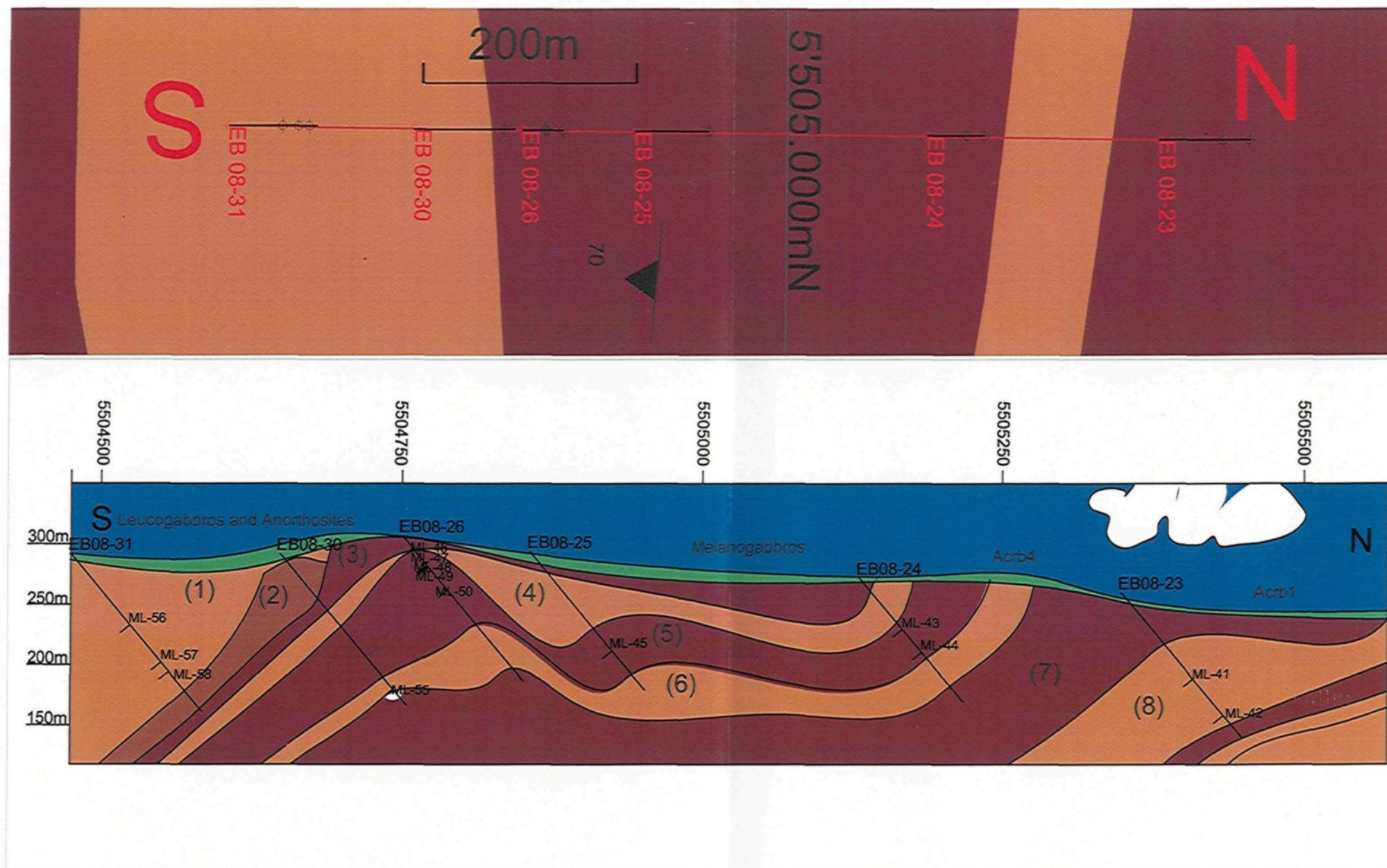
Layer (2) does not outcrop, but consists of a medium to dark-grey banded gabbro. It is very fine to medium grained, equigranular and massive. Minor disseminated pyrite is present. There is moderate pervasive alteration of amphibole to chlorite and minor potassic alteration of plagioclases towards the bottom of this interval.

Layer (3) corresponds to Acrb1 unit of Goutier (2005) and outcrops over a large area even though it is one of the thinnest units. It consists of a dark speckled green melanogabbro that is medium-grained and weakly foliated (dipping 50°). Minor disseminated sulphides are hosted in bands typically 5cm wide. There is weak pervasive alteration of amphiboles throughout. It is interbedded with bands of

leucogabbro. This layer is characterized by the presence of numerous dykes and veins of granite.

Layer (4) outcrops as Acrb4 of Goutier (2005); it is a pale-greenish white to dark green, medium-grained banded leucogabbro, and weakly foliated at 50° dip. There are some narrow bands of anorthosite and melanogabbro present.

Layer (5) does not appear on Goutier's map (2005) probably because it is in the middle of the leucocratic Acrb4 bands and its width is too small to be mapped. This layer is a banded pale to dark green speckled melanogabbro, fine to medium-grained. It has a strong foliation at 40°-50° (seen in the core samples). Some leucogabbro is present. There is a gradational contact with the speckled gabbro. Disseminated pyrrhotite, pyrite and chalcopyrite are present. There is weak pervasive alteration of amphibole in some cases.



Stratigraphic Legend
Abitibi Sub-Province,
Quebec

Bell River Complex
(2725+/-3Ma, Mortensen)

Layers (1), (4), (6) & (8):
leucogabbro Salt and
pepper medium to dark
grey-green, medium to
coarse grained
equigranular; massive
overall, minor sulphides;
some dykes intruded in
the rock.

Layer (2): Salt and pepper
medium to dark grey
banded gabbro; very fine
to medium grained,
equigranular; massive;
minor occasional
disseminated pyrite;
moderate pervasive
amphibole alteration.

Layers (3), (5) & (7): Dark
speckled green melanogabbro,
medium-grained, weakly
foliated at 50° with weak
pervasive amphibolite alteration
throughout, some bands of
leucogabbro interbedded. Minor
sulphides disseminated within
bands typically 5cm wide. Zone
characterized by numerous
dykes and veins


 UNIVERSITÉ DU QUÉBEC À CHICOUTIMI	UNIVERSITÉ DU QUÉBEC À CHICOUTIMI	HINTERLANDS METALS	PROFILES AND INTERPRETATION BY: CARLOS MARIO MUNOZ TABORDA	Figure 2.6: N-S profile, zoom map in the upper part with location of the holes, interpretative profile below.	<h1>2.6</h1>
	DEPARTAMENT DU SCIENCES DE LA TERRE	DISTRIBUTION OF PLATINUM GROUP ELEMENTS IN THE HINTERLAND'S EBAY CLAIM, CENTRAL PART OF THE BELL RIVER COMPLEX, MATAGAMI, QUEBEC	CARTOGRAPHY TAKEN FROM: GAUTIER AND MELANCON, 2007 REVISED BY: S-J BARNES, MARK FEKETE, EDWARD SAWYER	DATE: July, 2010	

Figure 2.6 Stratigraphic profile N-S

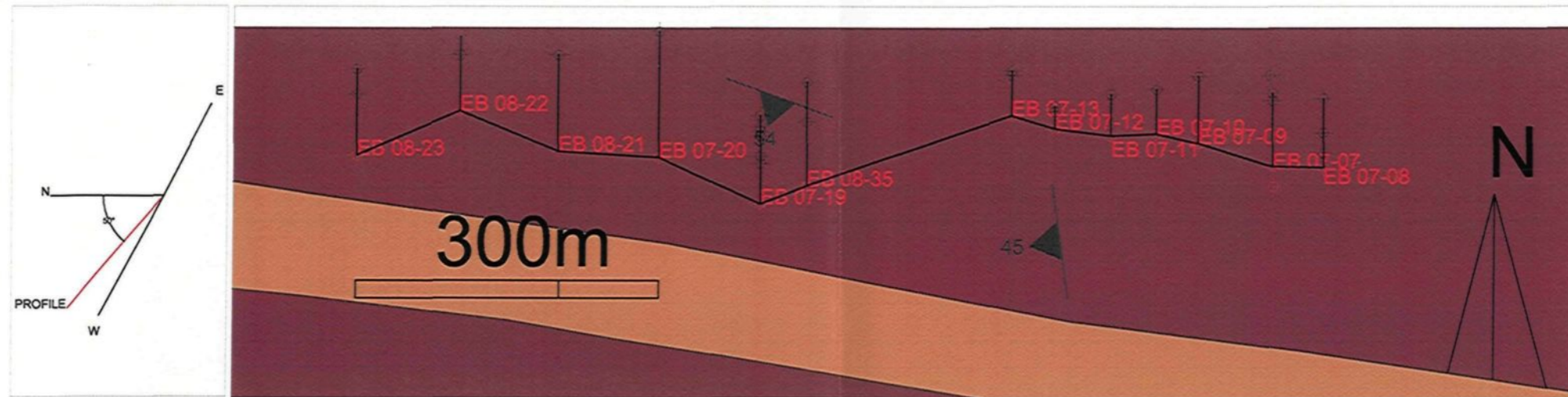
Layer (6) corresponds to the bottom of the EB08-24, EB08-26 and EB08-30 boreholes. This layer consists of greenish white to dark green, and medium to coarse grained speckled leucogabbro. It is weakly foliated at 45° - 50° (seen on core samples). This unit contains 20% melanogabbros. Minor disseminated sulphides are present throughout. There is a strong and pervasive retrogradation of amphibole in some portions.

Layer (7) is a melanogabbro present only in the EB08-23 hole in the N-S profile and probably continues towards the south at depth. It outcrops in the vicinity of borehole EB08-23 and probably towards the west. This melanogabbro is light green to grey, medium grained, and massive. There is weakly to moderate alteration of amphibole, intensifying at depth with minor potassic alteration.

The last three layers are only present into EB08-23 in the N-S profile and they are broadly distributed towards E-W profile, therefore they will be described in E-W profile below.

2.1.2. East-West profile

The E-W profile was drawn considering the dip of the holes, thus, our profile was drawn E-W, but is inclined 50 degrees towards the north as many of the holes are off course with respective corrections for holes with a different plunge. Thus the width is relative and corresponds to an inclined view (Figure 2.7).

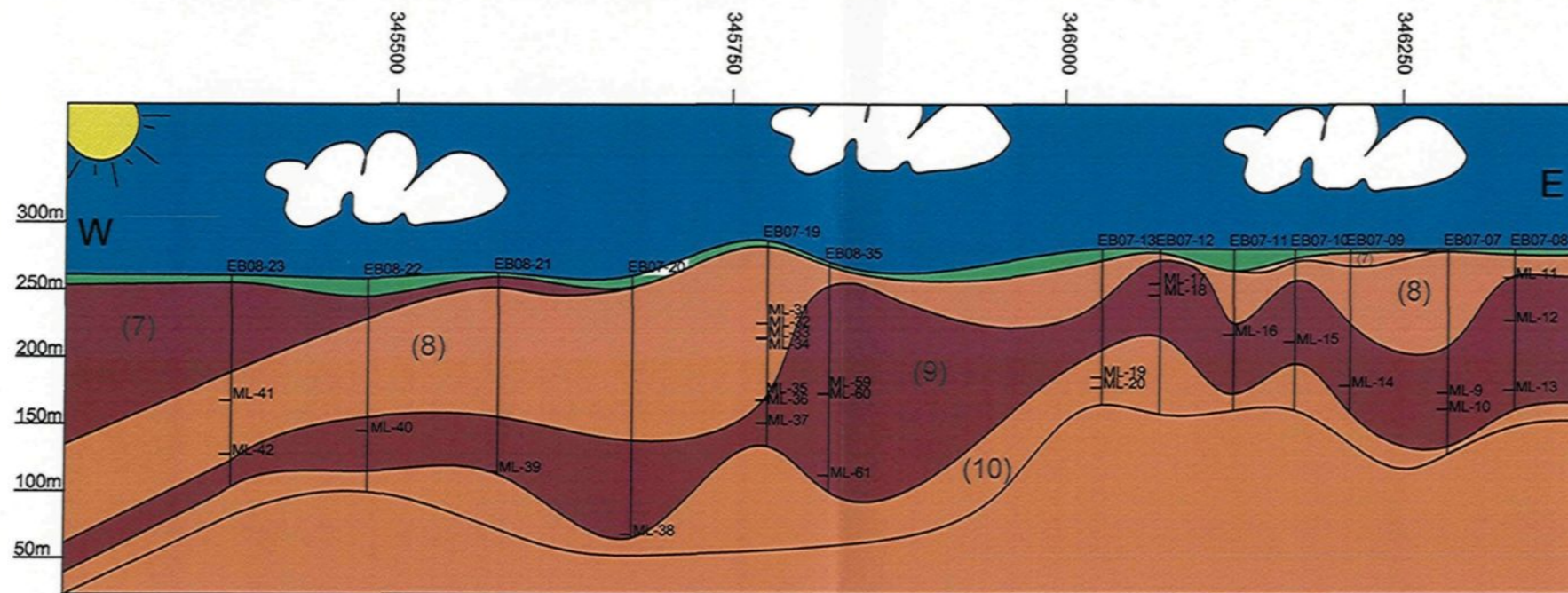


**Stratigraphic Legend
Abitibi Sub-Province,
Quebec**

**Bell River Complex
(2725 \pm 3Ma, Mortensen)**

Layers (7) & (9): melanocratic gabbro, light green to grey; medium grained; massive.

Layers (8) & (10): Leucogabbro White, light to dark grey, light green; medium grained; massive; numerous small grey dykes and small green melanogabbro sections



	UNIVERSITÉ DU QUÉBEC À CHICOUTIMI	HINTERLANDS METALS	PROFILES AND INTERPRETATION BY: CARLOS MARIO MUNOZ TABORDA	Figure 2.7: E-W profile, zoom map in the upper part with location of the holes, interpretative profiles in the lower box. DATE: July, 2010	2.7
	DEPARTAMENT DU SCIENCES DE LA TERRE	DISTRIBUTION OF PLATINUM GROUP ELEMENTS IN THE HINTERLAND'S EBAY CLAIM, CENTRAL PART OF THE BELL RIVER COMPLEX, MATAGAMI, QUEBEC	CARTOGRAPHY TAKEN FROM: GAUTIER AND MELANCON, 2007 REVISED BY: S-J BARNES, MARK FEKETE, EDWARD SAWYER		

Figure 2.7 Stratigraphic profile E-W

As mentioned above, the layers in the bottom of the N-S sequence correspond to beds on the top of the E-W profile. They cross the profile and a few are tilted towards the west. The first layer is best exposed to the east of EB08-23 hole and in minor proportions at the top of EB08-22 and EB08-21. This layer corresponds to layer (7) in the N-S profile described above and probably correlates with the layer on the top of EB07-09 and EB07-10, which was eroded along 450 meters.

Layer (8) is present in all of the holes on the E-W profile. It consists of a leucogabbro that is white, light to dark grey, light green in various parts, medium grained, and massive. There are numerous small grey dykes and small green melanogabbro layers interspersed. In some sections there may be up to 80% plagioclase. The rocks are massive to very weakly foliated. Minor disseminated pyrite and chalcopyrite are present. There is weak alteration of amphibole; there are large quartz bands in some places.

Layer (9) does not outcrop, but is present in all of the boreholes of the profile. It has a variable thickness (Figure 2.7). This layer is a dark grey-green, and fine to medium grained melanogabbro. There is pervasive alteration of amphibole throughout, but is variable in intensity. Some of the zones of altered amphibole are wispy and waxy in appearance, with an anastomosing appearance and these are soft when touched. Local potassic alteration is present, mainly affecting plagioclase crystals or along fracture surfaces (apple green alteration). Foliation is present locally.

The final layer (10) was only intersected in some holes and the true width is unknown. It consists of a white and medium grey leucogabbro that can also be described as "patchy", and in some cases is massive and medium grained. It has a foliation at 50° and contains abundant dykes and layers of melanogabbro. Some disseminated sulphides are present.

2.1.3. Generalized stratigraphic column

From the profiles described above, a generalized stratigraphic column can be constructed to summarize the sequence in the area of the Ebay claim.

This part of the BRC has a cyclic layering of melano- and leuco-gabbros which are sometimes referred to as anorthosite in field descriptions. The sequence is crosscut by numerous felsic dykes at all depths. Disseminated sulphides are present throughout the layers and in smaller proportion in the dykes (Figure 2.8).

From top to bottom, the stratigraphic column follows the same sequence as the profiles, where (1) represents the top and (10) the bottom, described above.

The samples taken have been re-projected onto this stratigraphic column in Table 2.1 which also shows their relative depths for further analyses. The location of many of the samples is not shown here considering that some of the boreholes are far away from the profiles and do not permit a projection.

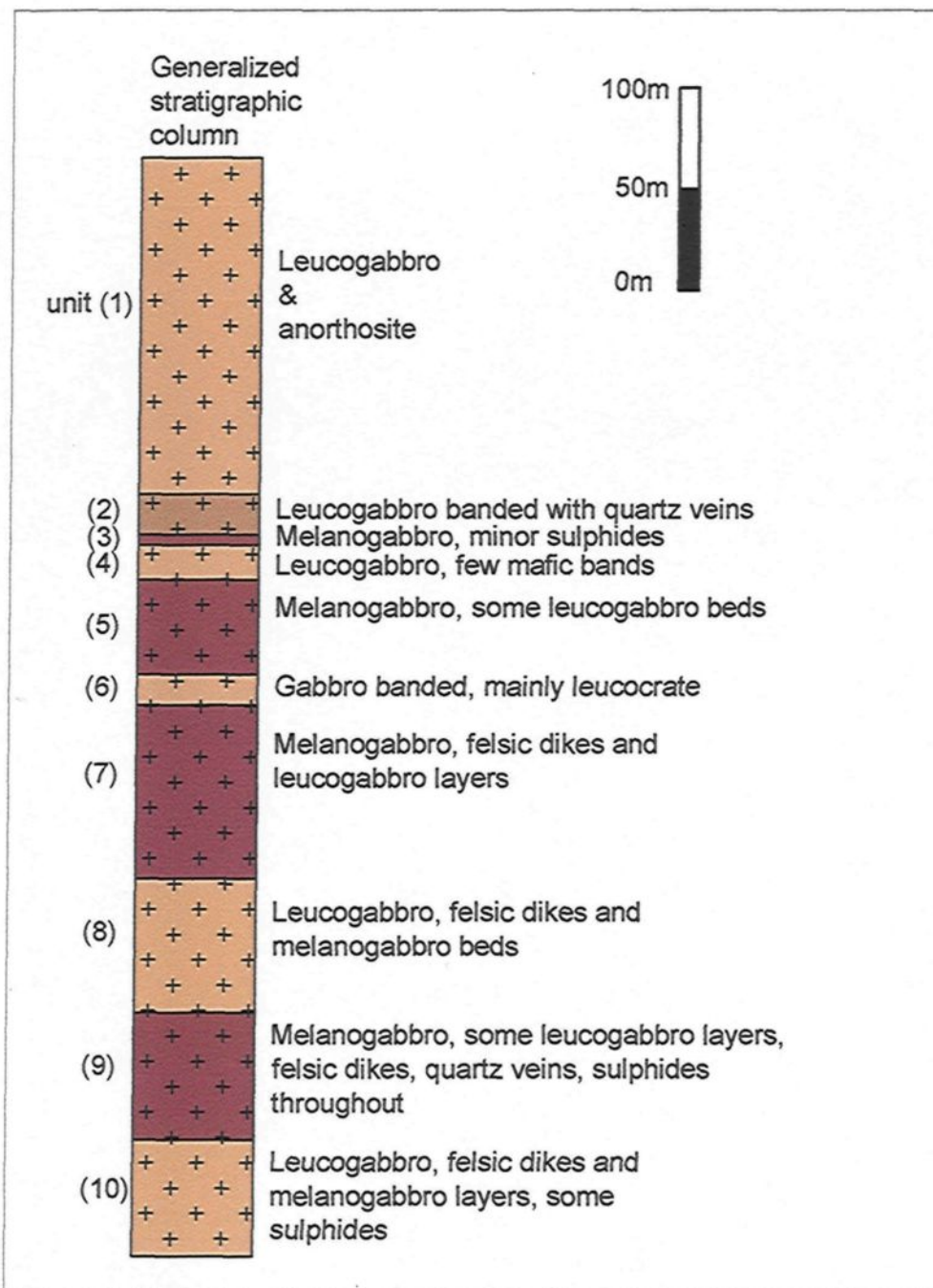


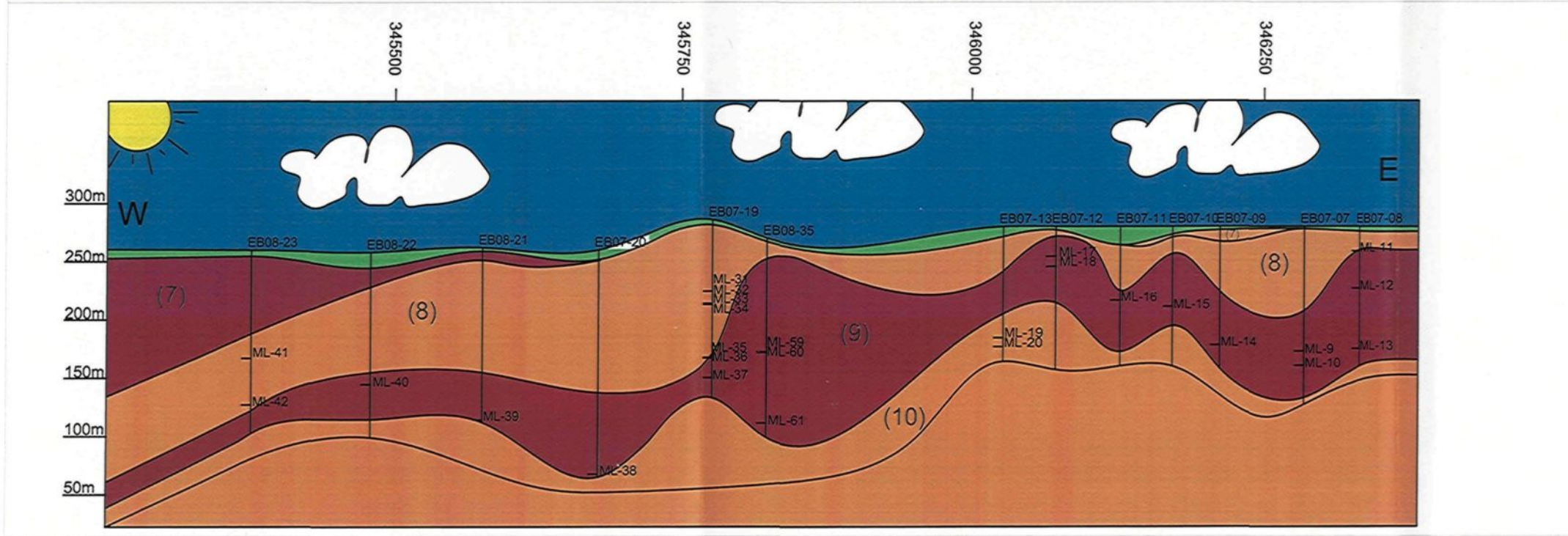
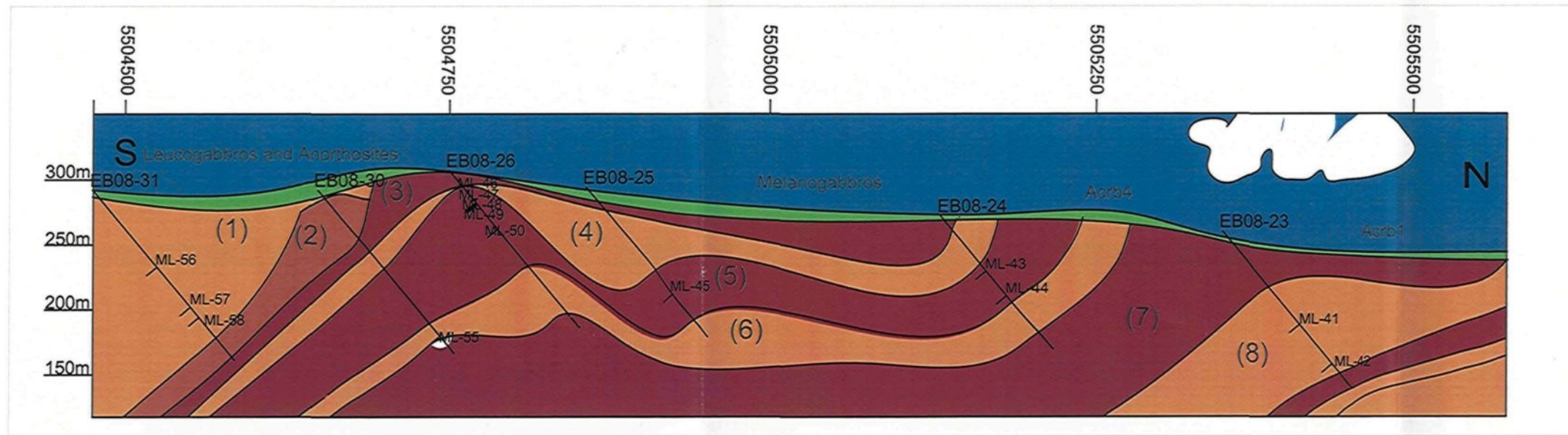
Figure 2.8 Generalized stratigraphic column

CHAPTER 3

PETROLOGY

Sixty-five samples were selected for petrographic and geochemical analyses (Fig. 3.1 & Table 2.1). Samples were selected so as to cover as wide a range of rock types and mineralization as possible based on an examination of the hand samples and on commercial analyses available from *Hinterland*.

Samples were further divided into sulphide-bearing and non-sulphide bearing based on the S content of the rocks with 0.1 wt% S being the dividing line.




 UNIVERSITÉ DU QUÉBEC À CHICOUTIMI	UNIVERSITÉ DU QUÉBEC À CHICOUTIMI	HINTERLANDS METALS	ELABORATED BY: CARLOS MARIO MUNOZ TABORDA	Figure 3.1: location of the samples, taken for geochemistry and petrology in both profiles. red samples are projected from other holes but closer DATE: July, 2010	3.1
	DEPARTAMENT DU SCIENCES DE LA TERRE	DISTRIBUTION OF PLATINUM GROUP ELEMENTS IN THE HINTERLAND'S EBAY CLAIM, CENTRAL PART OF THE BELL RIVER COMPLEX, MATAGAMI, QUEBEC	REVISED BY: S-J BARNES DIRECTED BY: S-J BARNES, MARK FEKETE, EDWARD SAWYER		

Figure 3.1 Location of the samples. Some of the samples contained in the profiles are not shown here. See Figure 2.3 for these.

3.1. Silicate assemblage

Two fundamental subdivisions were considered: meta-gabbros and granites.

3.1.1. Metagabbros

The rocks in this group vary from melanocratic to leucocratic meta-gabbros to meta-anorthosites. Some of the igneous minerals are preserved whereas many of the others are completely metamorphosed. Gabbroic texture and the presence of primary plagioclase and a minor proportion of primary amphibole remain.

These rocks have experienced greenschist to amphibolite facies regional metamorphism as reported by Goutier (2005). Contact metamorphism happened in the area due to intrusion of Opaoca and probably the Lac Olga plutons. The Lac Olga pluton is dated at 2693 ± 2 m.a. (U/Pb zircon Mortensen, 1993) and this intruded the Opaoca pluton (Goutier, 2004). Regional metamorphism occurred first and thermal metamorphism overprinted it (Figure 3.2).

The rocks are divided in three groups based on the metamorphism observed. The type 1 rocks correspond to greenschist or amphibolites facies rocks, type 2 rocks are albite-epidote hornfels, these rocks are granoblastic, medium grained, polymineralic and are not foliated in most cases and type 3 rocks with layering correspond to the inner layered complex, are relatively fresh and do not show any of the metamorphic events of the last two groups.

Type 1 Rocks: Rocks characterized by visible foliation in some samples (Figure 3.2 a,b). These rocks are composed in order of decreasing abundance: crystals of

tremolite–actinolite (green phase is the most abundant), plagioclase, the clinozoisite-zoisite-epidote group, chlorite and by a smaller proportion of titanite and apatite. Talc, in very small proportions, as well as a smaller amount of clinopyroxene is present in some cases. Tremolite-actinolite minerals are medium-grained, subidiomorphic, green to colourless, birefringent purple to green, and have poikiloblastic crystals that are typically aligned. They make up to 60% of the rock and some of these grains are thought to be replacing pyroxene or amphibole (in some cases small grains seem to be subidiomorphic poikiloblasts of chloritized crystals of pyroxene or hornblende). Plagioclase is subidiomorphic to xenomorphic, and medium to large in grain size. In some cases Carlsbad or albite twins enable the composition to be determined under the microscope (the grains identified are between An 60 to An 40). Furthermore, there is spindle texture developed in some plagioclase. Plagioclase makes up to 30% of the rock, and is commonly altered to produce sericite or saussurite. In hand specimen, plagioclase clearly shows red spots due to saussuritization. The clinozoisite-zoisite-epidote group form idiomorphic to subidiomorphic colourless crystals and make up to 5% of the rock. The interference colours are normally anomalous blue of first order or yellow to green maximum. Chlorite is green to colourless fine to medium grained and is commonly the alteration product of amphibole or pyroxene. Chlorite is xenomorphic in some places where some elongated crystals are present, kink bands or folded crystals are developed. The modal percentage of this mineral is very variable, but on average is 4 to 5%. Titanite and apatite are

accessory phases and they are very fine size grains and common as inclusions in amphibole or chlorite.

Type 2 Rocks: these are characterized by a lack of foliation and more obvious thermal metamorphic effects, these rocks are more abundant (Figure 3.2 c,d,e,f). They are granoblastic polymineralic rocks with various grain sizes from fine to medium, and are very altered. There is extensive growth of new coarse grained minerals that suggest an action of fluids in these rocks although some foliation has been preserved locally. These rocks are composed principally of plagioclase, tremolite-actinolite, a clinozoisite-zoisite-epidote group mineral and chlorite, with smaller proportions of titanite, apatite or relicts of pyroxene or amphibole. In some places veins of quartz and calcite are present, cross-cutting the rock (Figure 3.3). In most rocks plagioclase is the most abundant mineral making up to 60% of the rock. The grains are normally medium to coarse-grained and are visible in hand specimens, subidiomorphic, and in some places are highly affected by saussuritization or sericitization (the saussuritization is normally centered in the crystals and is seen on the hand specimen as red spots). They are colourless with twins of albite-Carlsbad in some places that permit classification (An60 to An40). The plagioclase crystals are rounded in shape and are frequently seen surrounded by chlorite and clinozoisite. There is also a spindle texture observed in some samples. Tremolite-actinolite series is dominantly green to colourless, pleochroic with an interference colour of purple and green. They are medium grain sized with

subidiomorphic, poikiloblastic crystals that are aligned in some places. They make up to 50% of the rock and some of those grains are thought to be relicts from pyroxene or amphibole (sometimes, a few high relief small grains seem to be subidiomorphic, poikiloblastic and chloritized pyroxene or hornblende crystals). The clinozoisite-zoisite-epidote group mineral forms idiomorphic to subidiomorphic colourless crystals with a high relief. The interference colours are normally blue anomalous of first order or yellow to green maximum. They commonly surround the plagioclase or are in the middle of amphibole and plagioclase along with chlorite. They make up to 5 to 20% of the rock. Chlorite tends to form a foliation that surrounds plagioclase or amphibole, and is subidiomorphic to xenomorphic. It is normally elongated and sigmoidal, and the grain size ranges from fine to medium-large. Chlorite is colourless although weakly pleochroic from brown to green and its interference colours are first order white to grey. Two groups of chlorite were recognized and make up to 15% of the rock. Titanite and apatite are considered to be accessory phases, and have very fine grain size and occur principally as inclusions in amphibole.

The spindle textures of plagioclase and folded chlorite, which indicate deformation, are not common. Mineral growth resulting from contact-metamorphism and associated fluids Interactions are very extensive and mask the regional metamorphism. Fluids have affected most rocks, but the proportions and assemblage of hydrous secondary minerals that were developed varies from place to place depending upon the previous igneous mineralogy. Development of the

epidote-clinozoisite group minerals is spatially related to plagioclase-rich rocks because of calcium and aluminium, whereas tremolite-actinolite is spatially related to pyroxene and/or amphibole-rich rocks because the magnesium and iron contents were large.

Where the fluid interaction was most extensive, plagioclase is less abundant or absent and tremolite-actinolite (the green, iron rich variety is the most common) is the most abundant mineral (70%). The subidiomorphic to amorphous and in some cases, poikiloblastic tremolite-actinolite replaces pyroxene or amphibole in some places. Where plagioclase remains, it shows albite-carlsbad and pericline twins, with some spindle texture indicating deformation of the crystals, and is sometimes altered. Clinopyroxene is present in some places in low quantities and is colourless, thus hard to classify under the microscope.

The distribution of the contact metamorphism it is not clear. Some samples closer to the contact with the plutons that preserve the regional foliation do not show the same contact related textures seen in the other samples. Possibly, the presence of joints facilitated the transport of fluids and this resulted in a heterogeneous distribution of the contact metamorphism.

The mineral and textural effects due to older ocean floor metamorphism in the BRC rocks are practically impossible to distinguish from the later thermal overprint: the mineral assemblages related to both facies are essentially similar and it is not possible to say which metamorphic paragenesis correspond to a particular rock. The mineralogy seen could be related to both facies. In addition, the Pouchot and

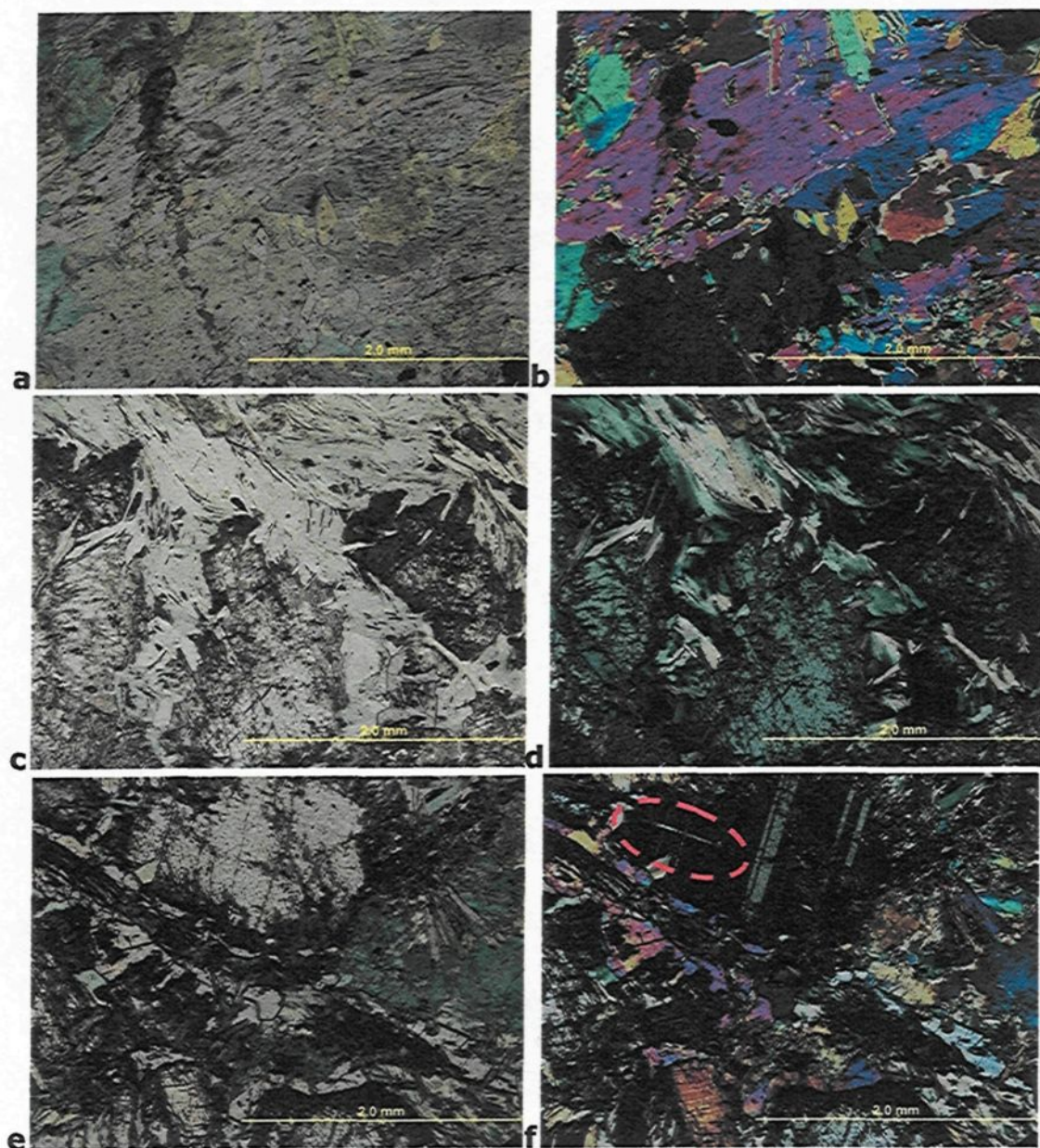


Figure 3.2 Meta-gabbroic samples. a,b) type 1 rock ML-48, Metamorphosed and foliated sample, poikilitic tremolite-actinolite; c,d) type 2 rock ML-46, altered plagioclase surrounded by chlorites e,f) type 2 rock ML-56, Spindle texture in plagioclase, epidote group and abundant in chlorite. Plan polarized light at left and crossed polars at right.

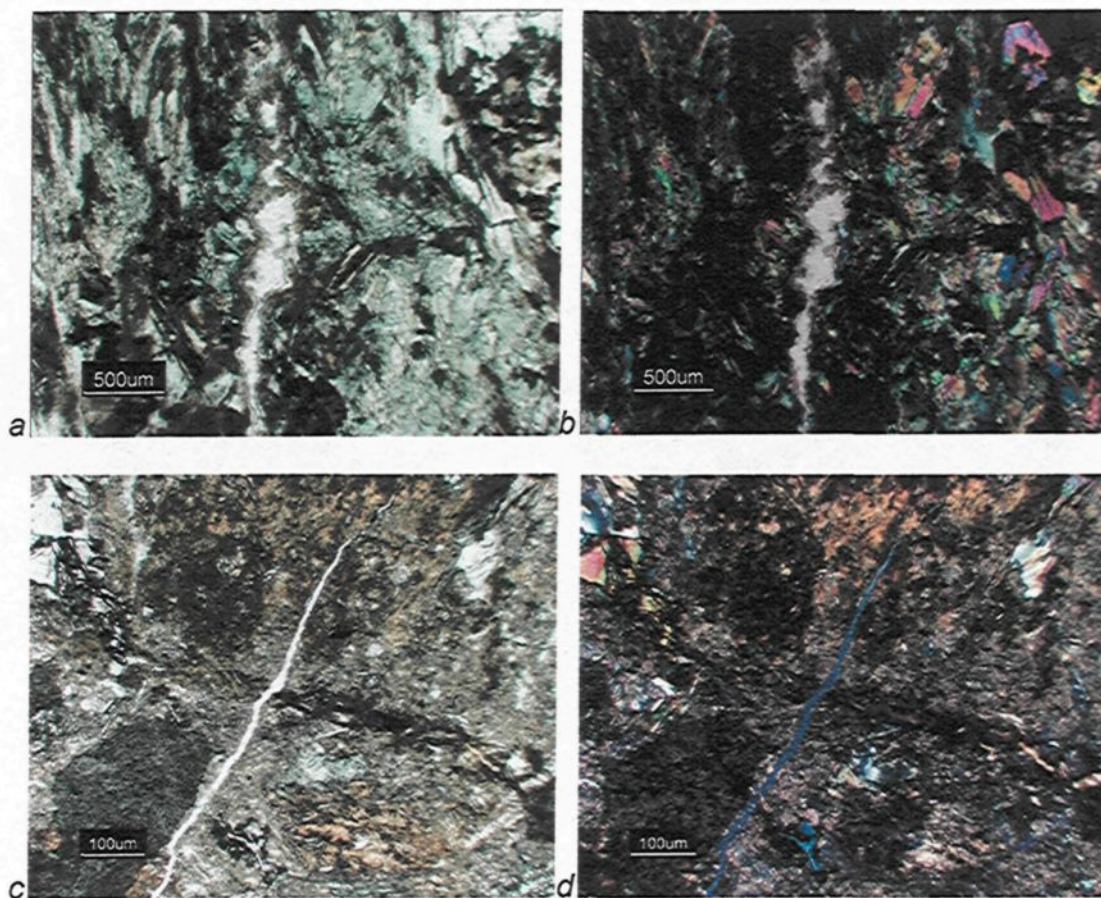


Figure 3.3 a,b)ML-19, calcite vein in the middle crosscutting the rock, surrounded by actinolite and saussuritized plagioclase; a) plane polarized light, b) cross polars; c,d)ML-13, quartz veins cross-cutting the rock, plagioclase very altered abundant in the section and clinzoisite in the upper left corner and in the bottom center.

Galinée anticlines, which have generated the foliation (Goutier, 2005), has most likely obliterated the ocean floor metamorphism.

Type 3 Rocks: Rocks which form part of the layers and have a foliation (inner of the layering of the complex) and have a very little alteration effects, they seem to be more felsic (Figure 3.4). Only two samples (ML-5, ML-26) were considered for detailed petrological and geochemical analysis. These foliated rocks are moderately fresh, equigranular idiomorphic to subidiomorphic and composed of plagioclase, hornblende, quartz, chlorite and biotite. The accessory minerals include zircon, titanite, apatite and sulphides.

ML-5 (Figure 3.4 a,b): Equigranular, fine-grained rock, with a foliation, alignment of hornblende and chlorite. This rock is composed mainly of hornblende and chlorite (~70%) with minor plagioclase (~20%), quartz (~10%) and biotite (~5%) and accessory titanite (~2%). Hornblende is subhedral, elongated, and has irregular grain boundaries. It is pleochroic, forest green to pale green or brownish colours, with interference colours of green, yellow, pink and blue of second order. Hornblende is strongly altered to chlorite. Plagioclase occurs as subhedral, tabular crystals with some elongation, a few display albite and Carlsbad twins. A few grains are altered to saussurite and sericite. Quartz is anhedral with the local formation of subgrains and shows undulated extinction in some grains. Biotite is subhedral, and oriented parallel to the foliation. It is pleochroic, colourless to dark brown, and its interference colours are pink, green to pastel yellow of second order. Titanite forms irregular masses or rounded, dispersed crystals.

In the sample ML-26 (Figure 3.4c,d) the foliation is not so evident as in ML-5. The rock is subidiomorphic and equigranular, relatively fresh and with variable grain size. This rock is composed of plagioclase (~70-80 %), hornblende (~ 15%), chlorite (~ 5%) and quartz (~ 10%). Plagioclase is medium-grained, anhedral with irregular borders and lightly sericitized. It has abundant albite and Carlsbad twins, is commonly zoned and possesses a spindle texture. Hornblende is subidiomorphic to xenomorphic, fine-grained with elongated crystals. It is pleochroic from green to pale green. Hornblende is moderately altered to chlorite. Quartz is present in subhedral to anhedral crystals with irregular contacts or lobate and the formation of subgrains is common. It is fine to medium-grained. This rock contains quartzitic veins that crosscut the sample.

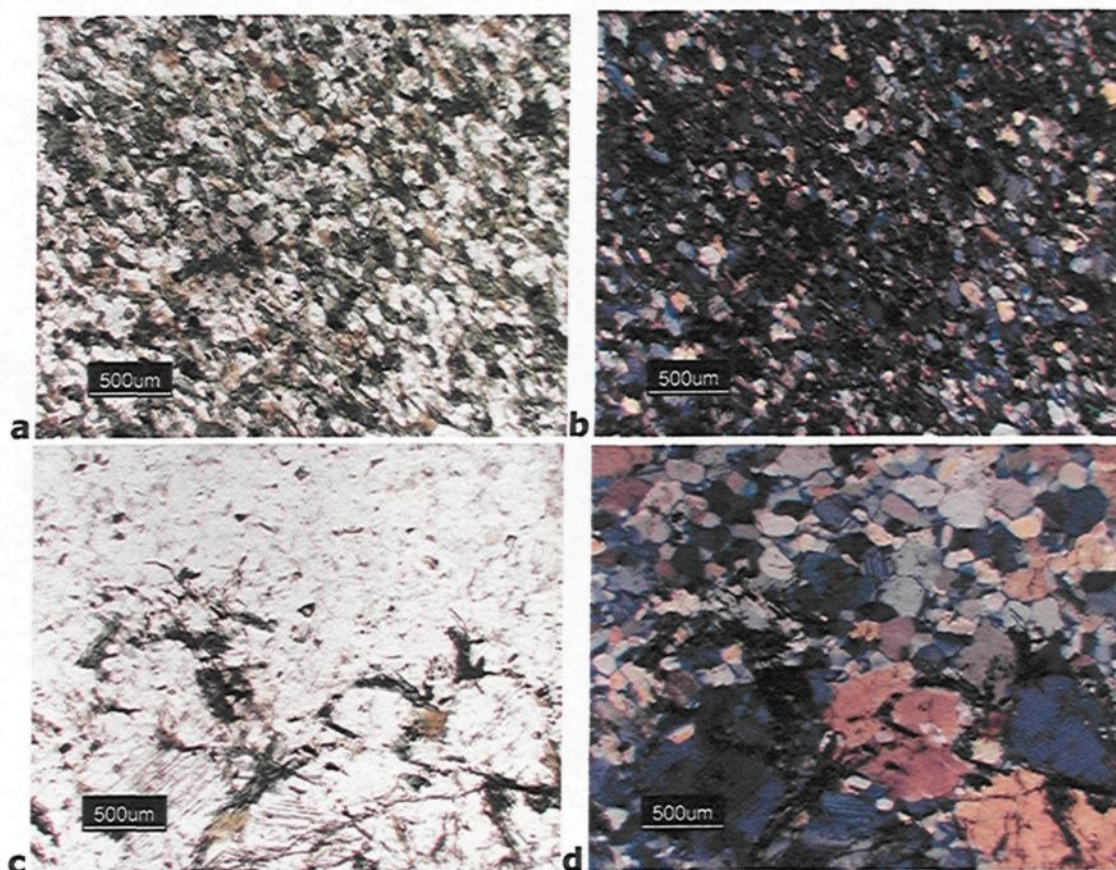


Figure 3.4 Type 3 rocks. a,b) ML-5, foliated sample, part of the layering of the BRC; c,d) ML-26, unfoliated sample but part of the layering of BRC, large plagioclase crystals with spindle texture and subgrain formation on quartz, minor green hornblende.

3.1.2. Granitic rock

This group is represented by rocks that have a more felsic composition and occur as dykes or sills that cross-cut the sequence (see Chapter two and Figure 3.5). Only one sample (ML-52) has been considered for detailed petrological and geochemical analyses. This massive rock is relatively fresh, equigranular idiomorphic to subidiomorphic, with plagioclase, hornblende, quartz, chlorite and biotite. The accessory minerals include zircon, titanite, apatite and sulphides.

Plagioclase is equigranular, subhedral, with a grain size ranging from medium to coarse. It is colourless with an unusual zonation and has abundant albite and pericline twins. There is some alteration to saussurite and sericite. Plagioclase makes up to 70% of the rock. Quartz crystals are subhedral with lobate grain boundaries and makes up to 10 % of the rock. Hornblende is subhedral, equigranular with irregular grain boundaries, fine to medium grained and pleochroic green to brown. Its interference colour is green to brown of second order which are masked by the strong colour of the mineral. In many cases it is altered to chlorite and contains inclusions of zircon and apatite and makes up to 15% of the rock. Chlorite is subhedral to anhedral, has a fine to medium grain size, is forest green, pleochroic to colourless brown, and its birefringence colours are anomalous white-brown to grey. It is seldom anomalous blue of first order. Chlorite makes up to 5% of the rock. Some chlorite is an alteration product of hornblende, and in a few places it preserves the pre-existing amphibole shape. Biotite is subhedral, fine-grain size, pleochroic brown to dark brown. The proportion of biotite in the rock is

less than 3%. The zircon, titanite and apatite are accessory phases in the rock, observed typically as inclusions in hornblende, chlorite or biotite (Figure 3.5).

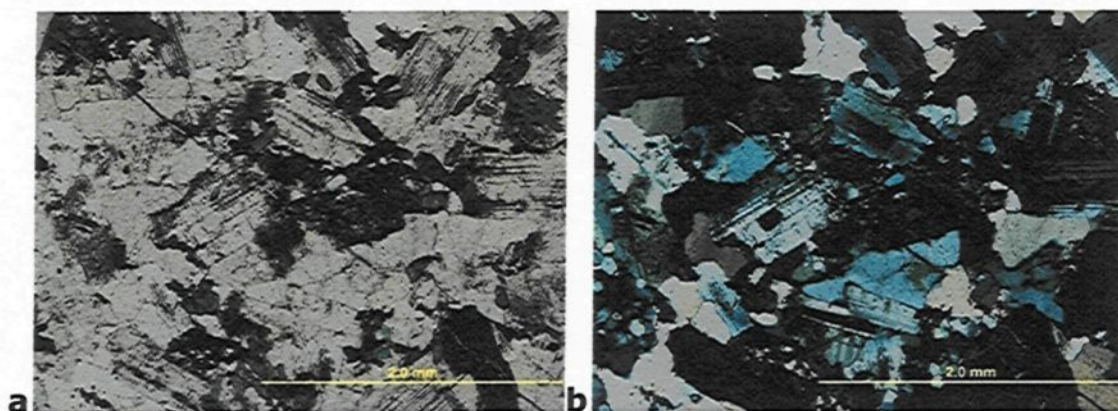


Figure 3.5 Felsic rock ML-52 with a little alteration, plagioclase, chlorite, biotite, quartz and minor hornblende. a) plane polarized light, b) cross polars.

3.2. Sulphide assemblage

Sulphide minerals occur in both the metagabbro and the felsic rocks. Two sulphide assemblages are present (Figure 3.6); one consists of pyrrhotite pentlandite and minor chalcopyrite which is thought to be magmatic; and the other is characterised by the presence of pyrite and chalcopyrite which is thought hydrothermal. Transitory assemblages from magmatic to hydrothermal are common and they consist of a mixture of both magmatic and hydrothermal sulphides (pyrrhotite, pentlandite, chalcopyrite and pyrite).

The magmatic group (Figure 3.6 a,b) contains pyrrhotite as the dominant mineral. It is brown to grey, the form is irregular to rounded, and is frequently associated with intergrowths of pentlandite. Pentlandite is pink-brown, anhedral or subhedral in some places, massive to rounded, and intergrown with pyrrhotite. Chalcopyrite is yellow to orange in colour, subhedral and in some places anhedral. In this group the average amount of sulphides is around 1 or 2% of the whole rock. The samples that contain this paragenesis are ML-6, ML-11, ML-26, ML-30, ML-40, ML-53 and ML-54.

The hydrothermal group (Figure 3.6 c,d) consists of sulphides that were either initially magmatic and altered by fluids along veins which are clearly visible in hand specimens and cross-cut the rock in random directions and masses of euhedral minerals disrupting the rock. Pyrite is bright yellow subidiomorphic, semi-rounded or semi-cubic with a few cracks. Chalcopyrite is orange-yellow, amorphous, and is

not cracked. It also has irregular grain boundaries. The samples that contain this paragenesis are ML-5, ML-7, ML-14, ML-62, and ML-65.

The most common paragenesis consists of an assemblage characterized by the presence of magmatic sulphides mixed with the hydrothermal sulphides (Figure 3.6 e,f). This transitional group consist of the presence of both mineral assemblages. The textural characteristics are similar to the hydrothermal group. Pyrite is bright yellow, anhedral in stringer grains aligned in some cases in the foliation or subidiomorphic and semi-cubic. Chalcopyrite is yellow to orange, subhedral to irregular. Pyrrhotite is brown to grey, forms small grains, sub-rounded to irregular in shape, generally into chalcopyrite. Pentlandite is pink-brown, normally found with chalcopyrite or pyrrhotite, is semi-rounded and in some places has chalcopyrite inclusions (Figure 3.6).

The rocks that have the magmatic sulphide assemblage correspond to sulphides that have been preserved and formed from the BRC magma. The hydrothermal sulphides are thought to be transported by veins over the complex that could be due to the interaction of the fluids of the Lac Olga or Opaoca intrusions. The transitional group correspond to the interaction of the magmatic sulphides already there that were altered by the fluids. Both sulphides were mixed by fluids and deposited together.

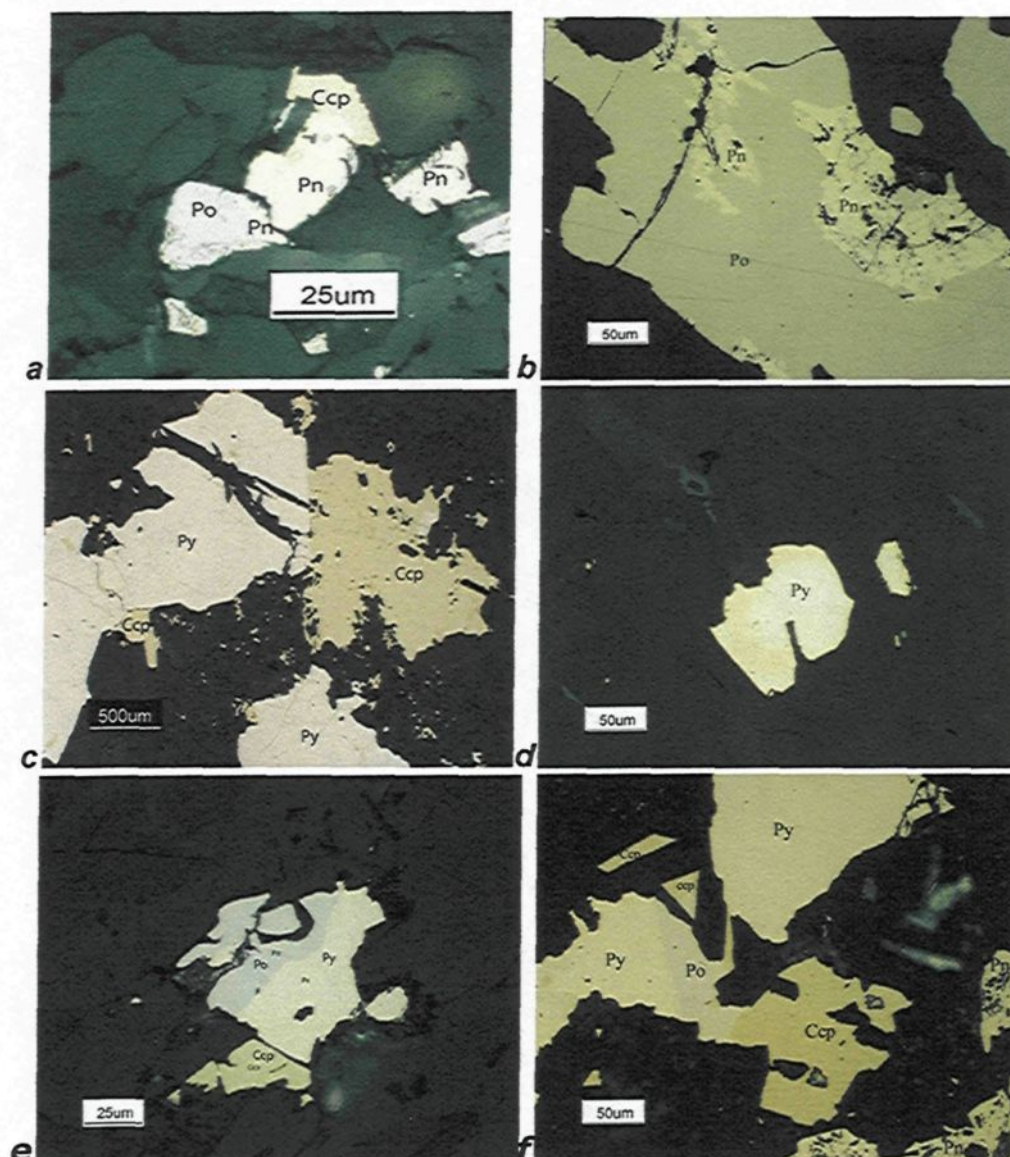


Figure 3.6 Sulphide assemblages. a) Magmatic assemblage of pentlandite, pyrrhotite and chalcopyrite, sample ML-30; b) Pyrrhotite and minor pentlandite in the magmatic assemblage, ML-54; c) ML-51 the most S rich sample, pyrite and chalcopyrite are the most abundant mineral phases, irregular shape, normally founded together, hydrothermal assemblage; d) ML-5, pyrite in the hydrothermal assemblage; e) pyrite, pyrrhotite and pentlandite from transitional the magmatic to hydrothermal sulphides, ML-30; f) ML-46, transitional magmatic to hydrothermal sulphides Py, Ccp, Po and Pn. Abbreviations: Pn: pentlandite, Po: pyrrhotite, Ccp: chalcopyrite, Py: Pyrite

3.3. Platinum Group Minerals (PGM)

Seven samples with the highest whole rock PGE values (ML-21, ML30, ML-35, ML-7, ML-46, ML-17 and ML-65) were selected to be investigated for platinum group minerals (PGM). All of these samples are sulphide-poor gabbro-norites, leucogabbro-norites and one leucogabbro. The sulphide-rich samples are poor in PGE (see Chapter 4). The PGM were detected using the scanning electron microscope (SEM) at *Laboratoire de Microanalyse Université Laval* using an accelerating voltage of 15KeV. The PGM were located by using the SEM in backscattered electron mode and conducting systematic transverse sections across the polished sections. The high atomic number of the PGM leads to a strong contrast with the silicate and sulphide minerals thus they can be readily located. The elements present in the PGM were identified using Energy Dispersive X-ray Spectroscopy (EDS). The results are shown in Tables 3.1 and 3.2, Figure 3.7 and appendix 10.

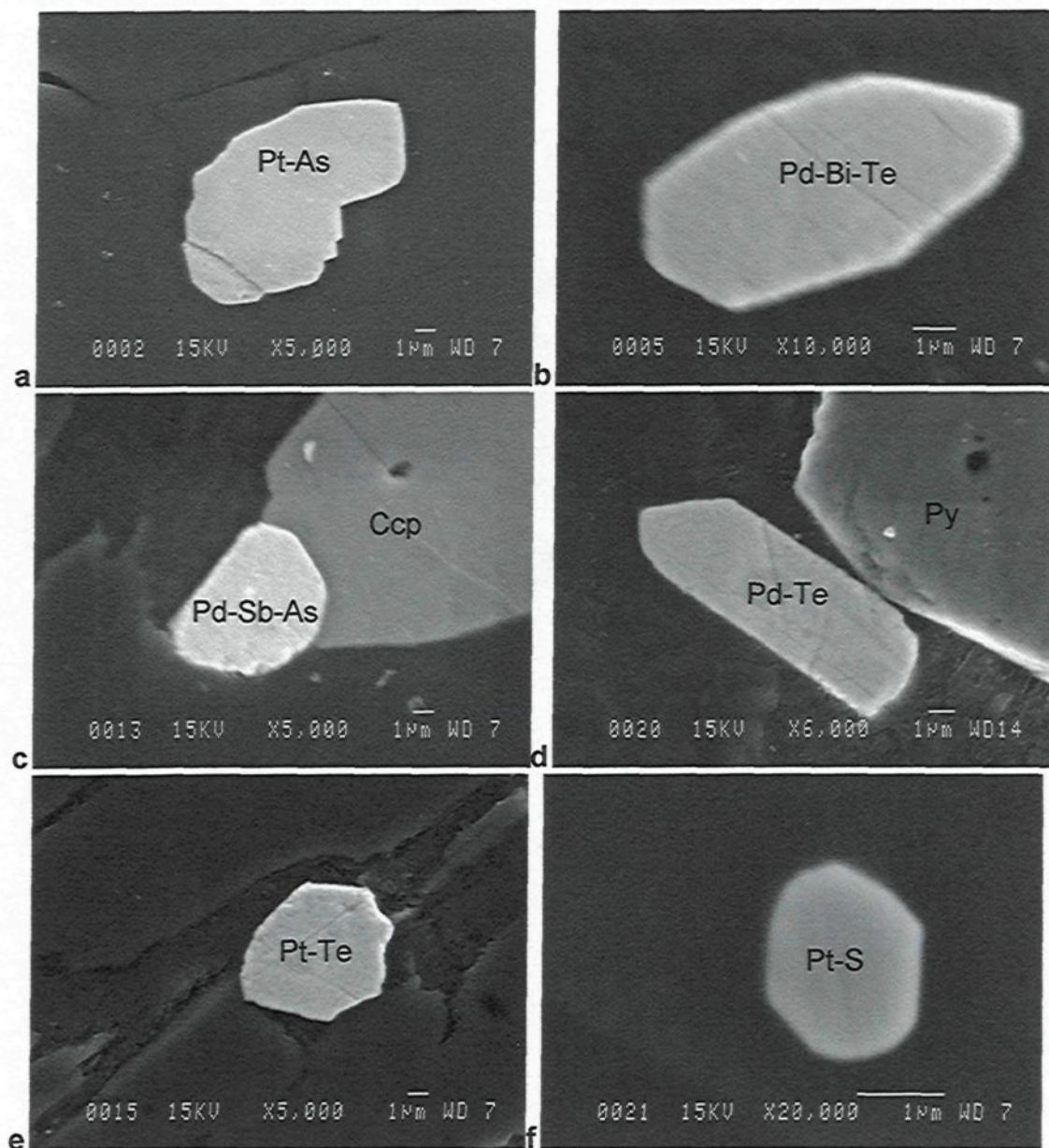


Figure 3.7 PGM pictures. a) Sample ML-21, Pt-As mineral; b) ML-30 Pd-Bi-Te; c) ML-35 Pd-Sb-As, Chalcopyrite grain upper right side, one of the two samples associated with sulphides; d) ML-46 Pd-Te, pyrite grain to the right side; e) ML-7, Pt-Te; f) ML-17, Pt-S. The host minerals on the pictures are silicates.

Table 3.1 Characterization of grains of Platinum-Group Minerals detected with the Scanning Electron Microscope

Sample	Present Elements (quantitative)	Possible Phases	Names of the Possible Phases	Size μm	Photo (Appendix)	Phase Associated	Host Rock	Unit/ Layer Number
ML-21	As,Pt	PtAs ₂	Sperrylite	10x5	2	silicate	Olivine gabbronorite	out of profile
ML-30	Te,Pt,Bi,Pd		n.i	8x3	3	silicate	Olivine - gabbronorite	out of profile
	Pd,Bi,Te	PdBiTe	Michenerite	5x3	4	silicate		
	Pd,Bi,Te	PdBiTe	Michenerite	7x4	5	silicate		
	Pd,Bi,Te	PdBiTe	Michenerite	4x3	6	silicate		
	Sn	Sn	tin	4x3	7	silicate		
ML-35	As,Pt	PtAs ₂	Sperrylite	5x5	8	silicate	Olivine - gabbronorite	9
	Pd,As	Pd ₈ As ₃	Stillwaterite	4x2	9	silicate		
	Pd,Sb	PdSb	Sudburyite	4x2	10	silicate		
	Pd,Sb,As	Pd ₁₁ (Sb,As) ₄ ; Pd ₈ (Sb,As) ₃	Mertieite I; II	4x3	11	silicate		
	Pd,Sb,As	Pd ₁₁ (Sb,As) ₄ ; Pd ₈ (Sb,As) ₃	Mertieite I; II	5x2	12	Ccp		
	Pd,Sb,As	Pd ₁₁ (Sb,As) ₄ ; Pd ₈ (Sb,As) ₃	Mertieite I; II	6x4	13	Ccp		
	Pd,As,Sb	Pd ₁₁ (Sb,As) ₄ ; Pd ₈ (Sb,As) ₃	Mertieite I; II	4x3	14	silicate		
ML-7	Pt,Te	PtTe ₂	Moncheite	7x5	15	silicate	Leuco- gabbronorite	9
	As,Pt	PtAs ₂	Sperrylite	4x2	16	silicate		
	Pd,Te,Bi	PdBiTe	Michenerite	11x7	17	silicate		
	Pd,Bi,Te	PdBiTe	Michenerite	5x3	18	silicate		
ML-46	Te,Pd,(Au)	PdTe ₂	Merenskyite	12x1	19	silicate	Olivine - gabbronorite	5
	Te,Pd,(Au)	PdTe ₂	Merenskyite	3x1	19	silicate		
	Te,Pd (Ir?)	PdTe ₂	Merenskyite	10x4	20	silicate		
ML-17	Pt,S	PtS	Cooperite	2x2	21	silicate	Olivine- gabbronorite	9
	Bi	Bi	Bismuth	5x3	22	silicate		
	As,Pt	PtAs ₂	Sperrylite	3x2	23	silicate		
ML-65	Pd,Sb	PdSb	Sudburyite	6x4	24	silicate	Leuco- troctolite	10
	Pd,Sb,As	Pd ₁₁ (Sb,As) ₄ ; Pd ₈ (Sb,As) ₃	Mertieite	4x3	25	silicate		

Table 3.2 Statistical Results of PGM grains

Possible PGM	Tentative Chemical Composition	Number Of Grains	Average Size (μm^2)
Michenerite	PdBiTe	5	29.4
Mertieite	$\text{Pd}_{11}(\text{Sb,As})_4$; $\text{Pd}_8(\text{Sb,As})_3$	5	14.0
Sperrylite	PtAs_2	4	22.3
Merenskyite	PdTe_2	3	18.3
Sudburyite	PdSb	2	16.0
Moncheite	PtTe_2	1	35.0
Not identified	Te, Pt, Bi, Pd	1	24.0
Bismuth	Bi	1	15.0
Tin	Sn	1	12.0
Stillwaterite	Pd_8As_3	1	8.0
Cooperite	PtS	1	4.0

A total of 25 grains with a high mean atomic number were recognized. Two of these were not PGE-bearing. For the PGM, Pd minerals are the most common in terms of the number of grains (Table 3.2). However, in terms of area Pd and Pt minerals are approximately equally abundant. The Pd minerals are predominantly bismuth-tellurides (Michenerite) and antimony-arsenides (Mertieite) (Figure 3.5). The dominant Pt mineral is an arsenide (sperrylite, PtAs_2). The PGM are normally associated with silicates. Only two grains were encountered in association with sulphides; both were grains of mertieite with chalcopyrite in sample ML-35. No PGM containing Os, Ru, Ir or Rh were found.

CHAPTER 4

GEOCHEMISTRY

4.1. Analytical Methods

4.1.1 Whole Rock Major and Trace Element Methods

Samples were cut, crushed and powdered in the University of Quebec in Chicoutimi (UQAC) laboratories using a carborundum blade saw, a steel jaw crusher and a W-Carbide shatter box.

The analyses of major elements were done at Geoscience Laboratories located in Sudbury (Ontario) by X-ray fluorescence (XRF). The samples were first run for loss for ignition (LOI) and then fused with a borate flux to produce a glass bead.

Trace elements were analyzed at Geoscience Laboratories by Inductively Coupled Plasma-Mass Spectrometry (ICP-MS) using a closed vessel multi-acid digestion.

4.1.2 Whole Rock Nickel, Copper, Sulphur and PGE-Au Analyses

Ni, Cu, S, PGE and Au contents in the whole rock were determined at *LabMater* at the UQAC. Ni and Cu were determined by atomic absorption spectrometry (AAS), 1 gram of each sample was dissolved in aqua regia solution; certified reference materials (CRM) run every ten analyses.

Sulphur analyses, were obtained by infrared light absorption (EMIA-220V of *HORIBA*, furnace method). The 0.5 grams of sample were mixed with accelerators (Fe, Sn, W) and put into a porcelain crucible which was heated in the induction furnace. Blank samples were run every ten analyses (details of the method are given in Bédard et al., 2008).

PGE were collected by Ni-S fire-assay followed by Te coprecipitation from 15 grams of sample. The solutions were then analyzed by ICP-MS (details in Savard et al., accepted).

4.2 Major elements

The values for the major elements (given in a weight percent wt. %) are listed in Appendix 2. Four groups of rocks were defined based on CIPW norm and PGE content. The blue diamonds in the diagrams correspond to olivine gabbros. The red squares correspond to pyroxene-rich rocks which are sulphur-rich and PGE-poor. The purple xs correspond to PGE rich rocks, which are olivine gabbros, and the green triangle corresponds to the felsic rock (ML-52) from a dyke.

The Harker (1909) diagrams in Figure 4.1 show the variation of major element oxides with respect to SiO₂. Silica content varies from 42.7 wt. % to 55.7 wt. %, except for sample ML-52 which corresponds to a felsic dyke with 67.7 wt. % SiO₂. Aluminium values generally vary from 14.0 wt. % to 30.0 wt. %, but some samples with very low aluminium content below 10 wt. %. Titanium varies from 0.05 wt. % to 0.61 wt. %, magnesium varies from 1.04 wt. % to 20.69 wt. %, and calcium varies

from 4.59 wt. % to 17.89 wt. %. The total FeO varies from 1.66 wt. % to 14.92 wt. %, sodium varies from 0.17 wt. % to 6.32 wt. % with a very tight alignment on the diagram. Manganese varies from 0.03 wt % to 0.31 wt % with samples slightly aligned until 0.20 wt %, while potassium varies from 0.01 wt % to 2.90 wt % and is widely distributed.

The major elements such as K, Ca, and Fe could be mobile during regional (at greenschist, amphibolite facies) or contact metamorphism, due to the injection of fluids and alteration. Ca, K and Fe were probably moved due to the reaction of plagioclase, pyroxene (hypersthene) and amphibole to form tremolite-actinolite (Fe rich is the most abundant) and epidote-zoisite. The potassium is highest in the muscovite bearing samples (Appendix 8).

In these diagrams, three magmatic series are recognized. The first and most important is represented by the olivine gabbros (blue diamonds). For this series SiO_2 shows a positive correlation with Al_2O_3 , CaO and Na_2O (Figure 4.1), a negative correlation with FeO_T , MnO and MgO and no correlation with K_2O and TiO_2 . These trends represent the processes of fractional crystallization and reflect the evolution of the magma. The samples evolved from the most mafic (olivine gabbro) to the more felsic, leucogabbro. The second magmatic series is represented by the pyroxene rich rocks (the samples in red squares ML-11, ML-14, ML-48, ML-49, ML-50, ML-53 and ML-54). This group does not follow the tendency defined by the first group and is generally richer in ferro magnesian component

for a given SiO_2 value. It is clearly not genetically related to the other group. Many of these samples contain hydrothermal sulphides as identified in the petrology chapter. The third group (felsic rock) is represented by just one sample and is entirely different from the other groups. This sample comes from one of the felsic dykes. A detailed study of these dykes is outside of the scope of this project.

The Ebay samples of the Bell River Complex have a tholeiitic composition. As it is seen on the classification diagrams of Irvine and Baragar (1971) (Figure 4.2), overall the rocks plot in the sub-alkaline field in the SiO_2 versus $\text{Na}_2\text{O}+\text{K}_2\text{O}$ diagram (Figure 4.2a), and in the tholeiitic field on the AFM diagram (Figure 4.2b).

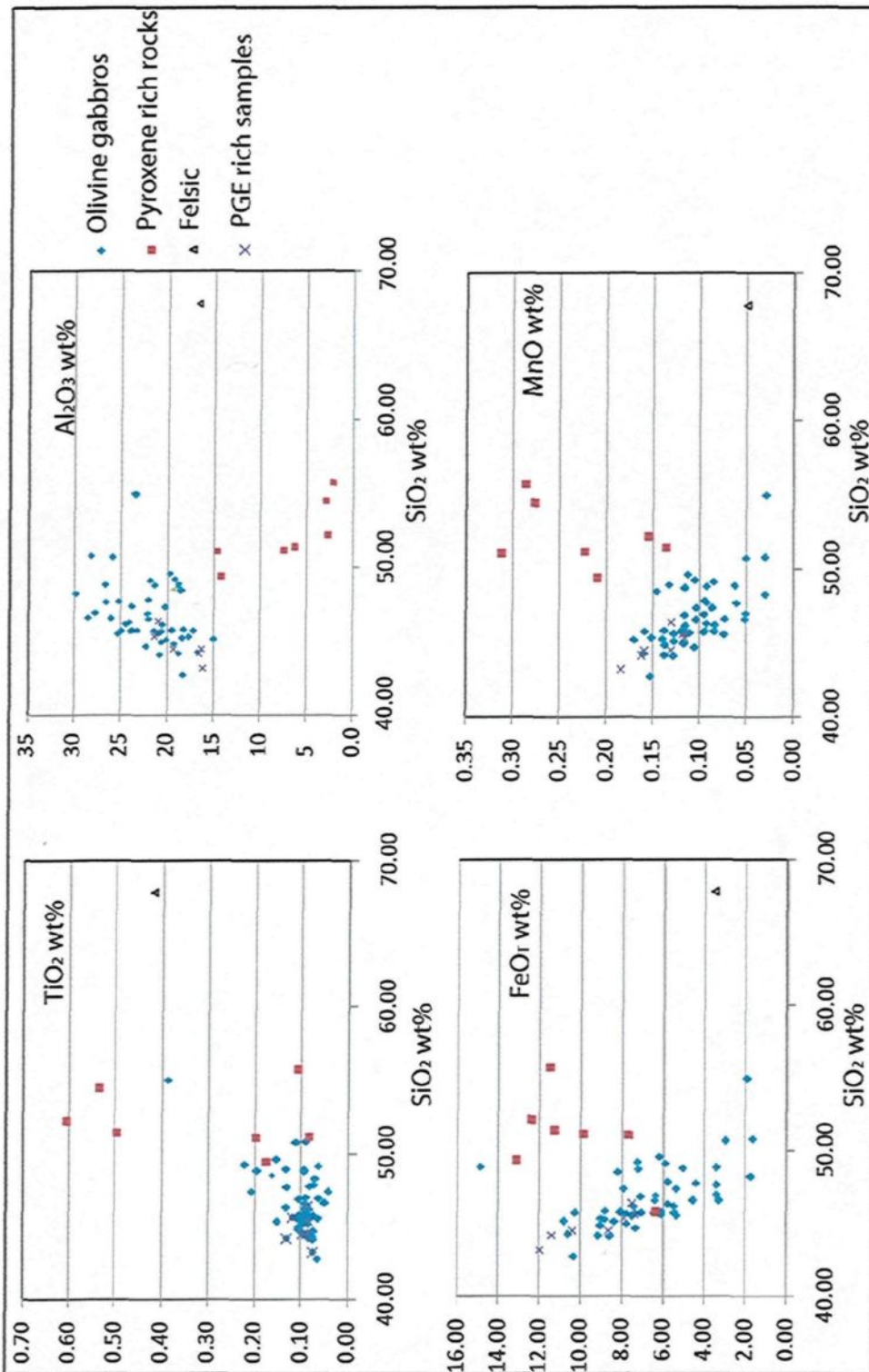


Figure 4.1 Major elements plotted on Harker diagrams (Harker, 1909) after corrections for LOI and sulfur.

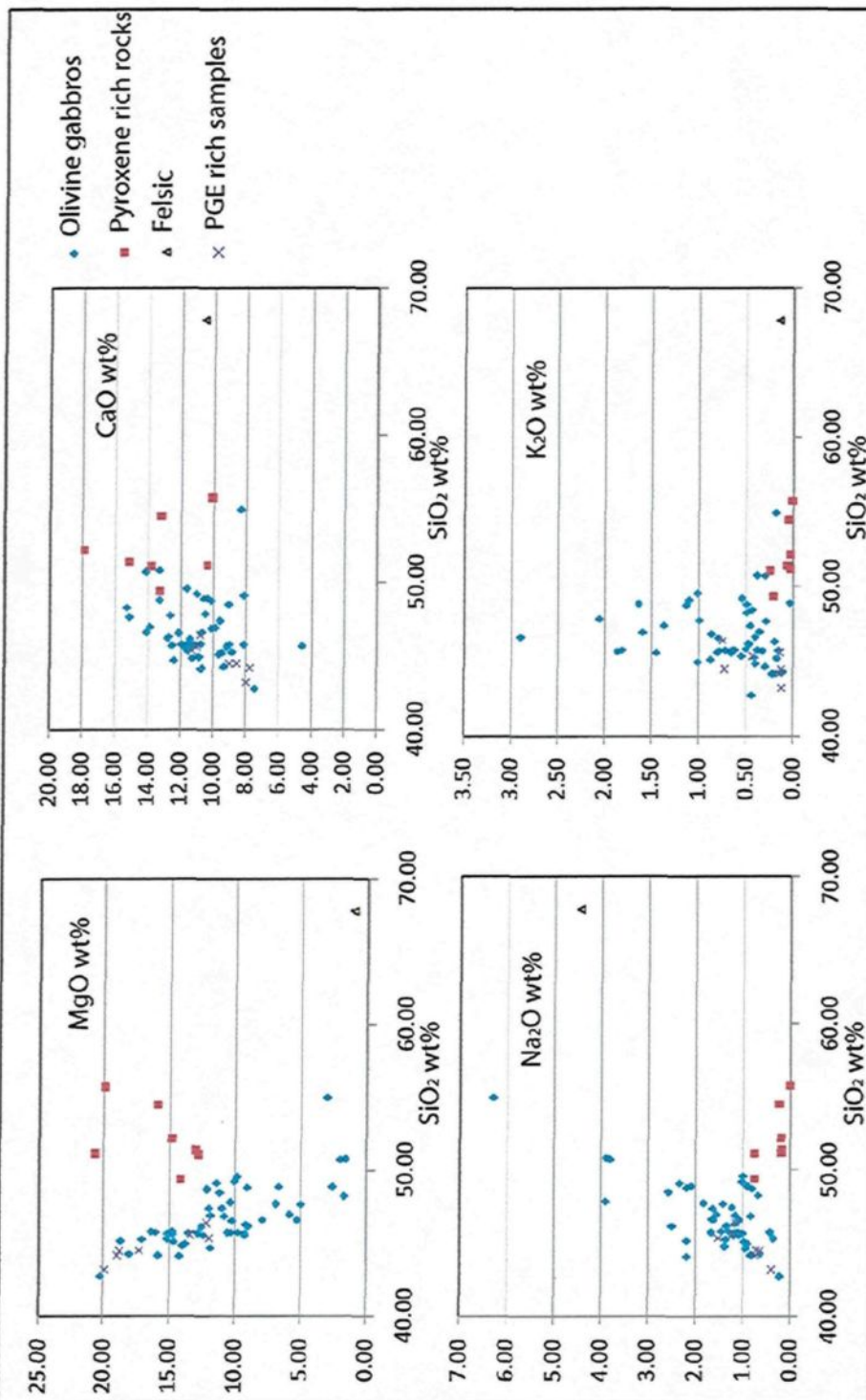


Figure 4.2 Major elements plotted on Harker diagrams (Harker, 1909) after corrections for LOI and sulfur. In blue diamonds are the olivine gabbros (first magma series), red squares are the pyroxene rich rocks (second magma series), the green triangle is the felsic (third magma series) and the purple x are the PGE rich samples (they belong to first magma series).

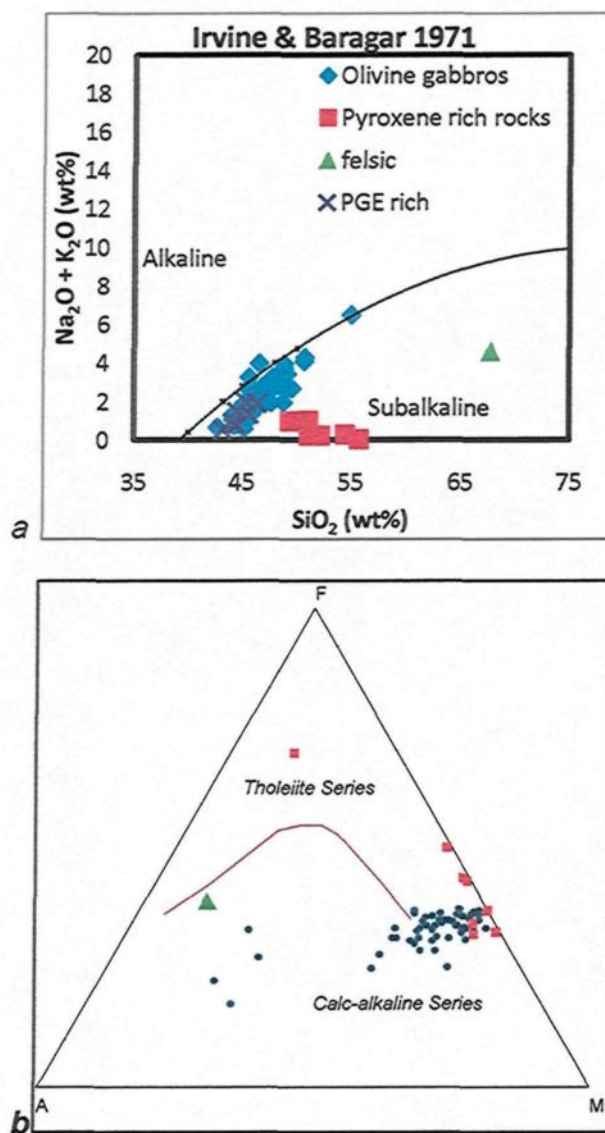


Figure 4.3 a) diagram of alkali versus silica and b) AFM of Irvine and Baragar (1971); blue diamonds are the olivine gabbros (first magma series), red squares are the pyroxene rich rocks (second magma series), green triangle is the felsic rock ML-52 and the purple x are the PGE rich samples.

4.2.1. CIPW Norm and Rock Classification

The original rock type is not clear due to the effects of metamorphism. Therefore the whole rock analyses have been used to calculate a CIPW norm with the aim of deducing the original rock types. A $\text{FeO}/(\text{FeO}+\text{Fe}_2\text{O}_3)$ ratio of 0.8 was used. The results of the calculation are reported in appendix 9.

The rocks were classified using Streckeisen (1976) diagrams based upon CIPW norm calculations. The CIPW norm was calculated using Minpet software and drawn on plagioclase (albite+ anorthite), pyroxene (hypersthene+diopside) and olivine ternary diagrams for gabbroic rocks (Figure. 4.3a), and on quartz, alkalis and plagioclase (QAP) for felsic rocks (Figure 4.3b).

The pyroxene rich rocks plot in the melagabbroite, gabbroite, olivine gabbroite and plagioclase bearing pyroxenite fields. Several of these rocks do not contain normative olivine. The remaining gabbroic rocks are basically olivine bearing gabbros and are classified as olivine-gabbroites and leucogabbroites in IUGS classification (Figure 4.3a). There are also a few leucotroctolites, leuconorites and anorthosites (Figure 4.3a). The felsic sample plot in the tonalite field (Figure 4.3b).

Because of the mobilization of the elements during metamorphism, rock classification using figure 4.3 should be considered with caution. However, an exception is the felsic sample which shows very little petrographic evidence of alteration, no metamorphism and in terms of mineral assemblage and microstructure the rock is well preserved.

In the protoliths of the Ebay zone the most common phase present is plagioclase with the vast majority of the rocks containing greater than 50 % plagioclase. Olivine is the next most commonly occurring phase with clinopyroxene and orthopyroxene occurring in slightly lower abundance in most cases. The presence of leucocratic gabbros as a part of the layering implies differentiation of the rocks of the complex. The second magma series (pyroxene rich rocks) are commonly more mafic gabbros, ranging from olivine-gabbronorite to gabbronorite, melagabbronorite and plagioclase bearing pyroxenite. They contain more pyroxene and less olivine.

Because olivine and plagioclase appear to be the most important phases present, Al_2O_3 versus MgO has been plotted (Figure 4.4). The Al_2O_3 has been plotted to consider plagioclase control and MgO to consider olivine or pyroxene control. On this plot it can be seen that the olivine bearing gabbros plot along a plagioclase-olivine tie line, while the second magma series plots along a plagioclase clinopyroxene or orthopyroxene tie lines. A few of the olivine gabbros show a pyroxene control as well and these correspond to leuconorites or leucogabbronorites with a major proportion of pyroxene over olivine (Figure 4.3. and 4.4a). On the plot of SiO_2 versus Al_2O_3 , similar relationships can be observed (Figure 4.4b).

On Figure 4.4 it is seen that in both plots, the second magma series shows a control of clinopyroxene.

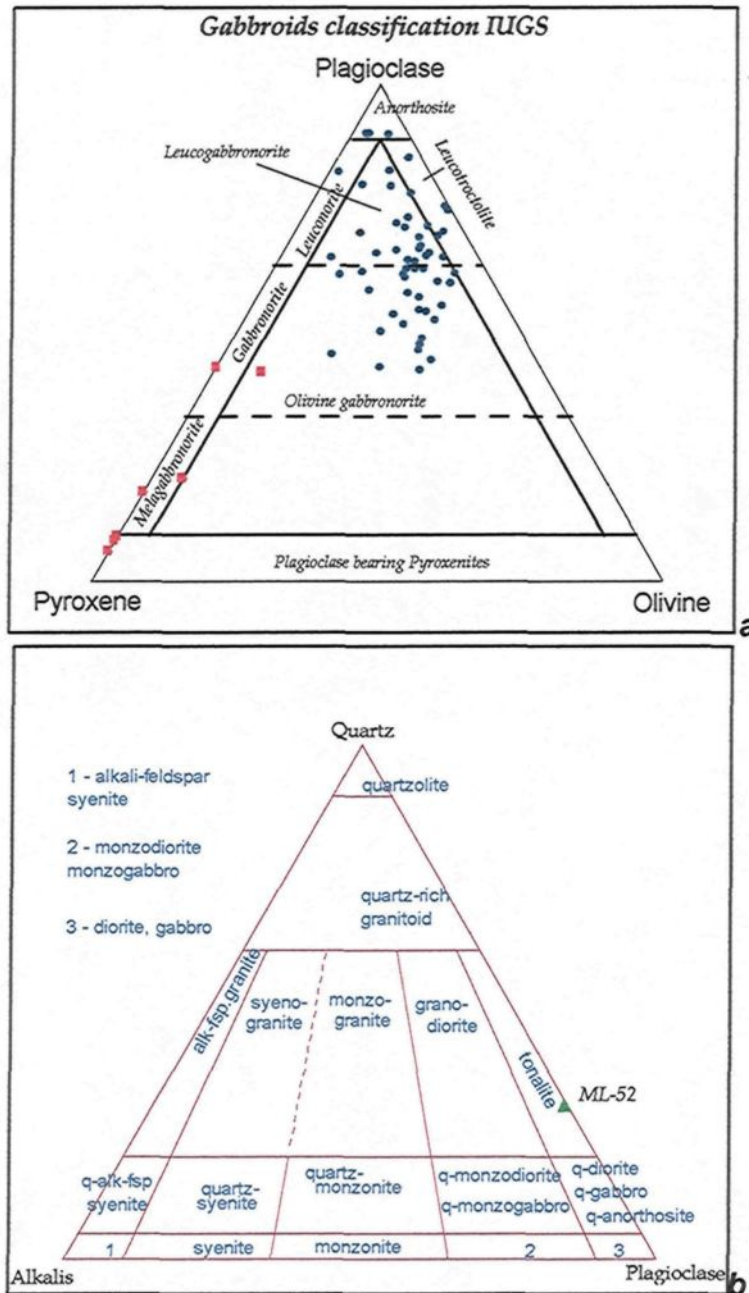


Figure 4.4 a) plagioclase, pyroxene and olivine diagram of Streckeisen (1979), for gabbroic samples. The blue diamonds represent the first magma series (olivine gabbros) and the red squares represent the second magma series (pyroxene rich rocks). b) QAP diagram of Streckeisen (1976) for felsic sample ML-52. ML-52 corresponds to a dyke from a later intrusion.

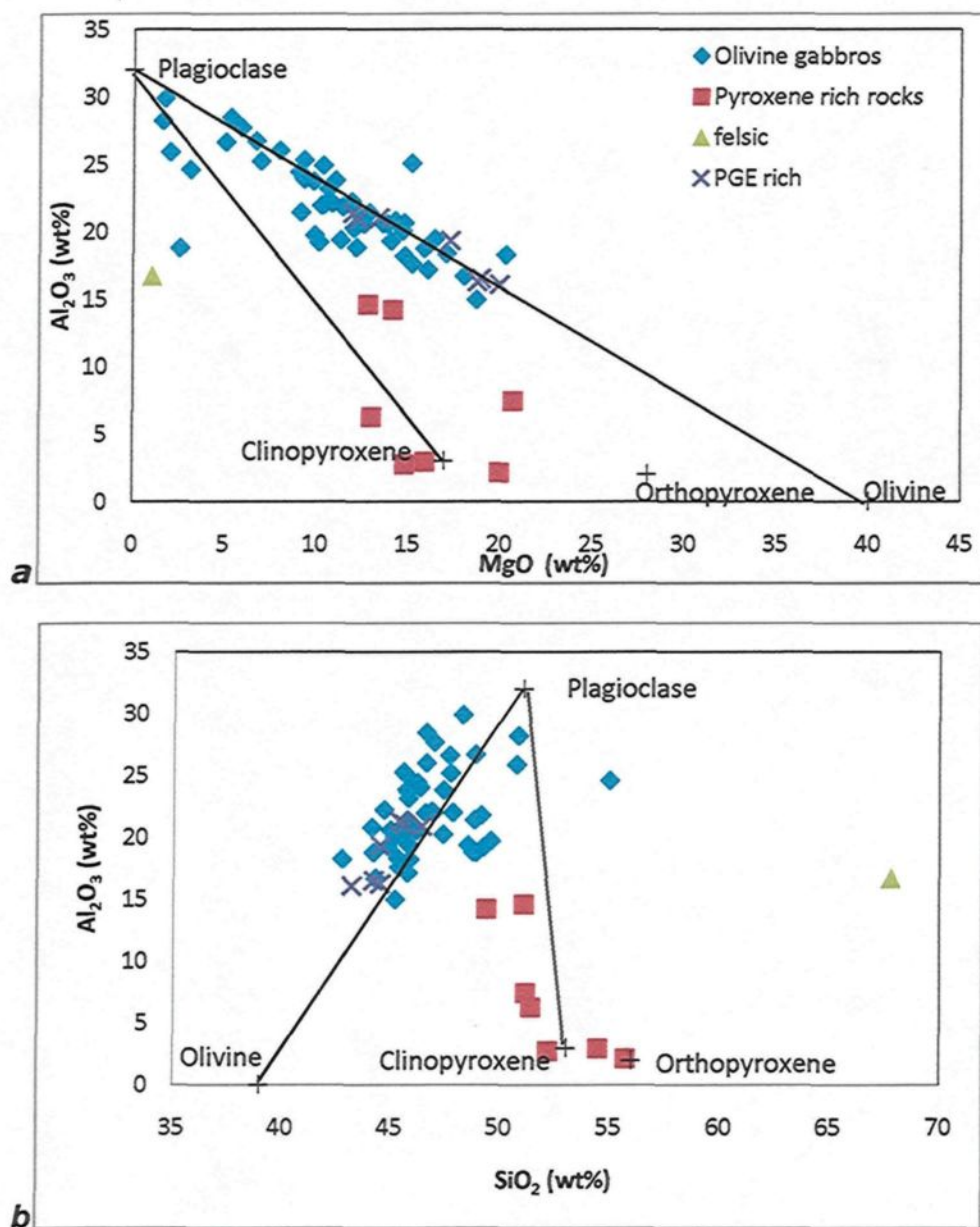


Figure 4. 5 MgO versus Al_2O_3 and SiO_2 versus Al_2O_3

4.3. Trace elements

The whole rock trace element analyses are given in Appendix 3. Figure 4.5 shows a multi-element diagram for the Ebay samples normalized to primitive mantle (Sun & McDonough, 1989). The samples have a semi-flat or flat pattern, for the high field strength elements with strong positive anomalies in K, Pb, Sr and less pronounced one for Eu.

The multi-element diagram shows a differentiated pattern for the rocks relative to its source (the primitive mantle), which is similar to the patterns characteristic of volcanic arc rocks. The pyroxene rich rocks have flat patterns, except for enrichment in Cs and Rb (Figure 4.5e). These patterns are influenced by the chemistry of the minerals due to the selective processes in the magmatic chamber where an elevated concentration of pyroxenes or plagioclase influence the shape of patterns (Figure 4.5). In the olivine gabbros the anomalies for K, Eu, Pb and Sr could be associated with the presence of abundant plagioclase. They become larger as the plagioclase content in the rocks increases (Figure 4.5b,c,d).

From the multi-element diagram (Figure 4.5), the enrichment in LREE and depletion in HREE from less to more differentiated are in the order: pyroxene rich rocks, olivine gabbros and felsics.

The Cs and Rb enrichment present in all of the rocks is thought to be influenced by the presence of fluids and the mobile behavior of the elements during

metamorphism. The LREE may also be disturbed during metamorphism and they become more enriched and compatible as the rock differentiates.

The ratio of La to Sm indicates the degree of enrichment of LREE for the different group of samples. In Figure 4.6 the pyroxene rich rocks are below the linear trend of the olivine gabbros and show a depletion of La with respect to the olivine gabbro trend. The difference could be due to the presence of cumulate clinopyroxene in the pyroxene rich rocks.

In addition, the diagram of Sm versus La (Figure 4.6) could be used as a measure of mobility of the elements and alteration of the samples. There is a positive correlation between the elements Sm and La. However, if we look at the blue diamonds (the olivine gabbros), the samples are slightly dispersed, which could indicate a relative alteration of the samples that could be related to different processes. In general, the most enriched samples in La are the most dispersed. This implies that these samples are the most affected by the different phenomena considering that they represent the last stages of crystallization of the BRC. In particular, the pyroxene rich rocks show a very tight alignment except for two samples. This shows that this magma is less evolved. Note the usefulness of this diagram and the small hydrothermal effect on these elements.

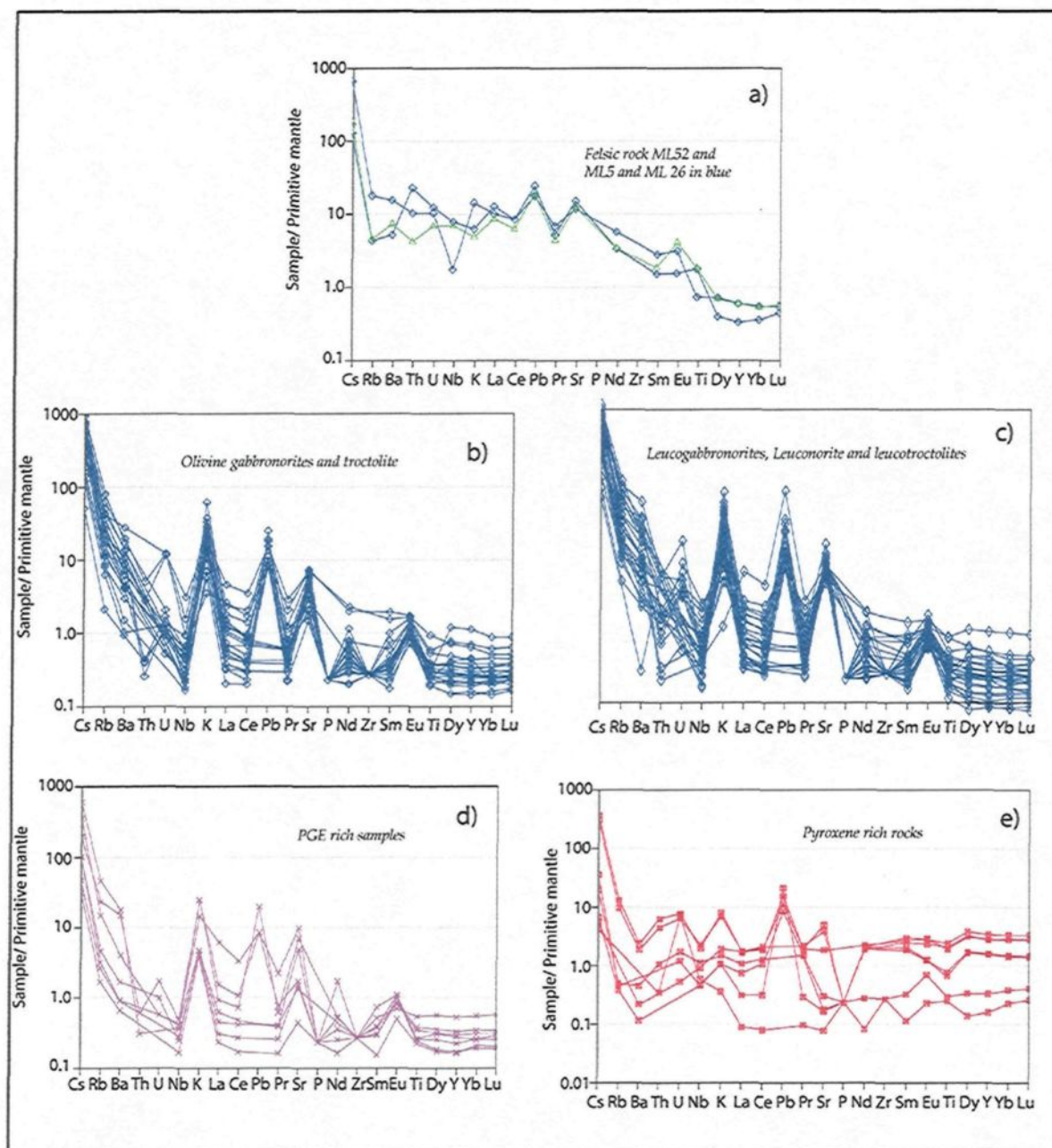


Figure 4.6 Multi-element spider diagrams for Ebay samples, normalized to the primitive mantle (Sun and McDonough, 1989) after CIPW.

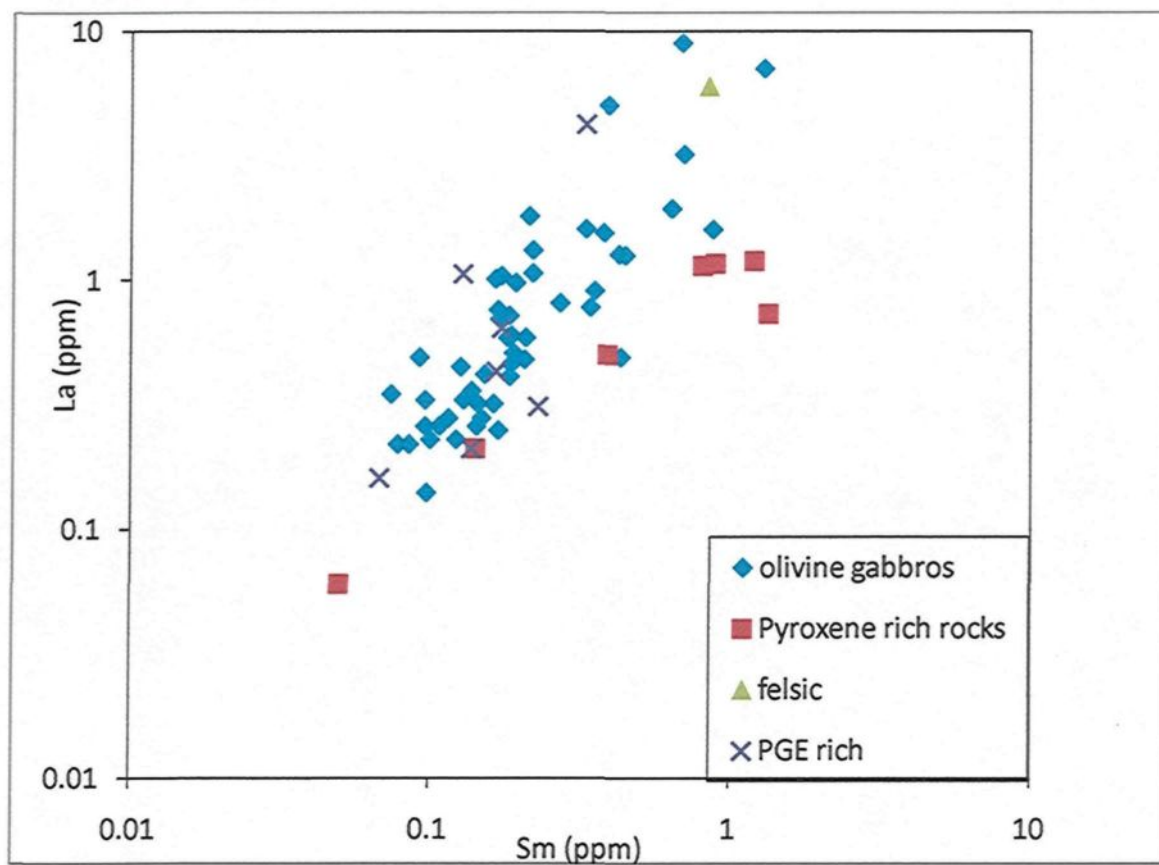


Figure 4.7 Sm versus La diagram showing that pyroxene rich rocks have a lower La/Sm ratio than the olivine gabbros

4.4. Sulphur, Ni-Cu & PGE-Au geochemistry

For many samples, the magmatic sulphide assemblage is still preserved as observed in many of the olivine gabbros (Figures 4.8 and 4.9); whereas for some of the olivine gabbros and all the pyroxene rich rocks, the magmatic sulphides were altered and formed the new assemblage that include the formation of pyrite from pyrrhotite and/or pentlandite. This implies that sulphur was mobile in some places.

Table 4.1 gives the values for S, Ni, Cu, Au and PGE (Os, Ir, Ru, Rh, Pt, Pd). Plots of these elements with depth (values after the height above mean sea level) are illustrated in Figure 4.7. The highest PGE values are for Pt and Pd which reach the 1170 and 845 ppb respectively, found within sample ML-21 at 111 meters depth [194 meters above sea level (masl)]. The next highest of Pd values are 804 ppb and 744 ppb and the next highest value for Pt is 471 ppb. Most of the samples vary from 1 ppb to 500 ppb in Pt+Pd. For other PGE however, concentrations do not exceed 300 ppb. Many of them are below 10 ppb including gold.

For the pyroxene rich rocks, sulphur varies from 0.11 to 4.17 wt. %, the PGE vary from 0.21 to 194 ppb with Pd being the highest. Ni values vary from 260 to 1583 ppm, and Cu from 281 to 2592 ppm.

In Figure 4.7 the PGE contents show peaks at 90 masl, 180 masl and 270 masl. Two of those peaks at 90 and 270 masl are related to local enrichments as

they are represented by only one sample each. The other peak at 180 masl is represented by multiple samples and has the highest Pd and Pt values.

In contrast to the PGE, the graph clearly shows a sulphur peak around 270 masl (Figure 4.7). This is represented by the pyroxene rich rocks and a leucogabbro (ML-51), some of which have a hydrothermal sulphide assemblage (Table 4.2). This concentration of hydrothermal sulphides does not show any positive correlation with PGE. In addition to this, the samples richest in sulphur show the lowest PGE values in the whole Ebay area.

Considering the presence of sulphides assemblages established in the petrology chapter, there is evidence of a hydrothermal event around the Ebay area. The phenomenon was observed in many samples, and therefore there should be evidence in the geochemical composition. The sulphide mineralogy described is pyrrhotite, pentlandite, chalcopyrite and pyrite. Thus, the phases are Ni, Cu, Fe and S bearing. Ni versus MgO shows a good correlation for the olivine gabbros. This suggests an olivine control for these samples. For the pyroxene rich rocks, Ni and Mg do not correlate well indicating enrichment in Ni due to the presence of sulphides.

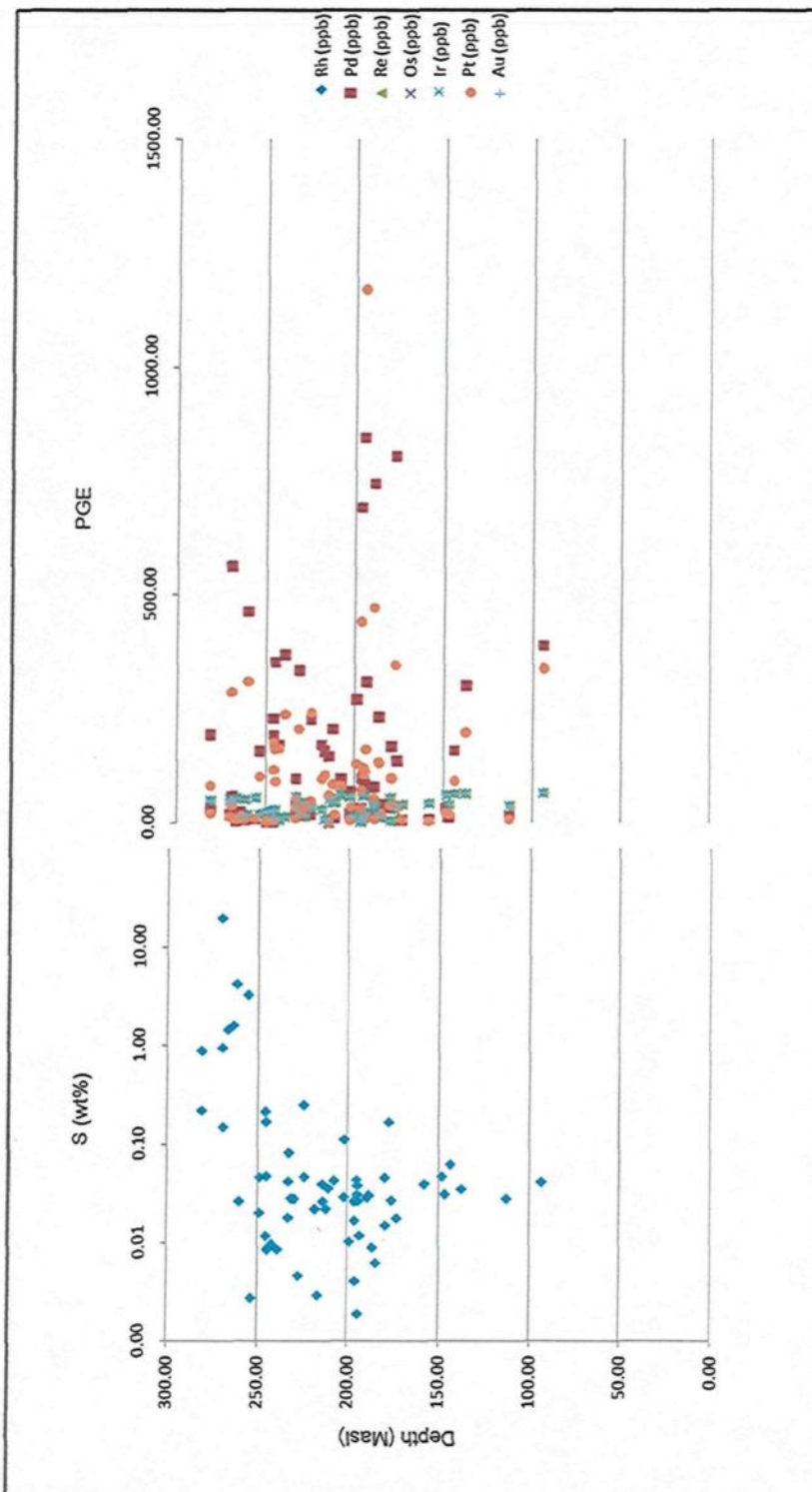


Figure 4.8 Variation of S and PGE with depth, shown as in meters above sea level; the surface is around 300 masl. The samples have been corrected to depth in the generalized stratigraphic column.

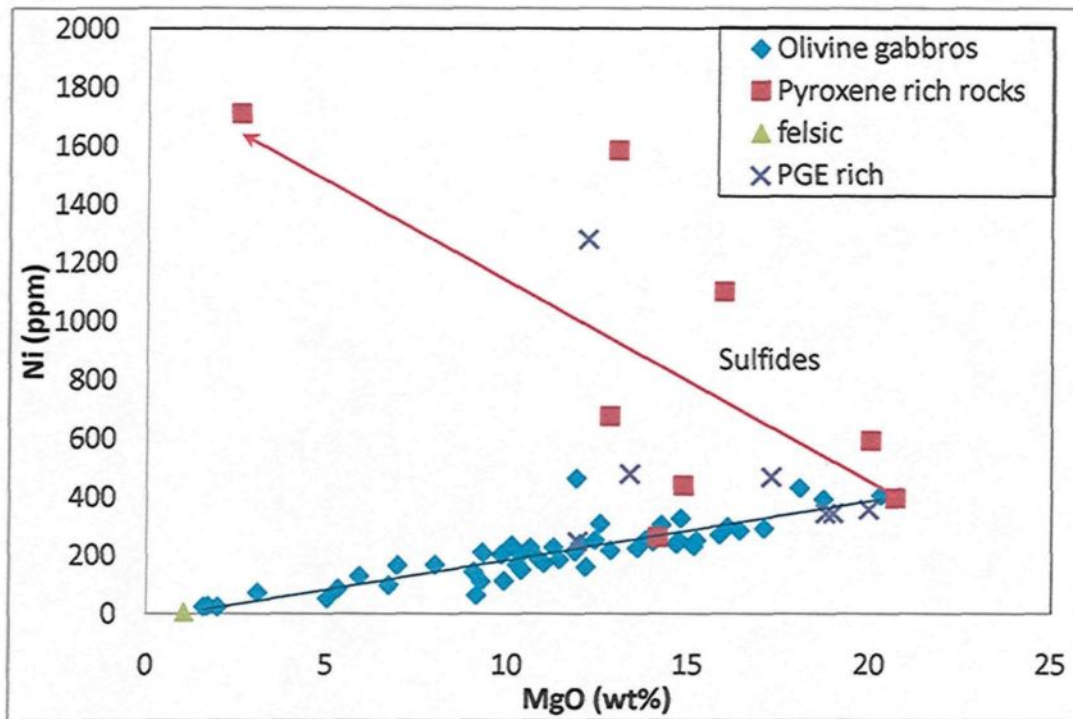


Figure 4.9 MgO versus Ni diagram showing the Ni controlled by olivine in olivine bearing gabbros and in some PGE rich samples (blue line). The Ni controlled by sulphides correspond to many of the pyroxene rich rocks (red line). Ni values by ICP-MS.

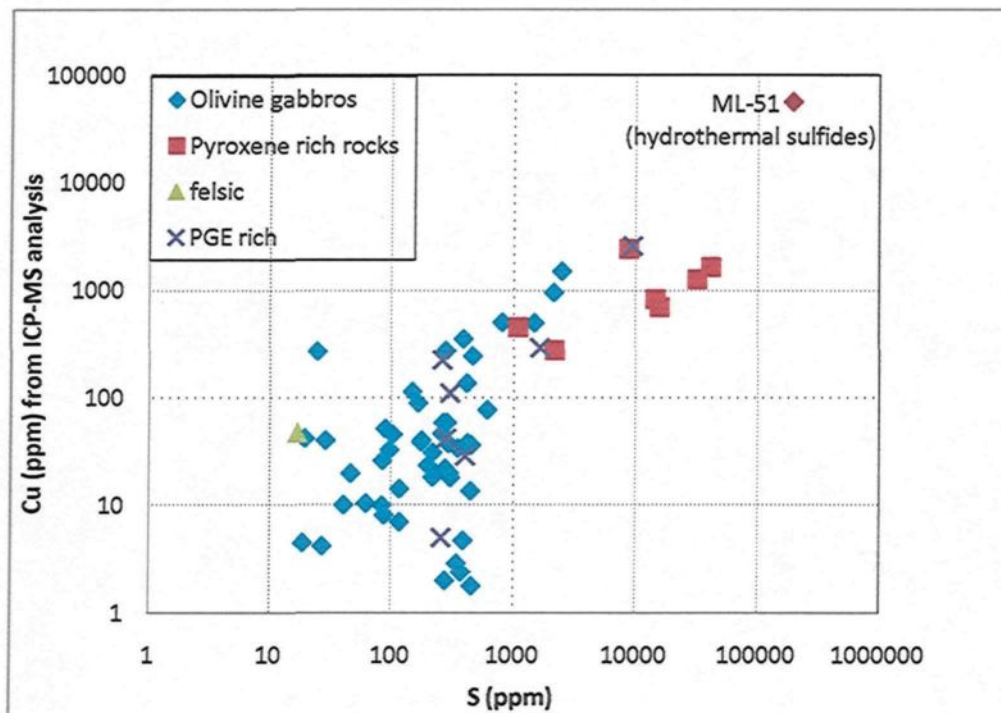


Figure 4.10 Diagram of sulphur versus Cu. The sample ML-51 has hydrothermal sulphides and is part of the Olivine gabbros group. Cu from ICP-MS results

In figure 4.9 the S and Cu show a positive correlation for the samples over 1000 ppm sulphur, most of these are the pyroxene rich rocks. In the olivine gabbros with S<1000 ppm there is no correlation between Cu and S. Many of the samples that correlate have a magmatic-hydrothermal assemblage.

In addition, diagrams of sulfur versus PGE, Bi and Sb (not shown), indicate that sulphur does not correlate with any of the PGE (Figure 4.10), Bi or Sb.

4.4.1. Relationships among the PGE

There is no correlation between Pt or Pd and S (Figure 4.10), however there is a positive linear correlation between Pt and Pd (Figure 4.11a), and a weaker correlation of Pd with Rh, Ir, Ru and Os (Figure 4.11b, c, d, e). The lack of a correlation between S and PGE suggests that the PGE are hosted by PGM rather than base metal sulphides. The PGM study showed that Pd-Bi-Te, Pd-Sb, Pt-As and Pt-S are present (Figure 3.5). However there is no correlation between Pd or Pt and Bi and Sb (figure 4.11f,g), suggesting that although the PGE are now present as Bi-tellurides and antimonides these were not collector phases.

However, the Pd versus Bi diagram (Figure 4.11f), shows a slight correlation of Pd with Bi for the PGE-rich samples. Also there are four samples which are poor in Pd but show correlation with Bi. This small group of samples is the same in every diagram and does not correspond to any of the groups defined before (i.e. the magma series).

The Pd versus Bi and Sb diagrams (Figures 4.11f,g) indicate that Bi and Sb in the BRC are unevenly distributed and therefore it is possible that enough Bi and Sb was available to form the Pd-Bi-Te and Pd-Sb-As phases locally.

With respect to Bi, this element has a great crustal affinity and its enrichment could be related to events such as the intrusion of the granite plutons and the dykes, which could have introduced the Bi to the BRC, or re-mobilized Bi already there. From the *Geochemistry of rocks of the oceans and continents GEOROC* web page (<http://georoc.mpch-mainz.gwdg.de/georoc/Start.asp>). The gabbros cover the 0.02-2 ppm range and the granites cover the range 0.1-11 ppm.

The other elements related to the PGE rich rocks (i.e. Te, As, Sb) are harder to explain in this way; however they could be related to mobilization of sulphides including Bi, which could have been removed by different processes occurring in confines of the BRC but driven by the regional and contact metamorphism.

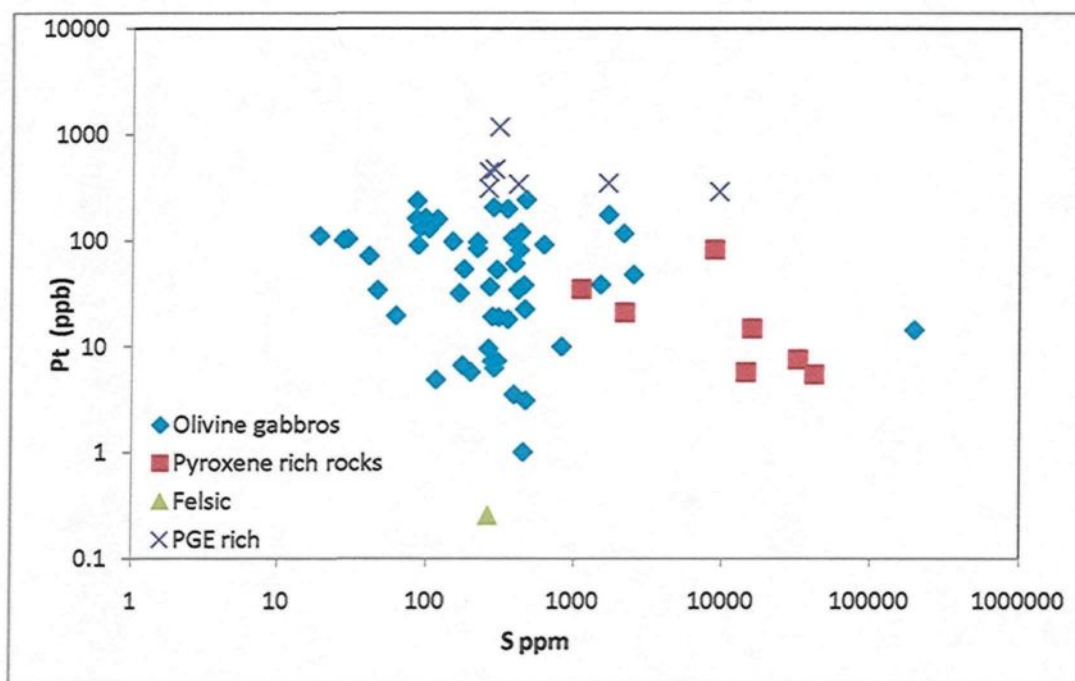
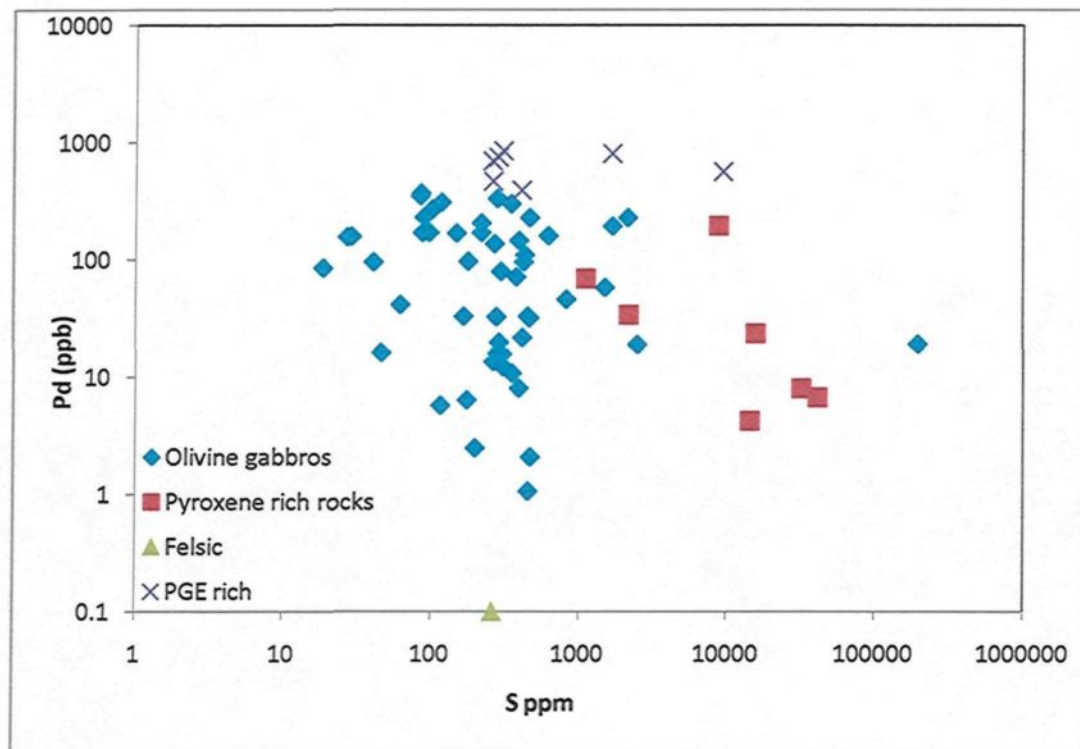


Figure 4.11 Sulphur versus Pt and Pd

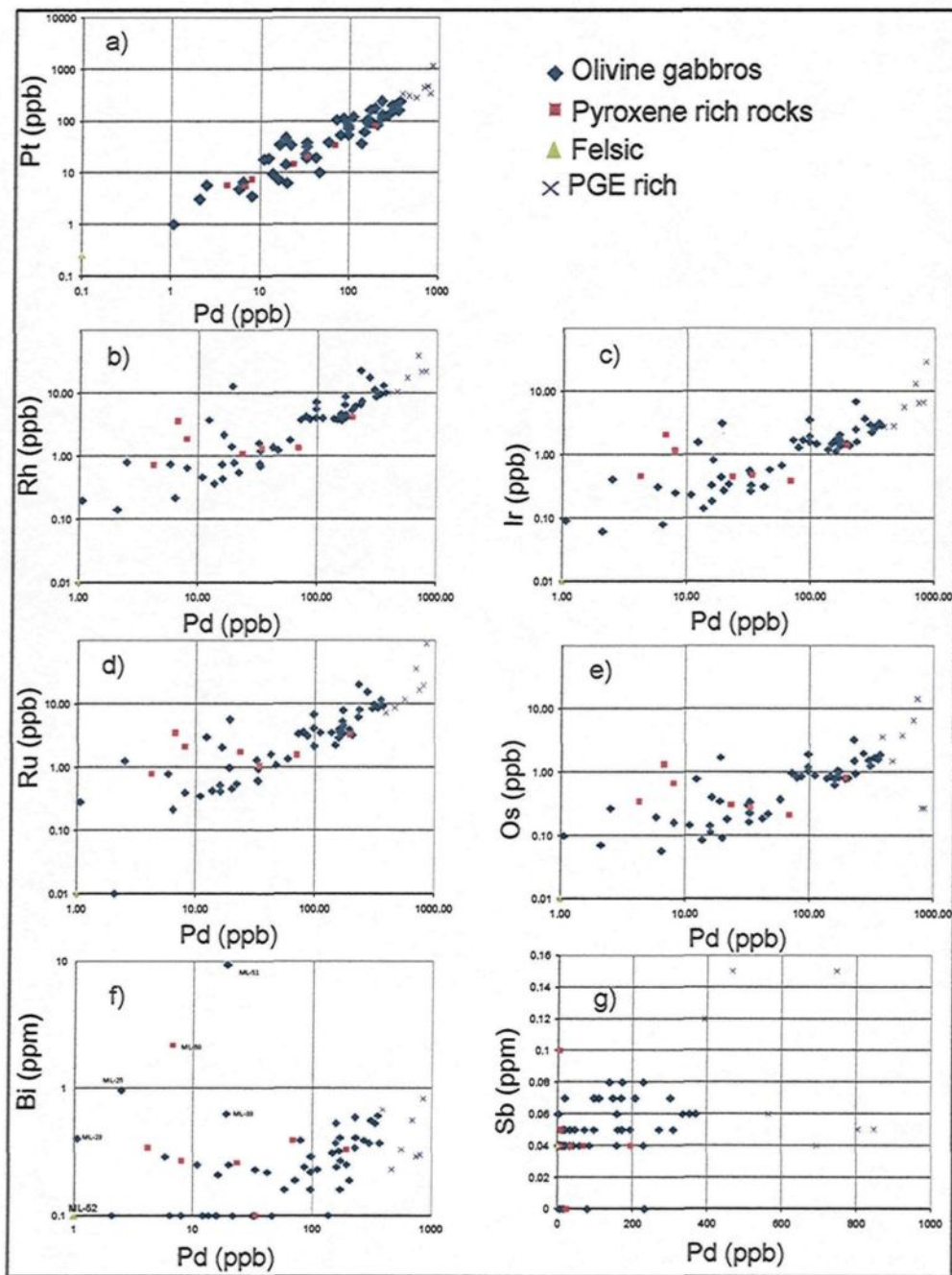


Figure 4.12 Pd vs PGE and Pd versus Bi and Sb (main constituents of PGM)

Figure 4.12 shows mantle normalized plots of PGE, Ni, Cu and Au. In this diagram, all the samples show a similar pattern, from the poorest in PGE (pyroxene-rich rocks, Figure 4.12 c) to the richest (PGE rich, Figure 4.12a). This diagram clearly shows the depletion of Ir and Ru relative to Pt and Pd.

For the mantle normalized plots of the PGE rich rocks (Figure 4.12a), the pattern represent a pronounced depletion in the IPGE respect to PPGE; the ratios of Pd/Ir for those samples are around 100. This diagram shows depletion of gold and copper relative to Pt and Pd. This pattern reflects the effects of metamorphism and a possible mobilization due to the circulation of fluids. Gold was one of the most remobilized elements by the fluid action, which produced the negative anomaly. This element was probably remobilized along with sulphides in some samples (some of the samples show negative anomalies in Cu as well).

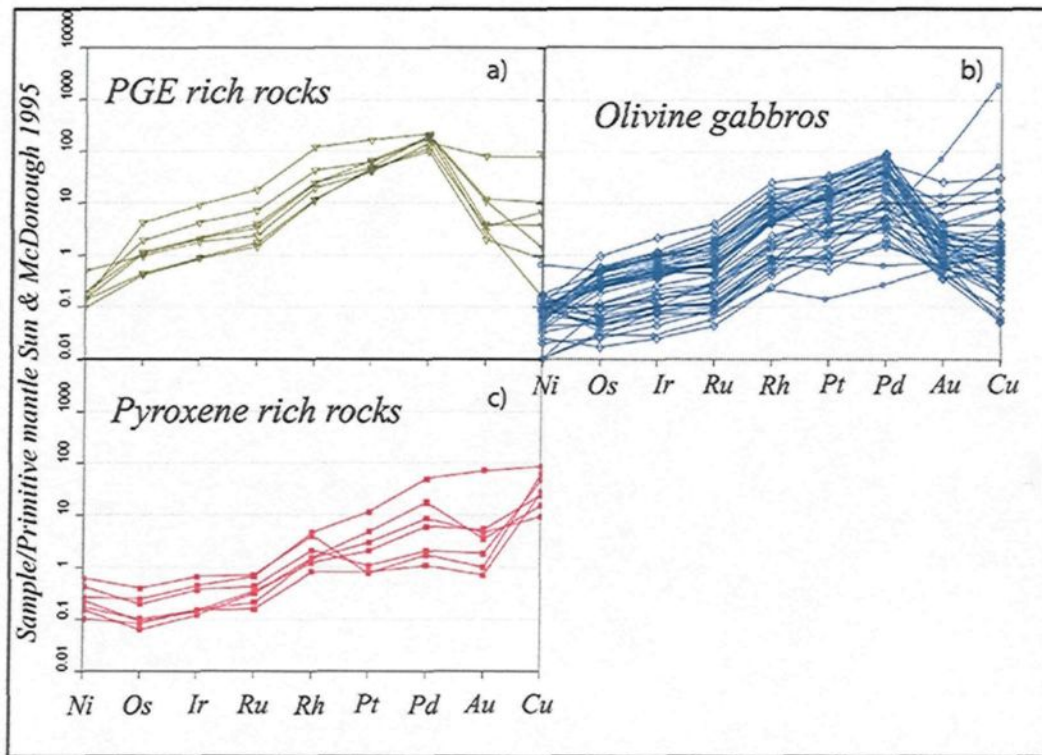


Figure 4.13 Ni-PGE-Cu normalized to primitive mantle. Normalization values taken from Sun & Mc Donough (1995).

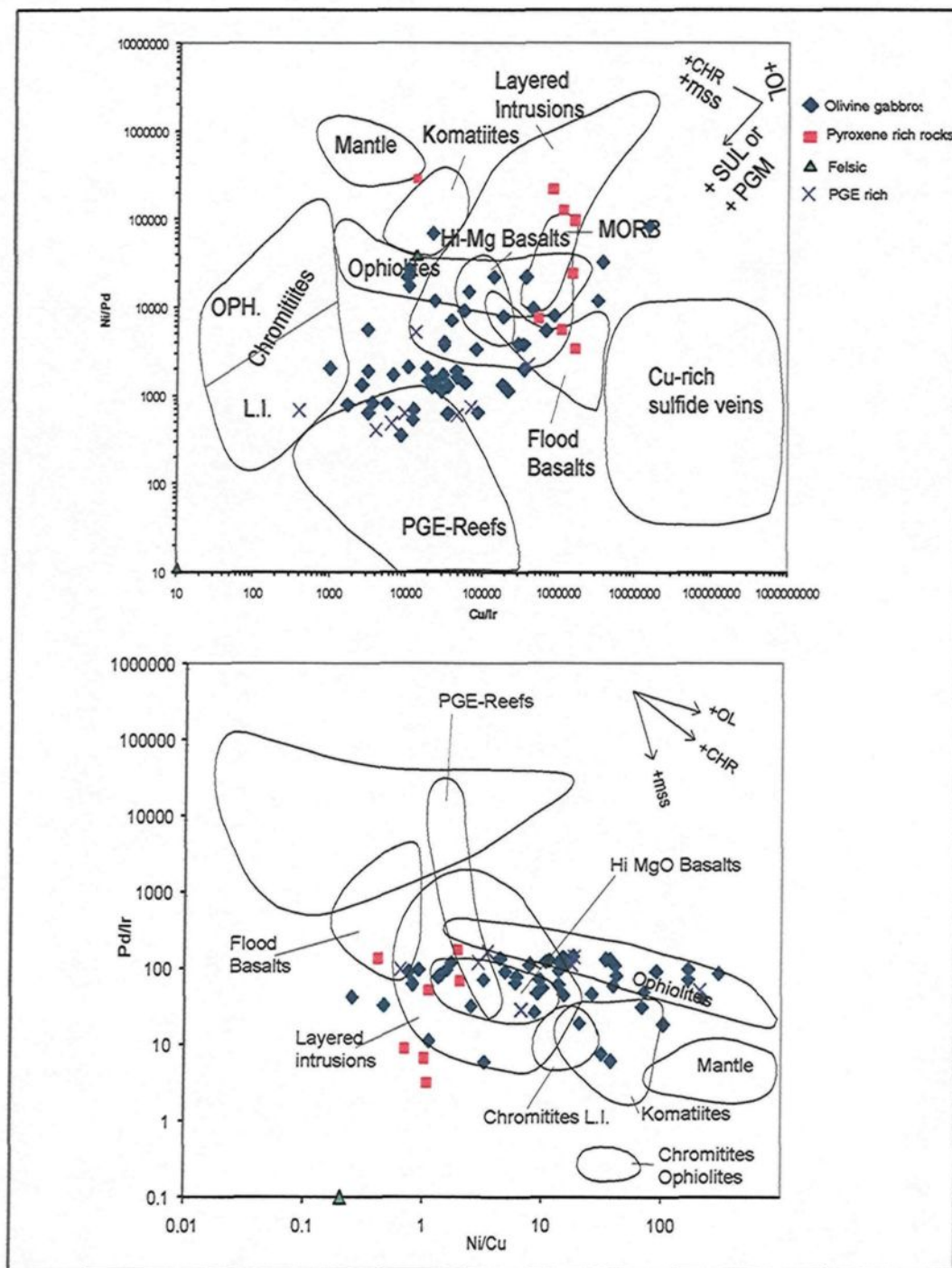


Figure 4.14 Cu/Ir versus Ni/Pd and Ni/Cu versus Pd/Ir after Barnes et al., 1993 for the Ebay samples. Ni and Cu are both ICP-MS values.

The diagram Cu/Ir versus Ni/Pd shows the different groups established before including the PGE-rich samples (Figure 4.13). This diagram shows the position of the BRC at Ebay with respect to the magma evolution in terms of gaining some minerals as illustrated by the vectors in the diagram. The hydrothermally affected samples have the highest Cu/Ir and Ni/Pd ratios as expected, because they have the highest values of Cu and Ni; they include ML-26, ML-51 and some of the pyroxene rich rocks, and as it was mentioned before, they have the lowest PGE values. The PGE rich samples, are slightly dispersed, nevertheless they are in the lower left corner. The others in blue that correspond to the olivine gabbros show a very dispersed pattern represented by a reduction in Ni/Pd ratio as Cu/Ir decreases. The pattern represented by all the samples follows a line that shows a gradual increase in the PGM (as illustrated in the top right). The trend of samples that are rich in sulphides, but low in the PGM gradually pass along trend to samples that have high PGM content, but low levels of sulphides (located in the bottom left corner). This gives to BRC an arched shaped pattern typical of reef type deposits. Hydrothermal effects have moved the samples towards a higher enrichment in Ni/Pd and Cu/Ir, which is the opposite to samples bearing PGM.

In the Ni/Cu versus Pd/Ir diagram, the samples show a flatter dispersion distributed across the diagram. All of the variation in samples encompasses a change in the Pd/Ir ratios between approximately 10 and 100, whereas the Ni/Cu ratios vary much more widely. In this diagram the hydrothermal samples plot in a field delimited by their similar content of Ni and Cu sulphides ($Ni/Cu \approx 1$). The rest

of the samples (the olivine gabbros) are widely dispersed including those with high PGE. In this diagram the increase of Ni over Cu is represented by the crystallization of olivine in the rocks (as indicated by the upper right), therefore representing the most mafic protoliths for Ebay.

Finally, this diagram shows that there is no correlation between the increases of Ni/Cu with the concentration of PGE. It is because many of the samples have been altered by hydrothermal sulphides which change the amounts of Cu on the samples. Table 4.1 shows that the Ni values do not change too much in comparison to Cu values for the PGE rich rocks.

CHAPTER 5

DISCUSSION

5.1. Magmatic events in the Bell River Complex

There are two magmatic events of importance to consider in the BRC. They are clearly represented in the Harker diagrams and have different patterns on all of the diagrams, except for CaO. The first group of samples defined on IUGS triangular diagram includes the majority of samples. These are olivine gabbros and they are composed principally of plagioclase and olivine. The second group has less plagioclase and olivine and has more pyroxene. The olivine gabbros follow a well defined trend of crystal fractionation on the Harker diagrams. These samples are slightly dispersed which possibly reflects a moderate mobilization of some elements. The pyroxene rich group does not follow this trend; rather, it follows another pattern that reflects a slightly higher content of silica and much lower content of alumina (Figure 4.1). Additionally, whereas the first group tends to be enriched with sodium and potassium, the second group is depleted in these elements and has characteristics that are more mafic and less fractionated.

Groups are clearly distinguishable on the Al_2O_3 versus FeO_T diagram (Figure 5.1). In this diagram, it can be clearly seen that the groups have different $Al_2O_3 /$

FeO_T proportions. Figure 5.1 clearly shows the trend related to the olivine gabbros, which follow a pattern represented by the enrichment of Al₂O₃ as the FeO decreases. In the mafic group no trend is evident.

In the CIPW norm calculation, the pyroxene rich samples have the lowest plagioclase content as well as high proportion of pyroxene (Appendix 9). The pyroxene rich group consist of pyroxenites, melagabbronorites, gabbronorites and olivine-gabbronorites. The pyroxene rich rocks are rich in MgO and CaO compared with the olivine gabbros and they have low PGE values (less than 200ppb) whereas their Cu and Ni contents are high (1wt. % Cu and 0.7 wt. % Ni on average).

The multielement mantle normalized diagrams (Figure 5.2) shows a less differentiated pattern for the pyroxene rich rocks. It is a flat pattern.

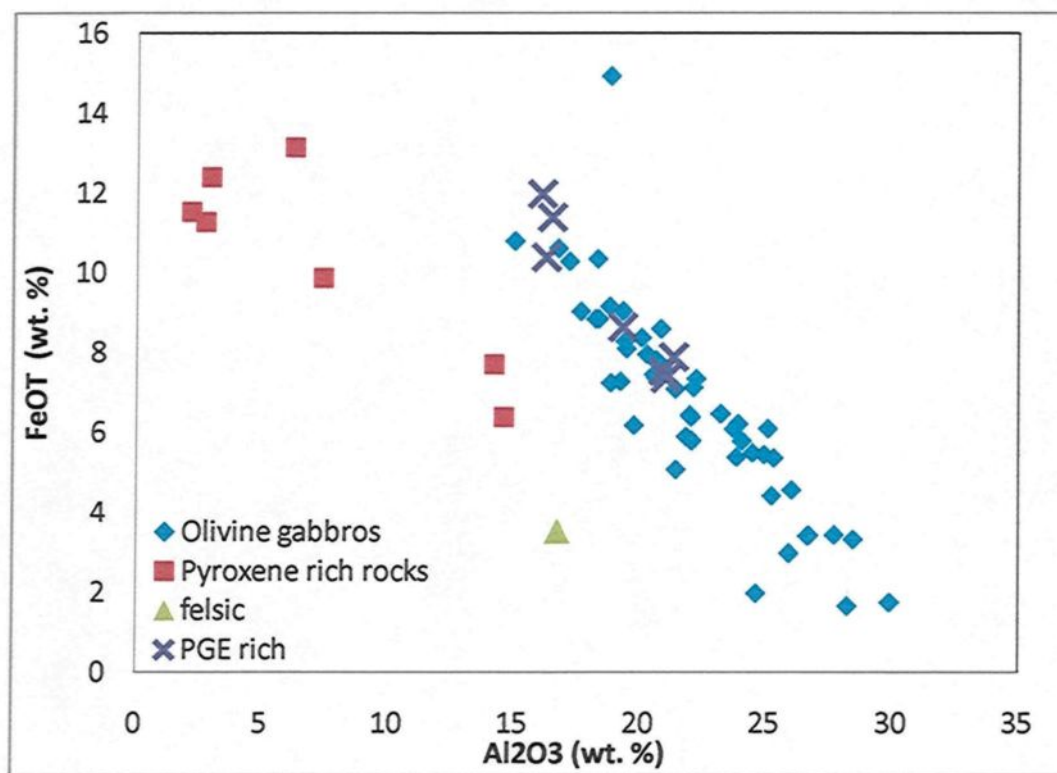


Figure 5.1 Al_2O_3 versus FeO_7 diagram

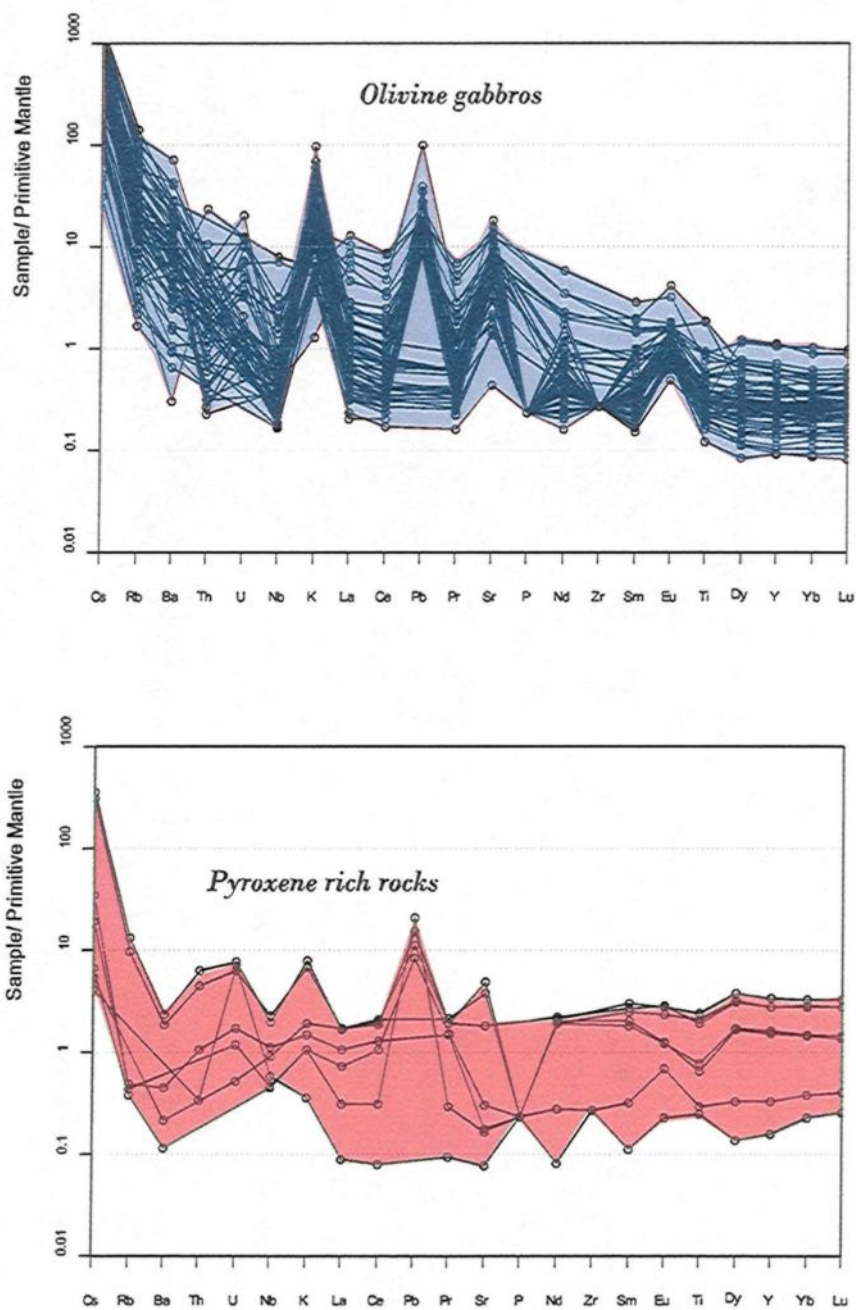


Figure 5.2 multi-element plots showing the patterns for the olivine gabbros and the pyroxene rich rocks. Normalized to Primitive Mantle (Sun & McDonough, 1989).

5.1.1 The sulphides

From the petrographic studies, the presence of three sulphide paragenesis was recognized. The first paragenesis contains pyrrhotite, pentlandite and chalcopyrite. The second paragenesis contains pyrite and chalcopyrite. The third paragenesis contains a mixture of the last two, pyrrhotite, pentlandite, pyrite and chalcopyrite.

The first paragenesis is considered magmatic whereas the second is considered hydrothermal. The evidence for the hydrothermal origin was firstly glimpsed from the outcrops observations that suggest a large interaction with the rocks of the Opaoca and Lac Olga intrusion. The outcrops show a large proportion of felsic dykes coming through pre-existing fractures of BRC or along the foliation (Figures 2.3 and 2.4). Thin sections show the presence of veins crosscutting the samples without the displacement of the rock, these veins are quartz rich and very locally they contain calcite (Figure 3.3). The presence of many of the silicate minerals that include H₂O in their structure (e.g. tremolite-actinolite, chlorite, epidote-clinzoisite and talc) along with the formation of calcite, suggests a source of fluids including H₂O. These fluids could come from different sources, the intrusion itself (juvenile water), the intrusive plutons (Opaoca or Lac Olga), surface, the overlying sediments or a mixture of them. A detailed study is necessary although considering the stratigraphic relationship the intrusive plutons play an important role in the process due to the fact that the granitic pluton reheated the rock. The presence of juvenile water could be abundant considering that the stages

of fractional crystallization of BRC were large and include up to leucotroctolites. Water could come from surface or sediments along fractures.

In the pyroxene rich rocks the presence of magmatic-hydrothermal assemblage (pyrite, chalcopyrite, pyrrhotite and pentlandite) is the most common. These rocks seem the most altered and show the highest values in Cu and Ni whereas the olivine gabbros are characterised by the presence of the three assemblages, but with lower values of Ni and Cu. Nevertheless the pyroxene rich rocks include samples with the highest PGE values. The diagram of Ni versus MgO (Figure 4.8) shows a control of sulphides for several samples including many of the pyroxene rich rocks, the diagram of S versus Cu shows a similar control (Figure 4.9). This supports the argument shown before that the pyroxene rich rocks were the most altered by fluids and that they are enriched in sulphides. Therefore many of these sulphides are from hydrothermal origin and mobilized.

However, the presence of sulphur of hydrothermal origin is not exclusive to the pyroxene rich rocks. The fact that some samples are enriched in sulphur does not mean that they are hydrothermal and viceversa (Appendix 8).

5.2. PGE behaviour and implications for exploration

The highest values of PGE are for Pt and Pd, 1170 and 845 ppb respectively. Besides these anomalies, there is a group of samples with values between 500

and 1000 ppb Pt or Pd. Thus some samples contain 1 to 2 ppm Pt+Pd. In figure 5.3 the values of Pt versus Pd from Ebay are compared with the Merensky and JM reef. Here it is clearly seen that the highest values of Ebay correspond to the lowest values of Merensky and JM reef. However, it is worthwhile to consider that in this project many samples that were taken do not have any economic interest, whereas for Bushveld and Stillwater, only the reefs are represented (Merensky and J-M reef for the Bushveld and Stillwater). It is probable that in the sampling we may have missed the richest parts of the zone. To ensure that we have located the enrichment, we should focus on the study of the distribution of the richest samples.

In order to understand the distribution of the PGE and their relationship to the layering, we should examine the distribution of the PGE in greater detail. Among the best indicators and exploration tools in the different PGE deposits are the distribution of sulphur, Ni and Cu along the layering. The relationship of PGE to these elements have been considered in many previous studies (e.g. Barnes et al., 1985; Naldrett, 2004; Barnes and Lightfoot, 2005; Peregoedova et al., 2006; Boudreau, 2008).

The $Cu/(Cu+Ni)$ index could be used as a tool in the exploration of PGE (Naldrett, 2004). This ratio is shown in Figure 5.4 and its correlation with the values of sulphides and PGE at depth. This figure shows how the Ni and Cu are distributed in the samples with respect to their proportion in sulphides or silicates. Thus high ratio values are related to the presence of Cu-sulphides, whereas low ratio values are related to Ni-bearing minerals either sulphides or silicates.

With regards to the Ebay samples, the $\text{Cu}/(\text{Cu}+\text{Ni})$ ratio is very low, because of low content of sulphides. However, the relationship of the sulphur and the $\text{Cu}/(\text{Cu}+\text{Ni})$ ratio is seen closer to the surface where there is a link with the pyroxene rich rocks (green area highlighted on figure 5.4).

In addition, in a basaltic magma, sulphur saturation occurs at 500-1000 ppm (Li and Ripley, 2005) and therefore for the cumulate rocks to contain cumulate sulphides requires S contents of 500 to 1000 ppm. The sulphur has a geometric mean of 400 ppm at Ebay. Therefore, if we use the value of 400 ppm S to define the enrichment or depletion of the samples, the only important enrichment of sulphur is around a depth of 30 meters (270 masl). The sulphide enrichment is coincident with the pyroxene rich rocks, which are concentrated towards the top (in yellow). An interesting depletion of S occurs at a depth of 120 meters (180 masl in green); other depletions are small.

The sulphide depletion is coincident with the PGE enrichment. This is represented by a group of samples which have the highest Pt and Pd values in Ebay. Such enrichment is represented by values of Pt + Pd that reach the 2 ppm and other less pronounced peaks that reach the 1 ppm Pt + Pd. These values change within a couple of meters and are probably related to an area of enrichment that is folded.

There are other concentrations of Pt and Pd at different depths, 210 m, 160 m, 60 m and 30 meters (90, 140, 240 and 270 masl). There are anomalies that are

worth consideration as they have values of Pt + Pd up to 720 ppb, 600 ppb, 700ppb and 1 ppm respectively.

The rest of PGE (Ru, Rh, Os, Ir) vary from 0.0 ppb to 300 ppb.

It is important to consider that not many PGE-rich samples have been taken (only 7 with PGE >1ppm). Furthermore just one or two enriched samples generate a peak in the profile and therefore, the two peaks at the top and the bottom correspond to the isolated PGE values (210 m and 30m depth).

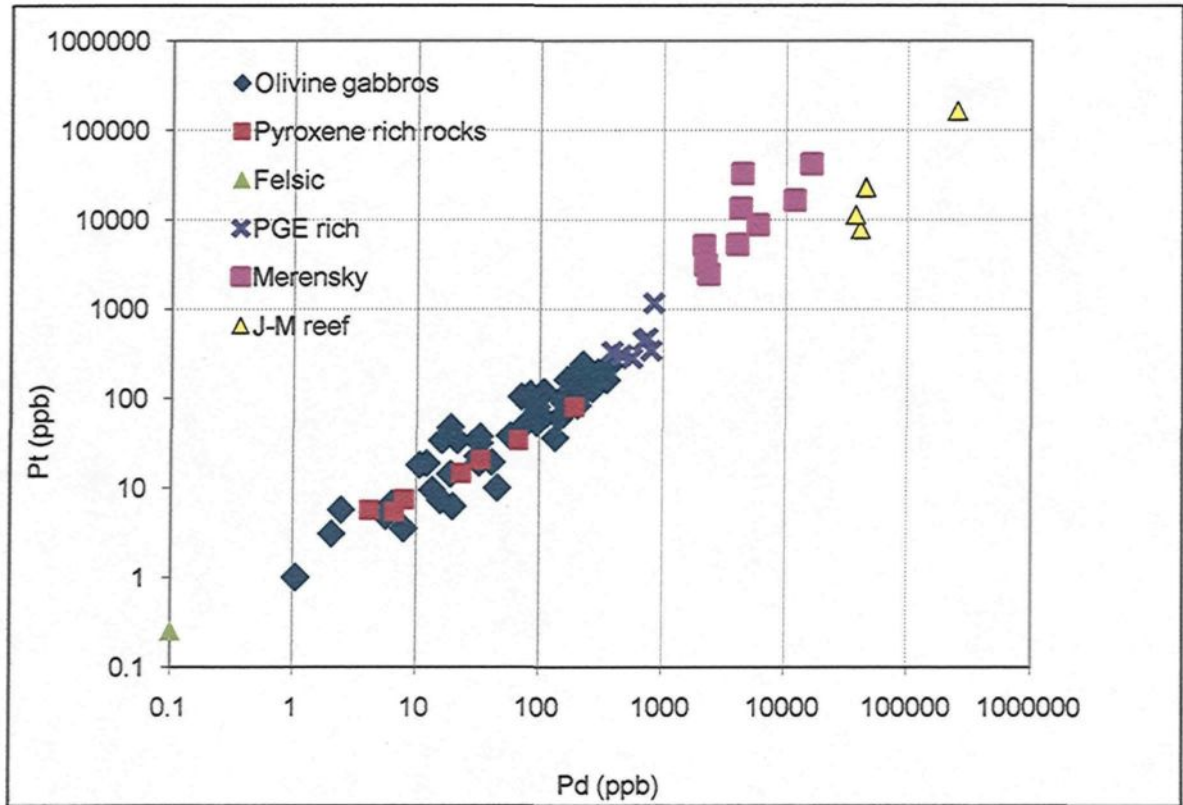


Figure 5.3 Pt versus Pd for the Ebay samples, compared to Merensky and J-M reef. Merensky reef from Godel et al., 2007; J-M reef from Godel et al., 2008.

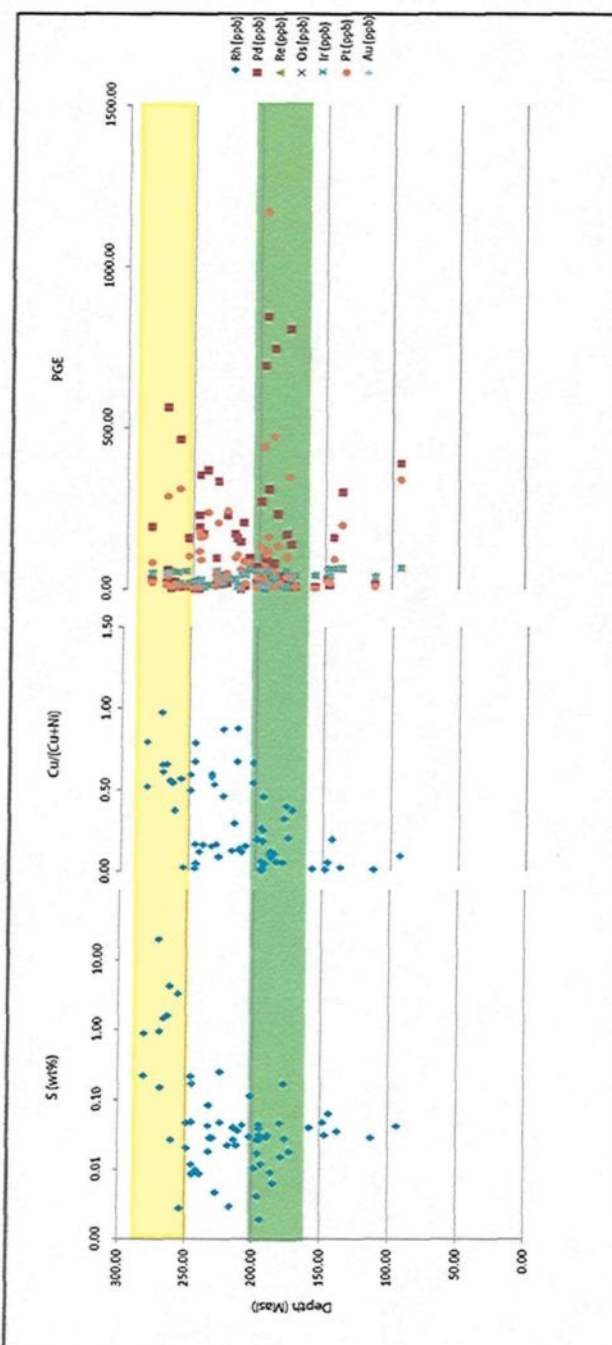


Figure 5.4 Variation of S, Cu/(Cu+Ni) and PGE at depth. The surface is approximately 300 meters above sea level (masl). The altitude values were considered to avoid topographical disparities in the surface in different places. The possible reef is highlighted in green and the Sulfur enrichment in yellow.

Before modelling the PGE values, we will concentrate on the feasibility of the project by means of discrimination diagrams for PGE deposits.

The Cu/Ir versus Ni/Pd and Ni/Cu versus Pd/Ir ratio diagrams are very useful PGE exploration tools. These diagrams of Barnes et al. (1993) detail many sorts of rocks, sulphides and PGE deposits. The diagrams presented in Figure 5.5 and include the reference values of Bushveld and Stillwater deposits (Godel et al., 2007; and Godel et al., 2008 respectively). The BRC samples have ratios that vary widely, and although some of them are PGE poor, a considerable number of samples have similar ratios to layered intrusions and PGE-reef deposits (e.g., Barnes et al., 1993, Figure 5.5). The samples that plot in the *PGE-reef* field are olivine gabbro-norites and leucogabbro-norites. The sulphur-rich samples, due to the high Ni and/or Cu content are, in Figure 5.5a towards the right side and in figure 5.5b towards the left.

The use of the Cu/Pd ratio is a common exploration tool. Rocks with Cu/Pd ratios greater than mantle values (~6000) were formed from magmas depleted in Pd, possibly due to the removal of a sulphide liquid from the magma. This implies that there is a potential for a PGE-bearing sulphide deposit at lower stratigraphic levels (Barnes et al., 1993). Thus, samples to search for are those with Cu/Pd ratios below 6000. Particularly in Ebay, the samples in Figure 5.6 with ratios over 6000 are in the uncoloured field and represent the samples with hydrothermal

sulphides. The rest of the samples below 6000 have promising values, and even when they do not reach the Merensky or J-M reef values, they deserve to be considered as a target.

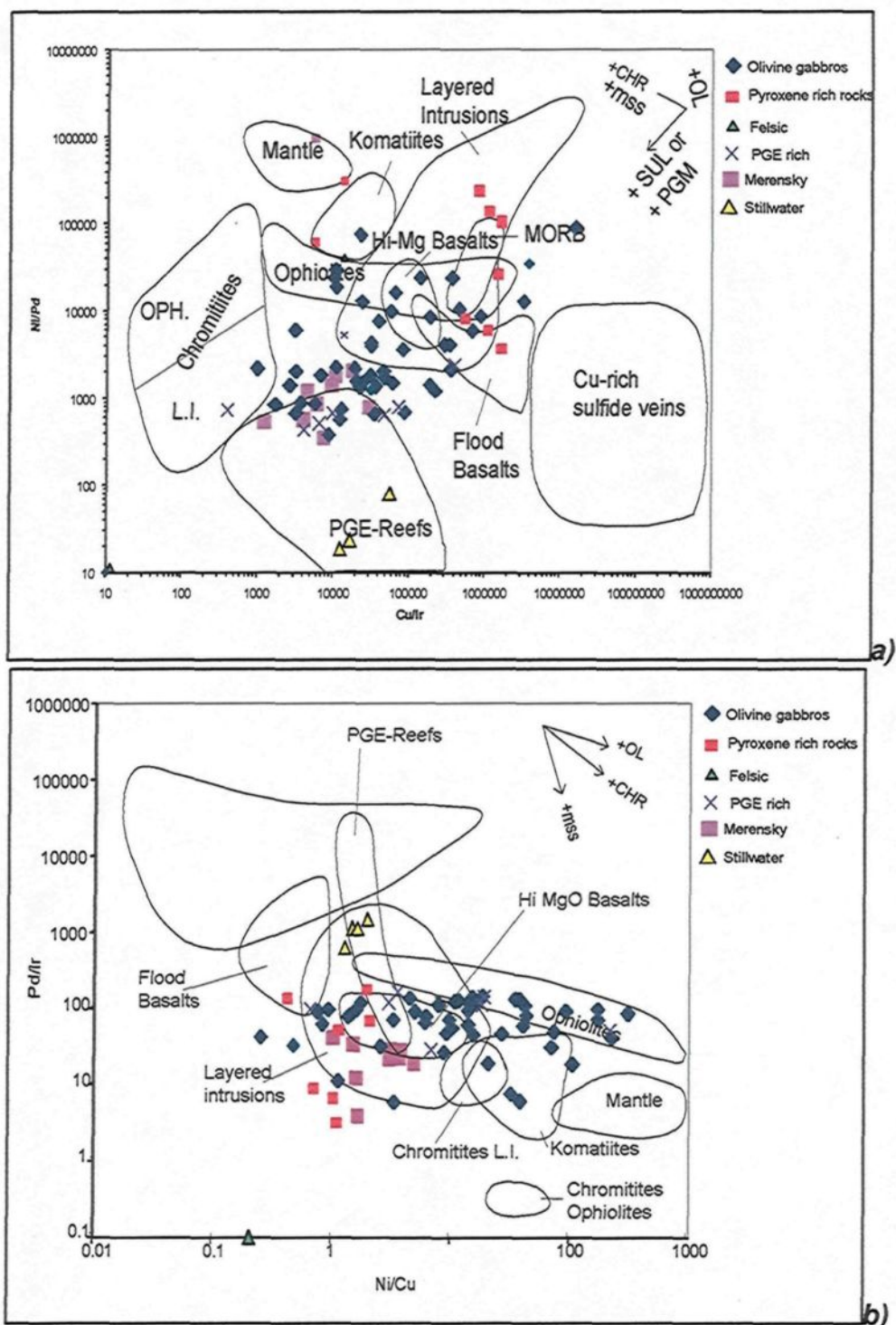


Figure 5.5 Cu/Ir versus Ni/Pd and Ni/Cu versus Pd/Ir after Barnes et al., 1993. Stillwater J-M reef from Godel et al., 2008; Merensky reef from Godel et al., 2007.

The Cu/Pd ratio has been applied to different mafic-ultramafic layered complexes of the Abitibi and Pontiac sub-provinces: the BRC (Barnes et al., 1993, Maier et al., 1996 and Goutier, 2005), the Lac Dore and Cummings (Barnes et al., 1993). The last two have Cu/Pd ratios greater than the mantle, suggesting that magmas from which these intrusions came from were depleted in PGE, and that the intrusions would not be good exploration targets at the stratigraphic levels sampled, although there could be PGE-rich sulphides below this (Barnes et al., 1993 and Goutier, 2005. Figure 5.6).

Considering the sampling made by Goutier (2005) in Bwest, Dotcom (the other showings in the BRC towards the south) and Ebay, the results show that Bwest and particularly Dotcom are richer in Pd with values very close to those of the Merensky reef. Furthermore they have Cu/Pd ratios similar to Ebay based on results of both Goutier (2005) and this study (Figure 5.6).

There are a great number of samples in the PGE rich field with Cu/Pd ratios as low as 10. Here the samples with the lowest Cu/Pd ratios are Pd rich, with values closer to 1000 ppb Pd (Figure 5.6). Comparing the Pt+Pd values from this study and the obtained by *Hinterland*, it is seen in the borehole EB 07-07 a value of Pd of 1003 ppb from 94.10 m to 94.90 m as compared with a value of 692 ppb Pd from 101.15 m to 101.30 m in the EB 06-05 in this study. Despite the fact that the samples did not come from the same bore holes, they are very close in the profile.

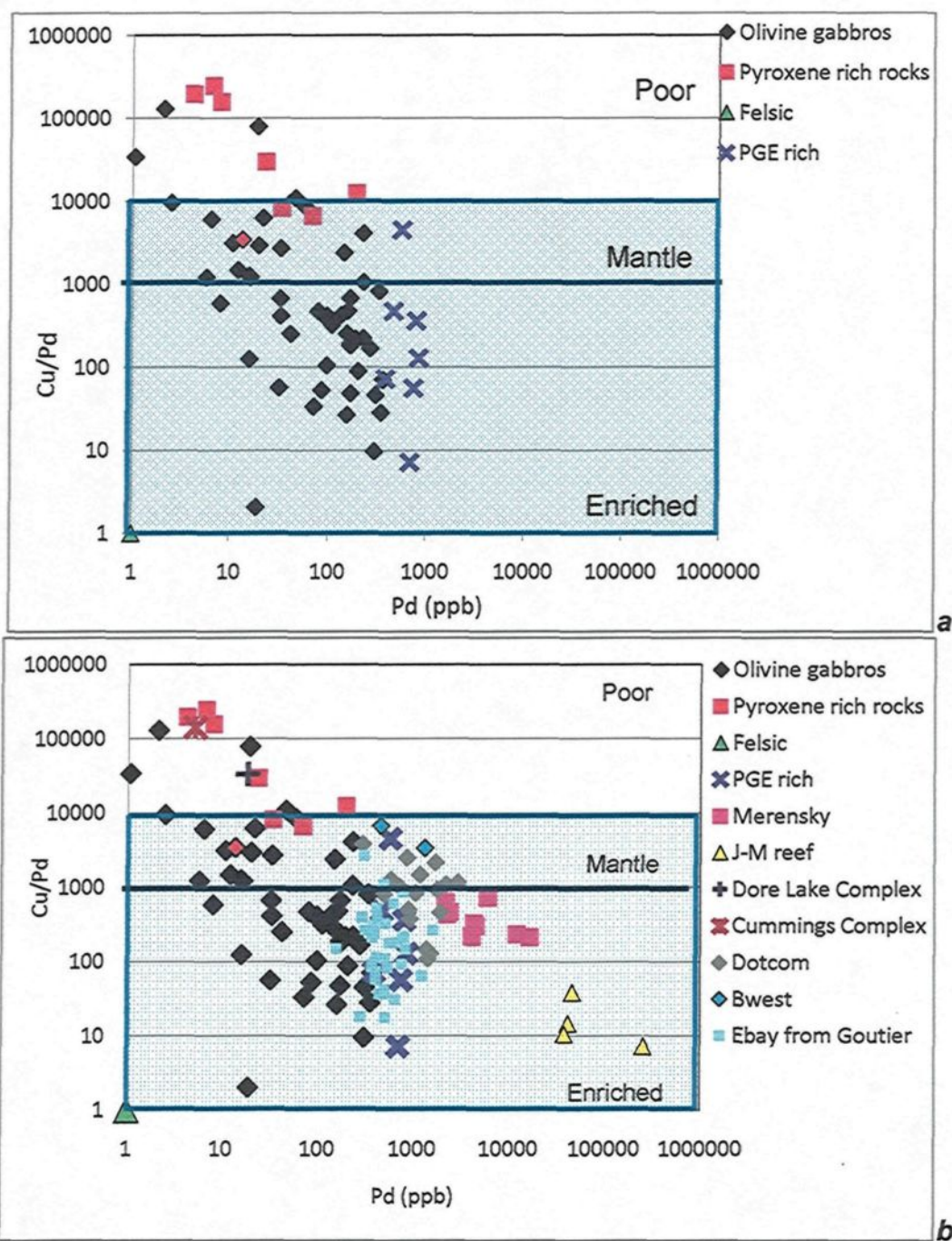


Figure 5.6 Pd versus Cu/Pd for BRC and other different layered complexes. a) Ebay samples from this project; b) Ebay compared to others. Bwest, Dotcom and Ebay from Goutier, 2005; J-M reef from Godel et al., 2008; Merensky reef from Godel et al., 2007; Lac Dore and Cummings from Barnes et al., 1993. Bwest, Dotcom and Ebay are located in BRC, Cummings and Dore Lake are in the Abitibi sub-province.

The sampling made in this project along with sampling made in the past exploration surveys leads us to consider that there is at Ebay an important concentration of PGE (composed of Pt+Pd).

5.3. PGE layer location

The position of the samples in the stratigraphic sequence reconstructed in this project for data from *Hinterland* and this study lead us to propose that there is an interesting concentration of PGE values at the top of one of the layers. Figure 5.4 shows a cluster of high values of Pt and Pd at approximately 120 meters deep (180 masl). The values on the graph change at a depth which cannot be used to determine the thickness of the PGE layer. This change is considered to be the product of the layering in the BRC. To clarify this point, the PGE values were placed at their respective depths in the sequence and some nearby values out of the profiles were projected into the section. In this profile only Pd was used but Pt could be, because it is present in the same chemical proportion ($Pt/Pd \approx 1$, Figure 5.3).

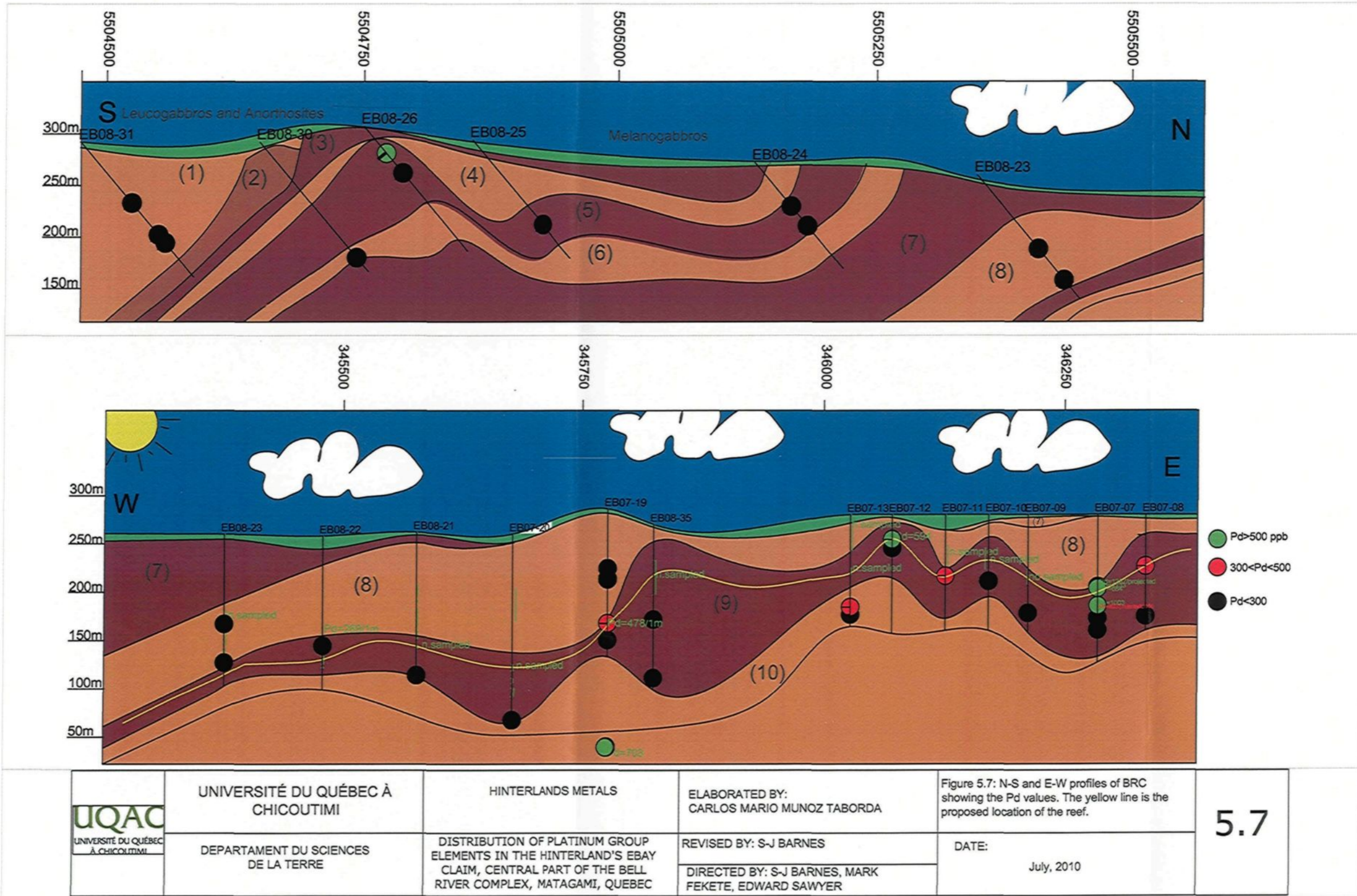
To separate the values of economic significance, the samples were divided into Pd-poor ($0 \text{ ppb} < Pd < 300 \text{ ppb}$), moderate ($300 \text{ ppb} < Pd < 500 \text{ ppb}$), and Pd-rich ($Pd > 500 \text{ ppb}$) (Figure 5.6). The graph shows an important concentration of Pd values towards the east. In the west there is insufficient sampling to define whether a Pd-rich layer is present.

Considering that our sampling was not exhaustive, we used the *Hinterland* sampling (commercial values). Many of the places where a possible concentration could be found have not been sampled. Such non-sampled places are featured in Figure 5.6 and are highlighted with green lines.

Therefore, gathering all the information together, the Pd-rich values and the non-sampled places highlight a possible reef at the top of the layer #9. The reef proposed is traced out on the most prominent places with a yellow line.

It is strongly recommended that sampling in the places demarcated by this line be carried out.

Some Pd rich samples have also been found in discrete locations. These places were analyzed and were discarded as a source of economic importance. Samples taken for *Hinterland* and others taken in this project in a close location to this isolated samples are PGE poor; and do not permit the extrapolation of such PGE concentrations.



UQAC
UNIVERSITÉ DU QUÉBEC
À CHICOUTIMI

UNIVERSITÉ DU QUÉBEC À
CHICOUTIMI

DEPARTAMENT DU SCIENCES
DE LA TERRE

HINTERLANDS METALS

DISTRIBUTION OF PLATINUM GROUP
ELEMENTS IN THE HINTERLAND'S EBAY
CLAIM, CENTRAL PART OF THE BELL
RIVER COMPLEX, MATAGAMI, QUEBEC

ELABORATED BY:
CARLOS MARIO MUNOZ TABORDA

REVISED BY: S-J BARNES

DIRECTED BY: S-J BARNES, MARK
FEKETE, EDWARD SAWYER

Figure 5.7: N-S and E-W profiles of BRC
showing the Pd values. The yellow line is the
proposed location of the reef.

DATE:

July, 2010

5.7

Figure 5.7 N-S and E-W profiles of BRC showing the Pd values, black dots are for values below 300ppb, red dots are for values between 300 and 500ppb and green dots are for values over 500ppb. The yellow line is the proposed location of the reef.

5.4. Formation processes of the Ebay's PGE reef

The Ebay zone of the BRC has experienced a number of processes; crystal fractionation, greenschist metamorphism, deformation, contact metamorphism and alteration due to the emplacement of the granitoid plutons. In order to consider the processes step by step, the first thing to understand is the process related to PGE collection that involves the formation of the reef.

To consider the concentration of the PGE and their appearance in the magmatic chamber we should consider previous work that explains their concentration. The PGE are chalcophile elements and therefore many studies consider them to be controlled by sulphides (Barnes et al., 1985; Barnes and Lightfoot, 2005; Naldrett, 2004). The model for the formation is that a mafic magma became saturated in a sulphide liquid. The sulphide liquid collected the platinum-group elements and the sulphide liquid in turn, was collected into the layers that now form the stratiform reef (Naldrett 2004). For the BRC, if the magma becomes saturated in sulphide, the process that includes the concentration of PGE and other metals associated like Ni, Au and Cu is illustrated in the spidergram (figure 5.8). In the Figure 5.8 the Ebay samples are normalized to primitive mantle for the PGE-rich rocks and the olivine gabbros. This diagram shows that the Ebay samples have Pd/Ir ratios ≈ 100 similar to basaltic liquids suggesting PGE were collected from a basaltic liquid. Ni/Cu varies because some samples contain cumulate olivine. The ratio of IPGE respect to PPGE is similar to deposits like Bushveld.

In the magmatic chamber, the layering processes including gravity settling, produces the concentration of sulphide droplets (and its PGE) in a layer. In the case of Ebay, is the layer #9. The cyclicity of the layering (mentioned in the chapter 2) probably formed the different showings in the central part of BRC such as Dotcom and Bwest (Figure 1.1). This gravity settling happened relatively efficiently, leaving some droplets isolated (Fig. 5.9a,b). These minor PGE concentrations are shown in the figure 5.4.

Mono-sulphide solid solution (MSS) crystallize from the sulphide liquid and the IPGE entered the MSS. The liquid that remained crystallized ISS and the final liquid between the MSS and the ISS became enriched in PPGE and crystallized the Pd + Pt as PGM. The PGE initially crystallized as PGM of Pt, Pd, Bi, Te, Sb and As.

As the temperature fell below 600°C, MSS exsolved to form Pentlandite + pyrrhotite and ISS forms chalcopyrite.

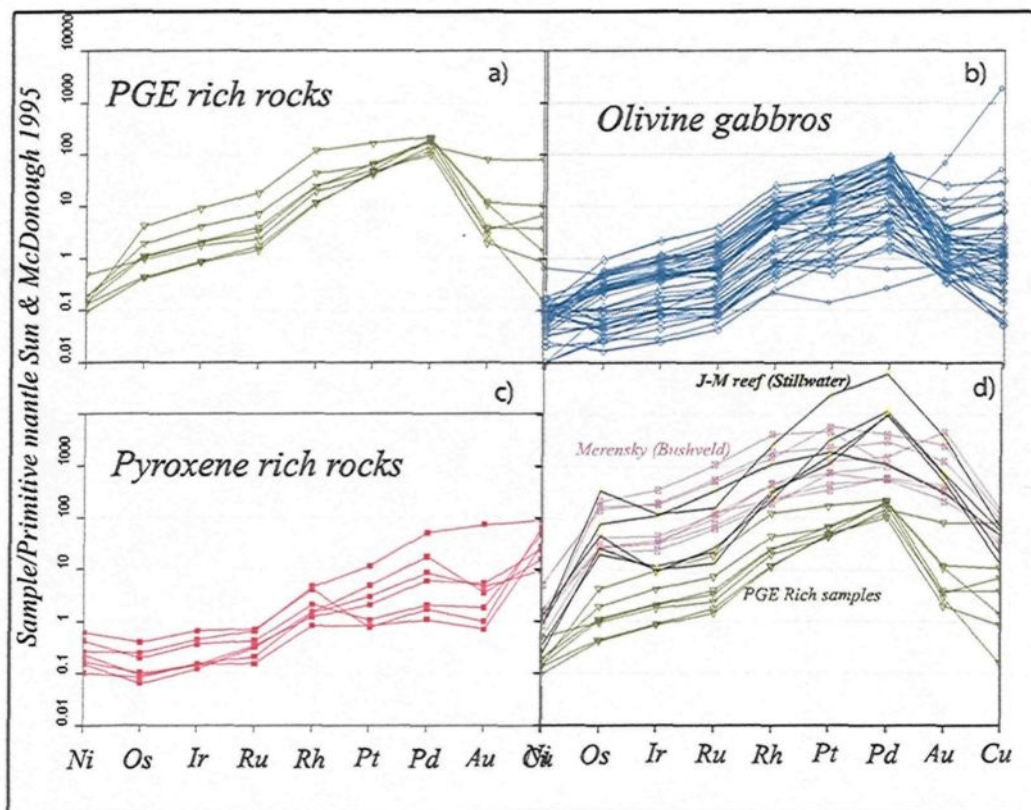


Figure 5.8 Ni-PGE-Au-Cu Spidergrams normalized to primitive mantle (Sun and Mc Donough, 1995) for Ebay and other PGE deposits. Stillwater from Godel et al., 2008; Merensky from Godel et al., 2007

The second magma arrived which formed the pyroxene rich rocks. This magma also become saturated in sulphides and collected PGE (Figure 5.8c).

Thereafter, the BRC suffered multiple metamorphic processes that modified the position of the layers and recrystallized the mineralogy (Chapter 3.1.1) including the PGM.

During metamorphism the S was remobilized from olivine gabbro samples resulting in mixed magmatic and hydrothermal sulphide mineral assemblages. The presence of fluids and textural signatures show that the sulphide minerals were strongly affected.

In contrast, the PGE were immobile and were left available for recrystallization of new PGM phases after sulphides were removed. Considering that metamorphism reached greenschist to amphibolite facies, temperatures could rise until they enabled the PGM to react with the surrounding fluids that were Bi-Te rich (Mihalik et al., 1974; Hoffman and MacLean, 1976). Probably some of the fluids came with the Lac Olga and Opaoca intrusions due to contact metamorphism considering that Bi and (Te?) are elements more abundant in the upper crust than in basaltic magmas (*Geochemical Earth Reference Model* web page <http://earthref.org/GERM/>). The diagram of Pd versus Bi (Figure 4.11) shows that Bi has been strongly modified and enriched in Ebay. The Bi values according to GEOROC and GERM for gabbros vary from 0.01 to 0.13 ppm and varies from 0.03 to 1.0 ppm for granites whereas the Bi values are from 0.16 to 0.96 for most Ebay

samples. This implies a strong interaction of the BRC with the granites of Opaoca and Lac Olga.

The PGM recrystallized, taking up Bi-Te from fluids in order to form the actual bismuth-tellurides and arsenides of PGE (Mihalik et al., 1974; Hoffman and MacLean, 1976). All of these processes happened without the addition of PGE.

With respect to the pyroxene-rich rocks; there are two possible hypotheses to consider for the formation of the present sulphide mineralogy. The pyroxene-rich rocks were initially rich in magmatic sulphides to explain S and Cu-rich nature of rocks; then, Fe-loss from sulphide during hydrothermal alteration resulting in pyrite formation from pyrrhotite. Or the pyroxene rich rocks have similar initial sulphide content to olivine gabbros and S + Cu was added during hydrothermal process. There is insufficient evidence to choose between these two possibilities.

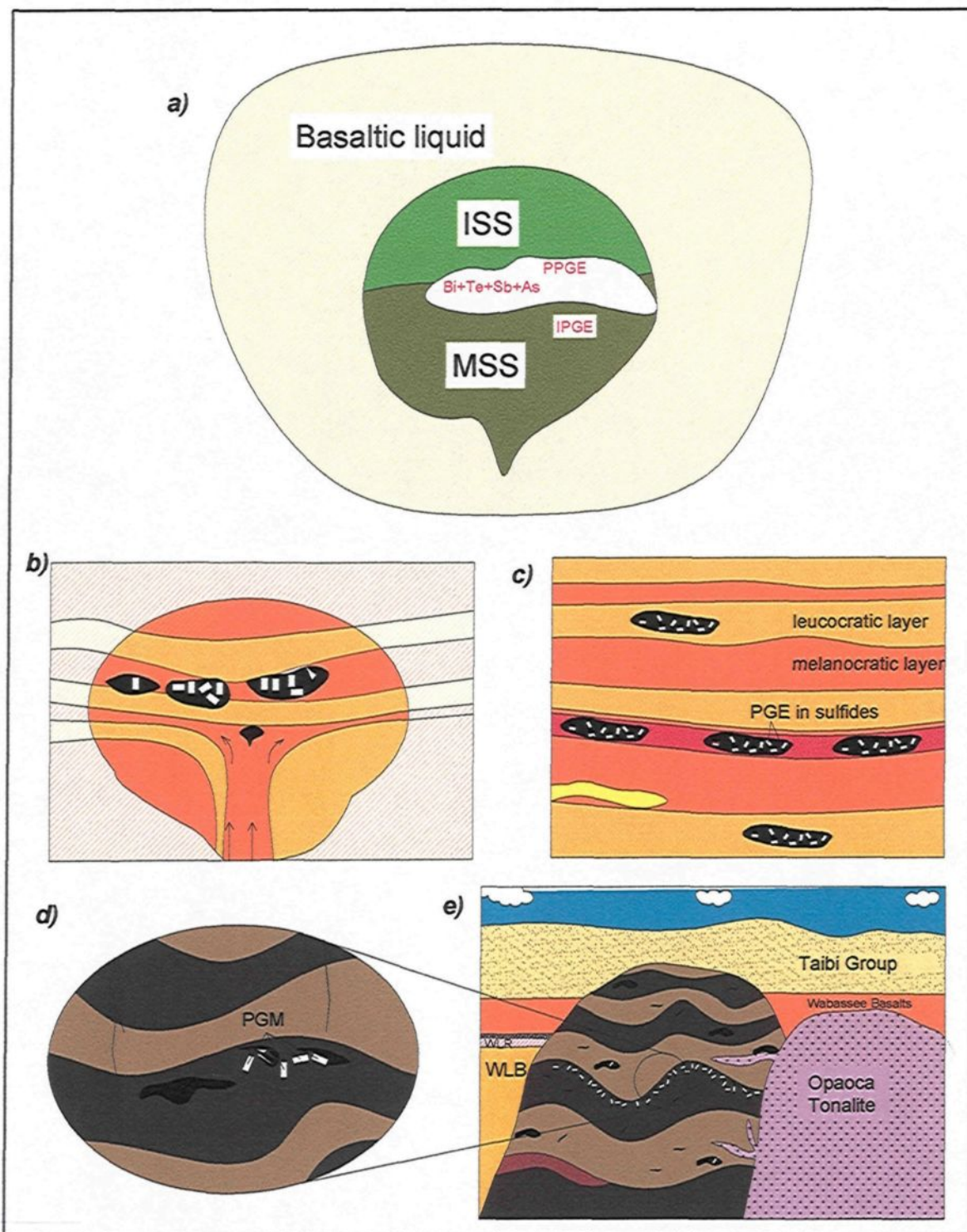


Figure 5.9 Diagram that represents the processes in the BRC at the Ebay zone and the PGM concentration. a) accumulation of PPGE between the MSS and the ISS in the sulphide liquid b) Magmatic chamber that shows the sulphide droplets (black) with the PGM (white crystals). c) Gravity settling the sulphide droplets principally at the top of layer #9. The bright yellow represents the second magma series (the pyroxene rich rocks). d) A detailed view of the processes in the reef during metamorphic events, the joints allowed the access of fluids into the rocks and permitted remobilized sulphides to leave behind the PGM that were able to react with fluids thereafter. e) The general context of BRC in the Ebay region. The Opaoca (the closest to BRC) and Lac Olga intrusions with their dykes crosscutting the layers. In this case the colors are the same used in the charts. The sequence around BRC from base to top is as follows: Watson Lake Basalts (orange), Watson Lake Rhyolite (dash red lines), Key Tuffite (black), Wabasseé Basalts (dark orange), and Taibi Group (beige).

5.5. Comparison to other PGE deposits

A detailed PGE spidergrams considering the PGE rich samples of Ebay and other PGE deposits is shown in Figure 5.8d and in Figure 5.10 upon Cu/Pd ratios. The diagrams, which are on the same scale, clearly illustrate the different behaviours. The olivine gabbros with Cu/Pd ratios over 6000 which include the hydrothermal sulphide bearing samples shown in the spidergrams (Figure 5.10d) appear to be rich in Cu and relatively poor in Pt and Pd with respect to the others. The samples whose Cu/Pd ratios are below 6000 (Figure 5.10b) clearly illustrate a process of enrichment of Pt and Pd with negative anomalies in copper and gold. The PGE rich rocks in the spidergram compared to Merensky and J-M Stillwater deposits (Figure 5.10d), show that the Ebay samples are clearly lower, but the trends are approximately similar.

The pyroxene rich rocks and the samples with $\text{Cu/Pd} > 6000$ show a pattern with very low Pt and Pd values.

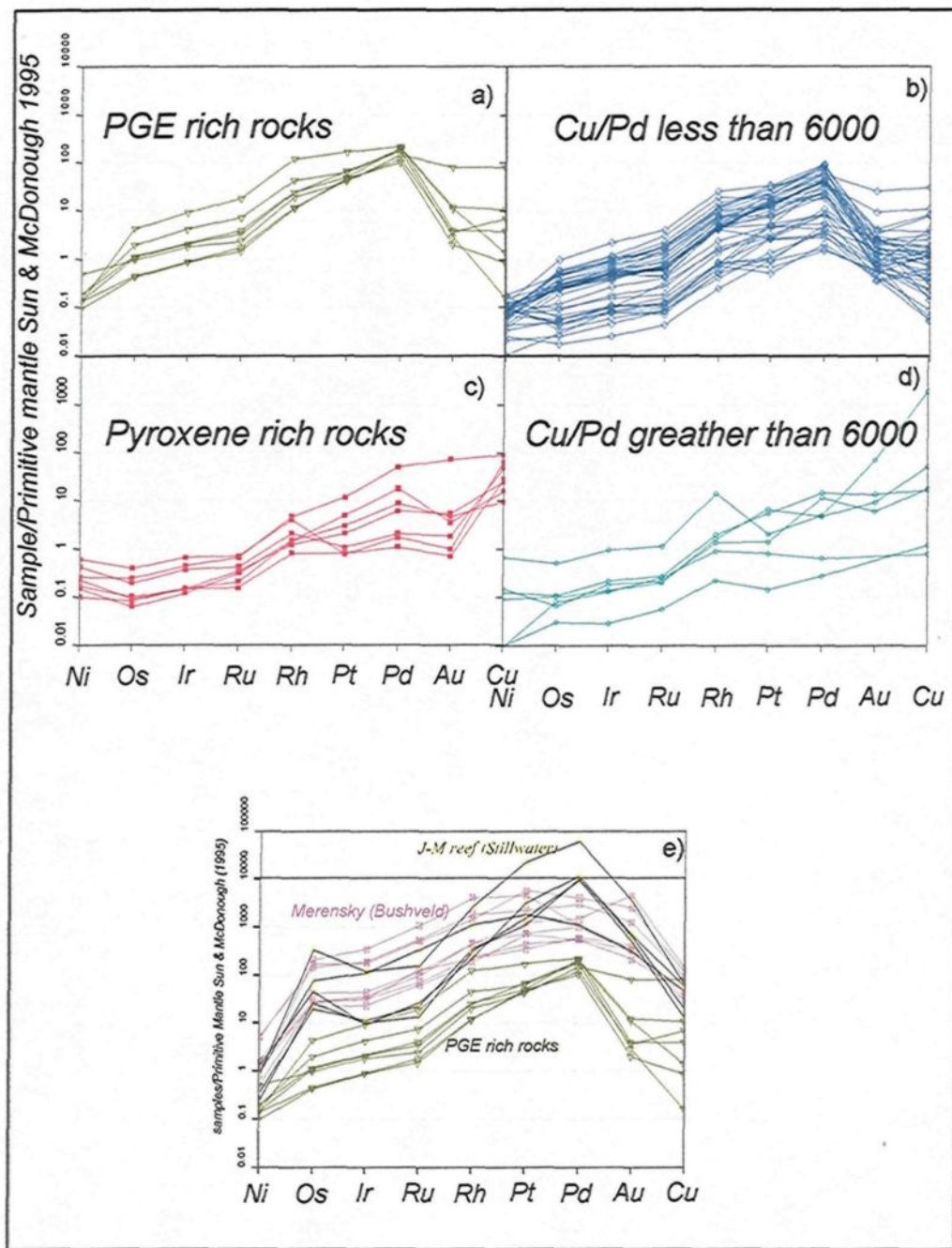


Figure 5.10 PGE Ni, Au and Cu Spidergrams after Cu/Pd ratios. Figures a,b and d correspond to olivine gabbros. Bushveld (Merensky reef pink) and Stillwater (J-M reef yellow). Stillwater from Godel et al., 2008; Merensky from Godel et al., 2007.

Regarding the Mg# for different deposits (Figure 5.11), the BRC has similar values to Merensky and Platreef. The magnesium number is on average 0.73 for BRC samples; for the Bushveld, the values change a little more; at depth the Mg# is over 0.80 including UG-1 and UG-2. In the Merensky reef, the values decrease and vary from 0.70 to 0.80 and finally, in the Main Zone, the values decrease to 0.70.

Considering the interval Critical-Main Zone of Bushveld and comparing this with BRC, both of which are on the same scale (Figure 5.12), it is clearly noticed how the interval related to the upper part of the Critical Zone, which includes the Merensky reef, resembles the BRC interval where the presence of the reef is proposed.

Table 5.1 summarizes the characteristics of the most important PGE deposits. In the table, the BRC's Ebay shares similar characteristics in terms of PGM to Ala Penikka (AP reef) of the Penikat layered intrusion. It suffered metamorphism (Halkoaho, 1994) as did Ebay. The olivine that is the most important phase for Ebay is not present in AP but is present in JM reef in Stillwater. The rock protoliths in Ebay hosting PGM are olivine gabbro-norites and leucogabbro-norites which comprise the mafic part of the complex. This part resembles many deposits but does not fit within magnetite- or chromite-bearing deposits, which have not been seen in Ebay.

We could say that BRC resembles the Stillwater's J-M reef regarding its silicate mineralogy (Table 5.1), however the Mg# for Stillwater varies from 76 to 86

(McCallum, 1996) whereas the Mg number for Ebay seems to indicate that we are in the corresponding interval of Critical-Main Zone of Bushveld. A look at the geological map and the petrography of BRC indicates that we are closer to the mafic-ultramafic border. The BRC composition is more mafic at Ebay and it closely resembles the Main Zone whereas structurally the Stillwater is very different to BRC. Stillwater "have an unknown size and shape and only a portion is exposed in a fault-bounded block along the northern margin of the Beartooth uplift" (Zientek et al., 2002). The PGM assemblage of BRC does resemble the AP reef of Penikat. The PGM in Stillwater are sulphides and alloys. Stillwater, Penikat and BRC have undergone metamorphic events which have not happened to Merensky reef.

In summary, Ebay does share similarities with many deposits but shares more characteristics with AP reef of the Penikat intrusion regarding the PGM phases, the position and the metamorphism.

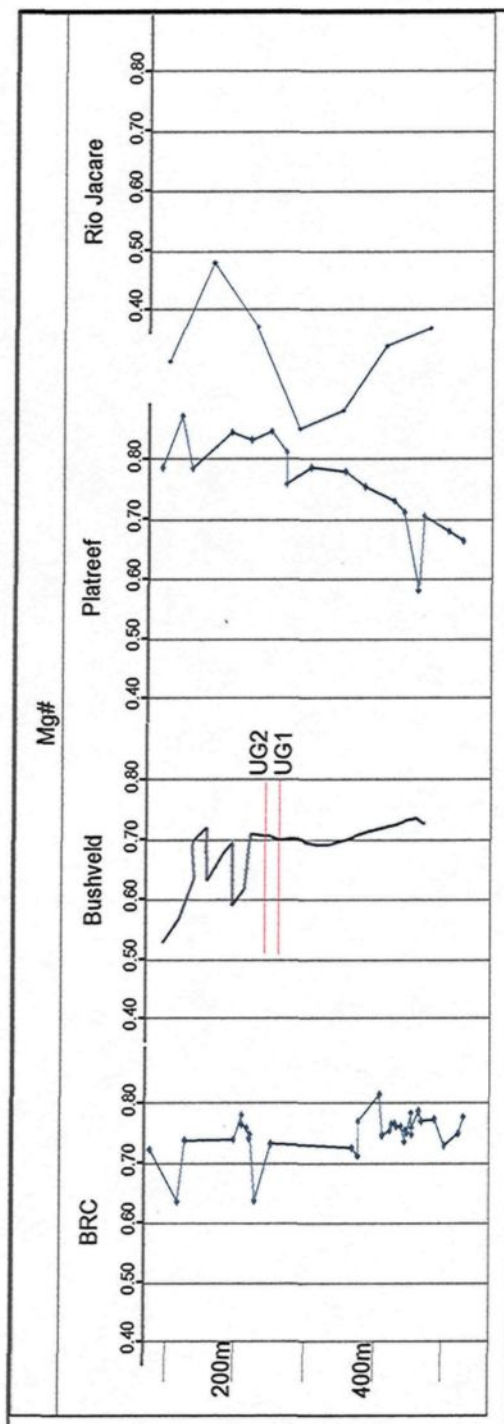


Figure 5.11 Mg number [$Mg\# = Mg/(Mg+Fe_T)$] for different PGE deposits, all at the same scale. Bushveld from Eales and Cawthorn, 1996; Platreef from Harris and Chaumba, 2001 and Rio Jacare from Sa et al., 2005.

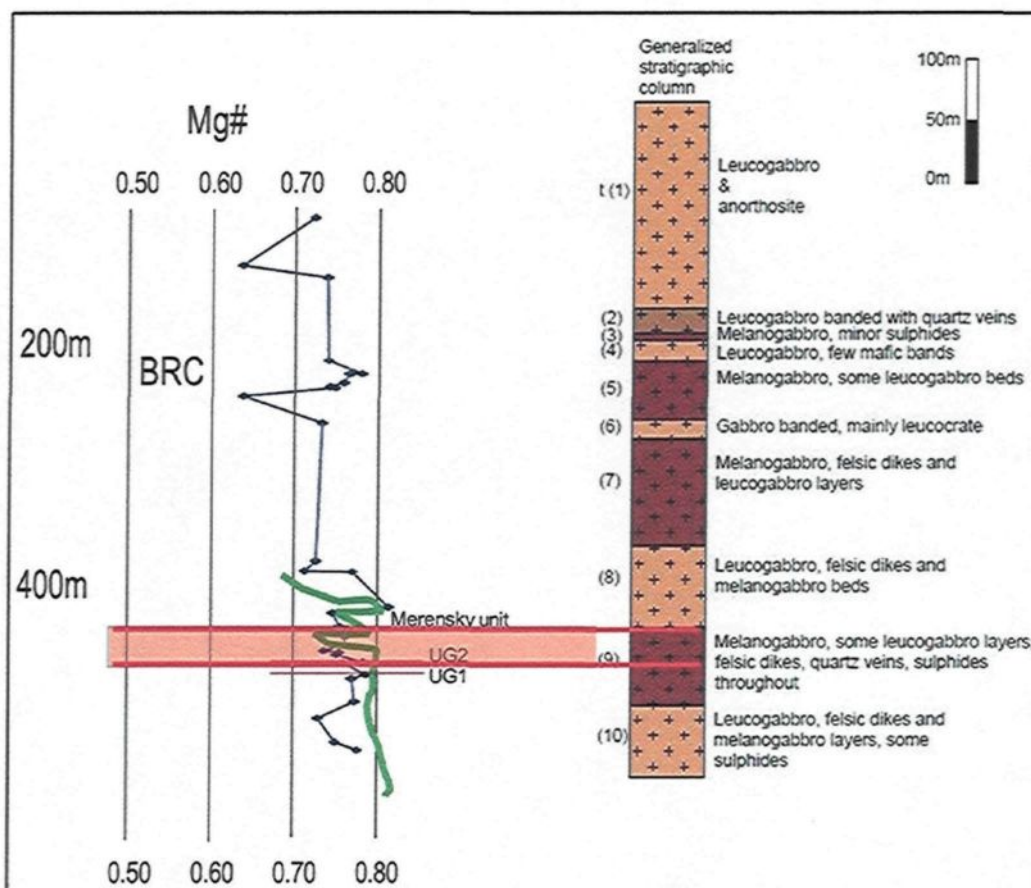


Figure 5.12 Comparison of the Mg# between BRC (blue) in a generalized stratigraphic column and the interval Critical-Main Zones of Bushveld (green). Bushveld data from Eales and Cawthorn, 1996.

Table 5.1 Characteristics of the different PGE deposits of the world

deposit	location	type	place in the intrusion	most important phase associated	type sulphides	host rocks	main PGE	main PGM	Px type
UG-2	Bushveld Complex	reef	Critical Zone	chromite	Pn, Ccp, Po, Py	Chromitite	Pt+Pd	RuS ₂ , PtS, Pt, Ir, Rh, Cu sulphide, (Pt, Pd, Ni)S (\$\$)	Opx
Merensky	Bushveld Complex	reef	Critical Zone	Sulphides	Po, Pn, Ccp	Chromitite	Pt+Pd (Au, Cu, Ni)	(Pt, Pd)S, PtS, RuS ₂ , Pt-Fe alloy(!)	Opx
Platreef	Bushveld Complex	broad zone	Mafic (main)	Sulphides	Pn, Po, Ccp	Pyroxenite, Norite, xenolites of dolomite	Pt+Pd	Pt-Pd tellurides, Pt Arsenides (*)	Cpx, Opx
Main sulphide zone	Great Dyke	reef	Layer 1/3	Sulphides	Po, Pn, Ccp	Pyroxenites	Pt+Pd	Pt-Pd bismuthotellurides, PtAs ₂ , PtS/(Pt, Pd)S, sulpharsenides(<)	Cpx
J-M reef	Stillwater Complex	reef	Midle	Sulphides	Po-Pn-Ccp	Olivine-Gabbro	Pd	Pd-Pt-Ru sulphides; Pt-Pd tellurides and arsenides; Pt-Fe, Pt-Pd-Sn, Pd-Pb, Pd-Hg, Au-Pt-Pd, Rh-Pt alloys(+)	Opx
Platinova	Skaergaard Complex	reef	Gabbroic	Sulphides	Bn, Dg, Ccp	Melagabbro to Leucogabbro	Pd	(Cu, Fe)(Au, Pd, Pt) (>) PdCu	Cpx
Upper Main, LG, Mid, Footwall reefs	Stella layered intrusion Kraipaan belt	reef	Gabbroic	Magnetite	Ccp, Py	Magnetite + Gabbros	Pt+Pd	PdTe ₂ , Pd ₅ +xSb ₂ -x, PtAs ₂ , PdTe, Pd ₆ As ₂ 5Sb _{0.5} , Ferroplatinum (:)	Cpx
Sompurjarvi (SJ)	Penikat layered intrusion	reef	bottom ultramafic	Sulphides & Chromite	Cr, Py-Pn-Ccp or Po-Pn-Ccp	Gabbroite, pokilitic plagioclase-bronzite orthocumulates; bronzite cumulates	Pt+Pd	Pd-As-Sb, PtAs ₂ , PGE-Fe-Cu-Mn hydroxides, PGE sulphides except RuS ₂ (†)	Opx
Aia-Penikka (AP)		reef	Midle Mafic	Sulphides	Po-Pn-Ccp	Metagabbroite	Pt+Pd	Pd-Te-(Bi), PtAs ₂ , Pd-As-Sb, Pt-Pd sulphides (†)	Opx, Cpx
Paasivaara (PV)		reef	Midle Mafic	Sulphides	Po-Pn-Ccp	Metagabbroite	Pt+Pd	PtS ₂ , PdTe, Pd ₁₁ Sb ₂ As ₂ , PdTe ₂ , Pd ₅ +xSb ₂ -x (‡), (Pt, Pd)S, PtS (x)	Opx
Rincon del Tigre	Rincon del Tigre Complex	reef	Gabbroic	Sulphides, magnetite	Bn-Cc-Ccp-Cv high Cu; low Fe, Ni	Magnetite gabbros	PGE	Pt-Co-Cu-S, Pt-Pd-S, Pt-S, Pt-As, Pd-(Pt)-Te, Pd(-Te, As), Pd-Te (!)	Opx sometimes
Rio Jacare	Rio Jacare Intrusion	reef	upper part of mafic zone	Magnetite	Mgt-Ilm-Pn PGE	Magnetite pyroxenite, gabbros	Pd+Pt	Pd (bismuthides and antimonides), PtAs (#)	Cpx
Roby zone	Lac des Iles Complex	breccia elipsoidal	Gabbroic	Sulphides	Ccp-Pn-Po-Py-Mil	Norite, breccia	Pd	PdS, PdSbAs, PdTe (~)	Opx

(\$\$) McLaren & Villiers, 1982

(!) Vermaak & Hendriks, 1976

(*) Holwell, D., McDonald, I. 2007

(<) Oberthur, T., 2002

(+) Zientek, M., et al, 2002

(>) Andersen, J., et al., 1998

(+) Zientek, M., et al, 2002

(>) Andersen, J., et al., 1998

(:) Richards, J., Martin, G., 2002 in Maier et al., 2003

(†) Halkoaho, T., 1994

({}) Huhtelin, T. et al., 1989

(x) Alapeti, T., Lahtinen, J., 1986

(!) Prichard H., 1996 Pers. Commun. as quoted by Prendergast, 2000

(#) Sa, J., et al., 2005

(-) Hinchey, J., et al., 2005

(-) Gowme, T., 2008

CHAPTER 6

CONCLUSIONS

The Bell River Complex is recognized as a layered intrusion based on numerous studies (Freeman, 1939, Maier *et al.*, 1996; Goutier, 2005). The layering occurs at different scales, from centimeters to meters. However, in our study the layering was modal, dependent upon the predominance of leuco- or melanocratic minerals. The description of the borehole samples was used to draw a stratigraphic column which was then correlated with other boreholes in order to establish a stratigraphic sequence.

The reconstruction has permitted us to define the layers in the Ebay zone. With this knowledge we realized that the layers sampled in the north-south profile do not correspond exactly to those that appear at the east-west profile. The layers in the north-south profile correspond to the uppermost layers of the east-west profile. The north-south layers are poor in PGE.

From the relationships between the major elements and the very low minor element contents (i.e. P_2O_5 and TiO_2), it can be concluded that most of the rocks are plagioclase-olivine cumulates with very little trapped liquid component. A small group of samples are rich in pyroxene and distinct from the olivine gabbros.

The petrological analyses have permitted us to discern the presence of magmatic and hydrothermal events originating from different places and different depths. The first metamorphic event is regional in scale, it was either ocean floor metamorphism and/or regional that also produced the Galinée and Puchot anticlines. This event was followed by contact metamorphism and associated circulation of hydrothermal fluids which occurred due to the intrusion of the nearby Opaoca and probably also the Lac Olga plutons. The presence of unmetamorphosed felsic dykes defines the hydrothermal event.

The pyroxene rich rocks are clearly different from the other groups and represent a second magma series. They have relatively high magnesium and calcium contents, low aluminium and alkalis. The normative CIPW compositions indicate more pyroxene for this group and are classified as plagioclase bearing pyroxenites, melagabbronorites, gabbronorites and olivine gabbronorites. The other samples, consists of olivine-plagioclase dominated rocks and are classified as olivine-gabbronorites, gabbronorites, leuconorites, leucogabbronorites, leucotroctolites and anorthosites. On the spidergrams, the pyroxene rich rocks are less evolved.

The rocks of the BRC correspond to cumulate rocks which were formed by the accumulation of the different crystals as a result of gravity settling.

The sample ML-52 corresponds to a quartz-bearing dyke and has a different geochemical behavior on the compositional diagrams. This sample does not

correspond with the main trends, and together with the pyroxene rich rocks, is not part of the main sequence of crystallization in the BRC.

The presence of a PGE reef at the top of the layer #9 is proposed for the Ebay showing. It consists of olivine gabbro-norites, leucogabbro-norites and a leucotroctolite. The PGM are hosted in silicates, and only a few grains were found in the sulphide minerals. The most important PGM phases are bismuth-tellurides and antimony-arsenides. The Pt and Pd are the most important elements. They are present in approximately the same proportion and together sum up to 1 or 2 ppm Pt + Pd. The layer hosting PGE is folded and had not been sampled in many places. It is for this reason that a more detailed sampling is proposed for this layer along the claim as well as in the places already stated. This is in order to more accurately establish its thickness and position (see Appendix 11 for the proposed sampling).

The phase that collected the PGE is not clear since there are not correlations between PGE and S, Bi, Cu or any chalcophile element. However, considering the presence of some PGM in sulphides, I propose that the formation of the reef could be attributed to collection by sulphides. The sulphide liquid collected the PGE, and then they were collected on the layer #9. Following this, metamorphism occurs and sulphur was mobilized from the PGE bearing layer.

Compared to other PGE deposits, Ebay share similarities with reef type deposits, in particular with AP reef of the Penikat intrusion.

The effect of hydrothermal activity, metamorphism and alteration on the samples plays an important role in the silicate minerals. Hydrothermal and metamorphic events at greenschist-amphibolite facies in the zone could have generated the recrystallization of PGE and brought other REE involved in the PGM phases.

BIBLIOGRAPHY

Adam, E., Milkereit, G., Mareschal, M. 1998. Seismic reflection and borehole geophysical investigations in the Matagami mining camp. *Canadian Journal of Earth Sciences* 35: 686-695.

Alapieti, T.T., and Lahtinen, J., J. 1986. Stratigraphy, petrology, and platinum-group element mineralization of the early Proterozoic Penikat layered intrusion, northern Finland. *Economic Geology* 81: 1126-1136.

Allard, G., O. 1970. The Doré Lake Complex, Chibougamau, Québec. A metamorphosed Bushveld type layered intrusion. In *Symposium on the Bushveld Igneous Complex and other layered intrusions*. Edited by J.L. Visser and G. Von Gruenewaldt. The Geological Society of South Africa. Special publication 1: 477-491.

Andersen, JCØ, Rasmussen, H., Nielsen, TFD, Ronsbø, JG. 1998. The Triple Group and the Platinova gold and palladium reefs in the Skaergaard intrusion: Stratigraphic and petrographic relations. *Economic Geology* 93:488–509.

Ayer, J., Amelin, Y., Corfu, F., Kamo, S., Ketchum, J., Kwok, K., Trowell, N. 2002. Evolution of the southern Abitibi greenstone belt based on U–Pb geochronology: autochthonous volcanic construction followed by plutonism, regional deformation and sedimentation. *Precambrian Research* 115: 63–95.

Bancroft, J. A. 1912. A report on the geology and natural resources of certain parts of the drainage basins of the Harricana and Nottaway Rivers, to the north of the National Transcontinental Railway in Northwestern Quebec. In *Quebec Bureau of Mines, Reports on Mining Operations*: 143 -216.

Barnes, S.-J., Maier, W.D. 2002. Platinum-group element distribution in the Rustenburg Layered Suite of the Bushveld Complex, South Africa. In: Cabri, L.J. (Ed.), *Geology, Geochemistry, Mineralogy and Mineral Benefication of Platinum Group Element*. Canadian Institute of Mining, Metallurgy and Petroleum, Special Volume 54: 459–481.

Barnes, S.-J., and Maier, W.D., 2002b. Platinum-group Elements and Microstructures of Normal Merensky Reef from Impala Platinum Mines, Bushveld Complex. *Journal of Petrology* 43: 103-128.

Barnes, S.-J., Maier W.D., Ashwal L.D. 2004. Platinum-group element distribution in the Main Zone and Upper Zone of the Bushveld Complex, South Africa. *Chemical Geology* 208: 293– 317.

Barnes, S.-J., Makovicky, E., Makovicky, M., Rose-Hansen, J., and Karup-Moller, S. 1997. Partition coefficients for Ni, Cu, Pd, Pt, Rh, and Ir between monosulphide solid solution and sulphide liquid and the formation of compositionally zoned Ni-Cu sulphide bodies by fractional crystallization of sulphide liquid. *Canadian Journal of Earth Sciences* 34: 366–374.

Barnes, S.-J., Naldrett, A.J., and Gorton, M.P. 1985. The origin of the fractionation of platinum-group elements in terrestrial magmas: *Chemical Geology* 53: 303-323.

Barnes, S.-J. and Picard, C.P. 1993. The behavior of platinum-group elements during partial melting, crystal fractionation and sulphide segregation: An example from the Cape Smith fold belt, northern Quebec; *Geochimica Cosmochimica Acta* 57: 79-87.

Barnes, S.-J., Prichard, H.M., Cox, R.A., Fisher, P.C., and Godel, B., 2008. The location of the chalcophile and siderophile elements in platinum-group element ore deposits (a textural, microbeam and whole rock geochemical study): Implications for the formation of the deposits. *Chemical Geology* 248: 295-317.

Barnes, S.-J., Sawyer, E.W. Mainville, M. Bouchaib, C., 1992. Reconnaissance results from the Belleterre Angliers Belt. In: *Lithoprobe, Abitibi-Grenville Transect: report n 25: 135-138.*

Barnes, S.-J., Couture, J. F., Poitras, A., Tremblay, C. 1993. Les éléments du groupe du platine dans la partie québécoise de la ceinture de roches vertes de l'Abitibi. *Ministère de l'Énergie et des ressources du Québec; ET 91-04, 100p.*

Barnes, S.-J., Couture, J. F., Sawyer, E.W., Bouchaib, C. 1993. Nickel-Copper Occurrences in the Belleterre-Angliers Belt of the Pontiac Subprovince and the use of Cu-Pd Ratios in interpreting Platinum-Group Elements Distributions. *Economic Geology* 88: 1403-1418.

Bédard, L.P., Savard D., and Barnes, S.-J. 2008. Total sulfur concentration in geological reference materials by elemental infrared analyser. *Geostandards and Geoanalytical Research*, 32: 203-208.

Card, K.D., and Ciesielski, A., 1986. Subdivisions of the Superior Province of the Canadian Shield. *Geoscience Canada* 13: 5-13.

Cawthorn, R.G., Barton, J.M., and Viljoen, M.J., 1985. Interaction of floor rocks with the Platreef on Overysel, Potgietersrus, northern Transvaal. *Economic Geology* 80: 988-1006.

Cawthorn, G., 1999. Platinum group element mineralization in the Bushveld Complex - A critical reassessment of geochemical models. *South African Journal of Geology* 102: 268-281.

Cawthorn, G., 2005. Stratiform platinum-group element deposits in layered intrusions, Chapter 3. In *Exploration for deposits of platinum-group elements*. Mungall, J. 2005 (ed.). Mineralogical Association of Canada Short Course Series Volume 35: 57-74.

Cousins, C., A. and Vermaak, C.F., 1976. The contribution of Southern African ore deposits to the geochemistry of the platinum group metals. *Economic Geology* 71: 287-305.

Davis, D.W., 2002. U-Pb geochronology of Archean metasedimentary rocks in the Pontiac and Abitibi subprovinces, Quebec, constraints on timing, provenance and regional tectonics. *Precambrian Research* 115: 97-117.

Eales, H., Cawthorn, R. 1996. The Bushveld complex. in *Layered intrusions*. Cawthorn (ed) 1996. p 181-229.

Farrow, C., Lightfoot, P. 2002. Sudbury PGE revisited: Towards an integrated model. In: Cabri, L.J. (Ed.), *Geology, Geochemistry, Mineralogy and Mineral Beneficiation of Platinum Group Element*. Canadian Institute of Mining, Metallurgy and Petroleum, Special Volume 54: 273-298.

Freeman, B., C. 1939. The Bell River Complex, northwestern Quebec. *Journal of Geology* 47: 29 -46.

Green, A., Peck D. 2005. PGE Exploration: Economic Considerations and Geological Criteria, in *Mineralogical Association of Canada. Short Course Series Volume 35*. Edited by James E. Mungall. University of Toronto: 247-274.

Godel, B., Barnes, S.-J., and Maier, W.D., 2007. Platinum-Group Elements in Sulphide Minerals, Platinum-Group Minerals, and Whole-Rocks of the Merensky Reef (Bushveld Complex, South Africa): Implications for the Formation of the Reef. *Journal of Petrology* 48: 1569-1604.

Godel, B., and Barnes, S.-J., 2008. Platinum-group elements in sulfide minerals and the whole rocks of the J-M Reef (Stillwater Complex): Implication for the formation of the reef. *Chemical Geology* 248: 272-294.

Goutier, J., 2005. Géologie de la région de la baie Ramsay (32F/10) et de la rivière Opaoca (32F/11). Ministère des Ressources naturelles et de la Faune, Québec; RG 2005-01, 56 pages et 8 cartes.

Goutier, J. Melançon, M., 2007. Compilation géologique de la Sous-province de l'Abitibi (version préliminaire). Ministère des Ressources naturelles et de la Faune, Québec; échelle 1/500 000.

Halkoaho, T., 1994. The Sompujärvi and Ala-Penikka PGE reefs in the Penikat layered intrusion, Northern Finland, Implications for PGE reef-Forming processes. Academic dissertation. 122p.

Harris C., Chaumba, J. 2001. Crustal contamination and fluid-rock interaction during the formation of the Platreef, Northern limb of the Bushveld complex, South Africa, *Journal of Petrology* 42: 1321-1347.

Hiemstra, S.A., 1979. The role of collectors in the formation of platinum deposits in the Bushveld Complex. *Canadian Mineralogy* 17: 469-482.

Hinchey, J., Hattori, K., Lavigne, M., 2005. Geology, Petrology, and controls on PGE Mineralization of the southern Roby and Twilight zones, Lac Des Iles Mine, Canada. *Economic Geology* 100: 43-61.

Hoatson, D.M., Keays, R.R., 1989. Formation of platiniferous sulfide horizons by crystal fractionation and magma mixing in the Munni Munni layered intrusion, west Pilbara block, Western Australia. *Economic Geology* 84: 1775–1804.

Hocq, M., 1994. Géologie du Québec. Gouvernement du Québec, Québec : 154p.

Hocq, M., 1990. Carte lithotectonique des sous-provinces de l'Abitibi et du Pontiac. Ministère de l'énergie et des ressources, Québec DV 89-04.

Hoffman, E. MacLean, W. H. 1976. Phase relations of the Michenerite and Merenskyite in the Pd-Bi-Te system. *Economic Geology* 71: 1461-1468.

Holwell, D., McDonald I., 2007. Distribution of platinum-group elements in the Platreef at Overysel, northern Bushveld Complex: a combined PGM and LA-ICP-MS study. *Contributions to Mineral Petrology* 154:171–190.

Huhtelin, T., Alapieti, T., Korvuo, E., Sotka, P. 1989. The Paasivaara PGE mineralization in the Penikat layered intrusion, Northern Finland. In: Alapieti, T., 1989 (ed.). 5th international Platinum symposium, Guide to the post-symposium field trip, August 4-11, 1989: 123-144.

Keays, R.R., Ross, J., R. and Woolrich, P., 1981. Precious metals in volcanic peridotite-associated nickel sulphide deposits in Western Australia, II. Distribution within the ores and host rocks at Kambalda. *Economic Geology* 76: 1645-1674.

Keays, R.R., Nickel, E.H., Groves, D.I. and McGoldrick, P.J., 1982. Iridium and alladium as discriminants of volcanic-exhalative hydrothermal and magmatic nickel sulfide mineralization. *Economic Geology* 77: 1535-1547.

Lavigne, M., J., Michaud, M., J. 2001. Geology of North American Palladium Ltd.'s Roby Zone Deposit. *Exploration and Mining Geology* 10: 1-17.

Le Maitre, R.W., Bateman, P., Dudek, A., Keller, J., Lameyre, J., Le Bas, M.J., Sabine, P.A., Schmid, R., Sorensen, H., Streckeisen, A., Woolley, A.R. & Zanettin, B., 1989. A Classification of Igneous Rocks and Glossary of terms: Recommendations of the International Union of Geological Sciences (IUGS) Subcommittee on the Systematics of Igneous Rocks. Blackwell Scientific Publications, Oxford, U.K. 193p.

Lavigne, M.J., and Michaud, M.J., 2001. Geology of North American Palladium Ltd.'s Roby zone deposit, Lac des Iles. *Exploration and Mining Geology* 10: 1-17.

Li, C., Ripley, E. 2005. Empirical equations to predict the sulfur content of mafic magmas at sulfide saturation and application to magmatic sulfide deposits. *Mineralium Deposita* 40: 218-230.

MacGeehan, P.J., and MacLean, W.H. 1980. Tholeiitic basalt -rhyolite magmatism and massive sulphide deposits at Matagami, Quebec. *Nature (London)* 283: 53- 57.

MacGeehan, P.J., 1978. The geochemistry of altered volcanic rocks at Matagami, Quebec: a geothermal model for massive sulphide genesis. *Canadian Journal of Earth Sciences* 15: 551-570.

MacLean, W.H. 1984. Geology and ore deposits of the Matagami district. In Chibougarnau-stratigraphy and mineralization. Edited by J. Guha and E.H. Chown. *Canadian Institute of Mining and Metallurgy* 34: 483-495.

McCallum, I. 1996. The Stillwater complex, in Layered intrusions. Cawthorn (ed.) 1996. p 441-483

Maier, W., D. 2005. Platinum-group element (PGE) deposits and occurrences: Mineralization styles, genetic concepts, and exploration criteria. *Journal of African Earth Sciences* 41: 165-191.

Maier, W., D., Barnes, S.-J., Pellet, T., 1996. The economic significance of the Bell River Complex, Abitibi Sub-province, Québec. *Canadian Journal of Earth Sciences* 33: 967–980.

Maier W., D., de Klerk, L., Blaine, J., Manyeruke, T., Barnes, S.-J., Stevens, M.V.A., Mavrogenes, J.A. 2008. Petrogenesis of contact-style PGE mineralization in the northern lobe of the Bushveld Complex: comparison of data from the farms Rooipoort, Townlands, Drenthe and Nonnenwerth. *Mineralium Deposita* 43: 255-280.

McCallum, M.E., Loucks, R.R., Carlson, R.R., Cooley, E.F., and Doerge, T.A., 1976. Platinum metals associated with hydrothermal copper ores of the New Rambler Mine, Medicine Bow Mountains, Wyoming. *Economic Geology* 71: 1429-1450.

McCallum, M.E., Lovacks, R.R., Carlson, R.R., Cooley, E.F. and Docrye, T.A., 1976. Platinum metals associated with hydrothermal copper ores of the New Rambler mine, Medicine Bow Mountains, Wyoming. *Economic Geology* 71: 1429-1450.

McLaren & De Villiers, 1982. The Platinum-Group Chemistry and Mineralogy of the UG-2 Chromitite Layer of the Bushveld Complex. *Economic Geology* 77:1348-1366.

Mercier, D., 1991. Leve geologique et analyses lithogeochemiques, project Opaoca (101089). Rapport statutaire depose au ministere des ressources naturelles et de la faune, Quebec ; GM 51240, 320 pages et 11 cartes.

Mercier, D., 1992. Rapport de la campagne de geologie, prospection, sondage pionjar et decapage, été-autumne 1992, project Opaoca (1089). Rapport statutaire depose au ministere des ressources naturelles et de la faune, Quebec ; GM 51857, 266 pages et 50 cartes.

Mihalik, P., Jacobsen, J. B. E. and Hiemstra, S. A. 1974. Platinum-group minerals from a hydrothermal environment. *Economic Geology* 69: 263-266.

Ministere de l'Energie et des Ressources du Quebec-Ontario Geological Survey, 1983. Lithostratigraphic map of the Abitibi subprovince Ontario Geological Survey-Quebec Ministere Energie Ressources, DV 83-16, 1:500 000.

Mortensen, J.K. 1993. U - Pb geochronology of the eastern Abitibi Subprovince, Part 1: Chibougamau - Matagami -Joutel region. *Canadian Journal of Earth Sciences* 30: 11-28.

Mungall, J. 2005. Exploration for deposits of platinum-group elements. Mineralogical Association of Canada. Short Course Series Volume 35. Edited by James E. Mungall. University of Toronto: 494p.

Nabil, H., 2003. Genèse des dépôts de Fe-Ti-P associés aux intrusions litées (exemples: l'intrusion mafique de Sept-Iles, au Québec; complexe de Duluth aux États-Unis). Thèse de doctorat Université du Québec à Chicoutimi et Université du Québec à Montréal : 537p.

Naldrett, A.J., 2004. Magmatic Sulfide Deposits: Geology, Geochemistry and Exploration, Springer Verlag : 728p.

Naldrett, A.J., Hoffman, E.L., Green, A.H., Chou, C.L., Naldrett, S.R., and Alcock, R.A., 1979. The composition of Ni-sulfide ores, with particular reference to their content of PGE and Au. *Canadian Mineralogy* 17: 403-415.

Nielsen, T., and Brooks C. 1995. Precious metals in magmas of East Greenland Factors important to the mineralization in the Skaergaard Intrusion. *Economic Geology* 90: 1911-1917.

Oberthür, T. 2002. Platinum-Group Element Mineralization of the Great Dyke, Zimbabwe. In: Cabri, L.J. (Ed.), *Geology, Geochemistry, Mineralogy and Mineral Beneficiation of Platinum Group Element*. Canadian Institute of Mining, Metallurgy and Petroleum, Special Volume 54: 459-481.

Peregoedova A., Barnes, S.-J., Baker, D., 2006. An experimental study of mass transfer of platinum-group elements, gold, nickel and copper in sulfur-dominated vapor at magmatic temperatures. *Chemical Geology* 235: 59-75.

Piche, M., Guha, J., and Daigneault, R., 1993. Stratigraphic and structural aspects of the volcanic rocks of the Matagami mining camp, Quebec; implications for the Norita ore deposit. *Economic Geology* 88: 1542-1558.

Prendergast, M. 1990. Platinum-group minerals and hydrosilicate 'alteration' in Wedza-Mimosa platinum deposit, Great Dyke, Zimbabwe -genetic and metallurgical implications. *Transactions of the Institution of Mining and Metallurgy (Section B: Applied earth science)* 99: B91-B105.

Prendergast, M., 2000. Layering and precious metals mineralization in the Rincon Del Tigre Complex, Eastern Bolivia. *Economic Geology* 95: 113-130.

Ripley, E., Shafer, P., Chusi Li, Hauck, S. 2008. Re–Os and O isotopic variations in magnetite from the contact zone of the Duluth Complex and the Biwabik Iron Formation, northeastern Minnesota. *Chemical Geology* 249: 213–226.

Rousell, D., Fedorowich, J., Dressler, B., 2003. Sudbury Breccia (Canada): a product of the 1850 Ma Sudbury Event and host to footwall Cu–Ni–PGE deposits. *Earth-Science Reviews* 60: 147–174.

Savard, D., Bédard, L.P., Meisel, T., and Barnes, S.-J. 2009. Comparison between nickel-sulfur-fire-assay Te-Co-precipitation and isotopic dilution with high-pressure techniques for determination of platinum-group elements, rhenium and gold. International Association of Geoanalysts annual meeting: *Geoanalysis 2009*, South Africa.

Sharpe, J. 1968. Geology and sulfide deposits of the Matagami area, Abitibi - East County. Quebec Department of Natural Resources. *Geological Report* 137.

Sa, J., Barnes, S.-J., Prichard, H., Fisher, P. 2005. The distribution of base metals and Platinum-group elements in magnetite and its host rocks in the Rio Jacare intrusion, Northeastern Brazil. *Economic Geology* 100: 333-348.

Scoon, R. and Mitchell, A. 2004. Petrogenesis of Discordant Magnesian Dunite Pipes from the Central Sector of the Eastern Bushveld Complex with Emphasis on the Winnaarshoek Pipe and Disruption of the Merensky Reef. *Economic Geology* 99: 517-541.

Tafadzwa, S. 2008. The formation of the palladium-rich Roby, Twilight and High grade zones of the Lac Des Iles Complex, Ontario. Thèse de doctorat Université du Québec à Chicoutimi: 278p.

Sun, S.-S. 1982. Chemical composition and origin of the earth's primitive mantle. *Geochimica et Cosmochimica Acta* 46: 179-192.

Tredoux, M., Lindsay, N.M., Davies, G., and McDonald, I., 1995. The fractionation of platinum-group elements in magmatic systems with the suggestion of a novel causal mechanism. *South African Journal of Geology* 98: 157–167.

Vermaak, C., Hendriks, L. 1976. A review of the mineralogy of the Merensky Reef, with specific reference to new data on the precious metal mineralogy. *Economic Geology* 71: 1244-1269.

Wood, S.A. 1987. Thermodynamic calculations of the volatility of the platinum group elements (PGE): the PGE content of fluids at magmatic temperatures. *Geochimica et Cosmochimica Acta* 51: 3041–3050.

Zientek, M.L., Cooper, R.W., Corson, S.R., Geraghty, E.P. 2002. Platinum-group element mineralization in the Stillwater Complex, Montana. In: Cabri, L.J. (Ed.), *Geology, Geochemistry, Mineralogy and Mineral Beneficiation of Platinum Group Element*. Canadian Institute of Mining, Metallurgy and Petroleum, Special Volume 54: 459–481.

ML 35	14.85	7.37	12.28	0.11	6.11	18.43	0.17	0.37	<0.01	39.85	0.07	99.61	93.5
ML 36	19.43	10.03	8.91	0.2	5.48	13.29	0.12	1.02	<0.01	41.12	0.07	99.66	94.18
ML 37	19.69	10.69	7.83	0.31	4.78	12.97	0.11	0.96	<0.01	43.6	0.09	101.04	96.26
ML 38	17.03	8.26	9.12	0.39	6.07	15.86	0.13	0.85	<0.01	41.99	0.09	99.79	93.72
ML 39	17.92	7.52	8.29	0.67	6.01	15.11	0.11	1.08	<0.01	42.14	0.08	98.94	92.93
ML 40	20.76	12.91	5.46	0.48	2.23	8.85	0.09	1.42	<0.01	47.25	0.19	99.65	97.42
ML 41	19.46	8.71	8.17	0.76	5.42	13.88	0.12	0.87	<0.01	42.97	0.08	100.44	95.02
ML 42	22.67	4.15	6.13	1.69	8.57	13.69	0.1	1.26	<0.01	41.26	0.07	99.6	91.03
ML 43	19.2	11.31	6.68	0.99	2.65	9.61	0.11	1.62	<0.01	48.13	0.15	100.44	97.79
ML 44	19.41	10.29	8.17	0.96	4.98	13.02	0.11	0.65	<0.01	42.34	0.1	100.04	95.06
ML 45	23.28	12.35	6.23	0.19	2.66	8.96	0.09	1.39	0.01	44.81	0.13	100.08	97.42
ML 46	19.27	9.98	9.49	0.69	4.16	11.24	0.12	1.07	0.01	42.73	0.08	98.85	94.69
ML 47	17.18	10.18	9.55	0.48	4.53	13.92	0.13	0.77	<0.01	43.17	0.09	100.01	95.48
ML 48	13.97	13.22	8.46	0.23	2.31	12.28	0.13	0.72	<0.01	48.92	0.19	100.43	98.12
ML 49	13.68	12.8	8.73	0.2	2.79	13.66	0.15	0.73	<0.01	47.63	0.17	100.52	97.73
ML 50	5.41	13.14	21.47	0.05	2.38	11.27	0.24	0.15	0.01	44.49	0.43	99.04	98.66
ML 51	9.84	5.56	33.11	0.02	10.03	1.34	0.07	2.05	0.01	25.59	0.07	87.69	77.66
ML 52	16.68	5.7	3.92	0.15	0.5	1.04	0.05	4.45	0.15	67.67	0.42	100.74	100.24
ML 53	2.55	18.85	14.88	0.03	1.19	13.98	0.27	0.18	<0.01	49.14	0.57	99.64	98.45
ML 54	2.62	11.83	19.2	0.04	2.06	14.3	0.2	0.22	<0.01	48.82	0.48	99.78	97.72
ML 55	18.32	10.73	9.53	0.39	4.62	13.3	0.13	0.81	<0.01	42.51	0.1	100.44	95.82
ML 56	27.64	13.7	3.59	0.4	2.36	5.14	0.05	1.63	<0.01	45.22	0.05	99.78	97.42
ML 57	29.22	14.93	1.9	0.49	1.83	1.68	0.03	2.44	0.02	47.12	0.07	99.74	97.91
ML 58	26.3	14.94	3.75	0.28	1.4	4.94	0.06	1.63	<0.01	47	0.13	100.43	99.03
ML 59	17.85	9.63	7.63	1.08	3.99	11.53	0.11	1.44	0.01	46.16	0.09	99.53	95.54
ML 60	20.84	9.96	6.09	1.95	4.57	9.82	0.09	1.13	<0.01	45.19	0.07	99.71	95.14
ML 61	20.92	9.61	7.49	0.82	5.17	10.25	0.11	1.72	<0.01	44.27	0.1	100.45	95.28
ML 62	22.67	11.11	6.47	1.74	4.88	9.38	0.08	0.94	<0.01	43.7	0.1	101.09	96.21
ML 63	19.63	10.94	7.91	0.45	4.04	11.99	0.11	1.12	<0.01	44.04	0.08	100.33	96.29
ML 64	19.41	9.21	8.47	0.44	3.92	11.51	0.1	1.87	0.04	45.32	0.2	100.48	96.56
ML 65	20.14	10.68	8.27	0.41	4.8	11.28	0.11	1.44	<0.01	42.81	0.08	100.02	95.22

ML-43	49.55	0.15	19.77	6.19	0.11	9.89	11.64	1.67	1.02	<0.01	100
ML-44	44.93	0.11	20.60	7.80	0.12	13.82	10.92	0.69	1.02	<0.01	100
ML-45	46.28	0.13	24.05	5.79	0.09	9.25	12.76	1.44	0.20	0.01	100
ML-46	46.38	0.09	20.92	7.54	0.13	12.20	10.83	1.16	0.75	0.01	100
ML-47	45.80	0.10	18.23	8.84	0.14	14.77	10.80	0.82	0.51	<0.01	100
ML-48	51.08	0.20	14.59	6.38	0.14	12.82	13.80	0.75	0.24	<0.01	100
ML-49	49.38	0.18	14.18	7.71	0.16	14.16	13.27	0.76	0.21	<0.01	100
ML-50	51.40	0.50	6.25	13.14	0.28	13.02	15.18	0.17	0.06	0.01	100
ML-51	48.87	0.13	18.79	14.92	0.13	2.56	10.62	3.91	0.04	0.02	100
ML-52	67.78	0.42	16.71	3.53	0.05	1.04	5.71	4.46	0.15	0.15	100
ML-53	52.17	0.61	2.71	11.27	0.29	14.84	17.89	0.19	0.03	<0.01	100
ML-54	54.48	0.54	2.92	12.39	0.22	15.96	13.20	0.25	0.04	<0.01	100
ML-55	44.81	0.11	19.31	9.04	0.14	14.02	11.31	0.85	0.41	<0.01	100
ML-56	46.59	0.05	28.48	3.33	0.05	5.30	14.11	1.68	0.41	<0.01	100
ML-57	48.22	0.07	29.90	1.75	0.03	1.72	15.28	2.50	0.50	0.02	100
ML-58	47.64	0.13	26.66	3.42	0.06	5.01	15.14	1.65	0.28	<0.01	100
ML-59	48.71	0.09	18.84	7.24	0.12	12.17	10.16	1.52	1.14	0.01	100
ML-60	47.81	0.07	22.05	5.80	0.10	10.39	10.54	1.20	2.06	<0.01	100
ML-61	46.83	0.11	22.13	7.13	0.12	10.84	10.17	1.82	0.87	<0.01	100
ML-62	45.74	0.10	23.73	6.09	0.08	9.82	11.63	0.98	1.82	<0.01	100
ML-63	46.13	0.08	20.56	7.45	0.12	12.56	11.46	1.17	0.47	<0.01	100
ML-64	47.35	0.21	20.28	7.96	0.10	12.02	9.62	1.95	0.46	0.04	100
ML-65	45.35	0.08	21.34	7.88	0.12	11.95	11.31	1.53	0.43	<0.01	100

White cells = Olivine gabbros

Red cells = pyroxene rich rocks

Green cells = felsic (type 3 rocks and the granite)

APPENDIX 3 Trace Elements determined by ICP-MS (in ppm)

sample	Ba	Be	Bi	Cd	Ce	Co	Cr	Cs	Cu
ML 1	196.6	0.07	0.31	0.03	0.52	61.19	40	11.337	351.8
ML 2	10.6	0.07	0.23	0.046	0.54	97.51	79	1.15	89.8
ML 3	85.2	0.16	0.22	0.043	3.42	83.34	63	5.903	10.1
ML 4	99.7	0.1	0.32	0.041	0.7	94.26	77	4.175	114
ML 5	110.8	0.53	0.25	0.059	15.16	86.99	71	5.402	42.3
ML 6	44.9	0.07	0.16	0.032	0.55	102.09	87	6.123	32.9
ML 7	104.2	0.24	0.56	0.04	1.88	106.9	110	1.568	5
ML 8	202.1	0.26	0.37	0.058	2.62	37.71	20	11.428	40.5
ML 9	153.8	0.38	0.24	0.036	1.91	60.4	44	7.721	4.5
ML 10	141.6	0.12	0.22	0.021	0.72	63.94	28	12.791	10.5
ML 11	<0.8	0.09	0.26	0.088	0.14	157.75	46	0.033	689
ML 12	36.8	0.13	0.37	0.022	0.56	70.23	79	3.161	26.1
ML 13	294.8	0.15	0.39	0.021	0.56	72.16	25	5.778	45.6
ML 14	<0.8	0.09	0.39	0.1	0.55	135.86	137	0.278	449.9
ML 15	82.6	0.1	0.21	0.031	1.29	71.47	37	6.951	19.8
ML 16	181	0.09	0.53	0.042	2.58	86.98	39	7.006	274.8
ML 17	6.3	0.09	0.23	0.051	0.48	125.33	146	0.369	222
ML 18	178.7	0.14	0.53	0.033	0.47	69.87	33	9.944	4.2
ML 19	74.2	0.11	0.56	0.059	1.7	86.5	56	3.374	14.2
ML 20	31.1	0.07	0.41	0.044	1.21	116.61	47	2.046	51.8
ML 21	6.4	0.08	0.83	0.042	0.74	116.72	180	0.797	110
ML 22	60	0.41	0.96	0.046	1.63	83.84	109	3.029	23.7
ML 23	66	0.42	0.4	0.033	1.22	71.18	62	4.146	36.4
ML 24	37.6	0.07	0.59	0.074	0.81	119.35	24	1.247	947.5
ML 25	6.6	0.1	0.29	0.041	3.11	126.28	69	0.41	7
ML 26	37.4	0.95	<0.15	0.093	15.23	83.36	26	1.045	270.3
ML 27	83.4	0.12	0.61	0.127	0.62	94.56	66	2.763	10
ML 28	48.9	0.12	0.41	0.026	0.6	68.86	61	2.424	8.2
ML 29	17.1	0.13	0.27	0.031	2.04	85.53	46	0.876	31.1
ML 30	11.7	0.13	0.3	0.034	0.84	99.25	150	0.809	291.6
ML 31	74.6	0.08	0.29	0.088	0.47	87.74	29	9.133	40.4
ML 32	7.3	0.04	<0.15	0.107	0.36	122.65	96	0.979	504.1
ML 33	77.4	0.25	0.63	0.08	6.33	105.26	29	6.254	1505.3
ML 34	63.5	0.14	0.34	0.066	1.23	115.29	85	2.433	243.2
ML 35	4.6	0.05	0.29	0.031	0.3	125.43	62	0.245	41.9
ML 36	20.9	0.05	0.39	0.029	0.41	97.96	43	4.355	37.8
ML 37	30.4	0.05	<0.15	0.039	0.53	101.82	58	5.53	58.5
ML 38	28.3	0.09	<0.15	0.042	1.35	102.05	66	1.277	2
ML 39	37.6	0.06	<0.15	0.036	1.45	99.71	30	2.377	18.1
ML 40	64.9	0.11	<0.15	0.042	1.09	64.47	632	3.133	38.9
ML 41	64.2	0.12	<0.15	0.04	1.62	90.37	59	7.877	19.9
ML 42	125.6	0.79	<0.15	0.024	1.53	60.36	33	7.356	4.7
ML 43	197.1	0.26	<0.15	0.073	2.51	69.38	457	4.796	22
ML 44	94.9	0.09	0.25	0.039	0.89	98.16	115	3.493	34

ML 45	22.2	0.09	0.19	0.041	1.05	78.19	46	2.331	18.3
ML 46	125.6	0.09	0.33	0.183	1.28	148.11	32	4.732	2550
ML 47	50.6	0.11	0.16	0.063	0.76	103.44	175	2.499	494.1
ML 48	16.3	0.06	0.33	0.173	3.48	105.99	719	2.872	2397.4
ML 49	13	0.12	<0.15	0.072	3.7	110.76	731	2.459	273.1
ML 50	1.5	0.38	2.17	0.108	3.26	>187	383	0.043	1621.7
ML 51	2.1	0.12	9.37	>4	8.39	>187	30	0.637	>2900
ML 52	52.6	0.55	<0.15	<0.013	11.37	95.45	11	1.478	47.3
ML 53	0.8	0.09	0.34	0.156	1.87	143.4	427	0.053	816.4
ML 54	3.1	0.16	0.27	0.156	2.26	>187	369	0.154	1249.4
ML 55	29.5	0.09	<0.15	0.058	0.71	112.36	88	5.597	13.7
ML 56	25.1	0.14	<0.15	0.07	0.47	51.84	11	3.524	136.5
ML 57	37.8	0.45	0.25	0.034	0.64	77.21	68	5.214	58.5
ML 58	18.7	0.09	<0.15	0.047	0.57	87.55	166	3.407	46.6
ML 59	139.5	0.19	0.23	0.053	3.75	78.36	34	5.214	35.4
ML 60	499.1	0.18	0.19	0.043	2.93	67.32	29	8.322	2.4
ML 61	113.3	0.18	<0.15	0.027	1.28	70.63	63	6.452	1.8
ML 62	281.5	0.09	0.16	0.02	0.99	77.54	52	7.524	37.9
ML 63	64.3	0.13	0.24	0.038	0.67	105.5	75	5.923	76.9
ML 64	50.5	0.36	0.37	0.025	4.34	102.65	84	8.535	2.9
ML 65	28.3	0.07	0.68	0.031	5.88	87.16	93	2.803	28.5

sample	Dy	Er	Eu	Ga	Gd	Hf	Ho	In	La
ML 1	0.107	0.065	0.114	13.73	0.109	<0.14	0.023	0.006	0.33
ML 2	0.145	0.1	0.2	12.69	0.123	<0.14	0.033	0.011	0.26
ML 3	0.233	0.134	0.203	14.26	0.265	0.2	0.047	0.011	1.61
ML 4	0.213	0.129	0.184	11.59	0.204	<0.14	0.044	0.009	0.42
ML 5	0.54	0.276	0.544	14.23	0.788	0.49	0.102	0.022	7.09
ML 6	0.241	0.146	0.175	12.67	0.197	<0.14	0.053	0.008	0.26
ML 7	0.135	0.088	0.166	13.82	0.129	<0.14	0.028	0.01	1.06
ML 8	0.354	0.172	0.205	15.84	0.446	0.17	0.066	0.007	1.27
ML 9	0.181	0.104	0.159	15.96	0.201	<0.14	0.038	0.006	1.07
ML 10	0.062	0.039	0.126	12.09	0.085	<0.14	0.014	0.007	0.49
ML 11	0.1	0.075	0.038	2.89	0.068	<0.14	0.023	0.008	0.06
ML 12	0.149	0.09	0.102	16.28	0.127	<0.14	0.031	0.005	0.28
ML 13	0.084	0.044	0.121	12.07	0.08	<0.14	0.016	0.005	0.35
ML 14	0.243	0.172	0.117	7.37	0.184	<0.14	0.056	0.012	0.21
ML 15	0.166	0.096	0.155	14.99	0.199	<0.14	0.035	0.006	0.59
ML 16	0.197	0.12	0.235	12.21	0.205	0.46	0.038	0.008	1.32
ML 17	0.23	0.162	0.135	10.08	0.184	<0.14	0.05	0.009	0.21
ML 18	0.093	0.053	0.146	13.54	0.094	<0.14	0.02	0.006	0.26
ML 19	0.356	0.203	0.247	14.62	0.311	0.17	0.071	0.017	0.81
ML 20	0.166	0.092	0.173	13.1	0.201	<0.14	0.033	0.012	0.46
ML 21	0.414	0.276	0.116	11.36	0.324	<0.14	0.089	0.01	0.31
ML 22	0.456	0.261	0.306	26.22	0.409	0.21	0.093	0.03	0.78
ML 23	0.228	0.14	0.203	22.52	0.203	<0.14	0.049	0.015	0.6

ML 24	0.137	0.085	0.217	13.85	0.13	<0.14	0.029	0.013	0.45
ML 25	0.191	0.11	0.25	12	0.198	<0.14	0.038	0.013	1.81
ML 26	0.297	0.162	0.269	19.78	0.454	3.15	0.055	0.004	8.96
ML 27	0.206	0.128	0.184	13.71	0.171	<0.14	0.045	0.009	0.28
ML 28	0.202	0.112	0.155	14.31	0.169	<0.14	0.044	0.007	0.32
ML 29	0.179	0.1	0.164	13.22	0.188	0.28	0.033	0.007	0.98
ML 30	0.261	0.163	0.143	13.06	0.207	<0.14	0.056	0.009	0.43
ML 31	0.113	0.062	0.13	14.28	0.107	<0.14	0.023	0.006	0.23
ML 32	0.155	0.106	0.122	9.27	0.126	<0.14	0.036	0.009	0.14
ML 33	0.535	0.277	0.279	14.54	0.671	1.23	0.102	0.012	3.2
ML 34	0.201	0.133	0.215	9.73	0.193	<0.14	0.045	0.016	0.7
ML 35	0.126	0.087	0.083	9.25	0.1	<0.14	0.028	0.008	0.16
ML 36	0.11	0.076	0.148	11.76	0.102	<0.14	0.024	0.007	0.22
ML 37	0.2	0.127	0.152	12.19	0.173	<0.14	0.043	0.007	0.23
ML 38	0.219	0.146	0.203	11.79	0.202	<0.14	0.048	0.012	0.76
ML 39	0.111	0.067	0.158	10.44	0.17	<0.14	0.025	0.008	1.04
ML 40	0.846	0.533	0.203	13.37	0.649	0.24	0.185	0.012	0.49
ML 41	0.16	0.102	0.165	12.29	0.168	<0.14	0.033	0.01	1.01
ML 42	0.305	0.141	0.134	15.84	0.467	<0.14	0.052	0.01	0.91
ML 43	0.573	0.348	0.265	13.86	0.531	0.16	0.121	0.019	1.26
ML 44	0.259	0.162	0.177	12.96	0.224	<0.14	0.052	0.01	0.51
ML 45	0.291	0.18	0.221	14.98	0.247	<0.14	0.062	0.011	0.48
ML 46	0.188	0.109	0.178	12.78	0.181	<0.14	0.038	0.019	0.64
ML 47	0.293	0.189	0.164	11.34	0.251	<0.14	0.068	0.014	0.41
ML 48	1.256	0.741	0.206	10.67	1.013	0.59	0.254	0.031	1.14
ML 49	1.215	0.718	0.211	10.34	1.026	0.45	0.254	0.025	1.16
ML 50	2.309	1.471	0.482	9.74	1.762	0.4	0.493	0.164	1.19
ML 51	0.187	0.101	0.136	13.26	0.288	<0.14	0.039	0.039	5.05
ML 52	0.523	0.278	0.702	17.98	0.659	5.1	0.099	0.015	5.99
ML 53	2.836	1.735	0.467	6.31	2.066	0.58	0.603	0.087	0.5
ML 54	2.325	1.467	0.39	6.11	1.684	0.48	0.502	0.091	0.73
ML 55	0.265	0.173	0.198	12.48	0.228	<0.14	0.058	0.011	0.32
ML 56	0.083	0.045	0.111	17.3	0.079	<0.14	0.017	0.006	0.22
ML 57	0.198	0.12	0.141	20.21	0.158	<0.14	0.04	0.008	0.33
ML 58	0.286	0.17	0.134	17.02	0.225	<0.14	0.059	0.011	0.25
ML 59	0.892	0.458	0.294	13.1	0.844	0.5	0.165	0.016	1.6
ML 60	0.343	0.199	0.213	13.48	0.352	0.3	0.069	0.011	1.55
ML 61	0.242	0.147	0.216	13.61	0.216	<0.14	0.051	0.011	0.72
ML 62	0.233	0.138	0.161	14.01	0.205	0.68	0.048	0.008	0.59
ML 63	0.199	0.127	0.171	12.8	0.174	<0.14	0.042	0.012	0.36
ML 64	0.481	0.245	0.256	12.97	0.603	0.9	0.089	0.013	1.94
ML 65	0.225	0.139	0.182	13.01	0.275	<0.14	0.046	0.009	4.22

sample	Li	Lu	Mo	Nb	Nd	Ni	Pb	Pr	Rb
ML 1	40.9	0.01	0.19	0.268	0.33	323.8	1.1	0.072	90.47
ML 2	51.6	0.017	0.13	0.12	0.38	535.2	<0.6	0.081	5.56
ML 3	36.4	0.022	0.36	0.636	1.78	396.8	0.9	0.456	22.91
ML 4	52.7	0.019	0.13	0.13	0.56	554.8	0.7	0.114	27.86
ML 5	41	0.041	0.19	1.283	7.91	479.6	1.3	1.922	11.71
ML 6	38.6	0.022	0.27	0.413	0.41	460.8	0.6	0.09	19.25
ML 7	67.1	0.014	>44	0.347	0.7	1038.1	0.6	0.209	14.78
ML 8	70.3	0.023	1.38	0.405	1.62	179.8	1.2	0.337	53.7
ML 9	31.3	0.016	0.2	0.535	1.03	320.9	1	0.243	29.65
ML 10	87.4	0.007	0.08	0.133	0.41	356.4	<0.6	0.087	48.62
ML 11	0.8	0.019	1.48	0.412	0.11	774.3	<0.6	0.026	<0.23
ML 12	20.8	0.011	0.31	0.491	0.39	279.5	<0.6	0.088	10.65
ML 13	61.5	0.008	0.11	0.126	0.31	430.7	<0.6	0.072	36.85
ML 14	11.3	0.03	0.44	0.333	0.37	876.9	1.5	0.08	0.28
ML 15	51.7	0.012	0.22	0.269	0.78	399.3	0.7	0.181	18.82
ML 16	63.2	0.018	0.26	0.394	1.22	472.7	0.6	0.302	56.8
ML 17	32.2	0.023	0.2	0.198	0.34	778.2	<0.6	0.071	1.66
ML 18	54.7	0.009	0.13	0.186	0.31	380.2	1.1	0.072	43.1
ML 19	92.6	0.033	0.12	0.671	1.04	525.8	0.8	0.228	14.16
ML 20	55	0.017	0.61	0.199	0.75	772	<0.6	0.163	10.23
ML 21	31.9	0.042	0.13	0.292	0.6	728.1	<0.6	0.112	2.02
ML 22	8.6	0.036	0.66	1.848	1.1	77.5	2.5	0.226	7.41
ML 23	23.2	0.018	0.47	1.683	0.68	40.4	2	0.157	8.94
ML 24	39.7	0.016	0.34	0.39	0.52	717.2	0.6	0.117	8.39
ML 25	43.4	0.019	0.23	0.432	1.09	725.3	0.6	0.316	1.37
ML 26	12.2	0.034	0.38	5.749	4.68	125.5	1.8	1.488	2.82
ML 27	34.1	0.019	0.61	0.384	0.49	408.8	<0.6	0.101	19.23
ML 28	30.8	0.018	0.37	0.24	0.41	342.9	<0.6	0.099	14.23
ML 29	37.9	0.015	0.11	0.387	0.92	519.8	<0.6	0.252	3.45
ML 30	35.5	0.025	0.17	0.176	0.48	859.1	<0.6	0.106	2.9
ML 31	40.3	0.011	0.36	0.3	0.32	347.4	1.9	0.086	23.36
ML 32	24.4	0.017	1.37	0.168	0.27	682.3	1.8	0.061	4.06
ML 33	37.4	0.038	0.49	2.261	3.09	378.4	1.1	0.789	14.26
ML 34	47.3	0.022	3.87	0.349	0.66	613.5	1.4	0.153	7.56
ML 35	21.6	0.015	0.15	0.118	0.22	742.9	<0.6	0.044	1.06
ML 36	47.5	0.013	0.14	0.173	0.28	518.2	0.8	0.063	5.25
ML 37	33	0.02	0.19	0.31	0.42	457.6	0.8	0.089	7.23
ML 38	61.5	0.023	0.66	0.274	0.62	594.3	<0.6	0.167	8.05
ML 39	57.7	0.012	0.23	0.154	0.82	564.2	<0.6	0.171	14.84
ML 40	39.7	0.072	0.19	0.55	1.16	237.7	<0.6	0.186	13.86
ML 41	45.9	0.019	0.12	0.155	0.79	521.2	0.6	0.2	23.32
ML 42	>207	0.015	0.1	0.156	0.97	320.9	1.1	0.194	50.5
ML 43	46.3	0.047	0.28	0.69	1.57	307.4	1.3	0.342	26.81
ML 44	65.8	0.026	0.22	0.276	0.57	510	0.7	0.12	32.56
ML 45	26.1	0.027	0.23	0.362	0.73	329.5	<0.6	0.151	6.25
ML 46	42.8	0.021	0.83	0.257	0.72	1643.3	1.4	0.169	28.99

ML 47	47.9	0.028	0.35	0.231	0.56	692.1	<0.6	0.118	17.5
ML 48	12	0.107	0.32	1.391	2.56	1004.2	0.8	0.524	8.4
ML 49	19.2	0.102	0.33	1.61	2.71	563.6	<0.6	0.594	6.15
ML 50	1.1	0.208	0.68	0.644	3.03	1769.8	1.1	0.532	<0.23
ML 51	11.3	0.018	0.29	0.314	2.74	1873.3	7.1	0.792	<0.23
ML 52	9.4	0.043	1.79	5.091	4.73	9.7	1.4	1.262	2.95
ML 53	1.2	0.245	0.31	0.324	2.84	574.7	0.6	0.418	0.24
ML 54	1.3	0.208	0.44	0.797	2.61	1286	<0.6	0.406	0.31
ML 55	62	0.029	0.22	0.376	0.5	510.8	<0.6	0.104	14.78
ML 56	16.8	0.006	0.19	0.239	0.32	216.1	0.6	0.068	12.46
ML 57	22.7	0.017	0.48	1.013	0.39	47.5	2.8	0.101	13.41
ML 58	3.6	0.022	0.48	0.704	0.47	150.3	1	0.09	7.55
ML 59	59.4	0.066	2.53	1.136	2.73	479.6	0.7	0.572	40.58
ML 60	57	0.027	0.28	0.613	1.62	400.6	0.8	0.369	76.23
ML 61	66.1	0.023	0.11	0.181	0.7	389.1	<0.6	0.166	28.59
ML 62	54.5	0.019	0.24	0.27	0.67	379.4	0.6	0.143	66.55
ML 63	41.5	0.018	0.25	0.482	0.48	696.3	0.7	0.103	11
ML 64	42.7	0.032	1	1.392	2.65	481.9	0.6	0.589	14.06
ML 65	55.8	0.019	0.19	0.298	2.3	527	0.6	0.605	9.42

sample	Sb	Sc	Sm	Sn	Sr	Ta	Tb	Th	Ti
ML 1	0.07	3.8	0.096	0.18	163.6	0.593	0.018	<0.018	264
ML 2	0.04	7.9	0.107	<0.16	71.9	0.245	0.023	<0.018	311
ML 3	0.05	5.3	0.327	0.43	158.5	0.869	0.041	0.062	398
ML 4	0.07	6.7	0.152	<0.16	103.3	0.247	0.031	<0.018	388
ML 5	0.05	9.8	1.284	0.86	256.4	0.42	0.095	0.905	978
ML 6	0.08	10	0.143	<0.16	127.3	0.966	0.037	<0.018	425
ML 7	0.04	6.1	0.128	0.43	36.2	0.218	0.019	0.051	317
ML 8	0.04	3.9	0.422	0.41	380.1	0.459	0.063	0.157	407
ML 9	0.04	4.1	0.219	0.5	203.6	0.538	0.028	<0.018	376
ML 10	0.04	2.8	0.092	0.23	257	0.176	0.012	<0.018	158
ML 11	<0.04	9.4	0.05	0.23	1.6	0.306	0.013	0.029	324
ML 12	0.06	3.2	0.115	0.2	205.6	1.281	0.022	0.028	400
ML 13	0.05	3	0.074	0.2	278.2	0.212	0.012	<0.018	207
ML 14	0.04	11.6	0.142	0.41	3.5	0.23	0.036	<0.018	377
ML 15	<0.04	3	0.208	<0.16	171.3	0.473	0.028	0.019	304
ML 16	0.06	4.7	0.219	0.26	204.9	0.568	0.032	0.179	295
ML 17	0.15	9.1	0.137	<0.16	32.2	0.309	0.035	<0.018	454
ML 18	0.06	3.2	0.096	0.19	233.6	0.433	0.014	<0.018	230
ML 19	0.05	9.3	0.269	0.47	36.7	0.147	0.051	0.022	700
ML 20	<0.04	5	0.185	0.23	42.8	0.14	0.027	<0.018	265
ML 21	0.05	14.2	0.229	0.19	28.5	0.172	0.06	<0.018	701
ML 22	0.06	6.6	0.339	0.7	191.9	2.589	0.071	0.087	720
ML 23	0.06	5.2	0.186	0.49	202.7	2.44	0.036	0.07	523
ML 24	0.04	4.5	0.126	0.26	146	1.104	0.021	<0.018	305
ML 25	<0.04	6.3	0.213	0.47	44.8	0.701	0.029	0.035	333

ML 26	0.04	3	0.686	0.18	326.9	3.271	0.057	2	2383
ML 27	0.06	6.4	0.148	0.18	160.6	0.962	0.032	<0.018	408
ML 28	0.05	6.3	0.144	0.17	186.2	0.416	0.03	<0.018	415
ML 29	0.05	4	0.192	0.19	106.6	0.31	0.029	0.116	299
ML 30	0.05	7.4	0.166	0.18	102.6	0.254	0.04	<0.018	497
ML 31	0.07	4.9	0.1	0.2	212.1	0.898	0.016	<0.018	250
ML 32	0.05	10.7	0.097	0.22	31.5	0.342	0.025	<0.018	345
ML 33	0.07	4.9	0.696	0.59	152	1.323	0.099	0.237	1223
ML 34	0.08	9.5	0.17	0.46	62	0.411	0.032	0.034	387
ML 35	0.15	7.8	0.068	<0.16	9.3	0.251	0.019	<0.018	289
ML 36	<0.04	5.8	0.078	<0.16	143.2	0.437	0.017	<0.018	252
ML 37	0.08	7.9	0.122	<0.16	157.5	0.691	0.029	<0.018	395
ML 38	0.04	7	0.168	0.37	61.8	0.279	0.036	0.038	437
ML 39	0.04	3.1	0.172	0.18	68.4	0.356	0.02	<0.018	250
ML 40	0.04	22.7	0.43	0.19	164.5	0.663	0.12	<0.018	1161
ML 41	0.05	4.9	0.165	0.31	122	0.295	0.026	<0.018	340
ML 42	0.04	2.2	0.351	0.33	91.3	0.094	0.054	<0.018	316
ML 43	0.05	18.4	0.444	0.93	135.1	0.535	0.086	<0.018	765
ML 44	0.05	7.7	0.189	0.27	120	0.645	0.04	<0.018	510
ML 45	0.07	7.3	0.206	0.18	133.2	0.804	0.044	<0.018	563
ML 46	0.06	5.9	0.173	0.22	147.3	0.586	0.027	0.026	330
ML 47	0.04	14.4	0.184	0.17	95.7	0.424	0.044	<0.018	469
ML 48	0.04	35.1	0.807	0.49	103.6	0.956	0.189	0.532	992
ML 49	0.04	33	0.888	0.57	81.1	1.614	0.183	0.381	849
ML 50	0.04	>63	1.193	0.38	38.5	0.912	0.332	<0.018	2477
ML 51	0.04	2.8	0.388	0.24	191.2	0.484	0.034	0.542	379
ML 52	0.04	3.5	0.84	0.38	270.6	3.008	0.092	0.367	2448
ML 53	0.1	>63	1.334	0.31	6.3	0.645	0.394	<0.018	3114
ML 54	0.05	>63	1.091	0.61	3.7	1.28	0.326	0.089	2707
ML 55	0.04	11.6	0.163	0.25	87.1	0.83	0.04	<0.018	485
ML 56	0.04	2	0.085	0.19	180.5	0.647	0.012	<0.018	275
ML 57	0.05	5.5	0.129	0.35	200	2.067	0.027	<0.018	429
ML 58	0.04	7.6	0.169	0.19	142.8	2.072	0.041	<0.018	625
ML 59	0.07	5.2	0.869	0.81	158.9	0.646	0.141	0.438	388
ML 60	0.05	4.2	0.376	0.58	138.7	0.349	0.054	0.537	319
ML 61	0.04	7.9	0.183	0.2	252.4	0.208	0.035	0.023	457
ML 62	0.07	4.9	0.181	0.22	180.8	0.653	0.035	<0.018	493
ML 63	0.05	7.4	0.137	0.67	111.2	0.841	0.028	<0.018	403
ML 64	0.07	9.1	0.633	0.4	125.1	1.107	0.086	0.141	1119
ML 65	0.12	9.3	0.327	0.26	209.7	0.495	0.036	<0.018	342

sample	Tl	Tm	U	V	W	Y	Yb	Zn	Zr
ML 1	0.333	0.009	<0.011	15.7	>141	0.6	0.068	28	<6
ML 2	0.019	0.015	<0.011	26	68.92	0.85	0.106	53	<6
ML 3	0.075	0.022	0.032	28.4	>141	1.36	0.141	43	7
ML 4	0.101	0.019	<0.011	32.7	67.12	1.19	0.128	50	<6
ML 5	0.045	0.04	0.224	52.3	90.58	2.77	0.275	94	19
ML 6	0.076	0.022	<0.011	41.1	>141	1.34	0.153	44	<6
ML 7	0.061	0.013	0.036	24.2	54.02	0.77	0.094	61	<6
ML 8	0.185	0.024	0.1	22.4	49.9	2.11	0.162	28	<6
ML 9	0.111	0.015	0.07	21.6	128.5	1.1	0.107	43	<6
ML 10	0.162	0.006	<0.011	10.6	43.97	0.41	0.045	32	<6
ML 11	0.035	0.014	0.151	23.9	50.6	0.71	0.111	64	<6
ML 12	0.045	0.013	<0.011	24.6	>141	0.81	0.083	21	<6
ML 13	0.176	0.007	0.015	11.5	50.61	0.46	0.052	37	<6
ML 14	0.008	0.026	0.025	37.1	43.98	1.49	0.188	68	<6
ML 15	0.049	0.013	<0.011	16	98.98	1.01	0.084	32	<6
ML 16	0.278	0.016	0.153	19.2	117.68	1.09	0.111	39	16
ML 17	0.01	0.022	<0.011	39	62.46	1.34	0.151	58	<6
ML 18	0.186	0.009	<0.011	13.1	89.13	0.5	0.061	34	<6
ML 19	0.033	0.031	0.028	44.1	28.77	1.99	0.226	70	6
ML 20	0.017	0.014	0.011	18.5	31.82	0.99	0.095	65	<6
ML 21	0.009	0.04	0.012	68.3	33.49	2.39	0.269	70	<6
ML 22	0.036	0.037	0.208	63.1	>141	2.57	0.244	17	6
ML 23	0.04	0.019	0.102	36.4	>141	1.3	0.136	15	<6
ML 24	0.038	0.013	<0.011	19.5	>141	0.78	0.092	43	<6
ML 25	0.006	0.017	0.036	25.5	133.41	1.06	0.119	65	<6
ML 26	0.011	0.024	0.267	9.3	>141	1.53	0.18	20	110
ML 27	0.062	0.018	<0.011	28.9	>141	1.14	0.131	36	<6
ML 28	0.059	0.018	0.012	28	78.89	1.1	0.123	33	<6
ML 29	0.015	0.015	0.073	17.2	59.21	0.99	0.101	43	10
ML 30	0.013	0.024	0.021	37.3	48.72	1.5	0.169	46	<6
ML 31	0.096	0.01	<0.011	21.3	>141	0.65	0.072	44	<6
ML 32	0.01	0.016	0.027	36.5	74.67	0.96	0.108	67	<6
ML 33	0.053	0.039	0.246	23.6	>141	2.95	0.251	46	49
ML 34	0.024	0.019	0.023	36.9	81.81	1.22	0.133	77	<6
ML 35	<0.005	0.014	<0.011	27.8	51.27	0.74	0.103	61	<6
ML 36	0.02	0.011	<0.011	22	83.15	0.65	0.079	45	<6
ML 37	0.02	0.019	<0.011	30.2	139.9	1.15	0.124	41	<6
ML 38	0.025	0.021	0.021	30.2	58.66	1.23	0.148	60	<6
ML 39	0.061	0.011	<0.011	14.1	80.9	0.73	0.071	45	<6
ML 40	0.081	0.077	<0.011	107.6	119.62	4.86	0.502	31	8
ML 41	0.076	0.014	0.016	22.3	66.74	0.94	0.113	49	<6
ML 42	0.182	0.017	0.044	18.6	23.89	2.08	0.107	80	<6
ML 43	0.118	0.047	0.259	73.2	96.11	3.22	0.303	53	<6
ML 44	0.148	0.024	<0.011	33.4	123.1	1.49	0.17	41	<6
ML 45	0.024	0.027	<0.011	35.4	135.7	1.68	0.183	40	<6
ML 46	0.242	0.017	<0.011	21.2	110.66	1.01	0.128	51	<6

ML 47	0.129	0.029	<0.011	50.4	80.94	1.74	0.188	49	<6
ML 48	0.141	0.112	0.161	134.8	127.24	7.27	0.74	45	12
ML 49	0.063	0.107	0.134	124.2	>141	7.04	0.703	45	8
ML 50	0.108	0.218	0.011	>370	>141	12.53	1.381	88	9
ML 51	0.731	0.015	0.423	108.4	111.55	1.08	0.114	296	<6
ML 52	0.014	0.04	0.146	37.9	>141	2.78	0.267	64	261
ML 53	0.032	0.254	<0.011	>370	123.81	15.49	1.636	67	14
ML 54	0.035	0.212	0.036	>370	>141	12.73	1.39	99	11
ML 55	0.073	0.028	<0.011	40.1	>141	1.55	0.169	61	<6
ML 56	0.066	0.006	<0.011	12	117.64	0.43	0.043	22	<6
ML 57	0.071	0.017	0.068	31.6	>141	1.15	0.109	15	<6
ML 58	0.029	0.025	<0.011	55.2	>141	1.52	0.164	23	<6
ML 59	0.168	0.067	0.258	25.8	74.62	5.14	0.436	54	16
ML 60	0.292	0.026	0.121	20.1	59.15	1.94	0.171	47	8
ML 61	0.133	0.02	0.015	33	42.02	1.32	0.146	50	<6
ML 62	0.297	0.022	<0.011	32.6	140.28	1.31	0.143	35	30
ML 63	0.032	0.019	0.021	33.7	>141	1.14	0.121	58	<6
ML 64	0.048	0.034	0.079	44.3	>141	2.43	0.216	57	44
ML 65	0.023	0.019	0.012	33.8	103.52	1.26	0.125	42	<6

APPENDIX 4 Ni, Cu analyses by atomic absorption spectrometry

	analyses Cu	Analyses Ni
Name:	Carlos Cu-2 lamp 100	Carlos Ni
Mode Instrument:	Aucun	Aucun
Dilution:	Non	Non
Date:	16-04-09	17-04-09

sample	Cu (ppm)	sample	Ni (ppm)
ML-1	342.26	ML-1	169.55
ML-2	96.75	ML-1	167.87
ML-3	10.35	ML-2	270.55
ML-4	111.97	ML-3	168.78
ML-5	44.84	ML-4	238.36
ML-6	33.22	ML-5	227.45
ML-7	4.74	ML-6	252.29
ML-8	39.95	ML-7	467.12
ML-9	5.05	ML-8	97.58
ML-10	9.84	ML-9	166.36
ML-11	737.95	ML-10	173.95
ML-12	24.30	ML-11	590.56
ML-13	45.27	ML-12	128.70
ML-14	461.48	ML-13	185.85
ML-15	19.23	ML-14	392.80
ML-16	243.02	ML-15	202.25
ML-17	204.87	ML-16	213.98
ML-18	4.22	ML-17	343.01
ML-19	12.10	ML-18	210.09
ML-20	48.69	ML-19	250.98
ML-21	113.30	ML-20	404.53
ML-22	23.60	ML-21	342.85
ML-23	36.00	ML-22	24.15
ML-24	946.06	ML-23	24.78
ML-25	6.83	ML-24	461.99
ML-26	267.88	ML-25	429.79
ML-27	9.52	ML-26	72.63
ML-28	7.12	ML-27	225.26
ML-29	30.43	ml-28	144.04
ML-30	312.97	ML-29	216.98
ML-31	36.99	ML-30	476.95
ML-32	543.37	ML-31	207.25
ML-33 1/2	1591.98	ML-32	391.66
ML-33 1/20	2327.85	ML-33	235.49
ML-34	252.68	ml-34	296.29
ML-35	40.99	ML-35	356.19

sample	Cu (ppm)	sample	Ni (ppm)
ML-36	40.10	ML-36	303.91
ML-37	57.36	ML-37	223.48
ML-38	1.90	ML-38	291.12
ML-39	15.50	ML-39	285.06
ML-40	38.21	ML-40	64.26
ML-41	21.84	ML-41	251.00
ML-42	2.63	ML-42	232.16
ML-43	22.35	ML-43	112.83
ML-44	33.48	ML-44	253.00
ML-45	16.84	ML-45	110.53
ml-46 1/20	2386.44	ML-46	1278.47
ML-47	507.62	ML-47	326.10
ml-48 1/20	2592.60	ML-48	673.29
ML-49	281.73	ML-49	260.88
ML-50 1/2	1877.93	ML-50	1560.13
ML-50-R 1/2	1850.28	ML-50R	1583.11
ML-51 1/100	59075.31	ML-51	1691.45
ML-51 R 1/100	53242.79	ML-51R	1708.97
ML-52	35.26	ML-52	5.08
ML-53	825.88	ML-53	437.41
ML-54 1/10	1458.45	ML-54	1100.91
ML-54 1/10 NEW	1339.30	ML-55	245.25
ML-54 1/100	1781.49	ML-56	85.78
ML-54 1/2	1432.08	ML-57	26.61
ML-55	12.93	ML-58	53.05
ML-56	127.03	ML-59	160.02
ML-57	52.78	ML-60	148.65
ML-58	44.34	ML-61	188.31
ML-59	35.76	ML-62	202.44
ML60	1.54	ML-63	308.31
ML-61	1.61	ML-64	240.76
ML-62	36.14	ML-65	246.28
ML-63	74.88		
ML-64	4.80		
ML-65	25.00		

APPENDIX 5 Whole rock sulphur by infrared light absorption

TECHNIQUE: Bedard *et al.*, 2008. *Geoanal. Geost. Res.*

Sample Name	C (ppm)	S (ppm)	CO ₂ (%)	S (%)
ml-1	149	391	0.055%	0.04%
ml-2	192	165	0.070%	0.02%
ml-3	134	40	0.049%	0.00%
ml-4	274	148	0.101%	0.01%
ml-5	136	1665	0.050%	0.17%
ml-6	229	96	0.084%	0.01%
ml-7	404	260	0.148%	0.03%
ml-8	169	29	0.062%	0.00%
ml-9	189	19	0.069%	0.00%
ml-10	243	62	0.089%	0.01%
ml-11	181	15821	0.067%	1.58%
ml-12	212	85	0.078%	0.01%
ml-13	199	101	0.073%	0.01%
ml-14	231	1101	0.085%	0.11%
ml-15	338	46	0.124%	0.00%
ml-16	612	279	0.224%	0.03%
ml-17	113	261	0.041%	0.03%
ml-18	169	27	0.062%	0.00%
ml-19	183	116	0.067%	0.01%
ml-20	306	88	0.112%	0.01%
ml-21	233	304	0.085%	0.03%
ml-22	608	199	0.223%	0.02%
ml-23	610	454	0.224%	0.05%
ml-24	478	2115	0.175%	0.21%
ml-25	429	116	0.157%	0.01%
ml-26	504	468	0.185%	0.05%
ml-27	388	83	0.142%	0.01%
ml-28	223	87	0.082%	0.01%
ml-29	297	219	0.109%	0.02%
ml-30	129	1653	0.047%	0.17%
ml-31	547	177	0.201%	0.02%
ml-32	519	812	0.190%	0.08%
ml-33	344	2481	0.126%	0.25%
ml-34	290	462	0.106%	0.05%
ml-35	267	285	0.098%	0.03%
ml-36	316	296	0.116%	0.03%
ml-37	534	267	0.196%	0.03%
ml-38	404	278	0.148%	0.03%
ml-39	613	306	0.225%	0.03%
ml-40	282	175	0.103%	0.02%

< 25 ppm

ml-41	463	300	0.170%	0.03%
ml-42	667	390	0.245%	0.04%
ml-43	199	278	0.073%	0.03%
ml-44	467	352	0.171%	0.04%
ml-45	206	218	0.076%	0.02%
ml-46	263	9420	0.096%	0.94%
ml-47	499	1484	0.183%	0.15%
ml-48	157	8804	0.058%	0.88%
ml-49	494	2177	0.181%	0.22%
ml-50	515	41349	0.189%	4.13%
ml-51	854	143349	0.266%	19.583 %
ml-52	205	261	0.075%	0.03%
ml-53	523	14502	0.192%	1.45%
ml-54	401	31349	0.147%	3.13%
ml-55	483	451	0.177%	0.05%
ml-56	197	414	0.072%	0.04%
ml-57	411	287	0.151%	0.03%
ml-58	389	262	0.143%	0.03%
ml-59	229	427	0.084%	0.04%
ml-60	411	376	0.151%	0.04%
ml-61	247	460	0.091%	0.05%
ml-62	605	421	0.222%	0.04%
ml-63	793	614	0.291%	0.06%
ml-64	516	346	0.189%	0.03%
ml-65	666	408	0.244%	0.04%
KPT	1910	10150	0.700%	1.02%
kpt	1991	10184	0.730%	1.02%
kpt	1874	10266	0.687%	1.03%
kpt	1921	10383	0.704%	1.04%
KPT	1886	10231	0.692%	1.02%
Average	1916	10243	0.703%	1.02%
Stdev	46	90	0.017%	0.01%
RSD %	2%	1%	2%	0.88%
Working KPT	1841	10430	0.675%	1.04%
+/-	216	520	0.079%	0.05%
LD (3s / 0.25g) (ppm)	82	25	0.030%	0.00%

APPENDIX 6 Whole rock PGE analyses by ICP-MS

PGE / NiS-Te-copr.

FOR: Carlos Munoz (SJ Barnes)

Analyst: D. Savard (ddsavard@uqac.ca), Julie Fredette

DATE: 8 mai 2009

NOTE: the Re is an approx. range - do not publish.



Université du Québec à Chicoutimi
595 Boulevard de l'Université
Chicoutimi, Québec, Canada
G7H 2B1

Paul Bédard, Responsable du laboratoire

Téléphone : 418-545-5011 poste 2276

Courriel : Paul.Bedard@uqac.ca

Dany Savard, Assistant de recherche

Téléphone : 418-545-5011 poste 2587

Courriel : dsavard@uqac.ca

Run	NO project	101Ru	103Rh	105Pd	185Re	189Os	193Ir	195Pt	197Au
		ppb	ppb	ppb	ppb	ppb	ppb	ppb	ppb
conc. (ppb)	ML-1 2009-05-05 09:27:26	2.230	3.873	146.30 0	<LD	0.856	1.479	61.300	9.556
s	ML-1 2009-05-05 09:27:26	0.058	0.036	1.359	--	0.043	0.018	0.930	0.110
%RSD	ML-1 2009-05-05 09:27:26	3%	1%	1%	--	5%	1%	2%	1%
conc. (ppb)	ML-2 2009-05-05 09:29:46	0.943	1.221	32.930	<LD	0.335	0.493	31.940	2.396
s	ML-2 2009-05-05 09:29:46	0.058	0.011	0.511	--	0.010	0.013	0.575	0.014
%RSD	ML-2 2009-05-05 09:29:46	6%	1%	2%	--	3%	3%	2%	1%
conc. (ppb)	ML-3 2009-05-05 09:32:01	2.143	4.119	96.280	0.2 ~ 0.6	1.043	1.591	72.030	0.531
s	ML-3 2009-05-05 09:32:01	0.012	0.041	1.745	--	0.025	0.031	0.647	0.025
%RSD	ML-3 2009-05-05 09:32:01	1%	1%	2%	--	2%	2%	1%	5%
conc. (ppb)	ML-4 2009-05-05 16:21:52	5.291	6.491	168.40 0	<LD	1.064	1.828	97.820	3.875
s	ML-4 2009-05-05 16:21:52	0.064	0.032	0.551	--	0.019	0.028	0.380	0.013
%RSD	ML-4 2009-05-05 16:21:52	1%	0%	0%	--	2%	2%	0%	0%
conc. (ppb)	ML-5 2009-05-05 09:36:23	3.965	5.415	192.40 0	<LD	0.784	1.482	175.40 0	1.318
s	ML-5 2009-05-05 09:36:23	0.051	0.037	1.670	--	0.029	0.022	1.577	0.010
%RSD	ML-5 2009-05-05 09:36:23	1%	1%	1%	--	4%	1%	1%	1%
conc. (ppb)	ML-6 2009-05-05 16:07:15	4.637	4.628	170.80 0	<LD	1.002	1.673	162.70 0	2.700
s	ML-6 2009-05-05 16:07:15	0.116	0.031	0.733	--	0.040	0.020	1.387	0.049
%RSD	ML-6 2009-05-05 16:07:15	3%	1%	0%	--	4%	1%	1%	2%
conc. (ppb)	ML-7 2009-05-05 16:24:26	35.850	38.930	692.30 0	3.8 ~ 11.5	6.545	13.200	441.40 0	2.857
s	ML-7 2009-05-05 16:24:26	0.520	0.739	4.991		0.130	0.124	6.295	0.111
%RSD	ML-7 2009-05-05 16:24:26	1%	2%	1%		2%	1%	1%	4%

conc. (ppb)	ML-8 2009-05-05 16:26:49	3.951	3.666	157.70 0	<LD	0.627	1.127	104.30 0	1.548
s	ML-8 2009-05-05 16:26:49	0.141	0.043	2.602	--	0.022	0.028	1.566	0.016
%RSD	ML-8 2009-05-05 16:26:49	4%	1%	2%	--	4%	2%	2%	1%
conc. (ppb)	ML-9 2009-05-05 16:29:01	3.127	3.866	85.040	<LD	0.866	1.691	112.20 0	0.590
s	ML-9 2009-05-05 16:29:01	0.043	0.006	0.342	--	0.040	0.018	0.404	0.023
%RSD	ML-9 2009-05-05 16:29:01	1%	0%	0%	--	5%	1%	0%	4%
conc. (ppb)	ML-10 2009-05-05 10:02:17	1.610	1.393	41.660	<LD	0.184	0.313	19.540	<LD
s	ML-10 2009-05-05 10:02:17	0.062	0.054	0.722	--	0.019	0.020	0.636	--
%RSD	ML-10 2009-05-05 10:02:17	4%	4%	2%	--	10%	6%	3%	--
conc. (ppb)	ML-11 2009-05-05 10:05:54	1.748	1.088	23.330	2.3 ~ 6.9	0.308	0.449	14.690	5.378
s	ML-11 2009-05-05 10:05:54	0.076	0.039	1.215		0.020	0.012	0.513	0.211
%RSD	ML-11 2009-05-05 10:05:54	4%	4%	5%		6%	3%	3%	4%
conc. (ppb)	ML-12 2009-05-05 16:39:17	9.294	10.330	368.50 0	<LD	1.869	2.941	237.60 0	2.610
s	ML-12 2009-05-05 16:39:17	0.122	0.037	3.166	--	0.031	0.040	1.046	0.051
%RSD	ML-12 2009-05-05 16:39:17	1%	0%	1%	--	2%	1%	0%	2%
conc. (ppb)	ML-13 2009-05-06 12:48:47	15.550	17.520	270.60 0	<LD	1.992	3.718	129.10 0	1.574
s	ML-13 2009-05-06 12:48:47	0.139	0.207	1.283	--	0.009	0.024	0.184	0.027
%RSD	ML-13 2009-05-06 12:48:47	1%	1%	0%	--	0%	1%	0%	2%
conc. (ppb)	ML-14 2009-05-06 12:46:28	1.568	1.344	68.480	<LD	0.213	0.387	34.480	3.521
s	ML-14 2009-05-06 12:46:28	0.049	0.002	0.231	--	0.005	0.011	0.275	0.027
%RSD	ML-14 2009-05-06 12:46:28	3%	0%	0%	--	2%	3%	1%	1%
conc. (ppb)	ML-15 2009-05-06 12:50:43	2.057	2.173	16.230	<LD	0.398	0.833	34.380	0.365
s	ML-15 2009-05-06 12:50:43	0.013	0.014	0.164	--	0.010	0.007	0.315	0.013
%RSD	ML-15 2009-05-06 12:50:43	1%	1%	1%	--	3%	1%	1%	4%
conc. (ppb)	ML-16 2009-05-06 12:52:36	8.577	9.645	334.30 0	<LD	1.687	2.750	205.90 0	3.402
s	ML-16 2009-05-06 12:52:36	0.117	0.101	2.493	--	0.055	0.006	0.309	0.018
%RSD	ML-16 2009-05-06 12:52:36	1%	1%	1%	--	3%	0%	0%	1%

conc. (ppb)	ML-17 2009-05-06 12:54:54	8.573	10.500	464.10 0	<LD	1.495	2.802	309.70 0	3.514
s	ML-17 2009-05-06 12:54:54	0.118	0.050	4.514	--	0.037	0.038	1.900	0.047
%RSD	ML-17 2009-05-06 12:54:54	1%	0%	1%	--	2%	1%	1%	1%
conc. (ppb)	ML-18 2009-05-06 12:57:20	2.855	4.729	157.40 0	<LD	0.798	1.697	101.60 0	<LD
s	ML-18 2009-05-06 12:57:20	0.068	0.021	1.188	--	0.024	0.016	0.196	--
%RSD	ML-18 2009-05-06 12:57:20	2%	0%	1%	--	3%	1%	0%	--
conc. (ppb)	ML-19 2009-05-06 12:59:52	9.854	8.800	308.90 0	<LD	1.258	2.287	160.70 0	0.627
s	ML-19 2009-05-06 12:59:52	0.253	0.060	0.326	--	0.025	0.032	0.916	0.027
%RSD	ML-19 2009-05-06 12:59:52	3%	1%	0%	--	2%	1%	1%	4%
conc. (ppb)	ML-20 2009-05-06 13:08:15	8.122	7.515	232.00 0	<LD	0.942	1.610	132.30 0	2.450
s	ML-20 2009-05-06 13:08:15	0.049	0.084	0.349	--	0.018	0.004	0.405	0.052
%RSD	ML-20 2009-05-06 13:08:15	1%	1%	0%	--	2%	0%	0%	2%
conc. (ppb)	ML-21 2009-05-06 13:10:40	89.800	107.50 0	845.70 0	<LD	14.300	29.360	1,170.0 00	3.868
s	ML-21 2009-05-06 13:10:40	0.761	1.018	8.496	--	0.095	0.264	13.850	0.039
%RSD	ML-21 2009-05-06 13:10:40	1%	1%	1%	--	1%	1%	1%	1%
conc. (ppb)	ML-22 2009-05-06 13:33:03	1.253	0.808	2.483	0.6 ~ 1.7	0.267	0.408	5.740	<LD
s	ML-22 2009-05-06 13:33:03	0.054	0.016	0.012		0.013	0.004	0.037	--
%RSD	ML-22 2009-05-06 13:33:03	4%	2%	0%		5%	1%	1%	--
conc. (ppb)	ML-23 2009-05-06 13:36:37	0.282	0.198	1.060	0.3 ~ 0.9	0.099	0.092	1.015	<LD
s	ML-23 2009-05-06 13:36:37	0.027	0.008	0.046		0.009	0.002	0.016	--
%RSD	ML-23 2009-05-06 13:36:37	10%	4%	4%		9%	2%	2%	--
conc. (ppb)	ML-24 2009-05-05 14:01:40	6.202	6.603	228.50 0	0.4 ~ 1.2	1.518	2.495	116.50 0	25.360
s	ML-24 2009-05-05 14:01:40	0.084	0.011	0.626		0.010	0.025	0.385	0.089
%RSD	ML-24 2009-05-05 14:01:40	1%	0%	0%		1%	1%	0%	0%
conc. (ppb)	ML-25 2009-05-05 14:04:00	0.787	0.754	5.751	<LD	0.195	0.311	4.873	<LD
s	ML-25 2009-05-05 14:04:00	0.022	0.017	0.159	--	0.006	0.007	0.029	--
%RSD	ML-25 2009-05-05 14:04:00	3%	2%	3%	--	3%	2%	1%	--

conc. (ppb)	ML-26 2009-05-05 14:05:52	<LD	0.143	2.082	0.2 ~ 0.5	0.071	0.062	3.095	7.167
s	ML-26 2009-05-05 14:05:52	--	0.004	0.040		0.006	0.003	0.041	0.025
%RSD	ML-26 2009-05-05 14:05:52	--	3%	2%		8%	5%	1%	0%
conc. (ppb)	ML-27 2009-05-05 14:07:42	11.440	13.200	352.200	0.4 ~ 1.2	1.597	3.161	161.800	1.523
s	ML-27 2009-05-05 14:07:42	0.121	0.042	0.924		0.039	0.031	0.663	0.025
%RSD	ML-27 2009-05-05 14:07:42	1%	0%	0%		2%	1%	0%	2%
conc. (ppb)	ML-28 2009-05-05 14:11:36	7.868	8.805	170.200	0.3 ~ 0.8	0.995	2.071	90.880	0.841
s	ML-28 2009-05-05 14:11:36	0.064	0.067	1.049		0.015	0.013	0.544	0.010
%RSD	ML-28 2009-05-05 14:11:36	1%	1%	1%		2%	1%	1%	1%
conc. (ppb)	ML-29 2009-05-05 14:13:36	3.444	4.095	171.000	<LD	0.836	1.372	97.320	1.002
s	ML-29 2009-05-05 14:13:36	0.058	0.023	0.076	--	0.028	0.014	1.063	0.023
%RSD	ML-29 2009-05-05 14:13:36	2%	1%	0%	--	3%	1%	1%	2%
conc. (ppb)	ML-30 2009-05-05 14:15:47	19.310	21.910	804.000	0.8 ~ 2.3	3.821	6.654	346.200	12.190
s	ML-30 2009-05-05 14:15:47	0.020	0.236	8.393		0.041	0.086	1.388	0.113
%RSD	ML-30 2009-05-05 14:15:47	0%	1%	1%		1%	1%	0%	1%
conc. (ppb)	ML-31 2009-05-05 14:17:49	6.744	7.206	96.650	<LD	1.912	3.554	54.100	0.631
s	ML-31 2009-05-05 14:17:49	0.110	0.043	0.710	--	0.008	0.036	0.163	0.027
%RSD	ML-31 2009-05-05 14:17:49	2%	1%	1%	--	0%	1%	0%	4%
conc. (ppb)	ML-32 2009-05-05 14:19:59	1.085	1.234	46.030	0.4 ~ 1.1	0.219	0.582	10.070	6.006
s	ML-32 2009-05-05 14:19:59	0.027	0.013	0.398		0.008	0.006	0.117	0.028
%RSD	ML-32 2009-05-05 14:19:59	2%	1%	1%		4%	1%	1%	0%
conc. (ppb)	ML-33 2009-05-05 14:32:22	0.980	1.431	18.910	<LD	0.345	0.442	47.810	9.395
s	ML-33 2009-05-05 14:32:22	0.058	0.018	0.128	--	0.009	0.004	0.044	0.062
%RSD	ML-33 2009-05-05 14:32:22	6%	1%	1%	--	3%	1%	0%	1%
conc. (ppb)	ML-34 2009-05-05 14:34:27	20.380	22.770	227.900	1.4 ~ 4.3	3.214	6.988	241.400	4.111
s	ML-34 2009-05-05 14:34:27	0.208	0.131	0.399		0.041	0.051	1.065	0.033
%RSD	ML-34 2009-05-05 14:34:27	1%	1%	0%		1%	1%	0%	1%

conc. (ppb)	ML-35 2009-05-05 14:36:33	16.570	21.590	744.50 0	<LD	3.578	6.591	471.80 0	10.780
s	ML-35 2009-05-05 14:36:33	0.181	0.113	1.936	--	0.036	0.027	1.492	0.022
%RSD	ML-35 2009-05-05 14:36:33	1%	1%	0%	--	1%	0%	0%	0%
conc. (ppb)	ML-36 2009-05-05 14:38:49	3.553	4.287	79.170	<LD	0.822	1.286	52.960	2.246
s	ML-36 2009-05-05 14:38:49	0.044	0.035	0.343	--	0.007	0.013	0.209	0.058
%RSD	ML-36 2009-05-05 14:38:49	1%	1%	0%	--	1%	1%	0%	3%
conc. (ppb)	ML-37 2009-05-05 14:40:48	3.499	3.959	136.50 0	<LD	0.796	1.203	36.520	1.937
s	ML-37 2009-05-05 14:40:48	0.036	0.046	0.851	--	0.021	0.004	0.222	0.046
%RSD	ML-37 2009-05-05 14:40:48	1%	1%	1%	--	3%	0%	1%	2%
conc. (ppb)	ML-38 2009-05-05 14:43:08	0.418	0.445	15.910	<LD	0.113	0.184	7.351	<LD
s	ML-38 2009-05-05 14:43:08	0.006	0.003	0.034	--	0.009	0.002	0.099	--
%RSD	ML-38 2009-05-05 14:43:08	1%	1%	0%	--	8%	1%	1%	--
conc. (ppb)	ML-39 2009-05-05 14:45:03	3.004	3.807	12.210	<LD	0.778	1.568	18.970	0.346
s	ML-39 2009-05-05 14:45:03	0.080	0.006	0.027	--	0.034	0.015	0.076	0.025
%RSD	ML-39 2009-05-05 14:45:03	3%	0%	0%	--	4%	1%	0%	7%
conc. (ppb)	ML-40 2009-05-05 14:47:07	0.214	0.219	6.387	0.3 ~ 0.8	0.057	0.080	6.655	0.522
s	ML-40 2009-05-05 14:47:07	0.007	0.007	0.137		0.008	0.006	0.044	0.021
%RSD	ML-40 2009-05-05 14:47:07	3%	3%	2%		14%	8%	1%	4%
conc. (ppb)	ML-41 2009-05-05 14:52:37	0.514	0.746	15.730	<LD	0.142	0.330	7.321	<LD
s	ML-41 2009-05-05 14:52:37	0.021	0.017	0.201	--	0.011	0.006	0.052	--
%RSD	ML-41 2009-05-05 14:52:37	4%	2%	1%	--	8%	2%	1%	--
conc. (ppb)	ML-42 2009-05-05 14:54:37	0.397	0.652	7.990	<LD	0.160	0.251	3.539	<LD
s	ML-42 2009-05-05 14:54:37	0.035	0.006	0.051	--	0.008	0.005	0.040	--
%RSD	ML-42 2009-05-05 14:54:37	9%	1%	1%	--	5%	2%	1%	--
conc. (ppb)	ML-43 2009-05-05 14:56:34	0.612	0.761	32.520	0.2 ~ 0.7	0.164	0.266	19.120	1.339
s	ML-43 2009-05-05 14:56:34	0.009	0.015	0.233		0.013	0.010	0.073	0.015
%RSD	ML-43 2009-05-05 14:56:34	1%	2%	1%		8%	4%	0%	1%
conc. (ppb)	ML-44 2009-05-06 13:06:18	0.352	0.471	10.760	<LD	0.146	0.234	18.130	0.730
s	ML-44 2009-05-06 13:06:18	0.020	0.002	0.333	--	0.007	0.009	0.030	0.017
%RSD	ML-44 2009-05-06 13:06:18	6%	0%	3%	--	5%	4%	0%	2%

conc. (ppb)	ML-45 2009-05-05 15:00:26	3.213	6.207	205.20 0	<LD	0.816	1.412	84.440	1.029
s	ML-45 2009-05-05 15:00:26	0.035	0.062	0.497	--	0.024	0.018	0.602	0.033
%RSD	ML-45 2009-05-05 15:00:26	1%	1%	0%	--	3%	1%	1%	3%
conc. (ppb)	ML-46 2009-05-05 15:02:44	11.790	17.520	562.80 0	1.6 ~ 4.7	3.218	5.650	287.10 0	79.710
s	ML-46 2009-05-05 15:02:44	0.045	0.116	3.857		0.062	0.057	0.428	0.308
%RSD	ML-46 2009-05-05 15:02:44	0%	1%	1%		2%	1%	0%	0%
conc. (ppb)	ML-47 2009-05-05 15:07:33	1.341	1.791	58.020	<LD	0.368	0.686	38.550	13.720
s	ML-47 2009-05-05 15:07:33	0.022	0.013	0.301	--	0.021	0.008	0.028	0.026
%RSD	ML-47 2009-05-05 15:07:33	2%	1%	1%	--	6%	1%	0%	0%
conc. (ppb)	ML-48 2009-05-05 15:11:48	3.275	4.169	194.00 0	1.6 ~ 4.9	0.823	1.415	81.700	72.180
s	ML-48 2009-05-05 15:11:48	0.052	0.047	0.536		0.008	0.015	0.392	0.451
%RSD	ML-48 2009-05-05 15:11:48	2%	1%	0%		1%	1%	0%	1%
conc. (ppb)	ML-49 2009-05-05 15:14:15	1.038	1.321	33.550	0.3 ~ 1.0	0.278	0.482	20.790	4.660
s	ML-49 2009-05-05 15:14:15	0.038	0.027	0.207		0.009	0.008	0.128	0.056
%RSD	ML-49 2009-05-05 15:14:15	4%	2%	1%		3%	2%	1%	1%
conc. (ppb)	ML-50 2009-05-05 15:25:12	3.478	3.625	6.662	12 ~ 37	1.336	2.079	5.456	0.987
s	ML-50 2009-05-05 15:25:12	0.029	0.007	0.047		0.020	0.025	0.060	0.025
%RSD	ML-50 2009-05-05 15:25:12	1%	0%	1%		1%	1%	1%	3%
conc. (ppb)	ML-51 2009-05-05 15:27:23	5.652	12.970	19.020	3 ~ 10	1.697	3.101	14.370	71.230
s	ML-51 2009-05-05 15:27:23	0.100	0.155	0.247		0.033	0.029	0.186	0.820
%RSD	ML-51 2009-05-05 15:27:23	2%	1%	1%		2%	1%	1%	1%
conc. (ppb)	ML-52 2009-05-05 15:32:11	<LD	<LD	<LD	<LD	<LD	<LD	0.256	0.338
s	ML-52 2009-05-05 15:32:11	--	--	--	--	--	--	0.013	0.013
%RSD	ML-52 2009-05-05 15:32:11	--	--	--	--	--	--	5%	4%
conc. (ppb)	ML-53 2009-05-05 15:34:23	0.780	0.732	4.187	7 ~ 22	0.344	0.462	5.660	0.701
s	ML-53 2009-05-05 15:34:23	0.025	0.010	0.033		0.025	0.011	0.060	0.047
%RSD	ML-53 2009-05-05 15:34:23	3%	1%	1%		7%	2%	1%	7%
conc. (ppb)	ML-54 2009-05-05 15:36:35	2.120	1.871	7.969	10 ~ 31	0.666	1.176	7.491	1.815
s	ML-54 2009-05-05 15:36:35	0.017	0.024	0.176		0.007	0.010	0.043	0.006
%RSD	ML-54 2009-05-05 15:36:35	1%	1%	2%		1%	1%	1%	0%

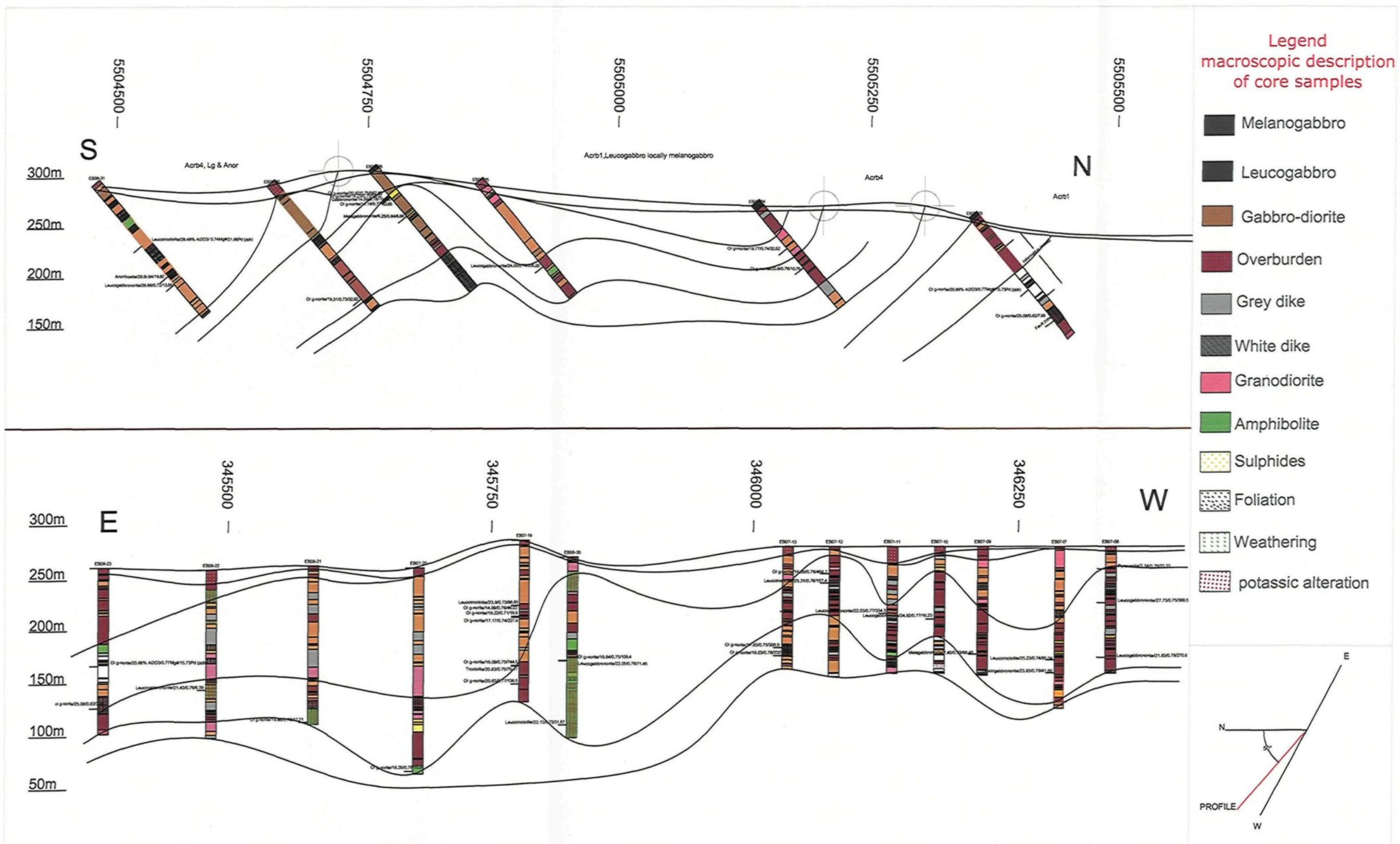
conc. (ppb)	ML-55 2009-05-05 15:38:41	0.605	0.698	32.920	<LD	0.226	0.330	37.820	1.262
s	ML-55 2009-05-05 15:38:41	0.036	0.004	0.234	--	0.006	0.002	0.289	0.039
%RSD	ML-55 2009-05-05 15:38:41	6%	1%	1%	--	3%	1%	1%	3%
conc. (ppb)	ML-56 2009-05-05 15:40:46	0.550	0.556	21.650	<LD	0.179	0.343	34.370	0.823
s	ML-56 2009-05-05 15:40:46	0.024	0.005	0.053	--	0.009	0.009	0.249	0.047
%RSD	ML-56 2009-05-05 15:40:46	4%	1%	0%	--	5%	3%	1%	6%
conc. (ppb)	ML-57 2009-05-05 15:42:56	0.464	0.791	19.820	<LD	0.092	0.271	6.281	<LD
s	ML-57 2009-05-05 15:42:56	0.010	0.008	0.102	--	0.005	0.004	0.108	--
%RSD	ML-57 2009-05-05 15:42:56	2%	1%	1%	--	5%	1%	2%	--
conc. (ppb)	ML-58 2009-05-05 15:45:07	0.423	0.369	13.560	<LD	0.085	0.143	9.539	0.772
s	ML-58 2009-05-05 15:45:07	0.028	0.006	0.188	--	0.009	0.008	0.147	0.036
%RSD	ML-58 2009-05-05 15:45:07	7%	2%	1%	--	11%	6%	2%	5%
conc. (ppb)	ML-59 2009-05-05 15:47:14	3.508	3.989	109.40 0	<LD	0.897	1.489	119.10 0	1.636
s	ML-59 2009-05-05 15:47:14	0.095	0.032	0.966	--	0.018	0.015	0.102	0.019
%RSD	ML-59 2009-05-05 15:47:14	3%	1%	1%	--	2%	1%	0%	1%
conc. (ppb)	ML-60 2009-05-05 15:49:34	3.369	3.819	71.450	<LD	0.958	1.704	104.90 0	0.752
s	ML-60 2009-05-05 15:49:34	0.051	0.026	0.469	--	0.011	0.028	0.656	0.013
%RSD	ML-60 2009-05-05 15:49:34	2%	1%	1%	--	1%	2%	1%	2%
conc. (ppb)	ML-61 2009-05-05 15:52:24	1.298	1.610	31.870	<LD	0.297	0.555	22.680	0.370
s	ML-61 2009-05-05 15:52:24	0.024	0.010	0.104	--	0.016	0.010	0.129	0.023
%RSD	ML-61 2009-05-05 15:52:24	2%	1%	0%	--	5%	2%	1%	6%
conc. (ppb)	ML-62 2009-05-05 15:54:38	4.115	5.639	95.950	0.5 ~ 1.5	1.191	1.960	81.380	1.277
s	ML-62 2009-05-05 15:54:38	0.094	0.058	0.327		0.020	0.016	0.898	0.011
%RSD	ML-62 2009-05-05 15:54:38	2%	1%	0%		2%	1%	1%	1%
conc. (ppb)	ML-63 2009-05-05 15:57:07	3.497	4.430	159.40 0	<LD	0.788	1.604	91.730	2.330
s	ML-63 2009-05-05 15:57:07	0.015	0.052	1.202	--	0.043	0.011	0.974	0.035
%RSD	ML-63 2009-05-05 15:57:07	0%	1%	1%	--	5%	1%	1%	2%
conc. (ppb)	ML-64 2009-05-05 15:59:29	8.491	11.330	300.20 0	<LD	1.544	3.005	198.40 0	1.022
s	ML-64 2009-05-05 15:59:29	0.079	0.076	1.177	--	0.024	0.029	0.958	0.020
%RSD	ML-64 2009-05-05 15:59:29	1%	1%	0%	--	2%	1%	0%	2%

conc. (ppb)	ML-65 2009-05-05 16:01:58	7.237	10.010	389.50 0	0.4 ~ 1.2	1.395	2.720	338.60 0	1.962
s	ML-65 2009-05-05 16:01:58	0.037	0.046	1.381		0.010	0.034	2.279	0.018
%RSD	ML-65 2009-05-05 16:01:58	1%	0%	0%		1%	1%	1%	1%

bb-235	Average	1.876	1.540	15.028	0.1 ~ 0.4	0.148	0.132	15.819	0.740
(20 run (4 samples)	STDEV	0.100	0.058	0.755		0.022	0.018	0.419	0.274
	RSD	5%	4%	5%		15%	14%	3%	37%
WORKING	bb-235	1.850	1.567	15.379	0.10 (ID)	0.165	0.125	15.656	1.073
WORKING	+/-	0.146	0.102	0.785	0.01 (ID)	0.039	0.019	0.868	0.512
		8%	7%	5%	10%	24%	15%	6%	48%

Limits of detection

This run	LD (3s on average blank bead) (ppb)	0.177	0.115	0.823	0.114	0.051	0.027	0.097	0.334
----------	-------------------------------------	-------	-------	-------	-------	-------	-------	-------	-------



 UNIVERSITÉ DU QUÉBEC À CHICOUTIMI	UNIVERSITÉ DU QUÉBEC À CHICOUTIMI	HINTERLANDS METALS	ELABORATED BY: CARLOS MARIO MUNOZ TABORDA	Appendix 7: Stratigraphic columns reconstruction upon borehole descriptions of Hinterland.	Appendix 7
	DEPARTAMENT DU SCIENCES DE LA TERRE	DISTRIBUTION OF PLATINUM GROUP ELEMENTS IN THE HINTERLAND'S EBAY CLAIM, CENTRAL PART OF THE BELL RIVER COMPLEX, MATAGAMI, QUEBEC	REVISED BY: S-J BARNES DIRECTED BY: S-J BARNES, MARK FEKETE, EDWARD SAWYER	DATE: July, 2010	

APPENDIX 8 Thin section descriptions

sample	mineralogy										Type of sulphides	S (ppm)	alterations	Musc	thin section description
	actinolite	plagioclase	epidote	clinozoisite	chlorite	Quartz	talc	titanite	relicts phases	sulphides					comments
ML-1	X		X	X	X	X			Hb	Ccp, Py		391.21	saussurite (sau)	X	weakly altered rock, euhedral crystals of Muscovite seen frequently, few Hb relicts, some Qz anhedral and some chlorites folded. metasomatism
ML-2			F e w	F e w	X	F e w			Cpx,Hb	Ccp		165.42	sau, sericite		altered sample, Cpx and Hb preserved, Plag altered and formation of epidote-clinoz. & Chl, some foliation visible
ML-3	X		X	X	F e w	F e w		X	Hb	Ccp, Py		40.35	sau		altered rock, plagioclases saussuritized and some hb relicts, formation of epidote-clinoz. and actinolite, veins are present(plag or epidote veins), some flux textures
ML-4	X		X	X	X	F e w		X	Hb,Cpx	Ccp		147.93	sau		weakly altered rock, particularly plag is totally altered, some relics of cpx & Hb, flux textures, some folded minerals (chl,act)
ML-5				F e w	X	X		X	Hb	Py	H	1665.32	sau		fresh rock composed by Qz, Hb & Chl, oriented, subhedral fine grains, silicified vein (various silicates) weakly altered.
ML-6	X	X	X	X	X	F e w		X	plag	Ccp, Pn		96.05	sau		partly altered rock,metamorphized, subgrains formation, no-foliated, various sizes
ML-7			X	X	X	F e w		X	Hb,Cpx	Ccp, Py	H	259.82	sau		foliated rock, chl abundant, highly sau, some Hb (and ver small cpx)
ML-8		X	F e w		X	X		X	Hb,Cpx	Ccp, Py		28.93	sau,chl		weakly altered rock,plag fresh, no oriented minerals,some Hb & Cpx remaining, cristals subhedral and sometimes broken
ML-9		X	X	X	F e w	X		X	Hb	Ccp		18.65	sau		weakly altered rock, plag. abundant, some sau. Hb are fresh & subhedrals, pressure effects on Hb and Chl
ML-10		X	X		X	X		X	Hb, plag	Ccp		61.68	sau, sericite		altered rock, plagioclases saussuritized and sericited,some epidote formation (few), few Hb

ML-11	X				F e w	F e w			Hb	Ccp, Po, Pn	M	15820.7 4	sericite		highly sericited rock, abundant actinolite, no foliated rock, medium to coarse grain size, fresh euhedral Hbs
ML-12	X	X	X	X	X			X	Hb	Ccp, Py, Pn	H/M	84.59	Chl		heterogeneous size crystals, anhedral, no foliated, spindle plag. and folded
ML-13		X	X	F e w	F e w	X			Hb	Ccp, Py		101.50	sau, musc, chl	X	plag highly altered (sau), some Hb relicts, formation of chl, musc. Local Qz veins
ML-14	X				X	X			few Hb	Py, Ccp	H	1100.56			metamorphized rocks with some Hb relicts, abundant actinolite and chl, anhedral to subhedral fine grains no oriented
ML-15	F e w	X	F e w	F e w	X	X		X	Hb	Ccp, Py		45.96	Chl, few sau		no foliated and anhedral crystals, green minerals surrounding plag., plag. and chl are the most abundant
ML-16		X	X	X	X	X			Hb	Ccp, Py		279.37	sau		this rock is composed of 2 parts, white and green, the white side is composed fundamentally by plag highly sau, and chl in few proportions, some hb relicts present. The green side is composed by abundant actinolite and chl. Some hb relicts as well. A Qz vein present
ML-17	X	X	X	X	X				Hb		0	260.63	few sau		subhedral to anhedral crystals, chl and actinolite fine grain size, plag are the biggest. No foliation
ML-18		f e w	X	X	X	f e w			Hb	Py		27.07	sau, musc	X	altered rock, fundamentally sau-plag and chl. Musc in long crystals, some foliation present
ML-19	X		X	f e w	X	F e w			Hb	Ccp, P y		116.39	sau		highly altered rock, anhedral crystals except epidote (subhedral), calcite vein
ML-20	X		f e w	f e w	X			X		Ccp		88.45	few sau		subhedral fine size crystals, fundamentally chl and actinolite, no foliated
ML-21	X				X	F e w				Po, Ccp, Py	H/M	304.33			actinolite and chl fundamentally, one vein of Qz. Some local flux textures. Anhedral crystals
ML-22		f e w	X			X				Py, Ccp		199.27	sau	X	epidote frequently, followed by Qz. Anhedral crystals, few musc.
ML-23			X	X		X				Py, Ccp		453.72	sau	X	abundant anhedral plag. (reaction borders) with epidote. Sau frequently, some Qz veins, few musc
ML-24	X	f e w	X	F e w	f e w	f e w				Ccp, Py	H	2115.39			abundant actinolite and anhedral plag. no foliated
ML-25	X		X	X	X	f e w				Py, Ccp		115.73	few sau		abundant actinolite subhedral no foliated, following epidote in amount, some foliation not so much pronounced

ML-26		X			f e w	X				Po, Ccp, Pn	M	467.76			fresh rock, abundant plag. Minor Qz and chl, Qz in veins too
ML-27	X	X	X	X	f e w	f e w				Ccp, Py, Po		83.42	weak sau		one part altered, one part metamorphized, plag sau, anhedral, abundant epidote, green part with abundant actinolite and chl in minor proportion neither actinolite nor chl have foliation, both anhedrals
ML-28	X	X	X			f e w				Ccp, Py		86.68			local flux textures, anhedral minerals, few plag fresh with a lot of apatite inclusions
ML-29	X	X	f e w			X	X			Ccp, Py		218.57			abundant actinolite, chl, anhedral crystals with abundant apatite inclusions, no foliated rock
ML-30	X	X	f e w			X	X			Po, Pn, Cc p	M	1652.83	few sau		abundant actinolite, plag weakly altered, anhedral plag. Subhedral actinolite and epidote
ML-31		X	X	X	X					Py, Ccp		177.25	sau	X	anhedral crystals of plag (more abundant with spindle texture). Highly altered rock, no foliated, epidote subhedral, big musc crystals
ML-32	F e w	X	X		f e w	X	f e w		Hb	Ccp, Py, Po		811.88	sau		weak chl and epidote formation (subhedrals and abundant), no foliated rock, plag weakly altered, little grains of actinolite (rare) associated with small Hb crystals, those anhedrals
ML-33	X	X	X	X	X	X			Hb	Po, Ccp, Py	H/M	2481.14	sau	X	2 parts, white and green, the white part are fundamentally plag, weakly altered and anhedral, Qz subgrains and chl; green part is actinolite fundamentally in small anhedral crystals, musc present, abundant epidote and minor chl, fine grains in the green part. In the whole sample epidote is the most abundant.
ML-34	X		X		f e w	X	f e w		Hb	Ccp, Py		461.99	sau	X	abundant actinolite in small grains, it is anhedral associated with fresh Hb. Abundant epidote, chl and megacrystals of musc. Some sau. Chl and epidote are subhedral.
ML-35	X		X		X	X				Po, Ccp, Py	H/M	284.55	sau		actinolite and chl are the principal phases, subhedral crystals. Few epidote, no foliated rock
ML-36	X		X		X	X				Ccp		295.88	sau, sericite	X	actinolite and chl are the most abundant minerals, actinolite is fine grained and subhedral, chl subhedral, few musc. No foliated rock
ML-37	X	f e w	X		X	X				Ccp		266.91	sau	X	very fine grains of actinolite (most abundant), subhedral epidote, musc. No foliated rock
ML-38	X		X		f e w	X	X		Hb	Ccp		277.69			very fine actinolite grains, abundant chl with brown patches, epidote subhedral are the biggest grains

ML-39	X		X	X	X	few			Hb	Ccp		305.67	sau	weak foliation, actinolite in fine grains are the most abundant, followed by chl, plag completely sau. sub to anhedral epidote fractured
ML-40	X	X	X	X	X		X	X	cpx, Plag	Po, Ccp, Mgt		174.87	sau	An66-An60, spindle texture on plag and folded crystals
ML-41	X	few	X	X	X	few	vn	X	cpx, Plag	Ccp,		299.63	talc, sau	granoblastic texture, polimineralic, subgrains on Qz, vein of talc, chl folded
ML-42		X	few	X		vn			plag			389.66	serp, sau+	altered rock, qz and talc veins.
ML-43	X	X	X	X	X	X	X	X	cpx, Plag	Po, Cc p, Pn		277.58	sau	px and amphibole poikiloblastic, clinozosites zoned
ML-44	X	X		X		X	vn		cpx, Plag	Ccp		352.19	Chl, sau	granoblastic texture, poikiloblastic amphiboles, chl deformed
ML-45	X	X	few	X	X	X		X	plag	Ccp, Po		217.80		oligoclase by Michel levi, spindle texture, subgrains, chl and plag folded
ML-46	X	X	X	X	X	few	X		opx	Py, Cc p, Po, Pn	H/M	9420.09	talc, sau, serp, chl	altered rock, some local foliation, An44 by Michel levi, chl folded
ML-47	X	X	X	X	X	few		X	Hb	Ccp, Py, Po	H/M	1484.45	Chl, sau	relict minerals, poikiloblastic texture, some chl folded
ML-48	X			X				X	Hb, px	Py, Cc p, Po, Pn	H/M	8804.29	Chl, arg, talc	partially metamorphosed rock, fresh minerals in one side and metamorphosed minerals in the other
ML-49	X	X	X	X	X			X	Hb, plag	Ccp, Py, Pn	H/M	2177.22	sau, chl	reaction borders in Hb of epidote, poikiloblastic texture, An45 by Michel levi
ML-50	X		X		few			X	hb	Po, Cc p, Pn	M	41654.00		Calcite as accessory phase, elongated crystals of actinolite associated with epidote
ML-51		X	X		few	X		X		Py, Cc p, Pn, Po	H/M	195834.000		An50 by levi, relatively fresh rock, plag and epidote abundant
ML-52		X			X	X				Pn		261.06	chl	qzodioritic rock, Plag, hb, bt, qz, chl are the main phases
ML-53	X		X		X		X			Po, Pn, Cc p	M	14502.28	talc, chl	altered phenocrystals of tremolite-actinolite towards chlorite and talc, anhedral, sprinkle epidotes
ML-54	X		X		X		X	X		Po, Cc p, Pn	M	32266.00	chl	altered rock, contact metamorphism with deformed phases, chloritized amphiboles
ML-55	X	X	X	X	X							450.66	sau	poikiloblastic crystals of actinolite, sometimes forming subgrains, weakly altered. Albite twins with saussurite

ML-56	f e w	X	X	X	X					plag	Ccp,Py,Pn		413.81	sau	An44 (andesine) by levi, labradorite by micro XRF, fluids evidence which form the ppal phases, abundant epidote on veins; plag altered and the most abundant on the rock	
ML-57		X	X	X	X						Po,Ccp		287.01	sau	partly altered rock, plag is the most abundant mineral, this saussuritized, albite twins and apatite inclusions, epidote clinozoisite anhedral colorless no pleochroic, some zoned. Chl filling spaces between plag and epidote	
ML-58	X	X	X	X	X					plag	Ccp,Py	H	262.12	sau,chl	actinolite subidiomorphic, poikiloblastic, altered to chl, An46 by levi, labradorite by micro XRF; anhedral plag with saussuritized borders, albite and pericline twins. Weakly altered rock	
ML-59		X	X	X	X					plag			427.16	chl,sau	altered rock, red points on plag possible by saussurite, epidote-clinozoisite fine to medium-grained some anhedral, some subhedral and pleochroic	
ML-60	X	X	X	X	X					MgHb			375.70	chl	chl folded, micro xrf tremolite and MgHb, altered rock, partially metamorphosed, strong sericitization and saussuritization, Hb retrograding to Chl.	
ML-61	X	X	X	X	X					plag, hb			460.07	sau,chl,ser	chl folded, hb sometimes in cores of actinolite, altered rock; some Hb retrograded to Chl, Plag very altered to saussurite or sericite, pseudomorphism in epidote and clinozoisite	
ML-62		X	X	X	X	X	X			plag,hb	Ccp,Py	H	421.03	sau,chl,talc	X	Altered rock, qz veins, zonation in epidotes, plag anhedral altered to saussurite, chl green to colourless, clinozoisite-epidot are subhedral, blue anomalous, very few Qz and fine-grained. Very few talc is present
ML-63	f e w	X	X	X	X					px,Plag	Py,Ccp,Po		613.81	Chl	X	altered rock, chl from px,epidote clinozoisite only phases formed on the metamorphism, they subhedral to anhedral, c.i. blue anomalous
ML-64		X	X	X	X	X				plag,hb,bt			345.77	chl,sau	vein of qz,plag, bt,chl. Plag partially altered, albite and pericline twins, some zoned. Abundant chl	
ML-65		X	X	X	X					cpx,hb,plag	Ccp,Py		407.55	sau,chl	X	altered rock,epidote-clinozoisite zoned, irregular fractures. Chl green pleochroic to colourless. Clinosoizite-epidote subhedral in some places anhedral, very few px and Hb being altered.

Ccp=chalcopyrite, Py=pyrite, Po=Pyrrhotite, Pn= pentlandite, Mgt=magnetite,H=hydrothermal sulphides, M=magmatic sulphides, H/M= transition magmatic-hydrothermal sulphides

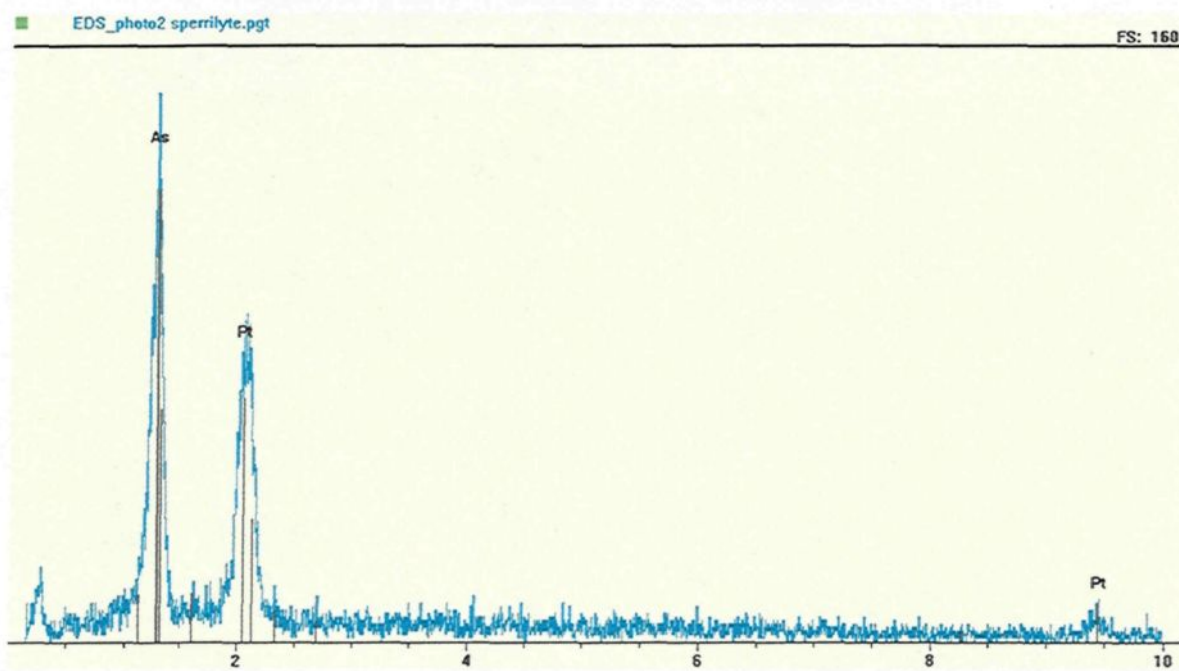
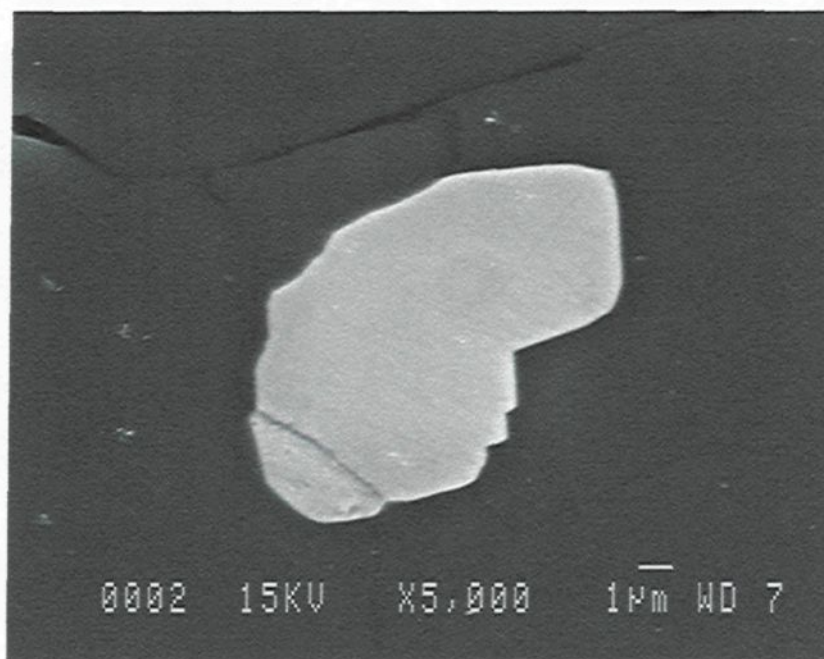
APPENDIX 9 CIPW norm classification

Sample	OI	Di	Hy	Ab	An	K-feldspar	Quartz	Magnetite	Ilmenite	Apatite	Pyrite	Total Plagioclase	Total Pyroxene	RockType
ML 01	19.1	0	0	6.58	55	17.72	0	1.52	0.1	0	0.08	61.53	0	leucotroctolite
ML 02	31.7	5.36	4.64	7.38	46.5	1.25	0	2.95	0.2	0	0.03	53.9	10	olivine-gabbronorite
ML 03	21.7	8.23	0	12.5	50.5	4.77	0	2.09	0.2	0	0.01	63.02	8.23	leucogabbronorite
ML 04	29.7	0.48	5.8	8.44	47.5	5.22	0	2.69	0.2	0	0.03	55.92	6.28	olivine-gabbronorite
ML 05	21.5	4.08	6.87	21.7	39.7	2.6	0	2.77	0.3	0.1	0.32	61.39	10.94	monzonite
ML 06	24.6	5.46	3.82	9.23	50.3	3.91	0	2.42	0.2	0	0.02	59.54	9.28	olivine-gabbronorite
ML 07	30.8	0	12.3	6.24	43.3	4.37	0	2.82	0.2	0	0.06	49.57	12.26	olivine-gabbronorite
ML 08	10.8	0	6.59	18.3	53.1	9.97	0	1.13	0.2	0	0.01	71.35	6.59	leucogabbronorite
ML 09	15.1	4.38	0	15.5	57.5	5.93	0	1.43	0.2	0	0	73.03	4.38	leucotroctolite
ML 10	14.7	0	14.8	10.8	49.4	8.38	0	1.78	0.1	0	0.01	60.18	14.81	leucogabbronorite
ML 11	0	34	46.5	0.08	5.48	0.06	6.05	4.54	0.2	0	3.03	5.57	80.55	pyroxenite
ML 12	10	1.3	4.5	13.4	67.4	2.11	0	1.11	0.2	0	0.02	80.78	5.81	leucogabbronorite
ML 13	17.9	0	11.8	20.2	41.4	6.64	0	1.94	0.1	0	0.02	61.56	11.83	leucogabbronorite
ML 14	5.43	25.6	44.5	1.5	19.2	0.19	0	3.22	0.2	0	0.22	20.67	70.11	melagabbronorite
ML 15	17.7	0	8.51	9.47	58.5	3.91	0	1.77	0.1	0	0.01	67.92	8.51	leucogabbronorite
ML 16	22.5	0	6.58	9.96	49.2	9.49	0	2.07	0.1	0	0.05	59.17	6.58	leucogabbronorite
ML 17	31.8	3.17	14.3	5.47	40.9	0.75	0	3.34	0.2	0	0.05	46.37	17.48	olivine-gabbronorite
ML 18	22	0	0	8.51	58.9	8.73	0	1.75	0.1	0	0.01	67.44	0	leucotroctolite
ML 19	23.4	10.3	12.1	3.12	44.6	3.27	0	2.91	0.3	0	0.02	47.71	22.4	olivine-gabbronorite
ML 20	33.7	0	19.5	2.03	38.5	2.7	0	3.45	0.1	0	0.02	40.51	19.46	olivine-gabbronorite
ML 21	31.9	0	18.1	6.38	38.7	0.84	0	3.69	0.3	0	0.07	45.1	18.11	olivine-gabbronorite
ML 22	1.31	14.8	0	26	54.9	1.82	0	1	0.2	0	0.04	80.81	14.77	leuconorite
ML 23	2.19	6.39	0	27.9	60.4	2.37	0	0.55	0.2	0	0.08	88.21	6.39	anorthosite
ML 24	24.4	5.05	2.74	8.09	55	1.74	0	2.47	0.1	0	0.42	63.08	7.79	leucogabbronorite
ML 25	31.6	3.26	13.3	5.44	42.2	0.63	0	3.41	0.1	0	0.02	47.67	16.58	olivine-gabbronorite
ML 26	6.1	2.94	0	48.6	39.6	1.17	0	0.66	0.8	0	0.09	88.21	2.94	monzonite
ML 27	20.9	2.75	4.43	9.94	56	3.72	0	2.09	0.2	0	0.02	65.93	7.18	leucogabbronorite
ML 28	17.4	3.55	3.68	11.4	59.2	2.83	0	1.77	0.2	0	0.02	70.54	7.23	leucogabbronorite
ML 29	23.2	3.09	7.39	10.9	52	0.94	0	2.28	0.2	0	0.04	62.88	10.48	leucogabbronorite
ML 30	23.8	2.68	8.36	10.3	51.1	0.82	0	2.46	0.2	0	0.33	61.37	11.04	olivine-gabbronorite
ML 31	21	4.62	0	10.5	56.9	4.69	0	2.01	0.2	0	0.03	67.47	4.62	leucotroctolite

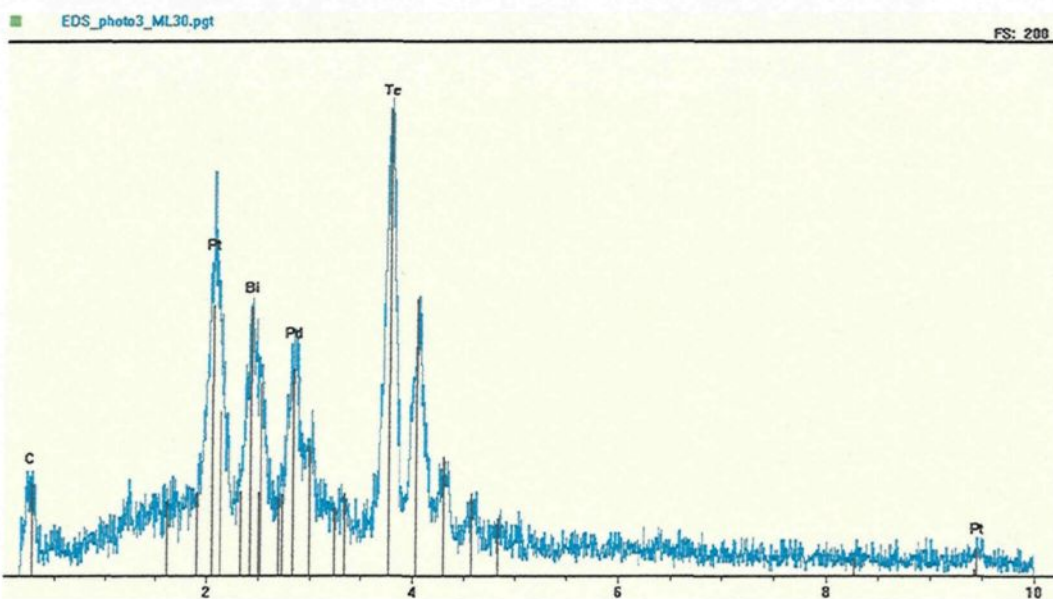
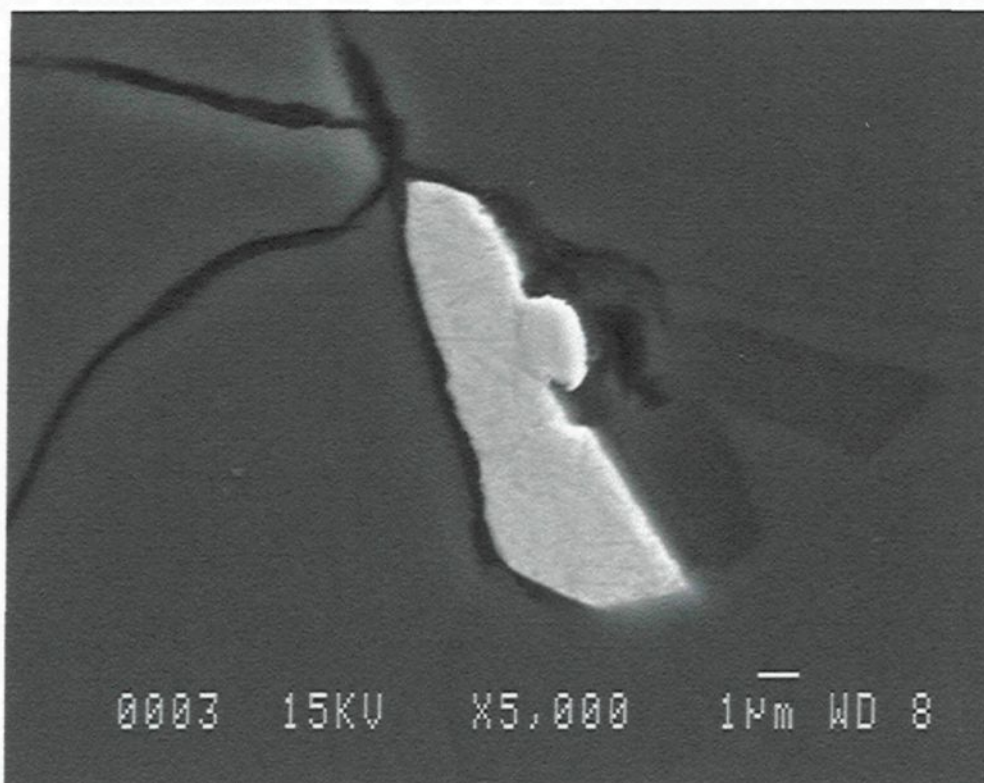
Sample	OI	Di	Hy	Ab	An	K-feldspar	Quartz	Magnetite	Ilmenite	Apatite	Pyrite	Total Plagioclase	Total Pyroxene	RockType
ML 32	27.3	6.94	19.1	3.6	38.3	1.01	0	3.47	0.2	0	0.16	41.88	26.06	olivine-gabbronorite
ML 33	14.6	10.9	8.75	18.5	40.6	3.24	0	2.45	0.4	0.1	0.48	59.06	19.64	olivine-gabbronorite
ML 34	26.5	3.08	15	8.62	41	2.26	0	3.31	0.2	0	0.1	49.56	18.04	olivine-gabbronorite
ML 35	35	0	17	3.41	39.8	0.71	0	3.88	0.1	0	0.05	43.21	16.97	olivine-gabbronorite
ML 36	30.8	1.77	2.85	9.23	51.1	1.26	0	2.76	0.1	0	0.06	60.33	4.61	troctolite
ML 37	22.9	3.89	9.53	8.49	50.7	1.92	0	2.37	0.2	0	0.05	59.14	13.42	olivine-gabbronorite
ML 38	29.3	0	13.2	7.75	44.2	2.49	0	2.84	0.2	0	0.05	51.94	13.16	olivine-gabbronorite
ML 39	27.5	0	13.9	10.1	41.2	4.38	0	2.65	0.2	0	0.07	51.34	13.91	olivine-gabbronorite
ML 40	8.54	12.6	11.1	12.4	50.4	2.93	0	1.63	0.4	0	0.03	62.75	23.75	leucogabbronorite
ML 41	24	0	14	7.91	46.5	4.84	0	2.55	0.2	0	0.06	54.42	13.99	olivine-gabbronorite
ML 42	16.1	0	29.4	13.4	26	12.6	0	2.24	0.2	0	0.09	39.43	29.41	olivine-gabbronorite
ML 43	11	11.6	11.6	14.1	43.3	6.03	0	2	0.3	0	0.05	57.42	23.19	olivine-gabbronorite
ML 44	27.4	3.41	4.66	5.83	49.9	6.03	0	2.51	0.2	0	0.07	55.73	8.08	olivine-gabbronorite
ML 45	16.2	3.79	6.11	12.1	58.5	1.17	0	1.87	0.3	0	0.04	70.59	9.89	leucogabbronorite
ML 46	21.2	3.27	8.5	9.55	48.2	4.32	0	2.9	0.2	0	1.86	57.74	11.78	olivine-gabbronorite
ML 47	24.1	7.3	11.2	6.87	44.2	3	0	2.92	0.2	0	0.3	51.08	18.48	olivine-gabbronorite
ML 48	0	25.5	27.2	6.2	34.8	1.39	0.31	2.5	0.4	0	1.68	41.03	52.74	gabbronorite
ML 49	8.17	24.7	21.8	6.36	34.4	1.21	0	2.6	0.3	0	0.42	40.75	46.52	olivine-gabbronorite
ML 50	0	42.4	24.7	1.29	14.2	0.31	2.11	6.34	0.8	0	7.88	15.48	67.04	melagabbronorite
ML 51	6.58	9.94	0	19.6	20.4	0.14	0	11.2	0.2	0	31.9	40.08	9.94	leucogabbronorite
ML 52	0	1.94	5.52	37.7	25.1	0.89	26.5	1.14	0.8	0.4	0.05	62.77	7.46	monzogranite
ML 53	0	63.4	19	1.54	6.16	0.18	1.46	4.38	1.1	0	2.75	7.7	82.42	pyroxenite
ML 54	0	43.1	31.1	1.89	6.12	0.24	5.06	5.65	0.9	0	5.95	8.01	74.17	pyroxenite
ML 55	26.7	6.91	6.07	7.21	47.4	2.43	0	2.9	0.2	0	0.08	54.65	12.99	olivine-gabbronorite
ML 56	11.8	0.94	0.5	14.2	68.9	2.44	0	1.07	0.1	0	0.08	83.04	1.44	leucotroctolite
ML 57	2.77	5.71	0	17.1	70.5	3.04	0	0.58	0.1	0.1	0.05	87.67	5.71	anorthosite
ML 58	6.74	8.56	3.24	14	64.4	1.68	0	1.1	0.3	0	0.05	78.37	11.8	leucogabbronorite
ML 59	17.3	7.47	12	12.8	41	6.74	0	2.33	0.2	0	0.08	53.88	19.52	olivine-gabbronorite
ML 60	20	3.08	4.05	10.1	48.5	12.2	0	1.87	0.1	0	0.07	58.63	7.13	leucogabbronorite
ML 61	23.4	0.82	3.2	15.4	49.5	5.13	0	2.29	0.2	0	0.1	64.84	4.02	leucotroctolite
ML 62	22.5	2.41	0	6.59	55.3	10.88	0	1.98	0.2	0	0.08	61.9	2.41	leucotroctolite
ML 63	22	6.02	7.38	9.91	49.3	2.78	0	2.39	0.2	0	0.11	59.17	13.4	olivine-gabbronorite
ML 64	21.5	1.92	9.25	16.5	45.1	2.72	0	2.57	0.4	0.1	0.06	61.54	11.17	leucogabbronorite
ML 65	27.1	5	0	12.6	50	2.57	0	2.54	0.2	0	0.08	62.58	5	leucotroctolite

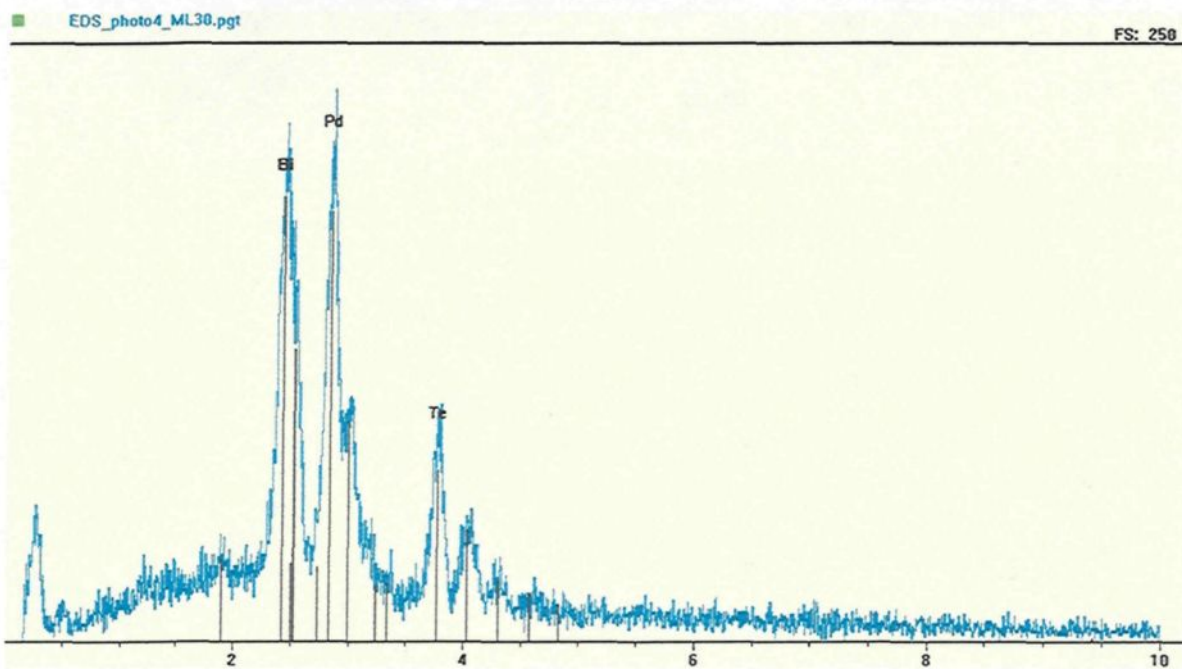
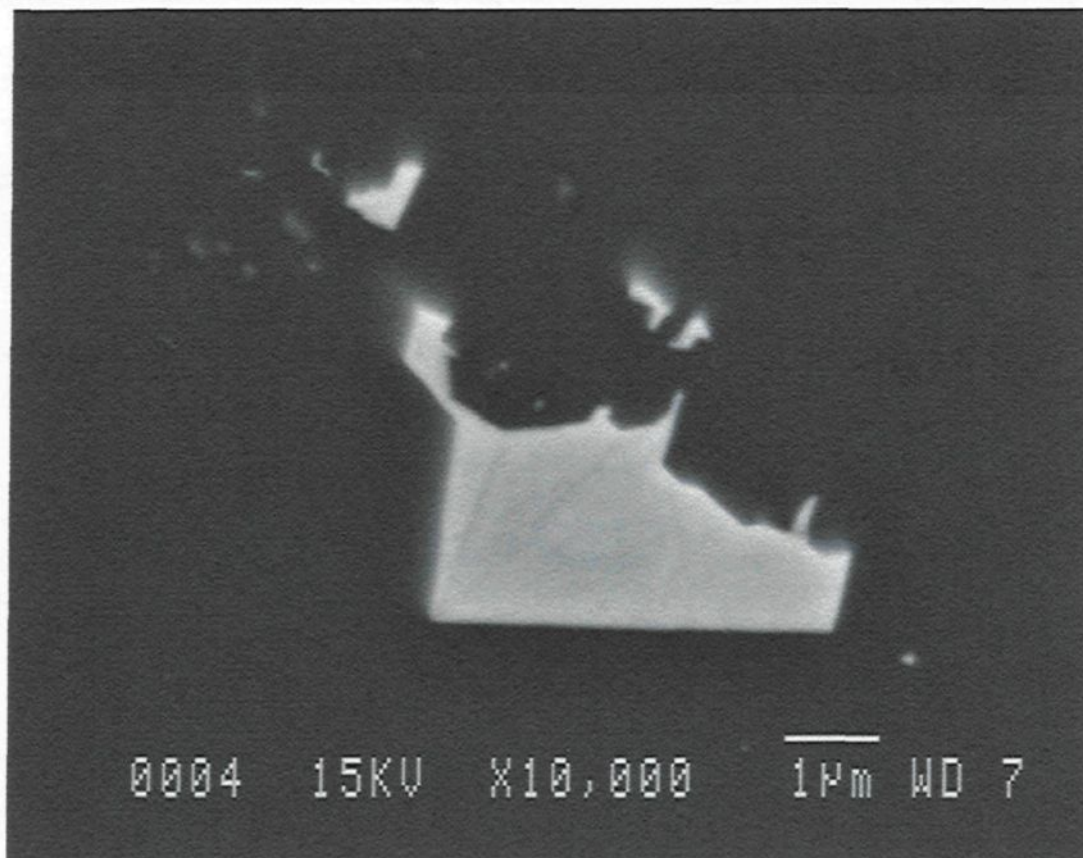
APPENDIX 10 SEM sessions, pictures and histograms

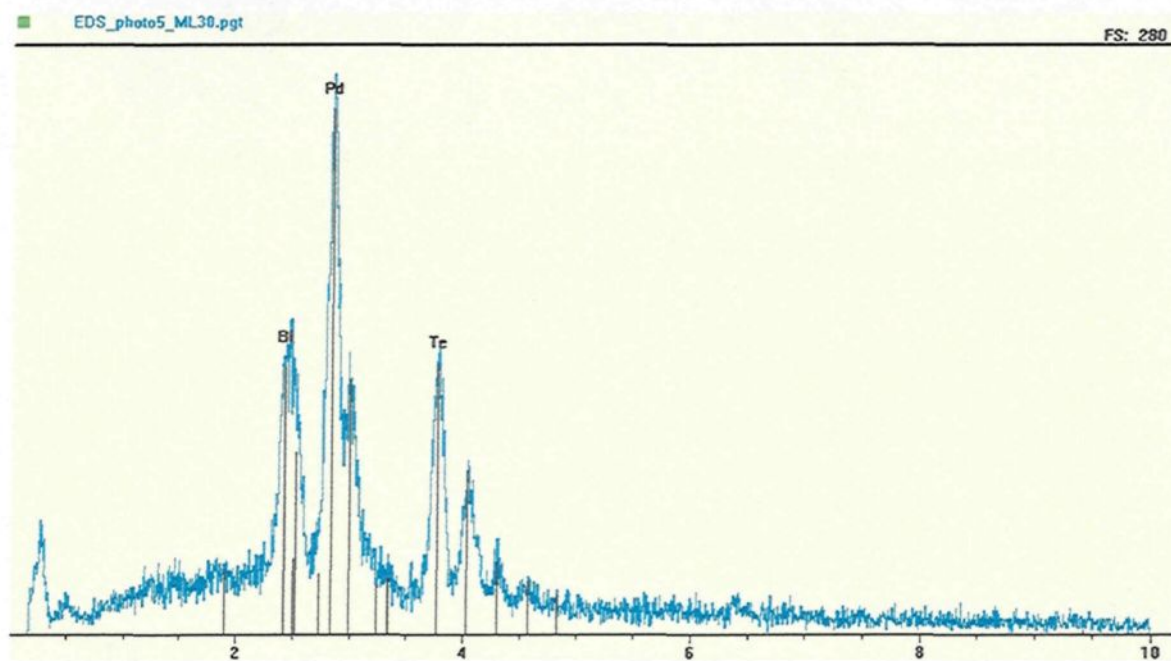
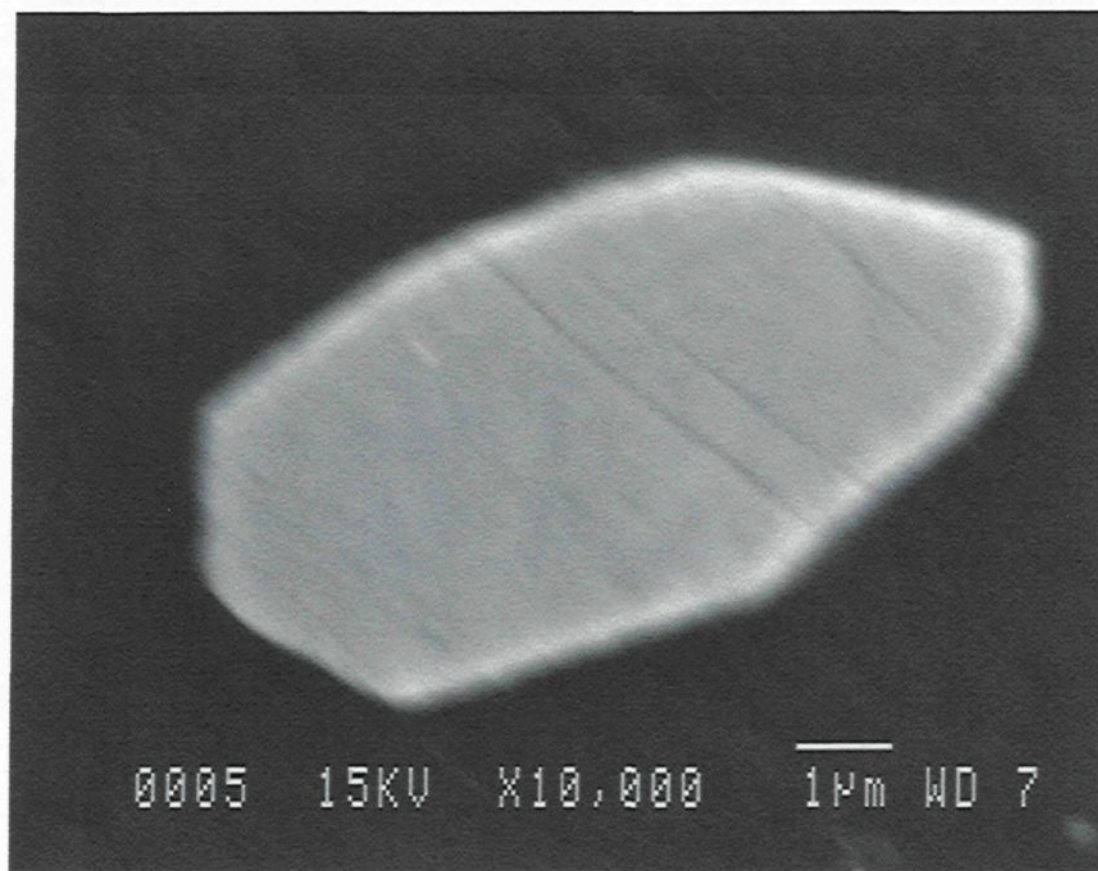
ML-21

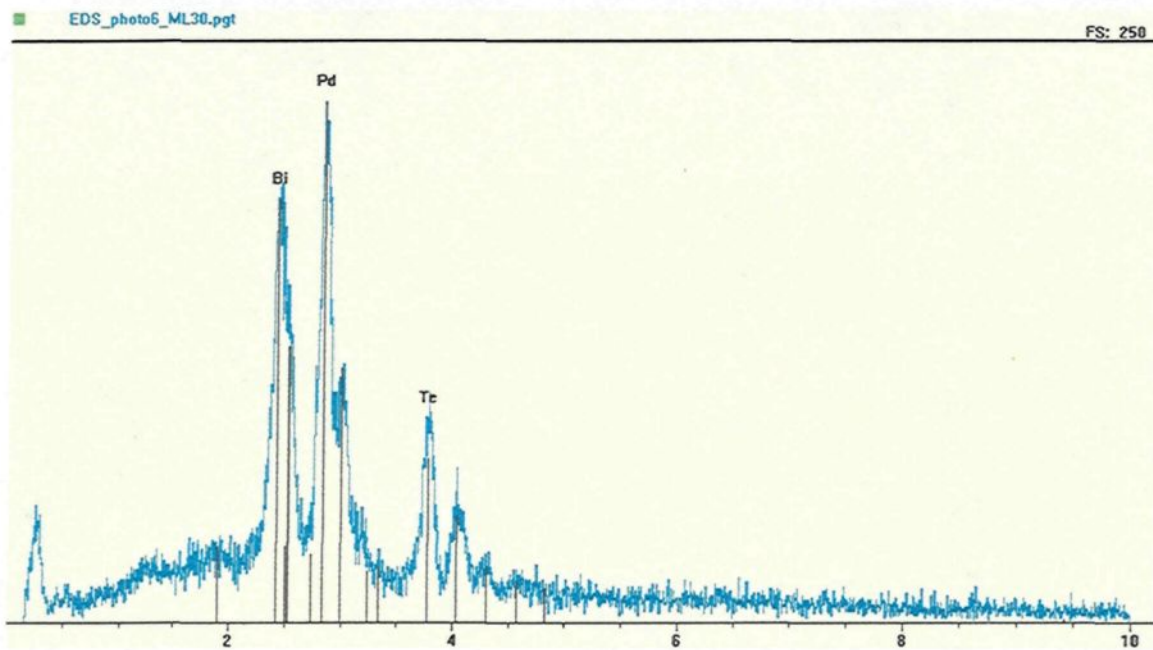
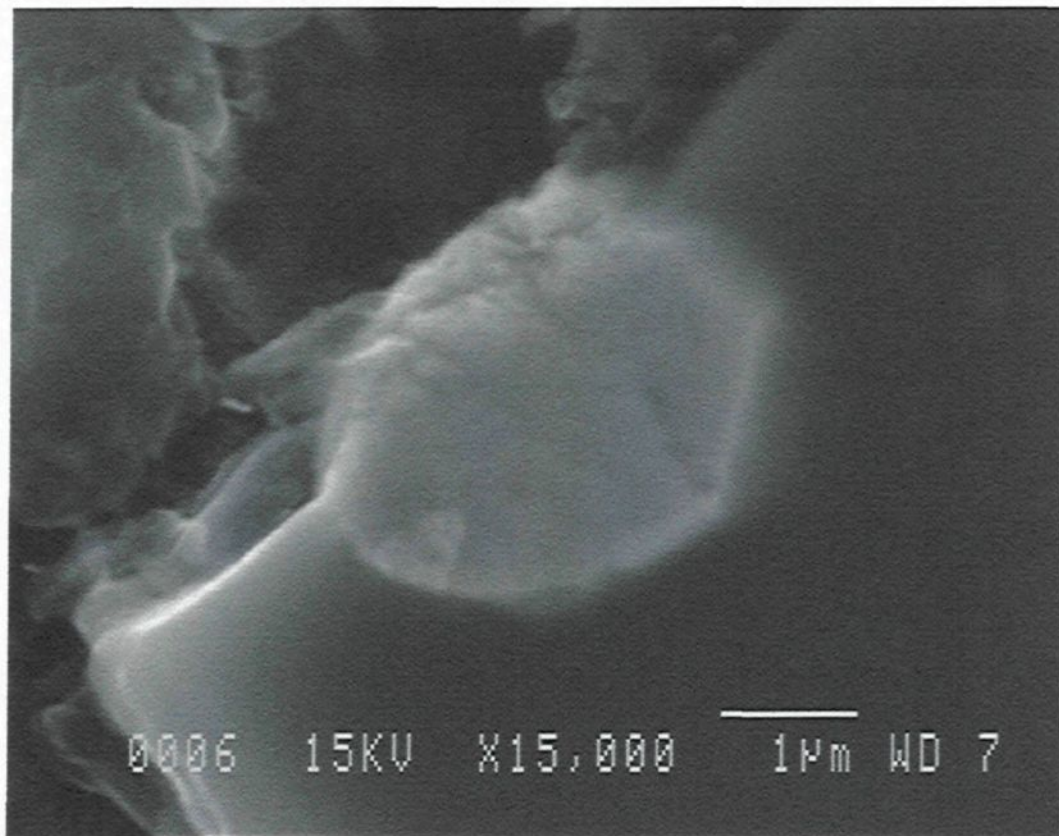


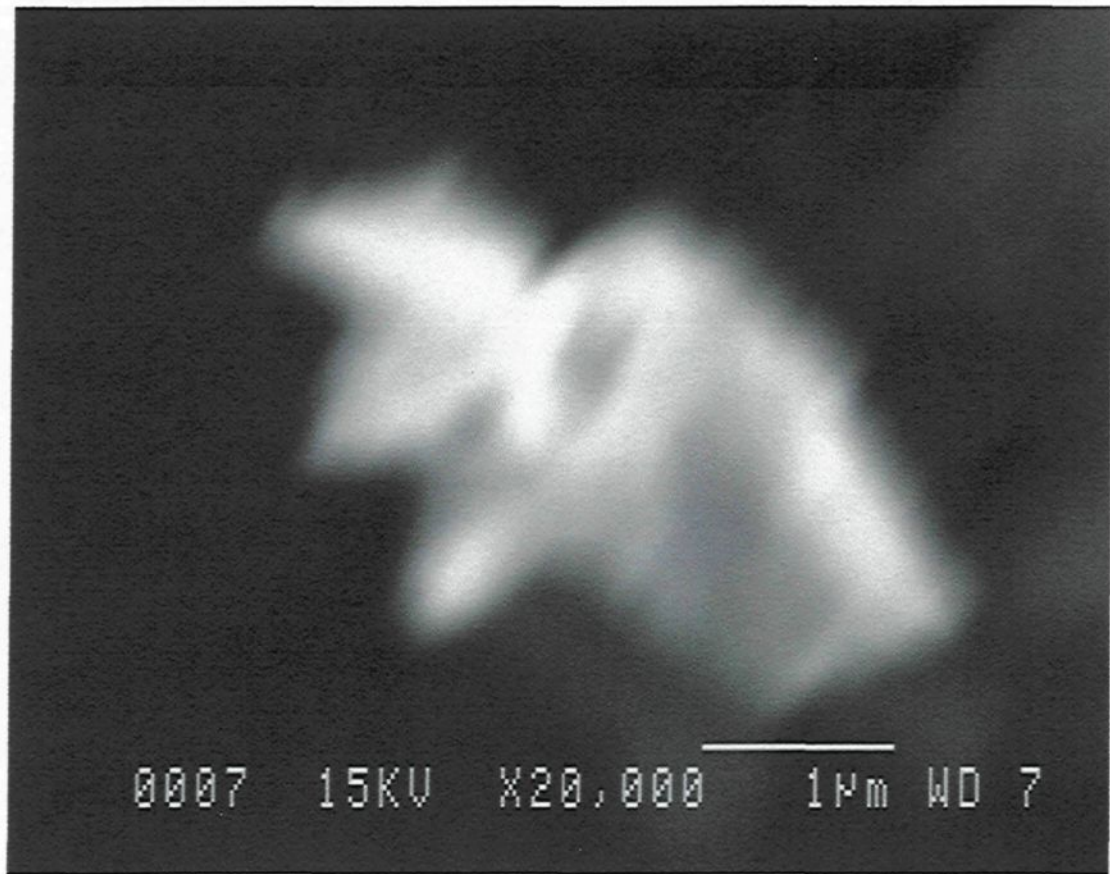
ML-30





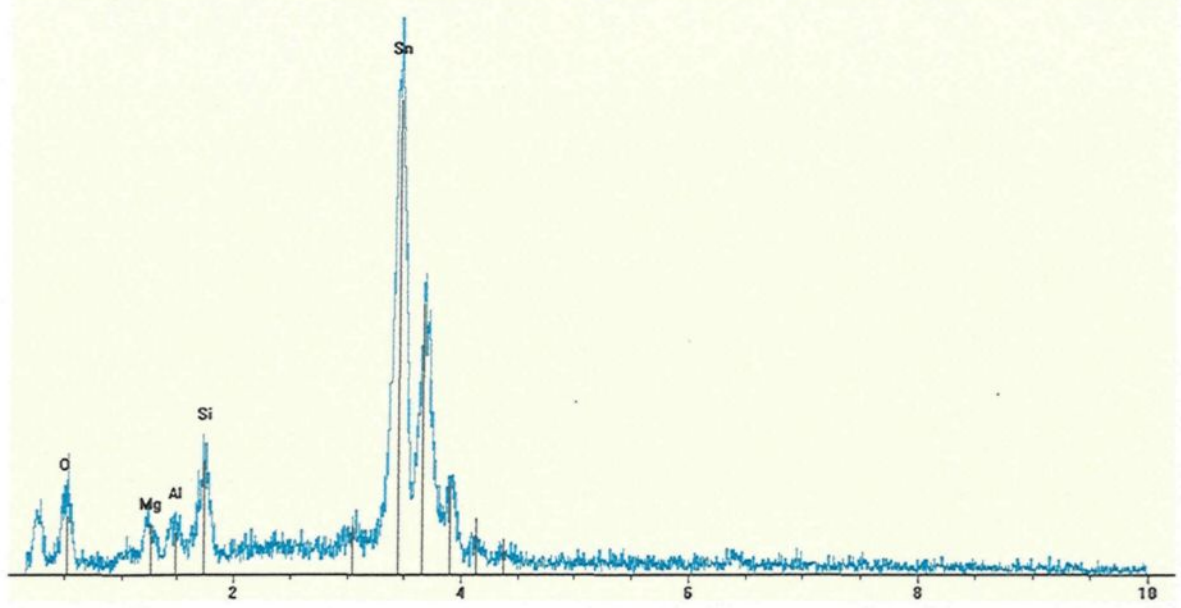


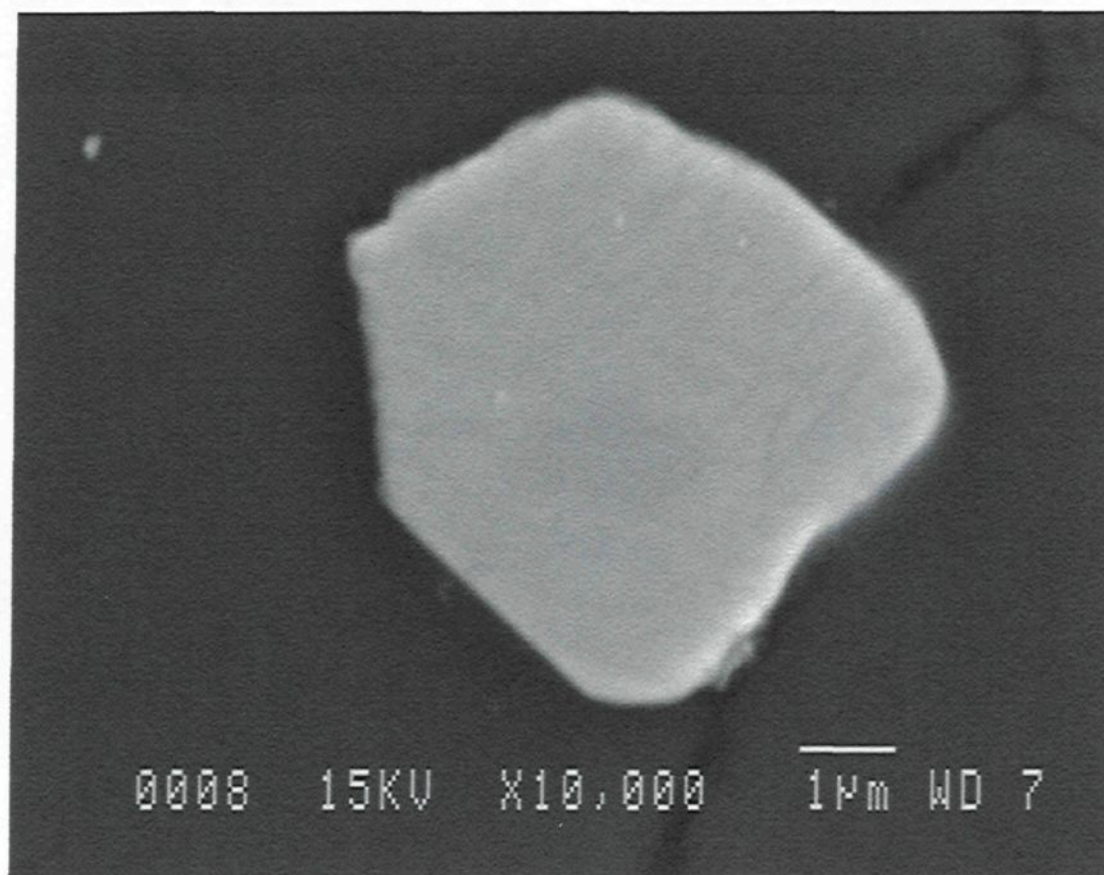




EDS_photo7_ML30 Sn.ppt

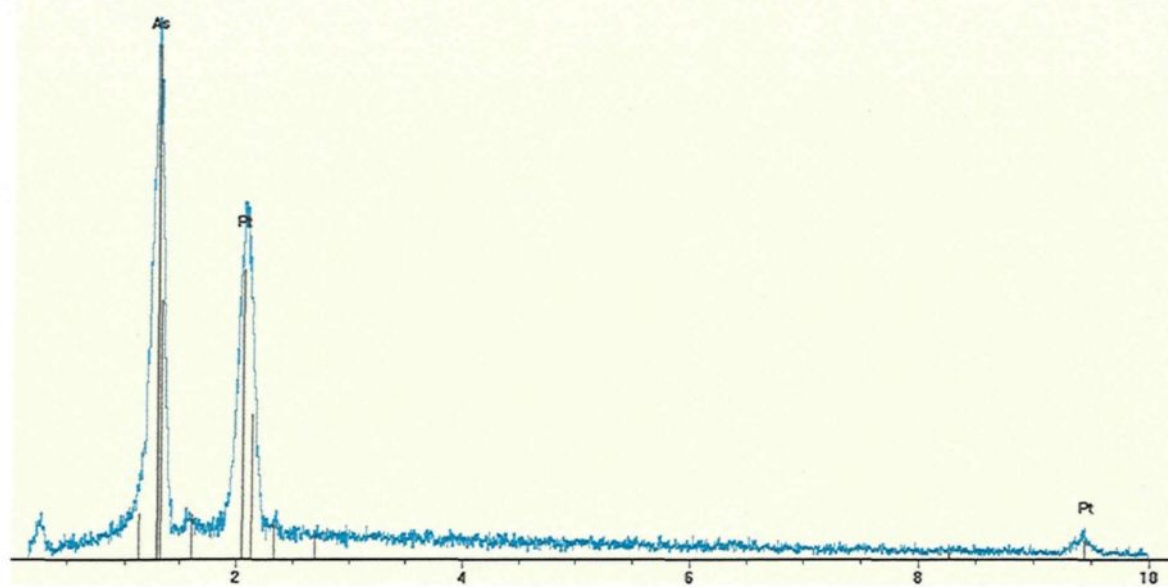
FS: 320



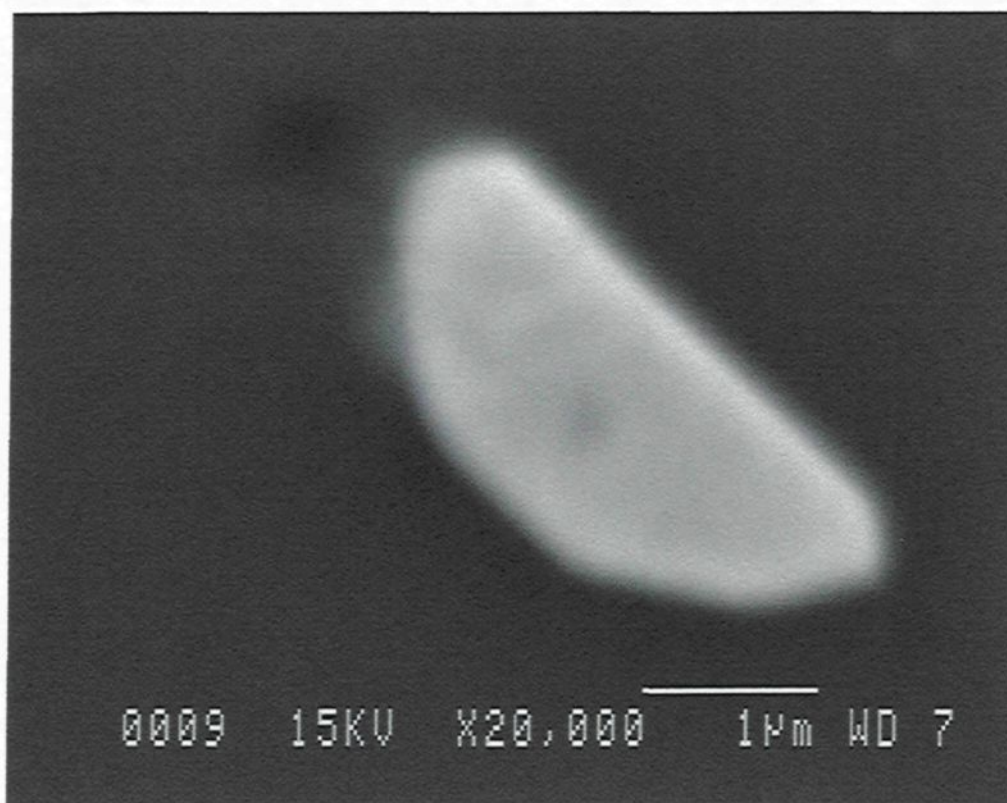


EDS_photo8_ML35 PtAs.pgt

FS: 640

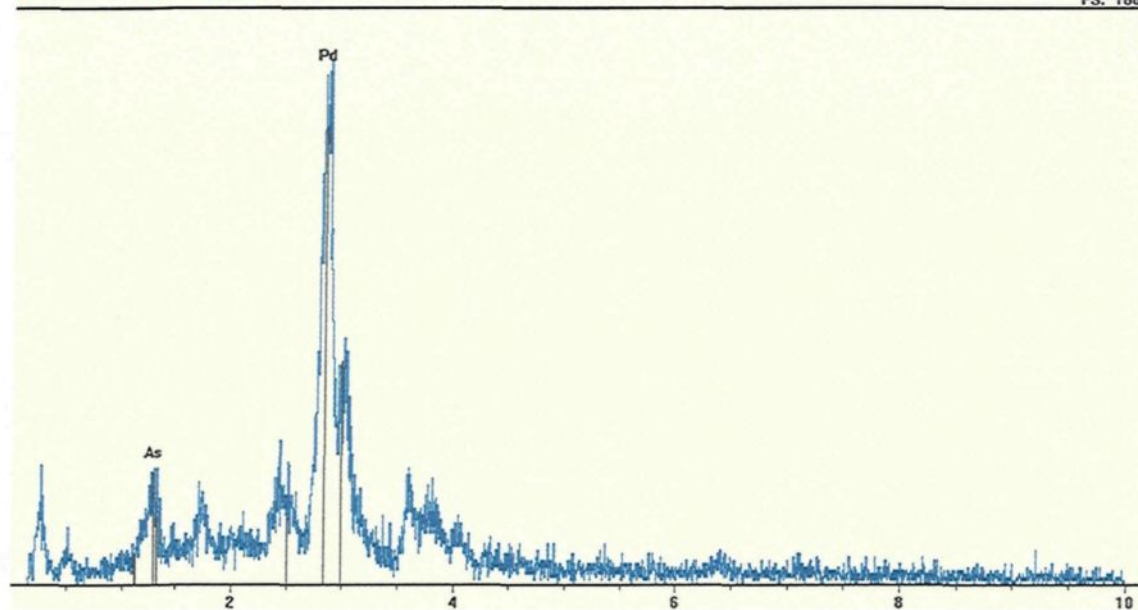


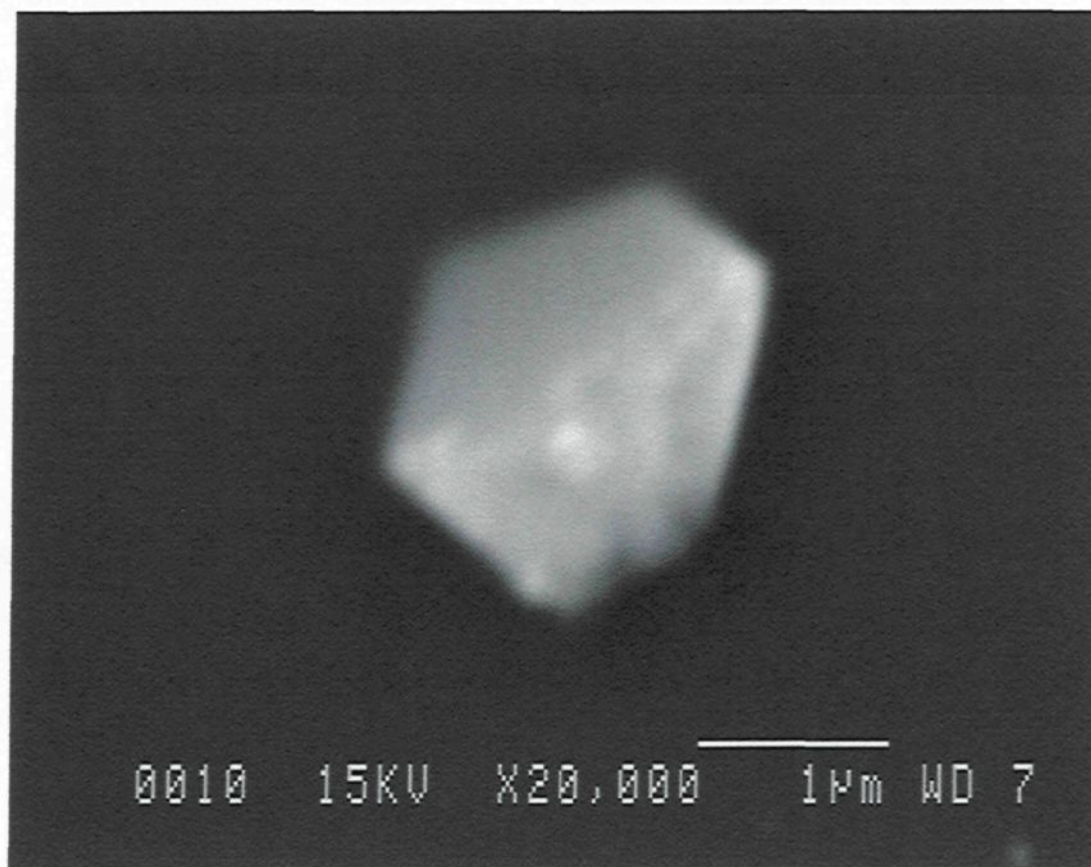
ML-35



EDS photo 9 ML 35 Pd.pgt

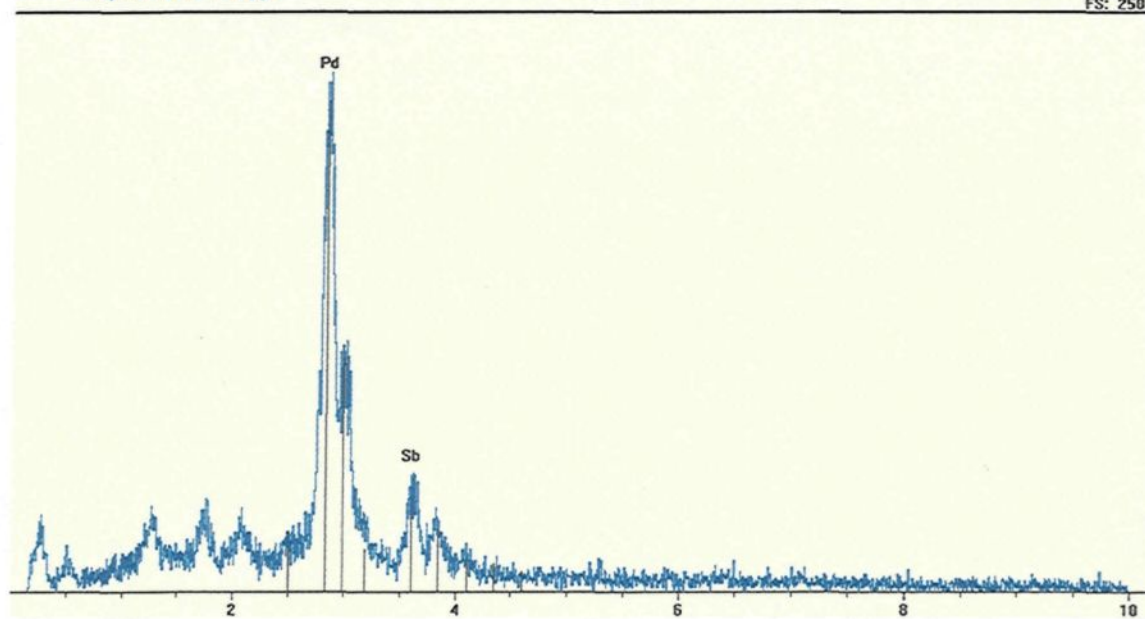
FS: 160

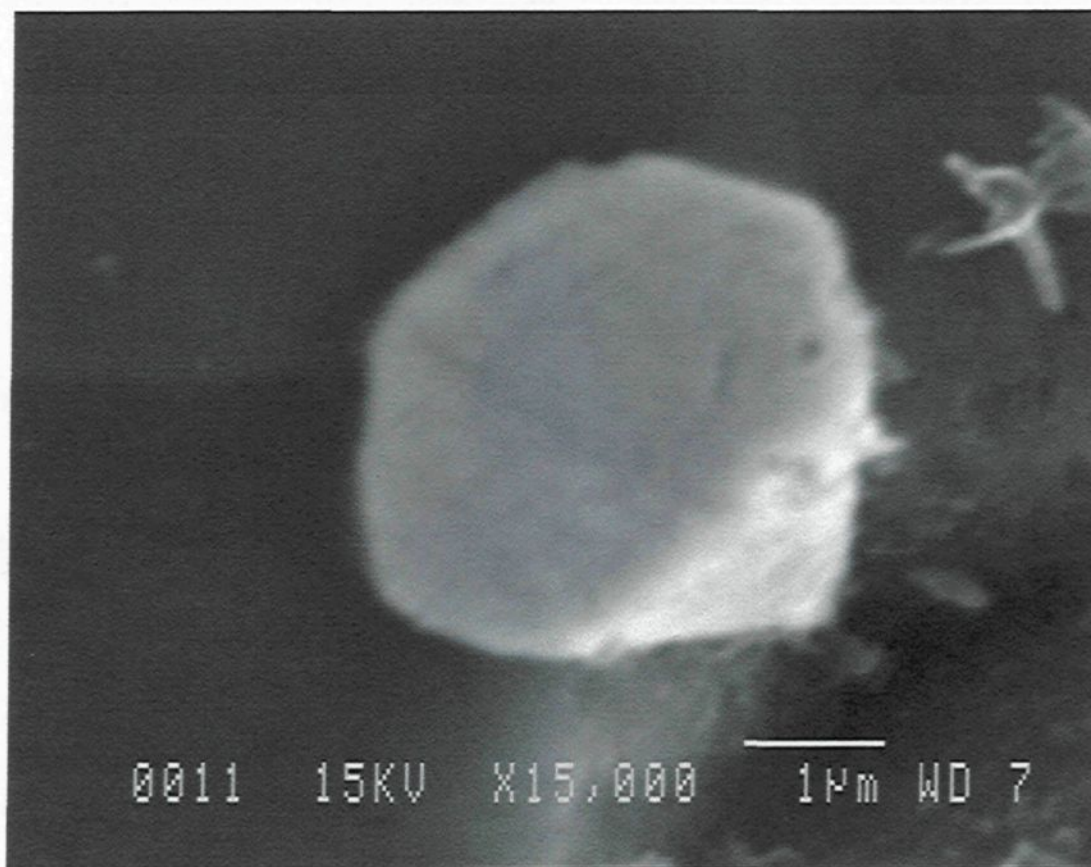




EDS photo 10 ML 35 Pd.pgt

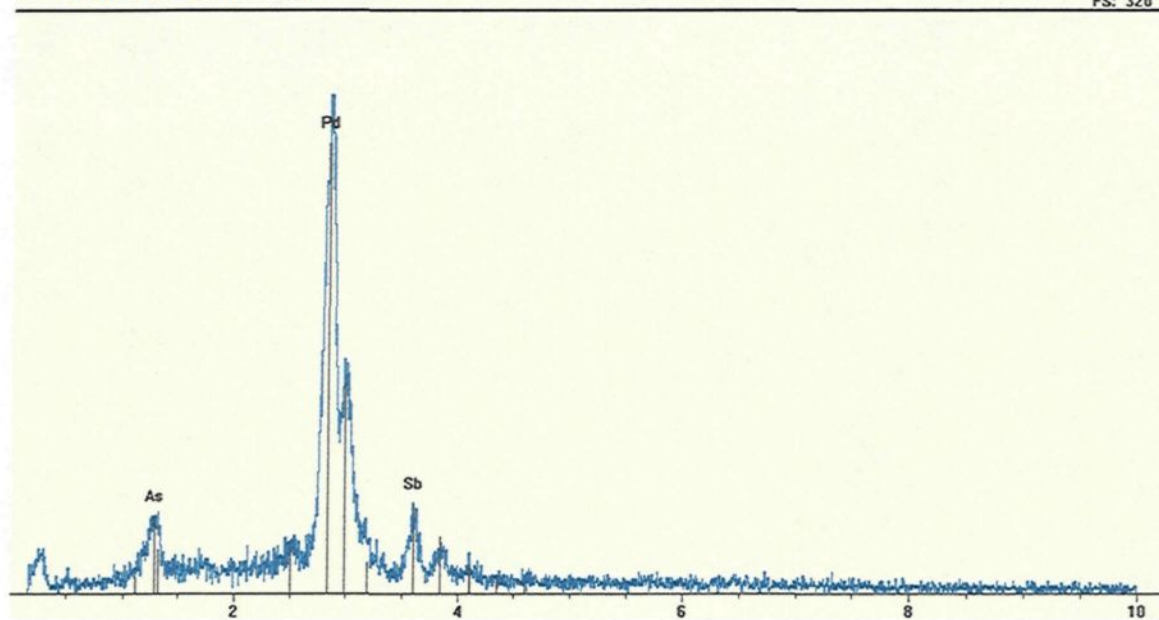
FS: 250

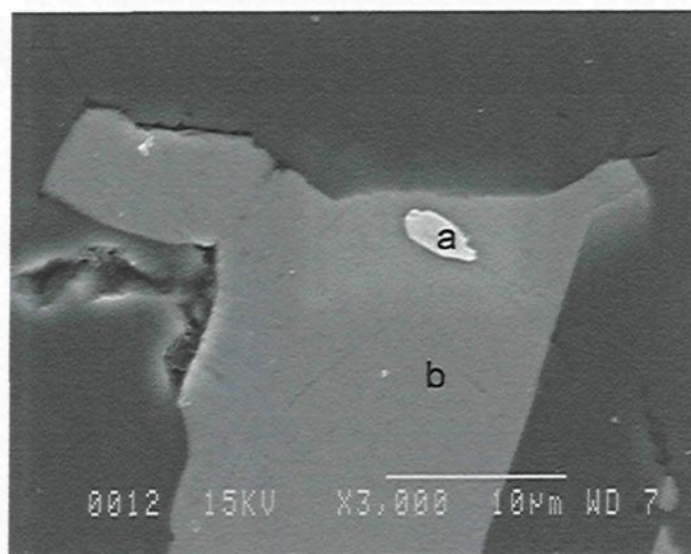




EDS photo 11 ML 35 PdSbAs.pgt

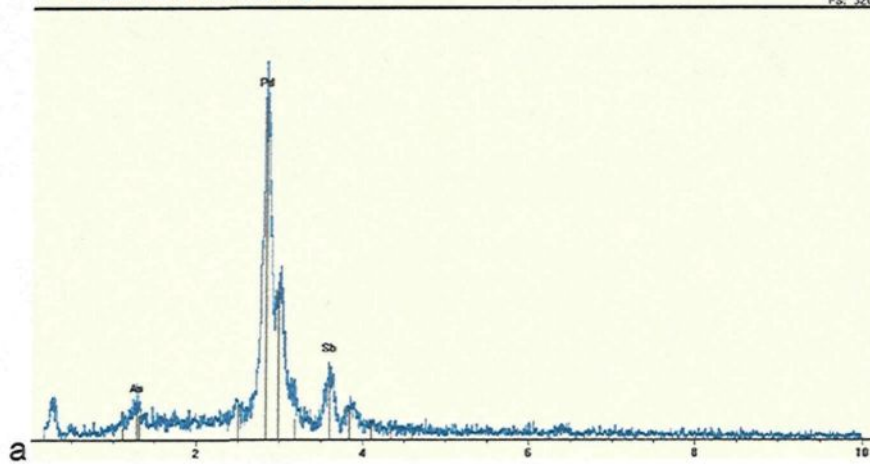
FS: 320





EDS photo 12 ML 35 PMSAs in sulphide.ppt

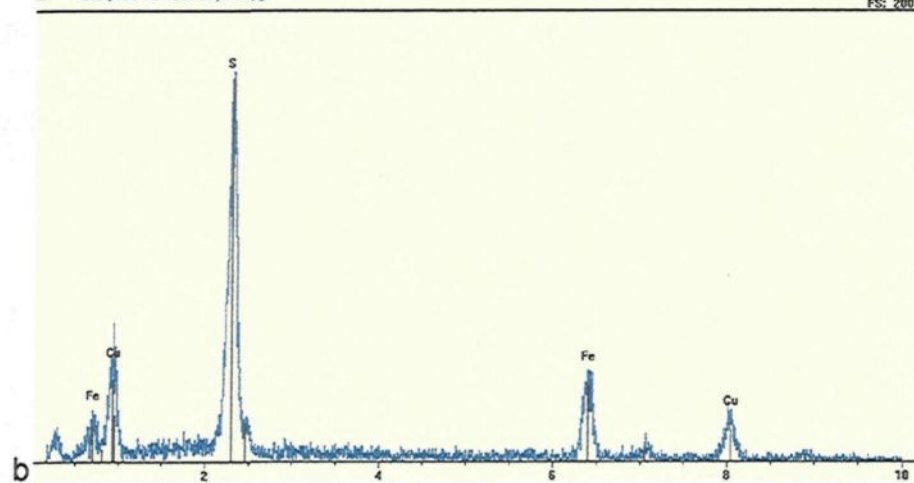
FS: 329



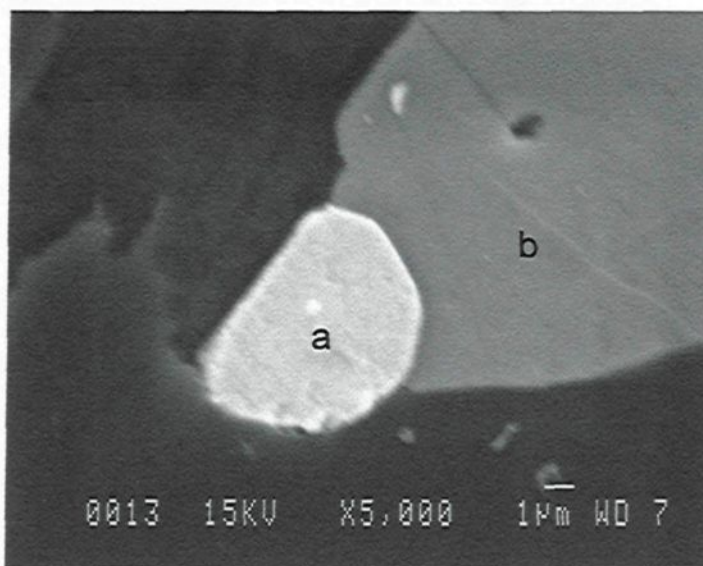
a

EDS photo 12 ML 35 sulphide.ppt

FS: 200

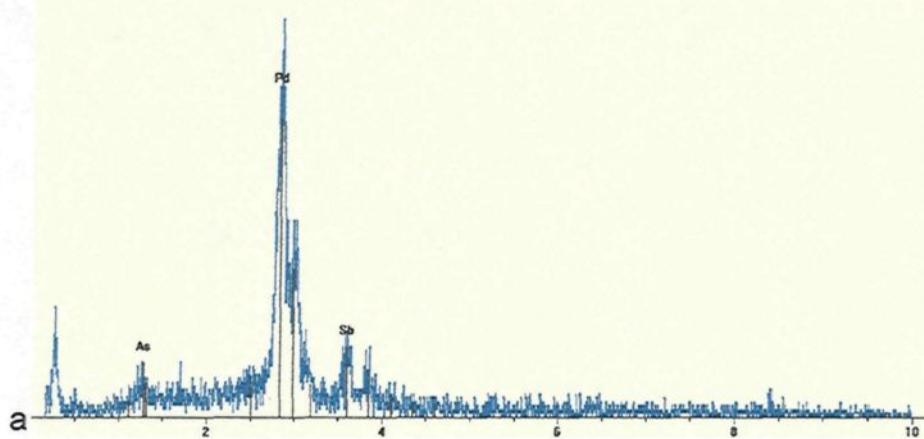


b



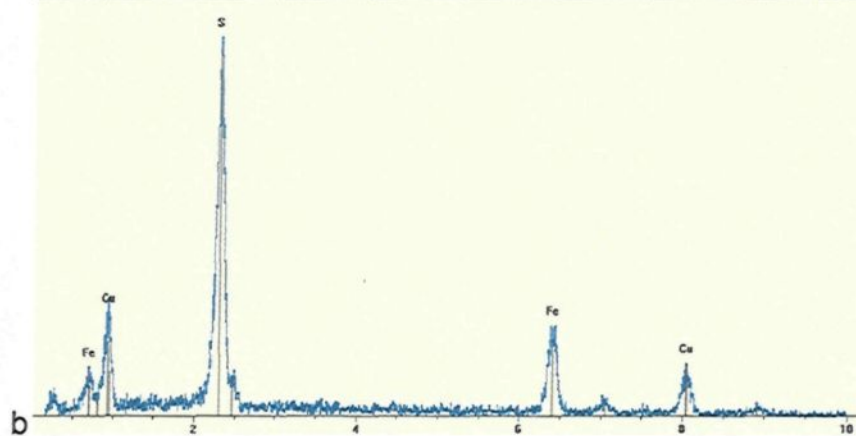
EDS photo 13 ML 35 PdSbAs borde sulphide.ppt

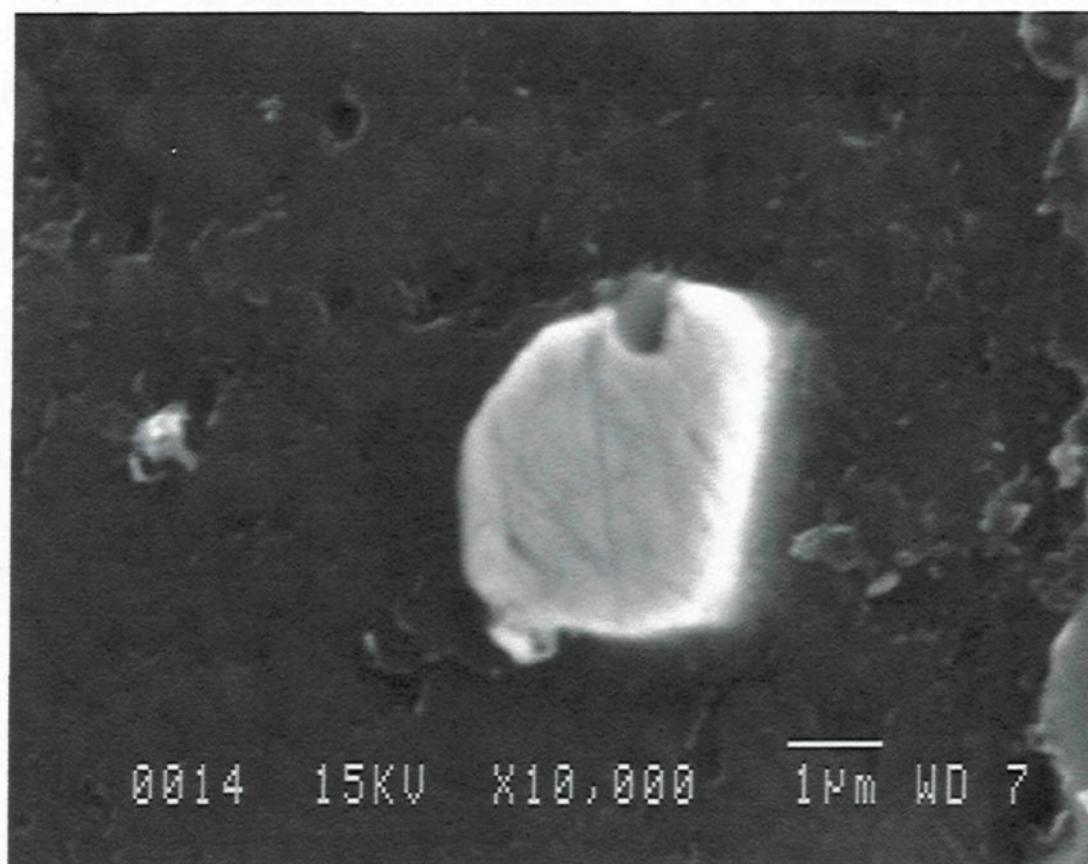
FS: 110



EDS photo 13 ML 35 sulphide.ppt

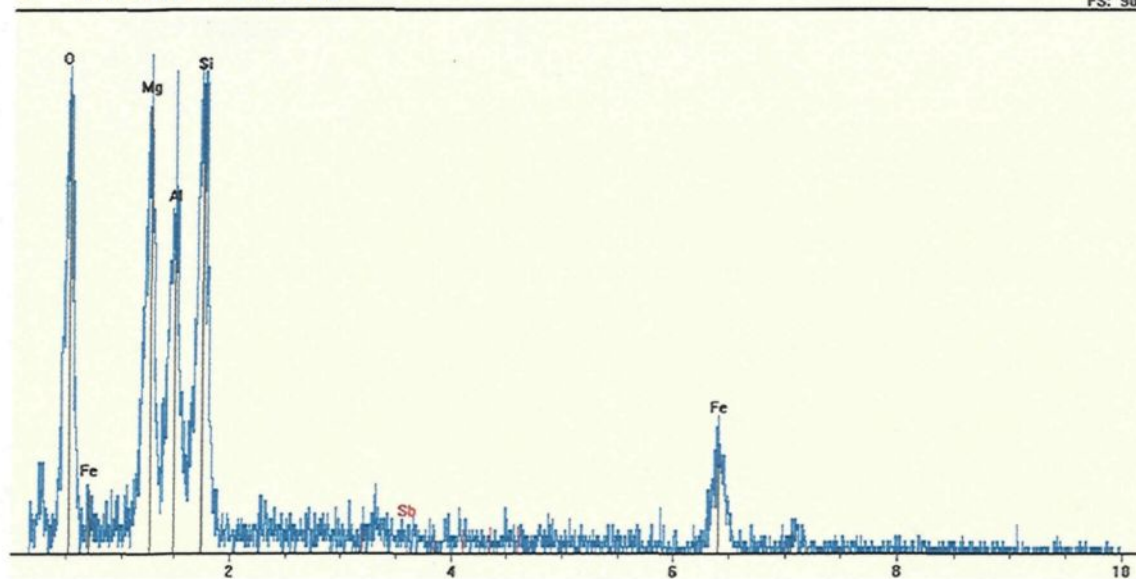
FS: 208



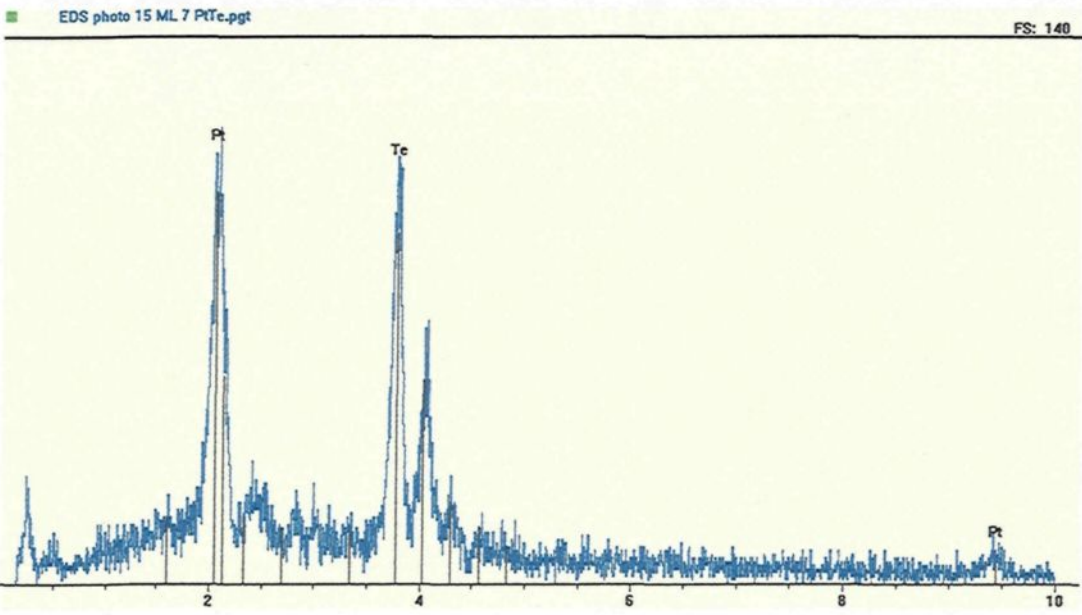
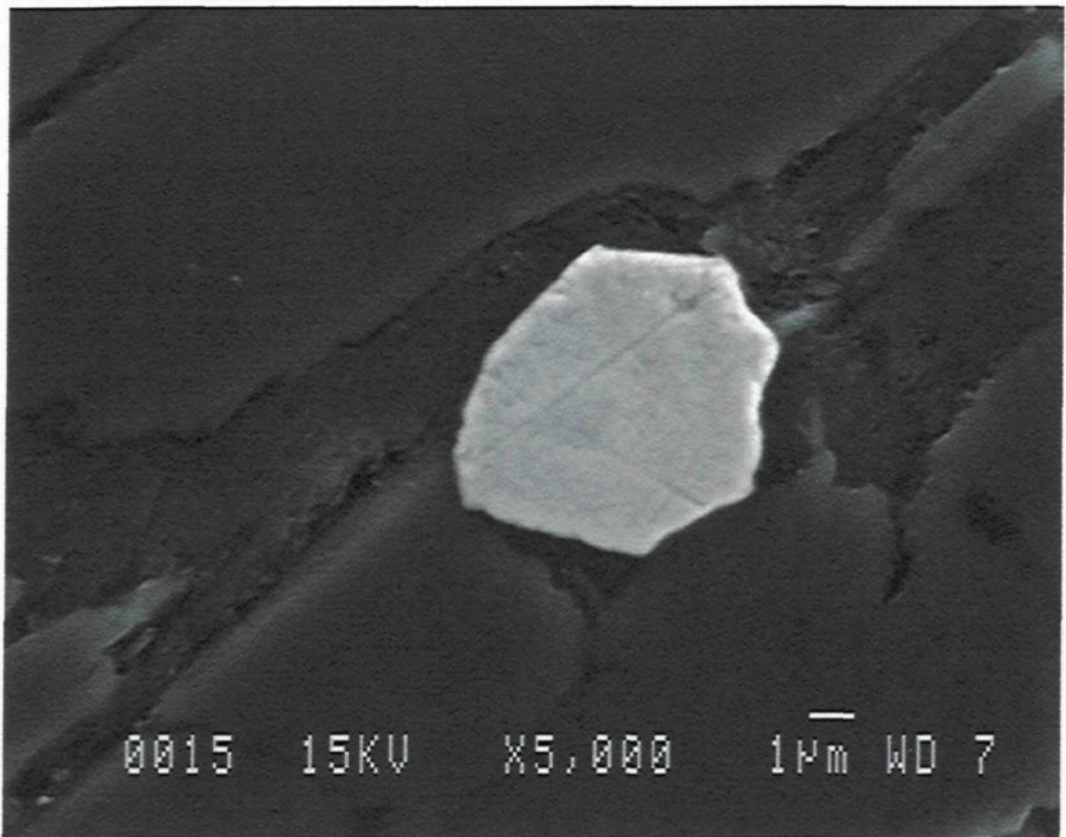


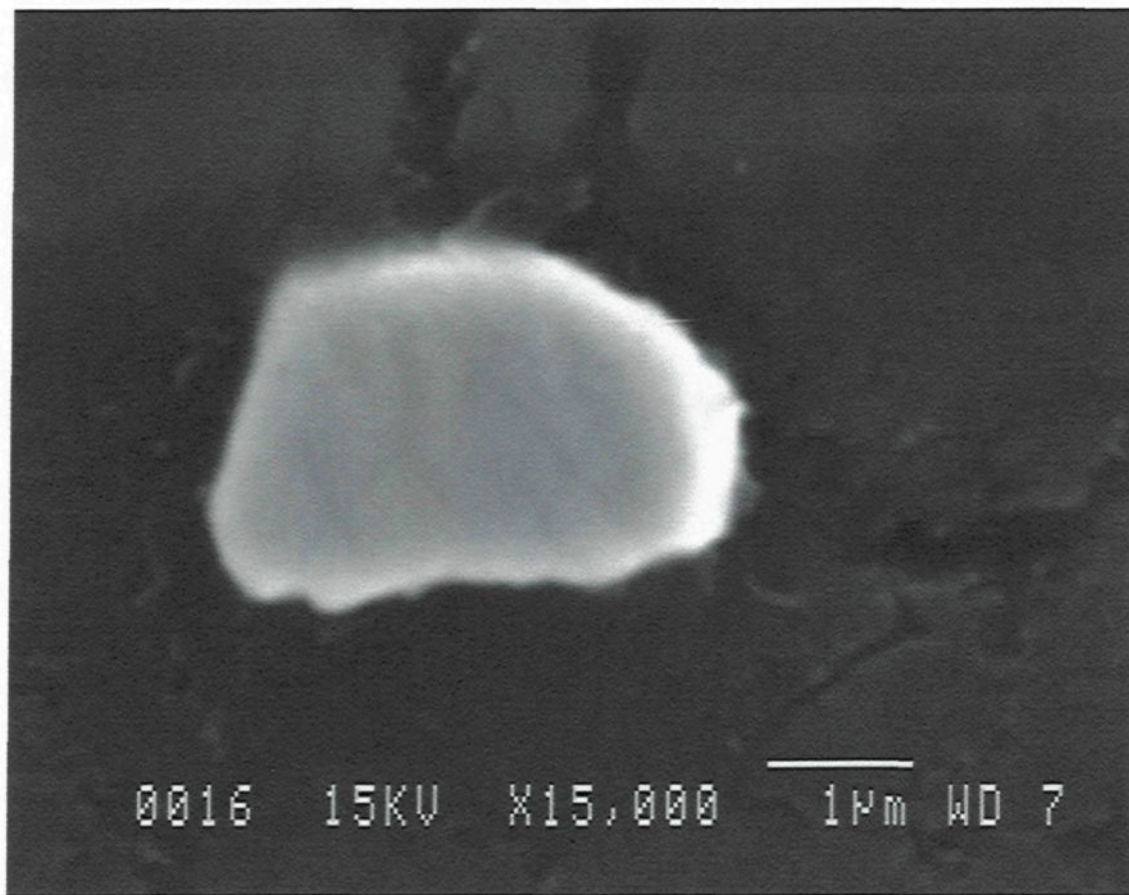
EDS photo 14 ML 35 AlMgFeSiO.pgt

FS: 90



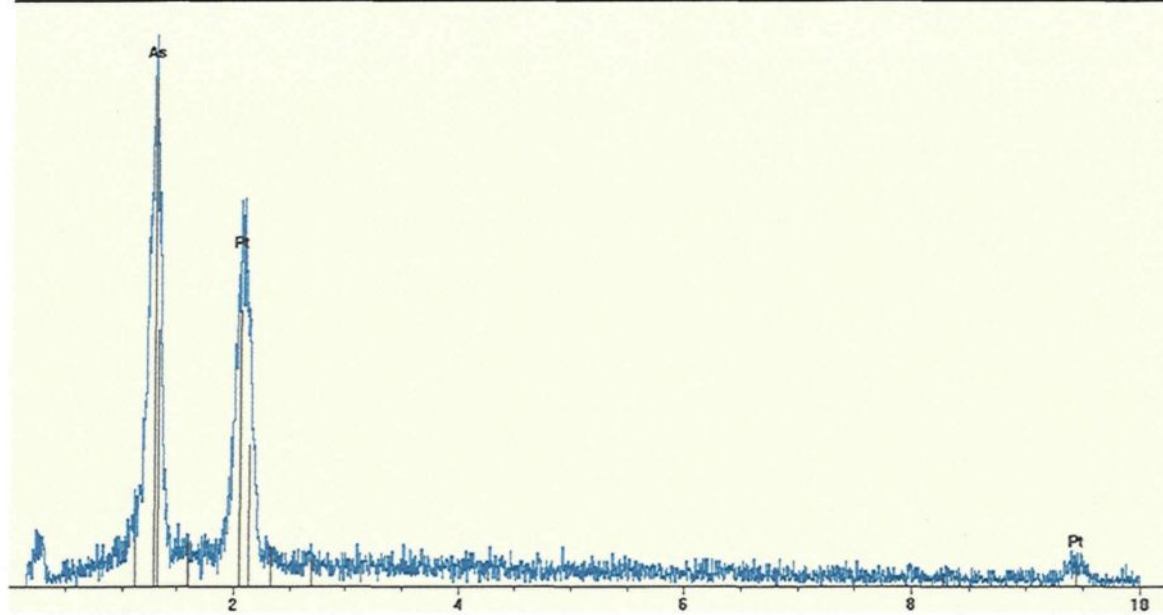
ML-7

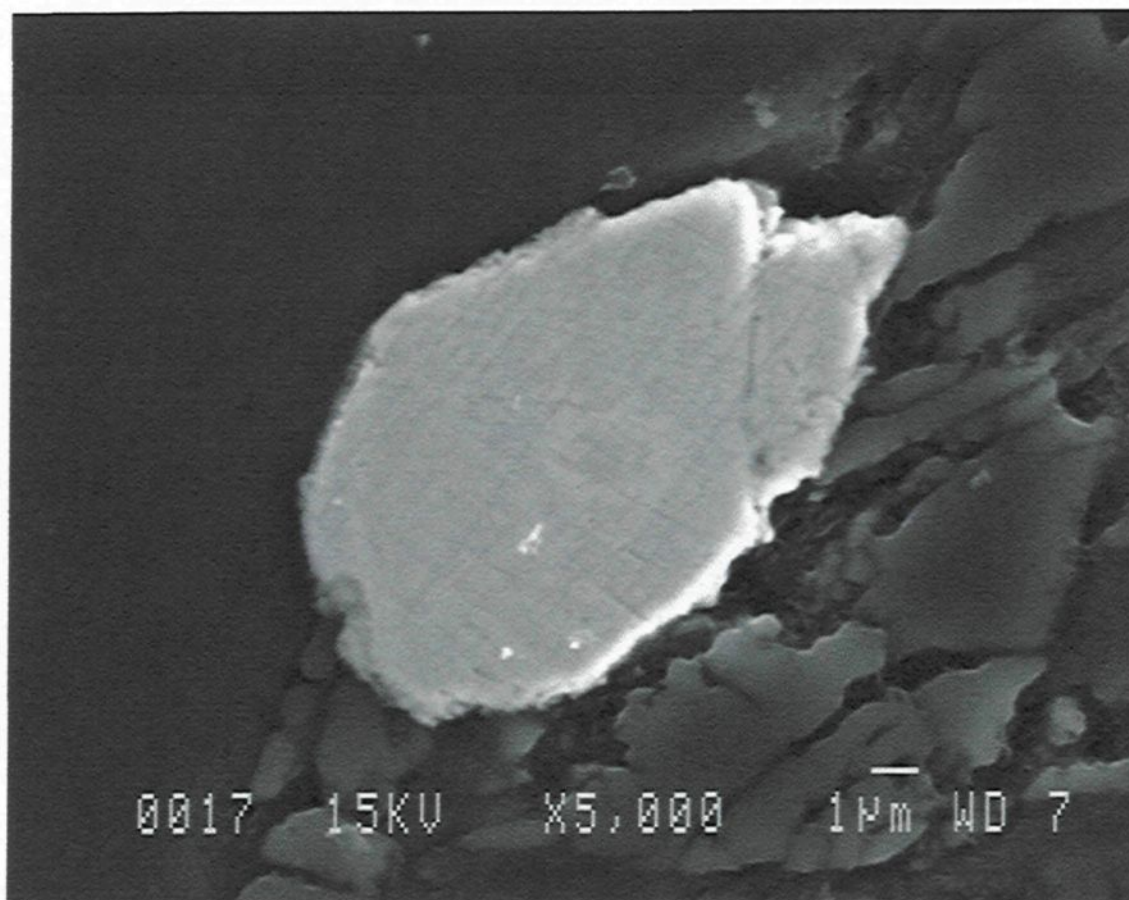




EDS photo 16 ML 7 PtAs.pgt

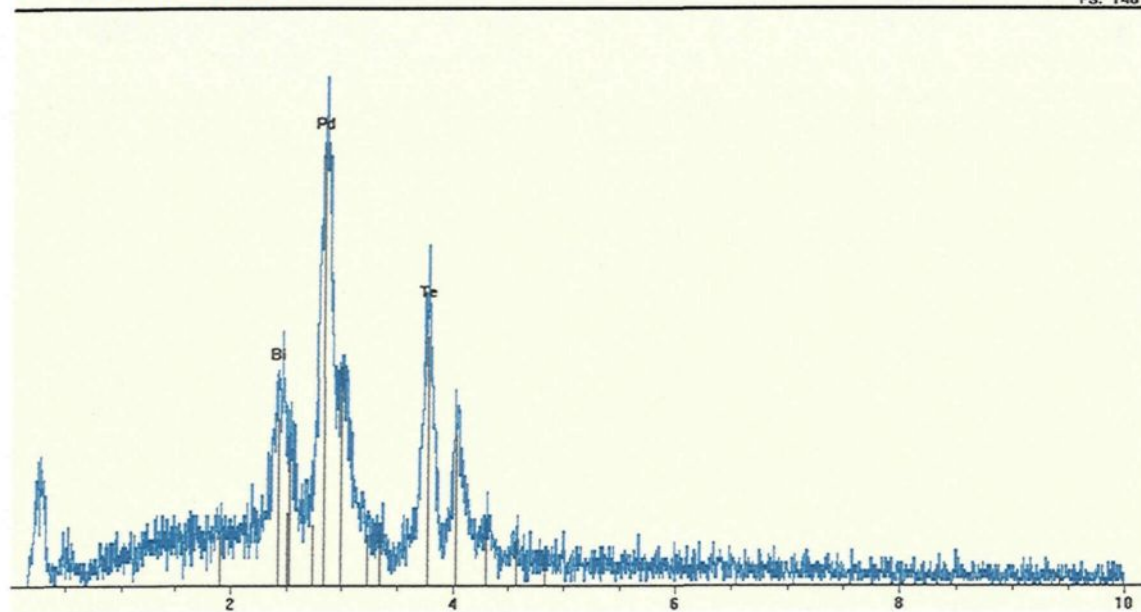
FS: 225

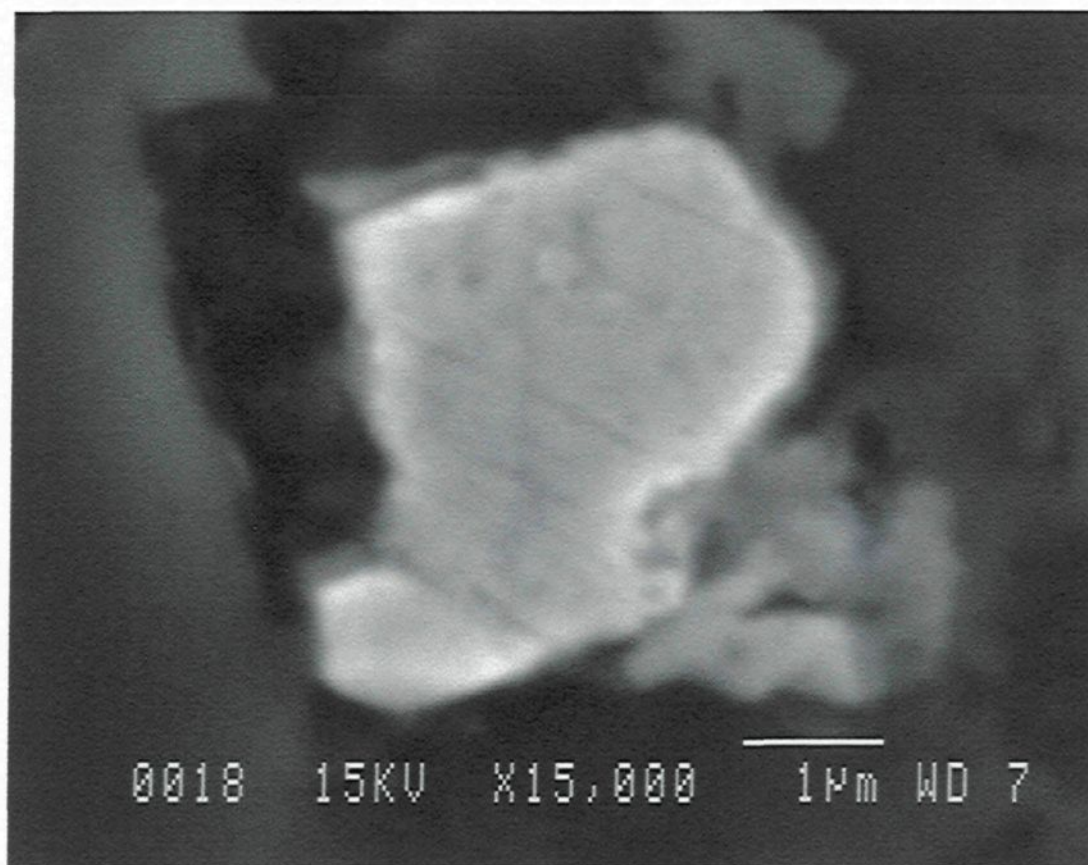




EDS photo 17 ML 7 PdBiTe.pgt

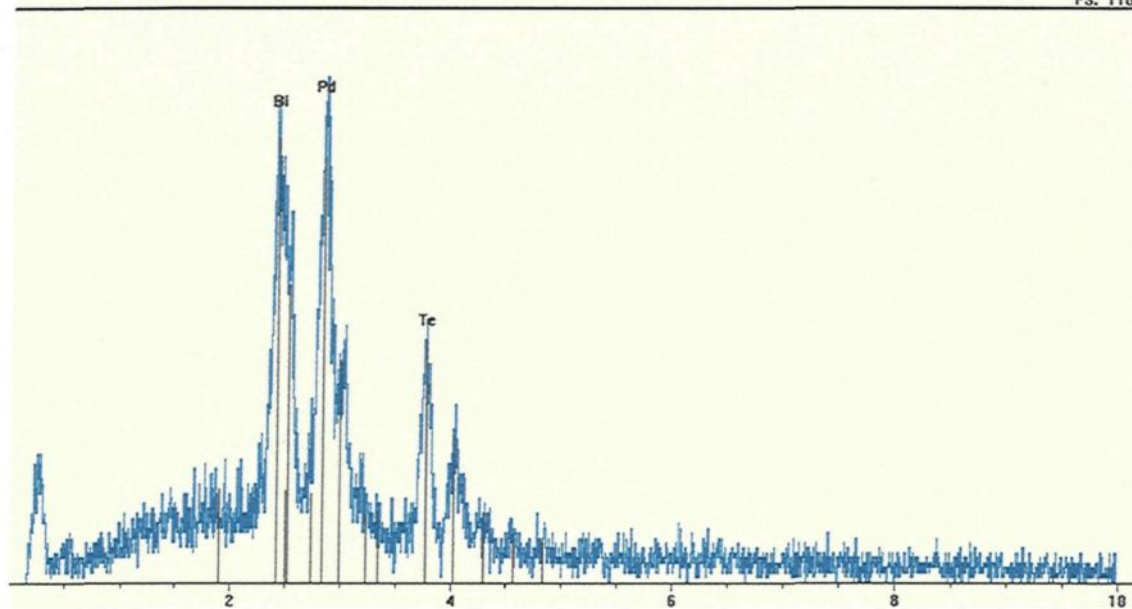
FS: 148



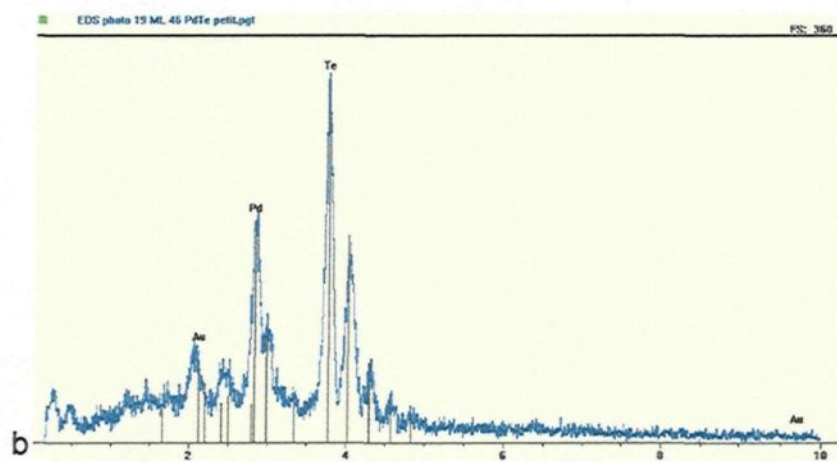
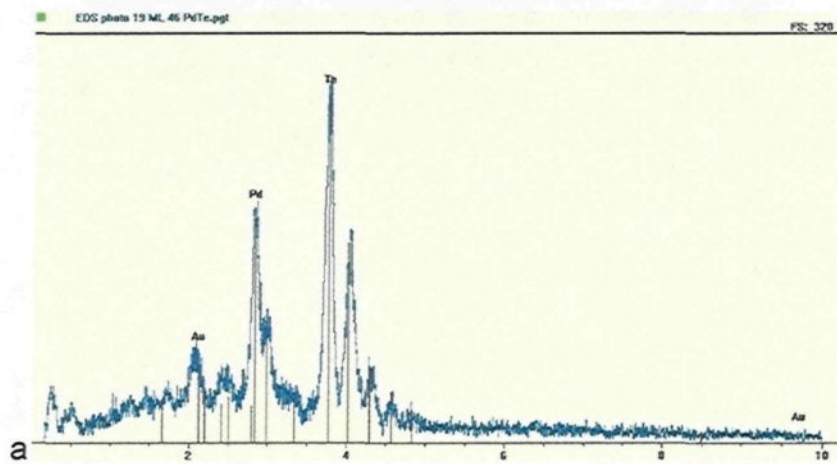
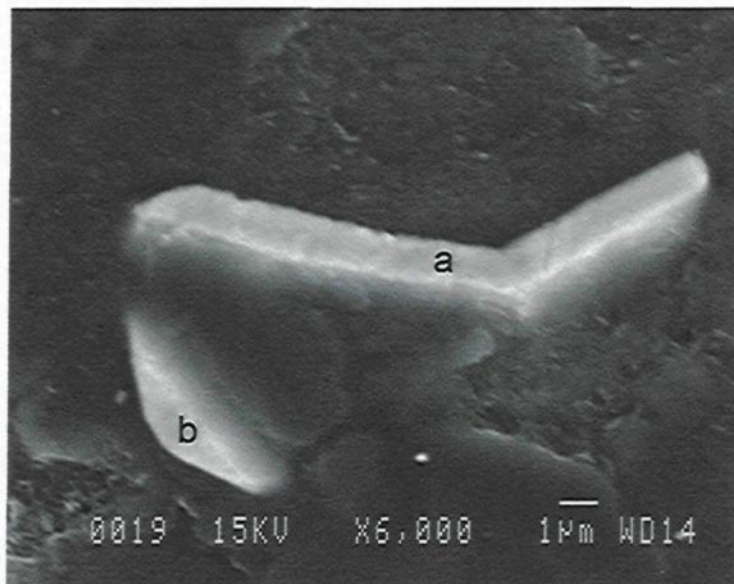


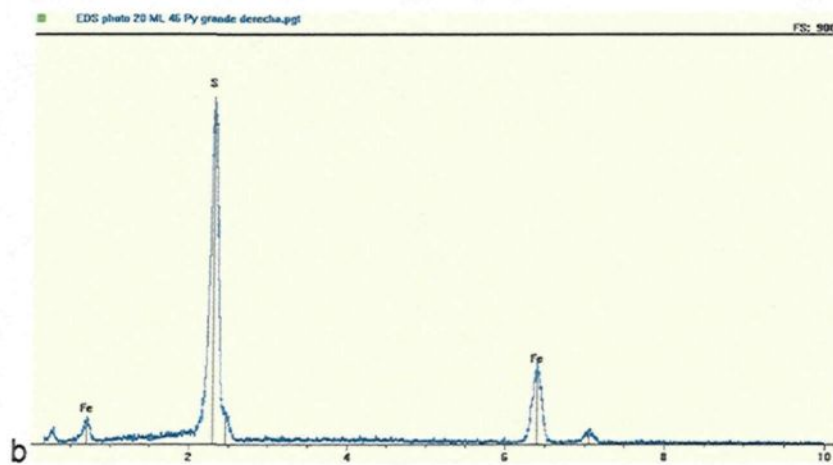
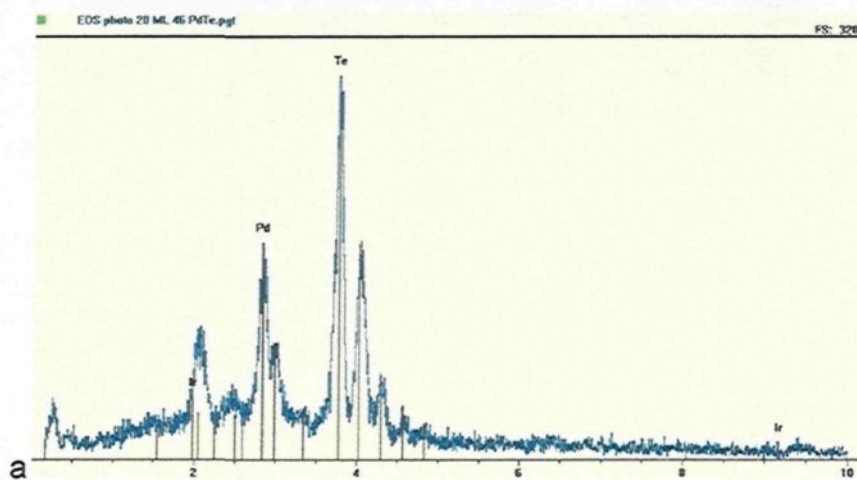
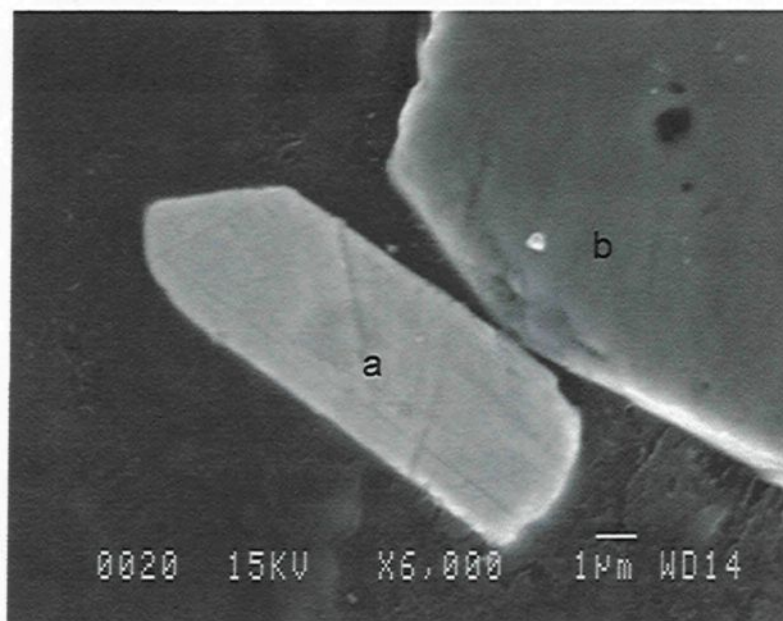
EDS photo 18 ML 7 PdBiTe.pgt

FS: 110

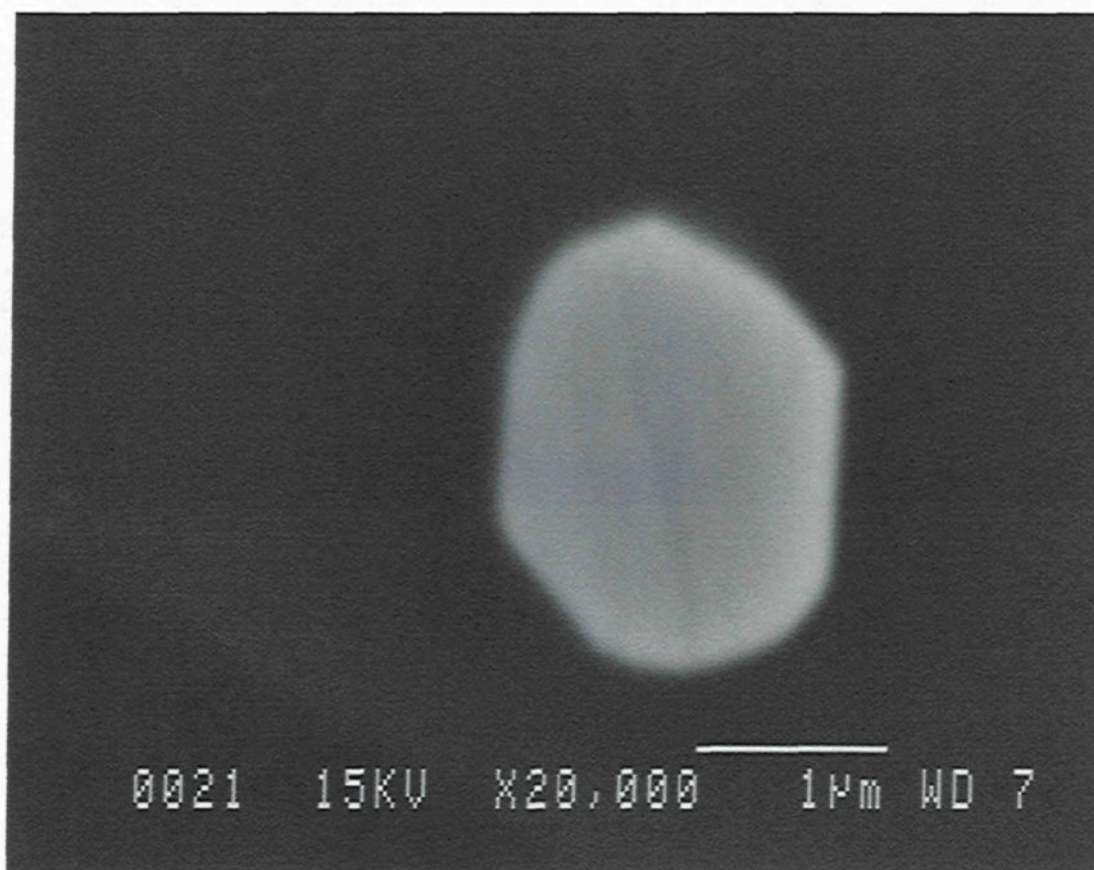


ML-46



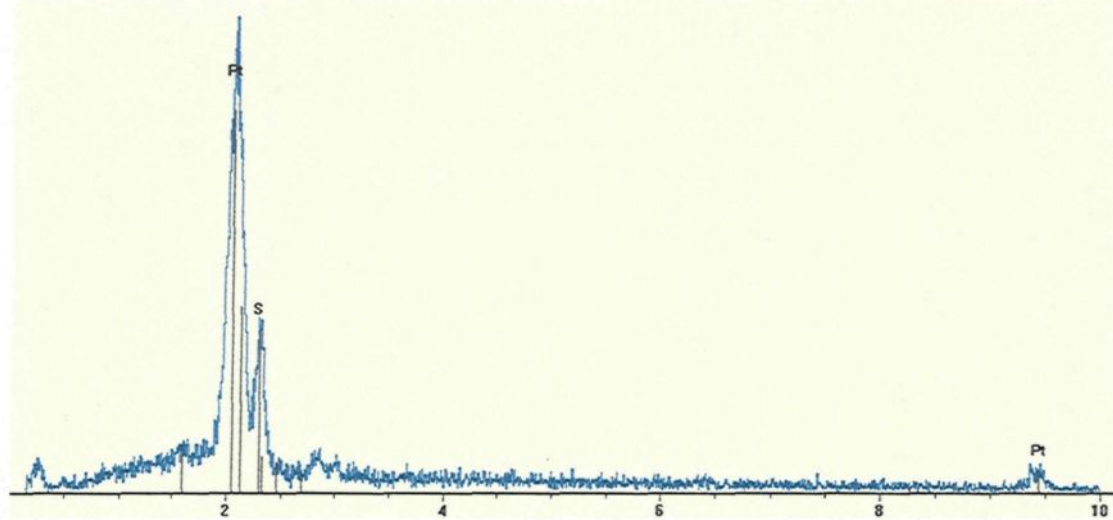


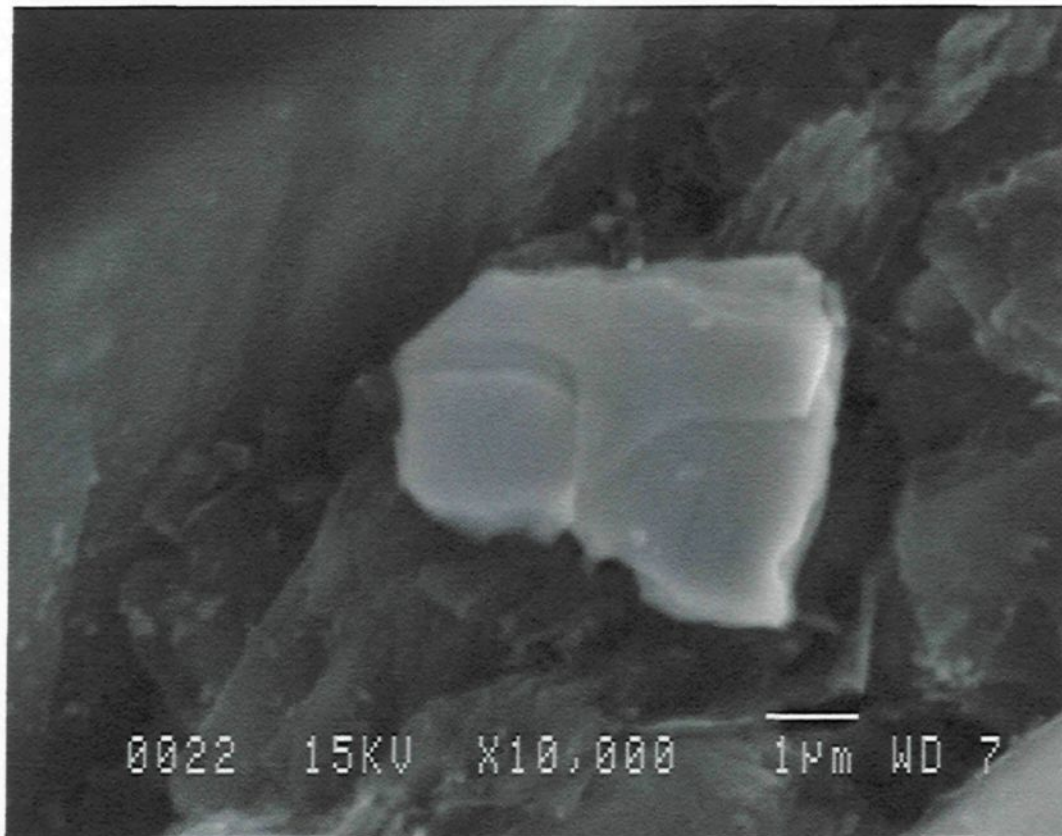
ML-17



EDS photo 21 ML 17 PtS.pgt

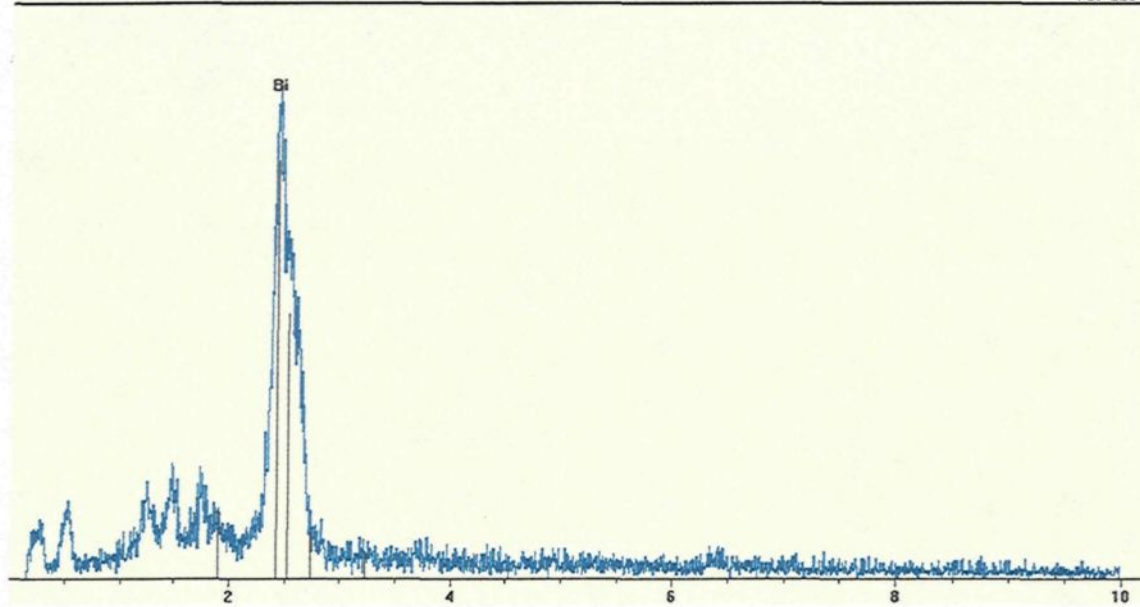
FS: 400

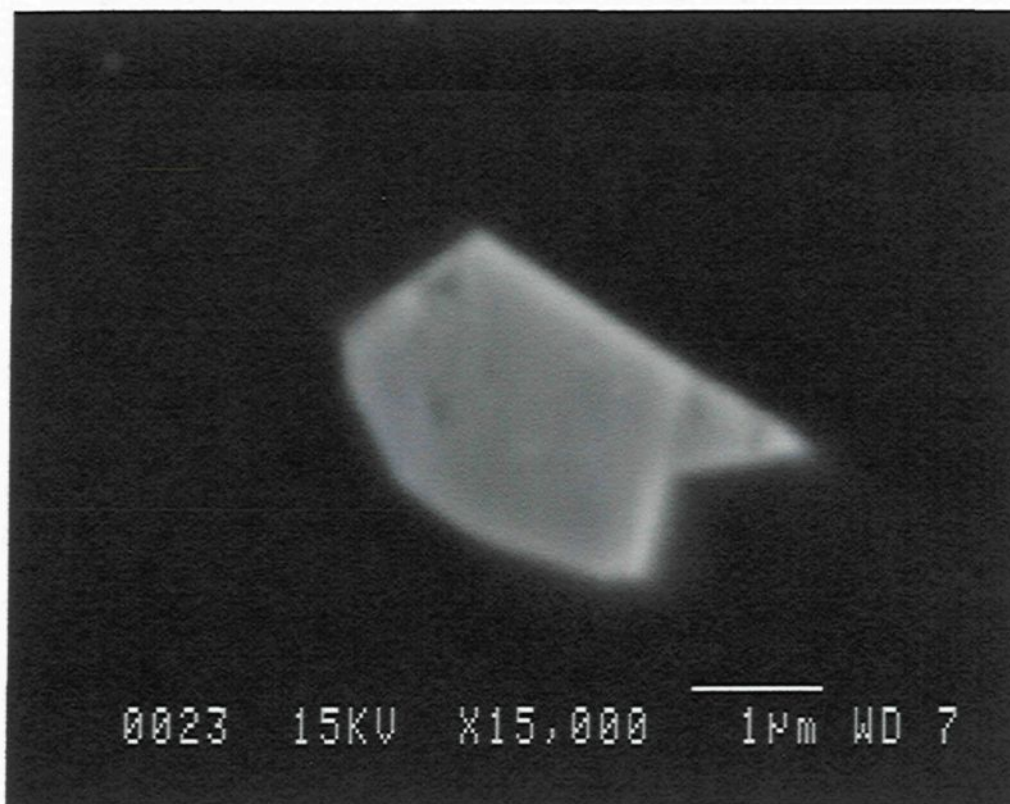




EDS photo 22 ML 17 Bi.pgt

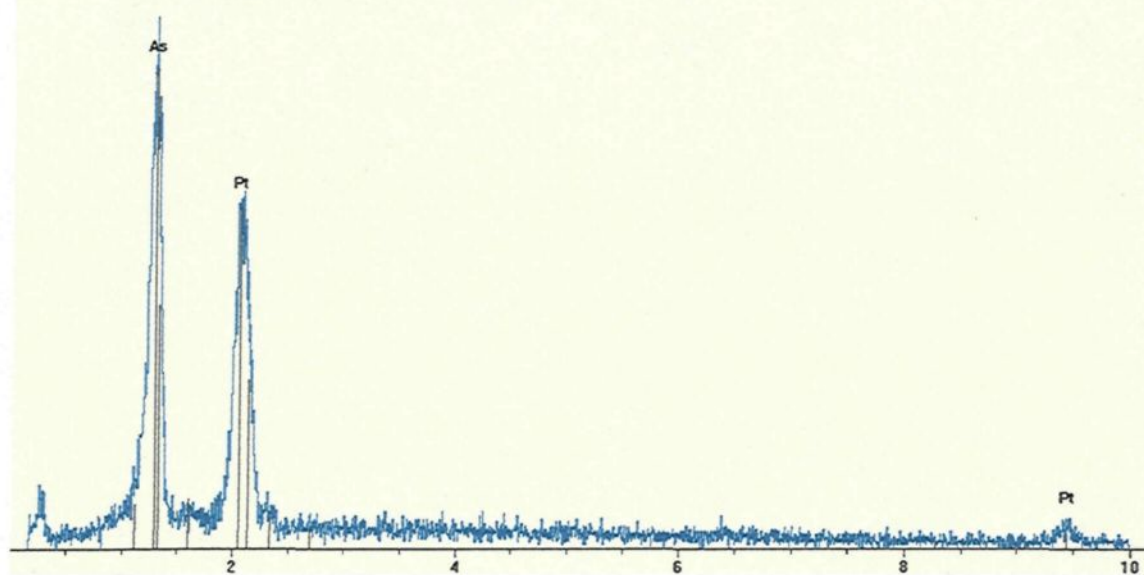
FS: 225



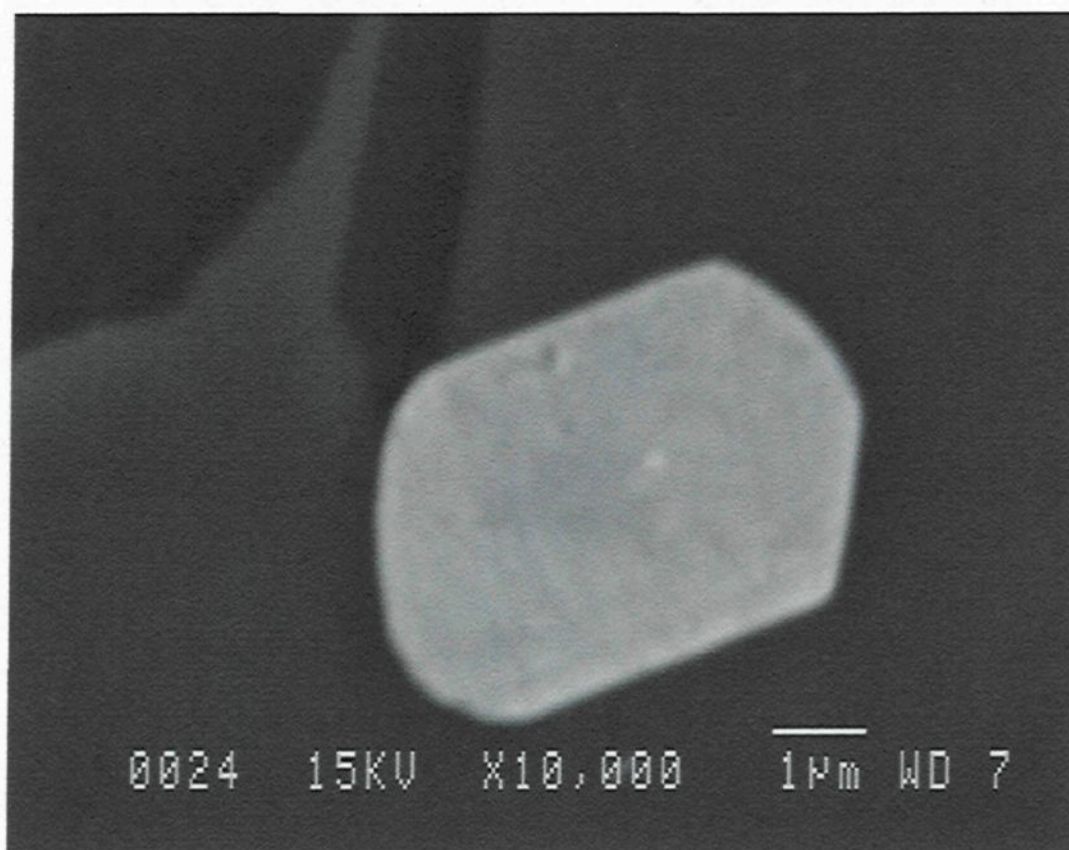


EDS photo 23 ML 17 PtAs.pgt

FS: 280

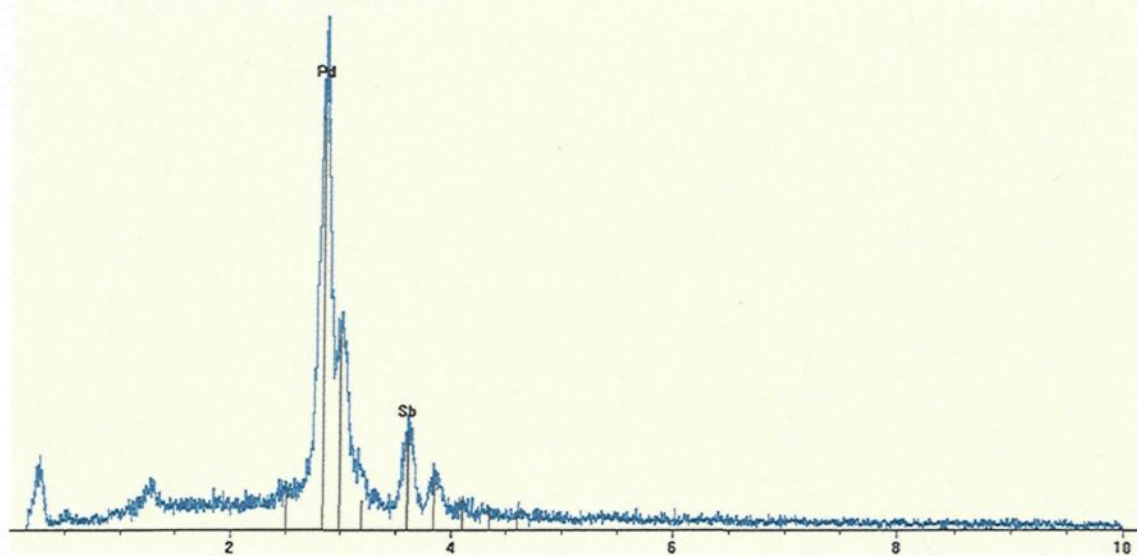


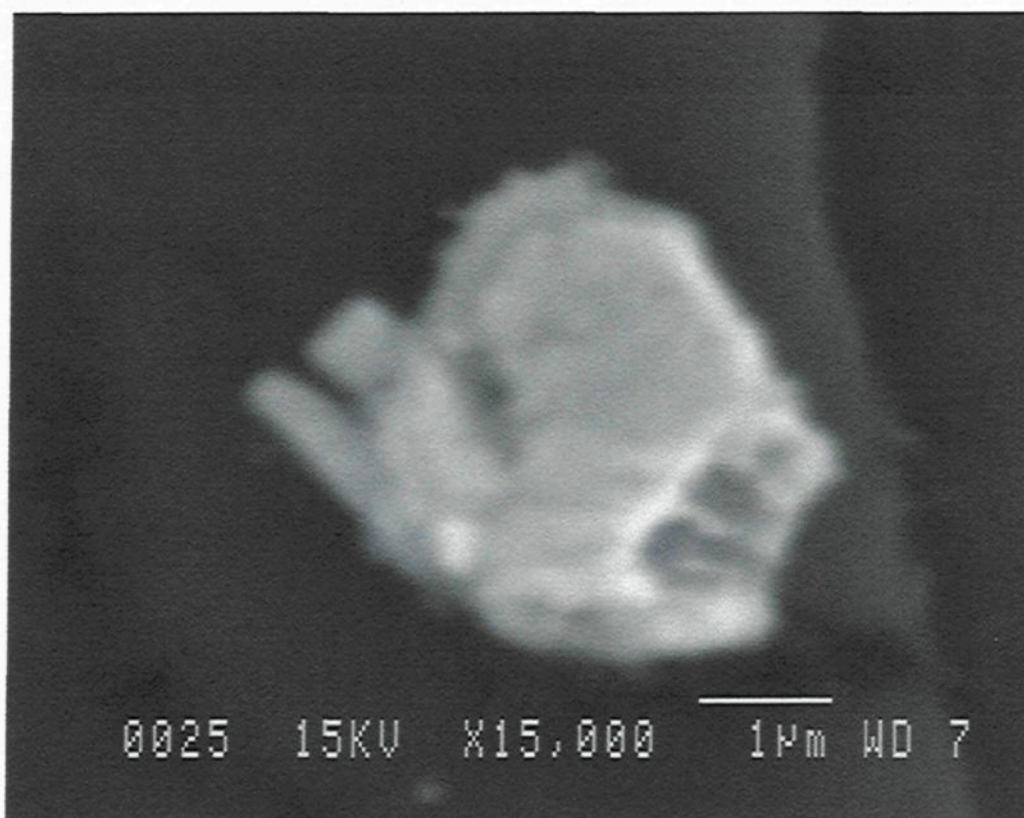
ML-65



EDS photo 24 ML 65 PdSb.pgt

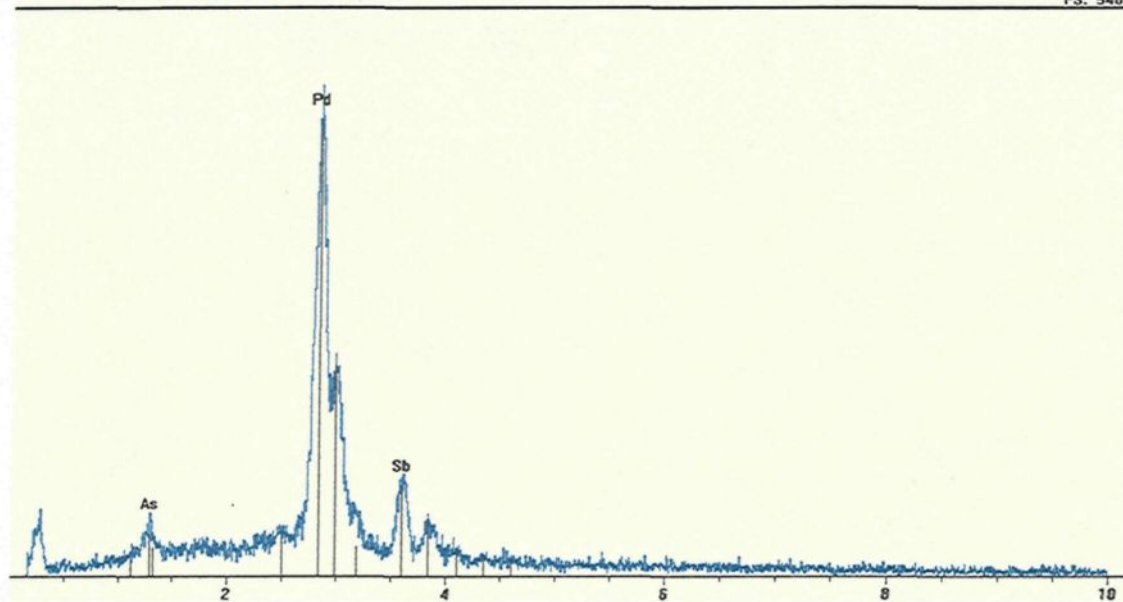
FS: 540





EDS photo 25 ML 65 PdSbAs.pgt

FS: 540



APPENDIX 111 Proposed sampling

Suggested sampling		
hole	depth	
	from	to
EB 07-09	56.00	72.50
EB 07-10	40.70	56.80
EB 07-11	31.90	55.30
EB 07-13	19.10	37.80
EB 07-13	55.20	61.80
EB 07-20	134.40	137.90
EB 07-20	137.90	138.70
EB 07-20	138.70	141.00
EB 07-20	149.30	154.20
EB 07-20	159.20	168.00
EB 08-21	55.00	66.40
EB 08-21	70.40	72.50
EB 08-21	78.10	98.80
EB 08-21	101.80	106.10
EB 08-21	109.10	110.30
EB 08-21	117.30	120.00
EB 08-22	124.60	132.40
EB 08-22	135.30	136.40
EB 08-23	80.00	90.70
EB 08-23	99.80	105.00
EB 08-23	109.30	114.50
EB 08-23	118.50	120.10
EB 08-23	121.10	122.20
EB 08-35	36.80	72.50

The sampling should be of only one kind of rock per sample and less than 1 meter long.